G. Höhne
W. Hemminger
H.-J. Flammersheim

Differential Scanning Calorimetry

An Introduction for Practitioners

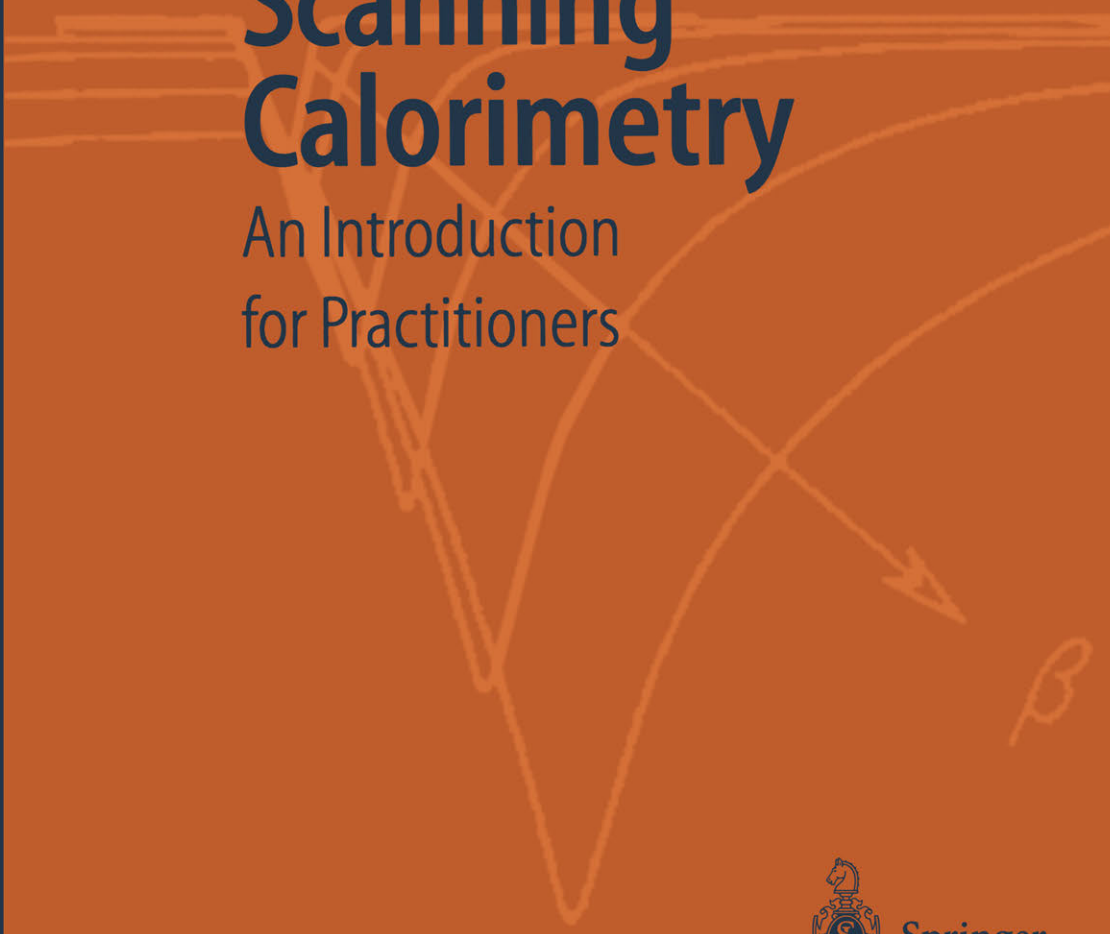

Springer

Differential Scanning Calorimetry

Springer-Verlag Berlin Heidelberg GmbH

G. W. H. Höhne, W. Hemminger,
H.-J. Flammersheim

Differential Scanning Calorimetry

An Introduction for Practitioners

With 136 Figures and 13 Tables

Springer

Dr. G. W. H. Höhne
Universität Ulm
Sektion Kalorimetrie
Albert-Einstein-Allee 11
D - 89069 Ulm

Dr. W. Hemminger
Physikalisch-Technische Bundesanstalt
Bundesallee 100
D - 38116 Braunschweig

Dr. H.-J. Flammersheim
Universität Jena
Institut für Physikalische Chemie
Lessingstraße 10
D - 07743 Jena

ISBN 978-3-662-03304-3 ISBN 978-3-662-03302-9 (eBook)
DOI 10.1007/978-3-662-03302-9

Library of Congress Cataloging-in-Publication Data
Höhne, G. W. H. (Günther, Walther, Heinrich)
Differential scanning calorimetry : an introduction for practitioners / G. W. H. Höhne, W. Hemminger, H.-J. Flammersheim.
Includes bibliographical references and index.

1. Calorimetry. I. Hemminger, W. II. Flammersheim, H.-J., III. Title.
QC291.H64 1995 95-20483

Originally published by Springer-Verlag Berlin Heidelberg New York in 1996.
Softcover reprint of the hardcover 1st edition 1996

Typesetting: Data-conversion by Fotosatz-Service Köhler OHG, Würzburg
SPIN:10077368 52/3020-5 4 3 2 1 0 - Printed on acid-free paper

Preface

Differential Scanning Calorimetry (DSC) is a well established measuring method which is used on a large scale in different areas of research, development, and quality inspection and testing. Over a large temperature range, thermal effects can be quickly identified and the relevant temperature and the characteristic caloric values determined using substance quantities in the mg range. Measurement values obtained by DSC allow heat capacity, heat of transition, kinetic data, purity and glass transition to be determined. DSC curves serve to identify substances, to set up phase diagrams and to determine degrees of crystallinity.

This book provides, for the first time, an overall description of the most important applications of Differential Scanning Calorimetry. Prerequisites for reliable measurement results, optimum evaluation of the measurement curves and estimation of the uncertainties of measurement are, however, the knowledge of the theoretical bases of DSC, a precise calibration of the calorimeter and the correct analysis of the measurement curve.

The largest part of this book deals with these basic aspects: The theory of DSC is discussed for both heat flux and power compensated instruments; temperature calibration and caloric calibration are described on the basis of thermodynamic principles. Desmearing of the measurement curve in different ways is presented as a method for evaluating the curves of fast transitions.

The instrumental data which are most important for the characterization of Differential Scanning Calorimeters are defined, and it is explained how they are determined experimentally. This enables every potential buyer to ask the manufacturer for measured characteristic data which will allow him to compare the different instruments available.

We are indebted to S.M. Sarge for a critical examination of the manuscript and valuable suggestions for improvement and especially to M.J. Richardson for helping us with the translation.

G.W.H. Höhne
W. Hemminger
H.-J. Flammersheim

Contents

List of Symbols

A	area, pre-exponential factor
C	heat capacity, electric capacity
E	energy
H	enthalpy
K	factor (calibration), coefficient
L	thermal conductance
P	electric power
Q	heat
R	resistance (thermal, electric), gas constant
S	entropy
T	temperature
U	internal energy, voltage
V	volume
W	work, electric energy
a	coefficient, apparatus function
c	specific heat capacity
d	distance
i	electric current
k	proportionality factor, calibration factor, rate constant
l	length, distance
m	mass
n	reaction order
p	pressure
r	rate of reaction
t	time
w	weight fraction
x	mole fraction
α	degree of reaction
β	heating rate
γ	expansivity coefficient
ε	emissivity
λ	thermal conductivity
ν	stoichiometric number
Φ	heat flow rate
ρ	density
σ	standard deviation
τ	time constant
χ	compressibility
ξ	extent of reaction, composition, conversion

Subscripts

A	activation
a	amorphous
bl	baseline
c	extrapolated offset, crystalline
cal	calorimeter
corr	correction
e	extrapolated onset
el	electric
eq	equilibrium
exp	experimental
F	furnace
f	final
fix	fixpoint
fus	fusion
g	glass
h, i, k, n	running numbers
i	initial
iso	isothermal
l	liquid
lit	literature
M	measurement point
m	measured
mix	mixing
o	onset
p	peak, constant pressure
prop	proportional
Φ	related to heat flow rate
Q	related to heat
R	reference sample
r	reaction
Ref	reference material used for calibration (e.g. Certified Reference Material)
S	sample
s	solid
st	steady state
th	thermal
tot	total
tr	true
trs	transition
V	constant volume
0	zero, zero line

1 Introduction

The objective of calorimetry is the measurement of heat. To measure heat means to exchange heat. The exchanged heat tends to effect a temperature change in a body that can be used as a measure of the heat exchanged, or the process of heat exchange is connected with a heat flow which leads to local temperature differences along its path which again serve as a measure of the flowing heat.

As chemical reactions and many physical transitions are connected with the generation or consumption of heat, calorimetry is a universal method for investigating such processes. Measuring devices in which an exactly known amount of heat is input into a sample, or abstracted from it, and the temperature change in the sample is measured (determination of the heat capacity, for example), are also referred to as calorimeters.

Caloric measurements have been carried out since the middle of the 18th century. Although modern Differential Scanning Calorimeters (DSC) are widely used today, the "classic" calorimeters cannot be dispensed with in precision measurements and for special applications. The most important classic calorimeters will be described only briefly in Appendix 2 to give the reader a more comprehensive survey of the field of calorimetry (for a more general presentation of calorimetry, cf. Hemminger, Höhne, 1984; Oscarson, Izatt, 1992).

The topic of this book is *Differential Scanning Calorimetry (DSC)* using as a measuring instrument the Differential Scanning Calorimeter (DSC) available in various designs (see Chapter 2).

According to the International Confederation for Thermal Analysis and Calorimetry (ICTAC) the definition of *Differential Scanning Calorimetry* is as follows:

A technique in which the heat-flow rate (power) to the sample is monitored against time or temperature while the temperature of the sample, in a specified atmosphere, is programmed.

Differential Thermal Analysis (DTA)

To distinguish a heat flux DSC from an apparatus for Differential Thermal Analysis (DTA), the latter will be characterized in the following.

Differential Thermal Analysis is applied to measure the temperature difference between the sample to be investigated and a reference sample as a function of temperature (or time). This temperature difference indicates a heat exchange qualitatively. DTA is more recent than classic calorimetry. Its advantages compared with conventional calorimetry are the dynamic mode of operation ("scanning") which allows reactions or processes to be investigated which can be thermally activated,

and the high sensitivity to anomalies of the temperature-time function. DTA allows characteristic temperatures to be determined and qualitative statements made on heat due to reaction. The further development of DTA has led to the construction of Differential Scanning Calorimeters (DSCs) with disk-type measuring systems.

The ICTAC definition of *Differential Thermal Analysis* is as follows:
A technique in which the difference in temperature between the sample and a reference material is monitored against time or temperature while the temperature of the sample, in a specified atmosphere, is programmed.

For a short description of the principle of DTA measuring systems in comparison with DSC, see Appendix 1.

Calorimetry and DTA Today

Owing to the new materials and sensors used and the application of modern electronic systems, all calorimeters available today – including the so-called "classic" calorimeters – are instruments which allow precise measurements to be carried out, their operation being relatively simple or perhaps even automated. Calorimetric methods are used in many fields for quality assurance purposes (cf. series of standards ISO 9000). The standards to be applied in the field of quality assurance (e.g. the standard EN 45001) demand a large variety of measures to ensure reliable measurement results, for example, the application of well-proven methods for the preparation of samples, reliable measurement methods, calibration methods and calibration materials traceable to standards (see also Sect. 4).

In the following, reference is made to some of the fields in which calorimeters are widely used today (see Hemminger, Höhne, 1984; Wunderlich, 1990; Oscarson, Izatt, 1992). A suggestion how to classify calorimeters in given in Appendix 2.

- With *bomb calorimeters*, combustion heats (gross calorific values) are measured on a large scale in industry (cost of fossil fuels) (Sunner, Månsson, 1979),
- *gas calorimeters* (flow calorimeters) are used for the continuous or discontinuous measurement of the calorific value of fuel gases (e.g. natural gas), both in frontier-crossing commercial transactions (between supplier and buyer) and for the calculation of the cost for the individual consumer (Hyde, Jones, 1960; Hemminger, 1988),
- *drop calorimeters* (usually home-made) allow mean heat capacities or enthalpy differences to be measured quickly. Drop sample temperatures of up to 2000 °C are realized (Chekhovskoi, 1984),
- different types of *isoperibol mixing calorimeters* are used to investigate reactions between two fluids or between a fluid and a solid (reaction heats, heats of solution, heats of mixing, adsorption heats) (see e.g. Parrish, 1986),
- *reaction calorimeters* and *safety calorimeters* allow model tests of procedures applied in industrial chemistry to be carried out. These instruments provide valuable support in development and optimization tasks since all test parameters (temperature, time, addition of substances etc.) are completely documented and can be varied automatically.

Questions of process technology which are also important for the dimensioning of production facilities, may be well in the fore here (Regenass, 1985). Reaction heat released is connected with the degree of conversion and exploitation, for example in biotechnology, where calorimetric studies are carried out on industrial production plants (large-scale calorimetry, mega-calorimetry, see e.g. von Stockar, Marison, 1991 in Lamprecht et al., 1991).
Special calorimeters (commercially available) are also used to investigate aspects of safety technique, for example, to determine characteristic temperatures of decomposition or the kinetics of reactions (decompositions, run-away reactions) under certain boundary conditions (see, for example, Grewer, 1987; Schwanebeck, 1991; Singh, 1993; for a survey, cf. Grewer, Steinbach, 1993),

- in highly sensitive *flow calorimeters* (usually of the isoperibol type, i.e. with surroundings at constant temperature), the heat generation of biological systems and their change under varying conditions of life are investigated (for example, addition of pharmaceuticals to bacterial cultures). In different types of biocalorimeters, the metabolism of organisms and their change due to external influences (optical, acoustical, mechanical, thermal, chemical) are studied (see e.g. Spink, Wadsö, 1976; Lamprecht, Schaarschmidt, 1977; Beezer, 1980; Lamprecht et al., 1991; Schmolz et al., 1993; Moratzky et al., 1993),
- heat capacities and heats of transition are measured directly with high accuracy using *adiabatic calorimeters*. The characteristic data of materials determined with their aid are an indispensable basis for the calibration of the DSCs (see e.g. Grønvold, 1967; Kagan, 1984; Jakobi et al., 1993; Grønvold, 1993). Properly calibrated DSCs allow specific heat capacities to be measured with an accuracy of 1 to 2% (see Sect. 6.2.1; cf. Richardson, 1992a).

New fields of application are constantly being opened up for the modern, highly automated DSCs. DSC is increasingly used in the field of quality assurance for many purposes: for the inspection of raw materials, as an accompanying measure in the manufacture and for checking the finished products. The basic limitations to, and the problems of these instruments should not, however, be forgotten in view of the ease of operation and evaluation.

DSCs allow reaction heats and heats of transition, or heat flow rates and their changes at characteristic temperatures, to be measured quickly using small sample masses (milligram range; in the case of classic calorimeters: gram range), in wide temperature ranges and with an accuracy which is usually sufficiently high for the respective purpose. DSCs are applied in the following fields (among others):

- characterization of materials,
- comparison (relative) measurements (quality control, identification of substances or mixtures),
- stability investigations,
- evaluation of phase diagrams,
- purity determinations,
- kinetic investigations,
- safety research.

Now as before, instruments used for *Differential Thermal Analysis* (DTA) offer particular advantages when special problems are to be investigated:

- they can be used at very high temperatures (up to about 2400 °C),
- they are highly sensitive,
- they are very flexible as regards the volume and form of the crucibles,
- their reasonably-priced measuring system can be easily exchanged.

Characteristic temperatures of transitions or reactions can be determined very well by DTA. Heats can still be estimated with an uncertainty between 20 and 50 %. DTA is applied in the following fields:

- comparison (relative) measurements (identification, control, comparison),
- safety research (stability investigations, also long-time investigations), see e. g. Hentze, 1984; Hentze, Krien, 1986,
- investigation of transitions, decompositions, reactions with gases,
- evaluation of phase diagrams.

DSC and DTA are also used together with other methods of thermal analysis or other analytical techniques (simultaneous thermal analysis), most frequently in connection with Thermogravimetry (TG), more rarely with Evolved Gas Analysis (EGA), Thermomicroscopy or Thermosonimetry.

The coupling of DSC or DTA with Thermogravimetry (TG) is of particular importance. In addition to information on changes in the heat flow rate (due, for example, to changes of heat capacity) and heats of transition, the TG signal provides information on whether volatile components are involved and which changes in mass can be attributed to a transition.

The different methods of gas analysis used together with DSC or DTA (usually together with TG/DSC or TG/DTA systems) are of increasing importance. Via a carrier gas stream, gaseous reaction products from the calorimeter or DTA device are transported to an apparatus in which these products are analyzed. This allows a correlation between the characteristic temperature of a reaction, gravimetric and/or enthalpic information and the composition of the volatile reaction product to be made (see examples in Mathot, 1994 a).

It is difficult to transfer the volatile products without alteration from the hot sample to the analysis system (condensation must be avoided). Various systems for coupling quadrupole mass spectrometers are commercially available (up to temperatures of 2400 °C). Examples of the investigation of volatile components applying methods of gas analysis can be found in Ohrbach et al., 1987; Matuschek et al., 1991; Matuschek et al., 1993.

The advantage of simultaneous measurements is that the same sample is investigated under identical conditions and that diverse information is obtained by one measurement run which is important for interpretation purposes. The following potential disadvantages of simultaneous instruments should be mentioned: lower sensitivity, higher susceptibility to failure, increased time and effort required for preparation and operation, higher instrument costs.

In Differential Scanning Calorimetry which is widely applied, there are still some actual problems of which one should be aware:

- there is not yet a theoretically well-founded complete understanding of DSC. The average user, therefore, does not yet know the limits to this method and the sources of the systematic errors by which it is affected,
- there are, as yet, no practicable and experimentally tested recommendations for temperature and heat calibration and for measurement procedures which are internationally accepted (see Sect. 4),
- there is no international agreement on a single set of substances for the temperature and heat calibration of DSC which have been measured with sufficient accuracy, including a metrologically sound traceability to national/international standards; instead there is a confusing variety of "certified reference materials" whose characteristic data are in part contradictory.

Due to the rapidly increasing use of DSCs in various fields of application, some negligence has gained ground – favoured by the ease of operation and evaluation – which would be inconceivable in "classic" calorimetry. Remedial measures should be taken; for example, the national societies of the International Confederation for Thermal Analysis and Calorimetry (ICTAC) should offer special training courses, and precise specifications for instruments and programs should be drawn up.

The following can frequently be observed:

- a realistic estimate of the uncertainty of measurement is rarely made. The calibration capability (cf. Sect. 4), different influencing quantities (cf. Sect. 5.2) and known theoretical considerations should be taken into account (cf. Chapter 3). In many cases, the *repeatability* of a DSC is, for example, simply, but wrongly, indicated as *accuracy* of the measured data (cf. Sect. 7.3),
- interpretation of the DSC measurement results is often insufficient or faulty, when
  - uncertainties of measurement are not taken into consideration,
  - systematic error sources are disregarded,
  - the measured curve is not "desmeared" (cf. Sect. 5.4),
  - the laws of thermodynamics, kinetics, are not taken into account,
  - uncritical confidence is placed in the evaluation programs provided by the manufacturer,
  - the results are not confirmed by other measuring methods.

A great number of calorimetric methods have not been mentioned here as, in comparison with DSC, they are used only in specific fields. To name a few examples:

- low-temperature calorimetry for measuring heat capacities (see e.g. Gmelin, 1987),
- more recent techniques of heat capacity measurement (see e.g. Lakshmikumar, Gopal, 1981; Maglic et al., 1984),
- measurement of the energy of particle radiation (see e.g. Domen, 1987),
- measurements on biological systems (see e.g. Lamprecht et al., 1991; Wadsö, 1993; Kemp, 1993),
- deformation calorimetry on polymers (see e.g. Kilian, Höhne, 1983; Godovsky, Höhne, 1994),

- high-temperature calorimetry in material science (see e.g. Bruzzone, 1985; Bros, 1989),
- (high-)pressure calorimetry (see e.g. in Mathot, 1994 b),
- "oscillating" ("temperature-modulated") DSC (see Wunderlich et al., 1994; Reading et al., 1994; Mayorga et al., 1994; Schawe, 1995) and AC calorimetry (Sullivan, Seidel, 1968).

2 Types of Differential Scanning Calorimeters

Two types of Differential Scanning Calorimeters (DSCs) must be distinguished:

- the heat flux DSC,
- the power compensation DSC.

They will be dealt with in this chapter. The theoretical bases are presented in Chapter 3.

Both types of DSC use a *differential method of measurement* which is defined as follows:

A method of measurement in which the measurand is compared with a quantity of the same kind, of known value only slightly different from the value of the measurand, and in which the difference between the two values is measured (International Vocabulary of Basic and General Terms in Metrology, 1984).

The characteristic feature of all DSC measuring systems is the twin-type design and the direct in-difference connection of the two measuring systems which are of the same kind. It is the decisive advantage of the differential principle that, in first approximation, disturbances such as temperature variations in the environment of the measuring system and the like, affect the two measuring systems in the same way and are compensated when the difference between the individual signals is formed.

Moreover, the differential signal – which is the measurement signal actually of interest – can be strongly amplified, as the high basic signal (signal of the individual measuring system) is also compensated when the difference is formed.

An extension to form multiple measuring systems (three or four) connected back to back does not mean a fundamental change in the differential principle.

The differential signal is the essential characteristic of each Differential Scanning Calorimeter. Another characteristic – by which distinguishes it from most classic calorimeters – is the dynamic mode of operation. The DSC can be heated or cooled at a preset heating or cooling rate (isothermal mode is possible as well).

A characteristic common to both types of DSC is that the measured signal is proportional to a heat flow rate Φ (and not to a heat as is the case with most of the classic calorimeters). This allows time dependences of a transition to be observed on the basis of the $\Phi(t)$ curve. This fact – directly measured heat flow rates – enables the DSCs to solve problems arising in many fields of application (see Chapter 6).

2.1 The Heat Flux DSC

The heat flux DSC belongs to the class of heat-exchanging calorimeters (for the classification, see Appendix 2). In heat flux DSCs a defined exchange of the heat to be measured with the environment takes place via a thermal resistance. The measurement signal is the temperature difference; it describes the intensity of the exchange and is proportional to the heat flow rate Φ.

In commercial heat flux DSCs, the well-defined heat conduction path is realized in different ways, with the measuring system being sufficiently dominating. The most important fundamental types are:

- the disk-type measuring system with solid sample support (disk).
  Features: It allows high heating rates, its time constants and the sample volume are small, but it has a high sensitivity per unit volume,
- the cylinder-type measuring system with integrated sample cavities.
  Features: Provided with large cavities and sample containers, it allows only low heating rates, its time constants and the sample volume are large, but it has a low sensitivity per unit volume.

2.1.1 Heat Flux DSC with a Disk-Type Measuring System

The characteristic feature of this measuring system is that the main heat flow from the furnace to the samples passes symmetrically through a disk of good thermal conductivity (Fig. 2.1a). The samples (or the sample containers) are positioned on this disk symmetrical to the centre. The temperature sensors are integrated into the disk or fixed on its surface. Each temperature sensor covers more or less the area supporting the respective container (crucible, pan) so that calibration can be carried out independently of the sample position inside the container (cf. Sect. 4.3). To keep the uncertainties of measurement as small as possible, the arrangement of sample and reference sample (or of the containers) and temperature sensor in relation to one another must always be the same (centre pin or the like on the container bottom).

Metals, quartz glass or ceramics are used as disk materials. Type and design of the temperature sensors differ (thermocouples, resistance thermometers).

When the furnace is heated (in general linearly in time, more recently also in a modulated way), heat flows through the disk to the samples. When the arrangement is ideally symmetrical (samples of the same kind), equally high heat flow rates flow into sample and reference sample. The differential temperature signal ΔT (originally a difference between electric potentials) is then zero. If this steady-state equilibrium is disturbed by a sample transition, a differential signal is generated which is proportional to the difference between the heat flow rates to the sample and to the reference sample:

$$\Phi_{FS} - \Phi_{FR} \sim -\Delta T \qquad (\Delta T = T_S - T_R)$$

As neither ideal thermal symmetry of the measuring system at all operating temperatures nor thermal identity of the samples can be attained in practical appli-

cation, not even outside the transition interval, there will always be a signal ΔT which depends on the temperature and the sample properties (cf. definition of zero line in Sect. 5.1). Chapter 3 is based on the assumption that this portion of the total signal is zero or has already been subtracted from the measurement signal proper.

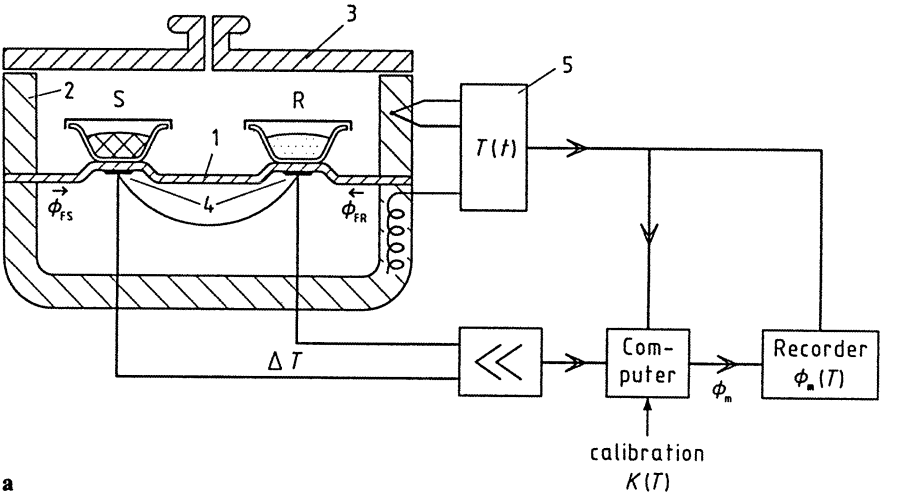

a

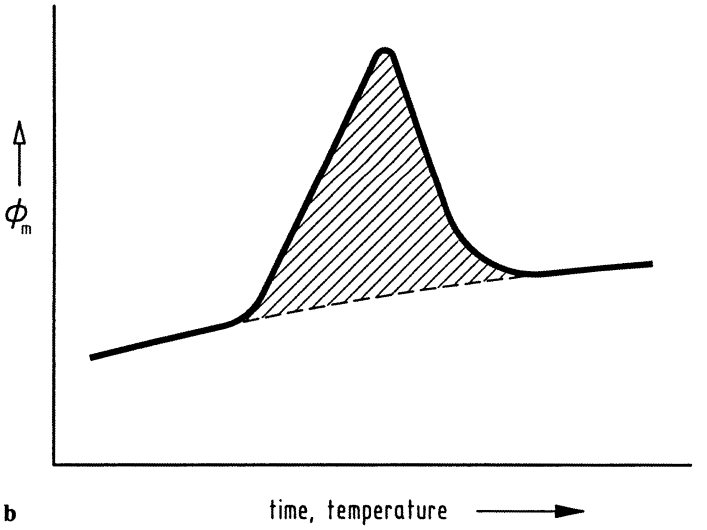

b

Fig. 2.1. **a** Heat flux DSC with disk-type measuring system. 1 disk, 2 furnace, 3 lid, 4 differential thermocouple(s), 5 programmer and controller, S crucible with sample substance, R crucible with reference sample substance, Φ_{FS} heat flow rate from furnace to sample crucible, Φ_{FR} heat flow rate from furnace to reference sample crucible, Φ_m measured heat flow rate, K calibration factor.
b Measured heat flow rate Φ_m (schematic curve) (acc. to Hemminger, 1994)

The measurement signal ΔT is always obtained as electrical voltage. In almost all heat flux DSCs, a heat flow rate Φ_m (m: measured) is internally (in the computer) assigned to this signal ΔT by factory-installed provisional calibration:

$$\Phi_m = -k' \cdot \Delta T$$

The measurement signal output by the DSC (Fig. 2.1 b) and accessible to the user is Φ_m (in µW or mW). The calibration of the DSC must be checked by the user: to what extent does Φ_m represent the true heat flow rate Φ_{true} which is released or consumed by the sample?

This test can be carried out:

- by measuring the steady-state heat flow rate into a sample of known heat capacity C, "charging" of a "heat capacity" in the quasi-steady-state of scanning with constant heating rate $\beta = dT/dt$:

$$C \cdot \beta = \Phi_{true} = K_\Phi \cdot \Phi_m \tag{2.1}$$

- by comparing the integral over a transition peak with the expected (known) heat of transition Q_r (energy balance):

$$Q_r = Q_{true} = K_Q \cdot \int (\Phi_m - \Phi_{bl})\, dt \tag{2.2}$$

(for definition of baseline Φ_{bl}, see Sect. 5.1)

(When resistance thermometers are used as temperature sensors, these thermometers can be used also as heaters which is advantageous in calibration procedures, see Wolf et al., 1994).

Questions of calibration capability and calibration are dealt with in Sect. 4.4; problems of "desmearing" arising in connection with it are discussed in Sect. 5.4.

Heat flux DSCs with disk-type measuring systems are available for temperatures between −190 and 1500 °C. The maximum heating rates are about 100 K min^{-1}. Typical time constants (empty systems, no samples) are between 3 and 10 s. The noise of the measurement signal (definition see Sect. 7.2) lies between 1 mW and 50 µW (it also depends on the temperature and the heating rate). The total uncertainty of the heat measurement amounts to about 5 %, and it is to be expected that it could not be reduced to less than 2 % even if more time and effort were spent (cf. Sect. 4.4).

Heat Flux DSC with Triple Measuring System

An extension of the disk-type measuring system described above has been presented by TA Instruments Inc. (formerly Du Pont). It is a "Dual Sample DSC" with three locations on the metallic (constantan) disk to receive sample crucibles.

The three locations are equipped with temperature sensors (cf. Fig. 2.1a for the normal DSC) which can measure the temperature differences between them. This configuration makes it possible to measure the heat capacity in a single run, using one measuring position for the sample, the second for an empty crucible, and the third for the calibration (reference) material with well known heat capacity; (Jin, Wunderlich, 1993; see Sect. 6.2.1.5). The temperature range of this Dual Sample DSC is from 125 to 1000 K with heating rates up to 100 K min^{-1}.

The development of an adiabatic high temperature triple-cell DSC system (up to 1500 K) has been described by Takahashi, Asou, 1993.

Pressure Heat Flux DSCs

Special containers for heat flux DSCs with disk-type measuring system allow higher pressure, in general up to 7 MPa (70 bar), to be applied. This makes it possible to determine, for example, vapour pressures and heats of evaporation by means of DSC (Wiedemann, 1991; Perrenot et al., 1992, see also articles in Mathot, 1994 b).

Heat Flux DSC with Modulated Heating Mode

A modification of the purely linear heating mode of heat flux DSCs with disk-type measuring system is realized if it is superimposed by a sine function (temperature modulated DSC). In addition to the heating rate the amplitude and the frequency of the modulating sine function can be changed. This operation mode is suitable for disk-type DSCs with a time constant (see Sect. 7.2) which is small compared with the modulation frequency. Otherwise a separation of the thermal effects due to the temperature and due to the heating rate (see Sect. 6.2.1.8) would not be possible.

2.1.2 Heat Flux DSC with a Cylinder-Type Measuring System

A block-type cylindrical furnace is provided with two cylindrical cavities, each containing a cylindrical, fixed sample container which is connected with the furnace or directly with the other container by means of several thermocouples (thermopiles), which are the characteristic features of this type of measuring system.

In the original cylinder-type measuring system (acc. to Calvet, 1948, Fig. 2.2), the outer surfaces of each sample container are in contact with a great number of thermocouples connected in series between the container and the furnace cavity. The thermocouple bands or wires are the dominating heat conduction path from the furnace to the samples. Heat conduction path and temperature difference sensors are identical. Both sample containers are thermally decoupled; heat exchange takes place only with parts of the massive furnace. The measurement signal proper is the temperature difference ΔT of both sample containers averaged over the surfaces; it is generated by differential connection of both thermopiles:

$$\Delta T = \Delta T_{FR} - \Delta T_{FF} = \Delta T_{SR}$$

The following is valid for the (steady-state) heat flow rates exchanged between furnace and sample, Φ_{FS}, between furnace and reference sample, Φ_{FR}, and for the measured heat (output) flow rate Φ_m and the true heat flow rate Φ_{true} into the sample:

$$\Phi_{FS} - \Phi_{FR} \sim -\Delta T$$

$$\Phi_m = -k' \cdot \Delta T$$

$$\Phi_{true} = K_\Phi \cdot \Phi_m$$

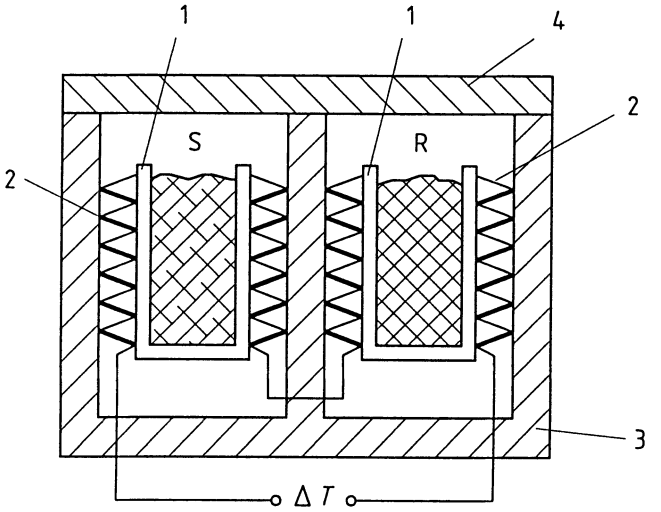

Fig. 2.2. Heat flux DSC with cylinder-type measuring system (Calvet, 1948; thermally decoupled sample containers) (acc. to Hemminger, 1994).
1 containers to take up sample and reference sample, 2 thermopile, 3 furnace (with programmable temperature controller), 4 lid, S sample substance, R reference sample substance, ΔT temperature difference between the containers

A voltage proportional to ΔT, or a heat flow rate signal internally calculated from ΔT (as in the case of the DSCs with disk-type measuring system, cf. Sect. 2.1.1) is put out as a measurement signal. It must be checked in both cases to what extent the measurement signal corresponds to the (steady-state) heat flow rate actually exchanged or to what extent the integral over the measured peak corresponds to the known heat of transition (cf. Sects. 4.4 and 5.4).

In modified cylinder-type measuring systems (for example, acc. to Petit et al., 1961), no heat flows from the furnace to the samples via thermocouples (Fig. 2.3). The heat exchange between furnace and samples takes place via the mechanical connections to the sample containers, via leads and gas layers between furnace and sample containers. Thermocouples are used to measure the temperature difference directly between sample and reference sample containers. Both containers are no longer thermally decoupled, however, the temperature difference measured between them is again proportional to the differential heat flow rate from the furnace to the samples, part of which is now also exchanged between the two containers.

In all cylinder-type measuring systems, the calibration factor may depend on the position and height of the sample in the container, the reason being that the efficiency of heat conduction paths, such as mechanical connections, leads and gas layers, depends on the position of the heat source (sample) in the container. When the sample comes close to the upper edge of the container, the calibration factor can change considerably, depending on the calorimeter type (cf. Sect. 4.4).

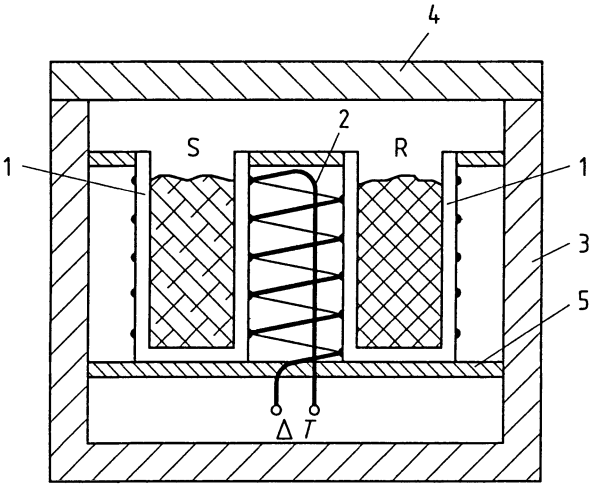

Fig. 2.3. Heat flux DSC with modified cylinder-type measuring system (thermally coupled sample containers) (acc. to Hemminger, 1994).
1 containers to take up sample and reference sample, 2 thermopile(s), 3 furnace (with programmable temperature controller), 4 lid, 5 support of containers, S sample substance, R reference sample substance, ΔT temperature difference between the containers

Compared with disk-type measuring systems, cylinder-type measuring systems have the advantage of a larger useful volume. In return, greater thermal inertia (time constants of up to 40 min) usually have to be accepted. The large cavity volume allows different special containers (for example, for electrical calibration, gas flow, mixture, high pressure etc.) to be used and makes intervention (electrical, mechanical, gas exchange, ...) and direct observations (acoustical, optical) in the sample cavity possible. The great number of thermocouples (up to 1000) generates a high output signal at relatively low noise.

Heat flux DSCs with cylinder-type measuring systems are available for a temperature range between – 190 and 1500 °C. Due to the relatively great time constants of the measuring systems, the maximum heating rates – depending on the cavity volume – lie at about 30 K min^{-1}. The instruments with large volumes (up to 100 cm^3) are used, for example, in biology for the investigation of small animals at constant temperature (cf. Moratzky et al., 1993; Schmolz et al., 1993). Other systems are used for highly sensitive measurements (detection limit about 1 μW). They can usually be heated with maximally 1 K min^{-1}; in most cases operation is isoperibol (isoperibol: surroundings at constant temperature) within a restricted temperature range.

High temperature systems can be used in an isoperibol mode of operation as drop calorimeters (cf. Appendix 2), to measure, for example, enthalpies of mixing (see e.g. Fan et al., 1993).

For heat flux DSCs with cylinder-type measuring systems according to E. Calvet (decoupled sample containers), a rather simple theory has been developed which

quantitatively describes the functional correlation between the instantaneous measurement signal Φ_m and the original event Φ_r in the calorimeter (cf. Sect. 3.1). According to this theory, "desmearing" of the measured curve – to obtain the $\Phi_r(t)$ function – can be performed rather easily "on-line", for example by means of an electronic device.

For disk-type DSCs, the desmearing procedure is not so simple but can be performed as well (see Sect. 5.4).

2.2 The Power Compensation DSC

The power compensation DSC belongs to the class of heat-compensating calorimeters (see Appendix 2). The heat to be measured is (almost totally) compensated with electric energy, by increasing or decreasing an adjustable Joule's heat.

The commercial power compensation DSC* most frequently used is an instrument with isoperibol mode of operation. The measuring system (Fig. 2.4) consists of two microfurnaces of the same type made of a platinum-iridium alloy, each of which contains a temperature sensor (platinum resistance thermometer) and a heat-

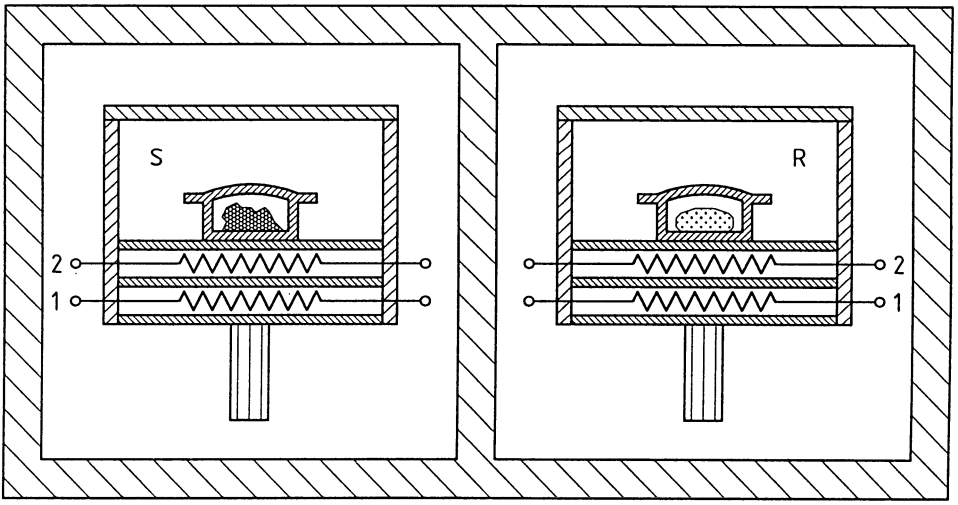

Fig. 2.4. Power compensation DSC (Perkin-Elmer Corp.). Set-up of the measuring system (acc. to Hemminger, 1994).
S sample measuring system with sample crucible, microfurnace and lid, R reference sample system (analogous to S), 1 heating wire, 2 resistance thermometer. Both measuring systems – separated from each other – are positioned in a surrounding (block) at constant temperature

* The description of a power compensation DSC is based on the widely used DSC of the Perkin-Elmer Corp.

ing resistor (made of platinum wire). The microfurnace is about 9 mm in diameter, approx. 6 mm in height and has a mass of approx. 2 g. The time constant is slightly smaller than 2 s, and the isothermal noise is about 2 μW. The maximum heating power of a microfurnace is about 14 W, the maximum heating rate is 500 K min^{-1} (Perkin-Elmer DSC 7).

Both microfurnaces – separated from each other (thermally decoupled) – are positioned in an aluminium block of constant temperature. The measuring range extends from – 175 (block cooled with liquid nitrogen) to 725 °C.

During heating-up, the same heating power is supplied to both microfurnaces via a control circuit (Fig. 2.5) in order to change their mean temperature in accordance with the preset heating rate (see Watson et al., 1964 *). If there is ideal thermal symmetry, the temperature of both microfurnaces is always the same. When an asymmetry occurs, for example as a result of a sample reaction, a temperature difference results between the microfurnace accommodating the sample and the

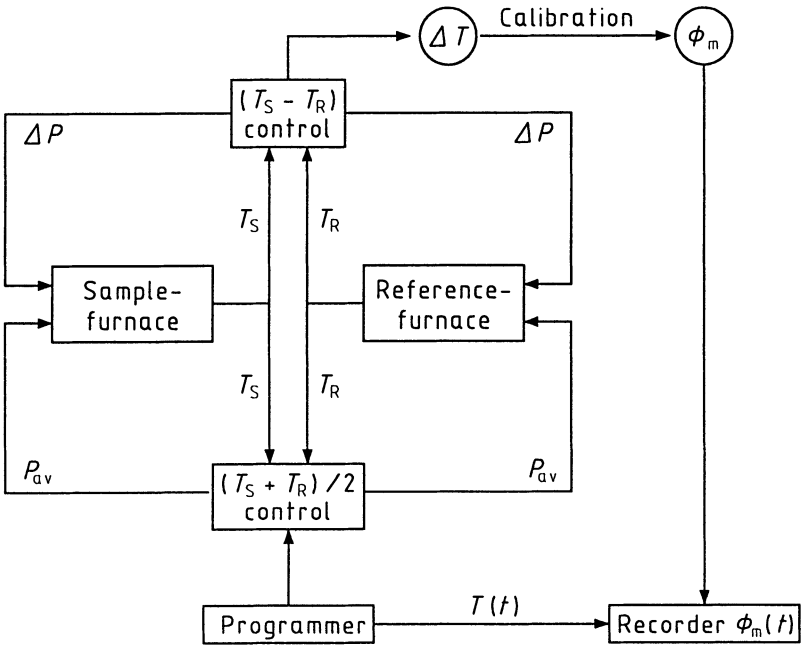

Fig. 2.5. Power compensation DSC (Perkin-Elmer Corp.). Block diagram showing the function principle (acc. to Hemminger, 1994).
T_S temperature of the sample furnace, T_R temperature of the reference sample furnace, $\Delta T = T_S - T_R$, P_{av} average heating power, ΔP compensation heating power, Φ_m measured heat flow rate (measurement signal)

* In the basic paper by Watson et al., the term Differential Scanning Calorimeter (DSC) is coined, but the title of the paper is: A Differential Scanning Calorimeter for Quantitative Differential Thermal Analysis, i.e. the inventors of this DSC recognized clearly the systematic relationship between this type of DSC and classic DTA.

microfurnace containing the reference sample. The temperature difference is both the measurement signal and the input signal of a second control circuit. This second circuit tries to compensate the reaction heat flow rate by proportional control by increasing or decreasing an additional heating power. The compensating heating power provided for this purpose amounts to up to ± 700 mW. The compensating heating power ΔP is proportional to the remaining temperature difference ΔT (because of the proportional controller). The time integral over the compensating heating power is proportional to the heat Q_r which was consumed or released in the sample (Fig. 2.6).

Again, a heat flow rate Φ_m is assigned to the real measurement signal ΔT as a result of a factory-installed calibration, and fed in. The relations between ΔT, Φ_m and the compensating heating power ΔP are as follows:

$$\Delta P = -k_1 \cdot \Delta T \qquad \Phi_m = -k_2 \cdot \Delta T$$

The factor k_1 is a factory-set fixed quantity of the proportional controller, k_2 can be changed at the instrument with the aid of a potentiometer or it is adjusted via the software (calibration). The factor k_2 is almost independent of measurement parameters (e.g. temperature), as – via k_1 – a given compensating heating power always corresponds to a given ΔT; k_2 can therefore – in principle – be determined by one calibration measurement.

As regards the formal aspects (cf. Sect. 2.1, heat flux DSC), the output signal is also given as a heat flow rate signal Φ_m (e.g. in mW), and the relation between Φ_m and the true heat flow rate exchanged with the sample, $\Phi_{true} = K_\Phi \cdot \Phi_m$, must also be determined by caloric calibration (see Sect. 4.4).

Thermal asymmetries of the measuring system, which become apparent as a curvature of the zero line, can be electronically compensated. In this way, it is also possible to "straighten" the measured curve outside the peaks and/or incline it as desired.

At higher temperatures of the measuring system, the heat flows exchanged with the (isoperibol) surroundings (by conduction, radiation, convection) are relatively large compared with the quantity to be measured. High requirements must, therefore, be met as far as the uniformity of the heat exchange between the two microfurnaces and the surroundings is concerned in order to keep the uncertainties of measurement small. Moreover, the shares of the various heat exchange mechanisms and their respective amounts must depend only on the temperature, and strict repeatability must be ensured. Conclusion: The microfurnaces must be covered with lids of the same kind in order to "cover up" inhomogeneities of sample and reference sample; the thermophysical properties of the crucibles and lids must depend only on the temperature.

Compared with heat flux DSCs, the power compensation DSC offers the following advantages:

- the short heat conduction path between samples and heater and the relatively small masses of the microfurnaces allow an almost instantaneous response to a sample reaction. Due to the small time constant, desmearing is required only in a few cases (cf. Sect. 5.4),

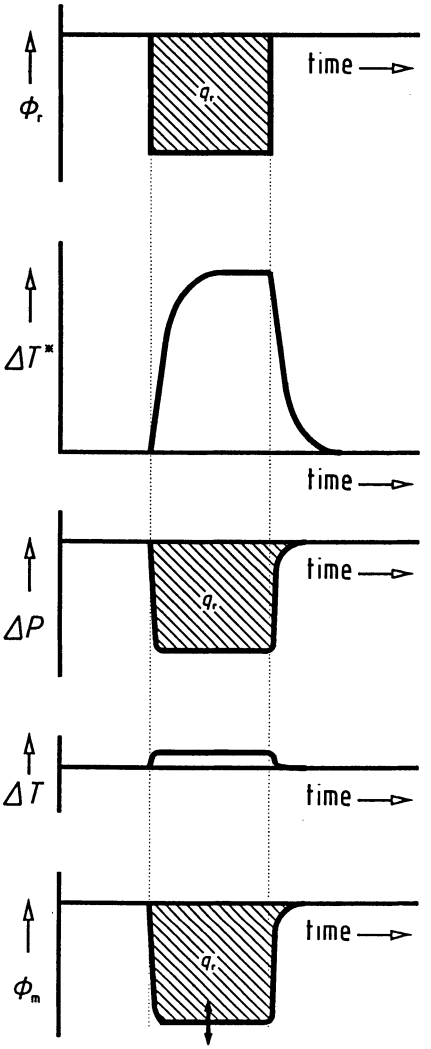

Fig. 2.6. Power compensation DSC. Diagrammatic view of the signals in question (acc. to Hemminger, 1994).
Φ_r heat flow rate released in the sample (exothermic, therefore negative), q_r heat released in the sample, ΔT^* temperature increase in the sample furnace which would build up due to the exothermic effect unless it was compensated (as in heat flux DSC), ΔP compensation heating power (negative, to compensate the exothermic effect), ΔT temperature increase actually occurring in the sample furnace (corresponds to the residual deviation from the theoretical value, which cannot be completely compensated by the proportional control), Φ_m output signal (proportional to the (negative) amplified ΔT signal)

- reaction heat flow rates are rapidly and to a large extent compensated by electrical heating power. As a result, only small temperature differences ΔT occur between the microfurnaces of sample and reference sample (approx. 1/10 of those occurring in heat flux DSCs between sample and reference sample supports). This means that the calibration factor K_Φ is practically independent of the intensity and kinetics of the sample reaction,
- the total compensating energy ($\int \Delta P \, dt$) is equal to the reaction heat or heat of transition,
- the temperature dependence of the control circuit properties (above all of the temperature sensors and the heating elements) is known and strictly repeatable. It can be taken into account with the aid of electronic circuits or by the software. A single caloric calibration is then – in principle – sufficient to determine the correlation between Φ_m (or Φ_r) and ΔP (cf. Sect. 3.2).

The user must, however, keep in mind that the temperature difference between the two microfurnaces is not totally compensated for in commercial power compensation DSCs. During the peak there is still a temperature difference ΔT proportional to the reaction heat flow rate. That is to say, the power compensation DSC can be considered a kind of DTA instrument with a ΔT as the measurement signal, but with a ΔT (arising from a specific thermal event) which is much smaller than that developed in a heat flux DSC measuring system.

In conclusion, it may be said that all the attributes of heat flux DSC systems which depend on this temperature difference can also be found in the "real" power compensation DSC, but to a lesser degree. The calibration factor in particular is not a constant figure but depends in principle on temperature, heat flow rate, heating rate and peak area (cf. Sects. 3.2, 4.4). Though these effects are not very pronounced, they should be carefully tested and a thorough calibration (with the relevant parameters varied) should be performed if the demands on the accuracy of the measurements are high (Höhne, Glöggler, 1989).

The design, specifications and application of a power compensated DSC (based on the Perkin-Elmer DSC-7) used under high pressure (up to 500 MPa) have been described by Blankenhorn, Höhne, 1991.

Photo-DSC

Slight changes in the design of a DSC make it possible to irradiate the sample with light. A DSC modified in this way is referred to as Photo-DSC.

Irradiation of the sample with light having enough energy leads to a reaction in the Photo-DSC. The heat generated during these reactions is recorded. First applications of this type of DSC were described by Wight, Hicks, 1978; Tryson, Shultz, 1979; Flammersheim, 1981. The DPA-7 of Perkin-Elmer has been commercially available as a supplementary device for the DSC-7 since 1987. (Heat flux DSCs are also available with suitable additional devices.) The principle is shown in Fig. 2.7.

Sample and reference substance are contained in the calorimeter at constant temperature. The sample crucibles are either open or covered by quartz disks. The lid of the microfurnace is provided with openings sealed with quartz disks. If light high

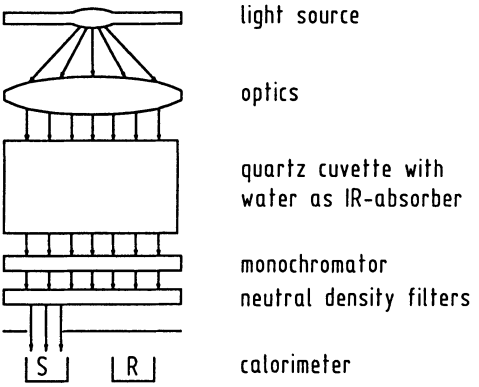

Fig. 2.7. Photo-DSC, schematic representation

in energy is incident on the sample, it is either absorbed directly or – as is usually the case – with the aid of a photo-initiator. A reaction usually takes place only as long as energy is supplied by irradiation. High-pressure mercury vapour lamps with a large number of spectral lines are frequently used as a light source; however, hydrogen, deuterium or xenon lamps are also suitable. The undesired infrared portion of the spectrum can be quantitatively absorbed by quartz cells filled with water. The portion of the spectrum which is of interest is selected using monochromatic filters and the desired intensity is adjusted by means of neutral density filters or metal sieves with different mesh width. It is a particular advantage that the DSC is also suitable for the direct measurement of the incoming radiation flow (light intensity). For this purpose, a graphite disk of known emissivity is substituted for the sample. This disk absorbs the greater portion of the incident light and transfers it to the calorimeter in the form of a heat flow. For most applications, it is of secondary importance whether sample and reference cells are irradiated or the sample cell alone. For precise measurements electronic stabilization of the light intensity of the lamp is important. Otherwise the total noise of the observed curve will be substantially higher than the noise of the DSC measuring system.

Light-activated reactions under conditions closely related to practice are usually very fast. The greatest part of the reaction takes place within a few seconds (cf. Figs. 6.19 and 6.20). There are two consequences:

- there is a considerable change in the measurement signal in periods comparable with that of the DSC time constant. The measured and true heat flow rates differ substantially. Desmearing is necessary prior to every evaluation in which the time variable is involved, for example, when calculating the conversion versus time curve (cf. Sect. 5.4),
- heat flow rates (cf. Fig. 6.19) are so great that the sample temperature deviates considerably from the temperature of the microfurnace, even in power compensated DSCs. If a thermal resistance of 40 K W^{-1} between sample and temperature sensor is assumed, temperature differences of 5 to 10 K would result even

for samples with very good thermal conductivity. For organic samples, these differences are even greater. This means that the measurements are no longer isothermal, not even as an approximation. Kinetic analysis must allow for this.

Adiabatic DSC

For precise biochemical investigations, commercial power compensation DSCs are often used that are operated adiabatically. There are different types with a sample volume of approx. 5 ml and a noise (cf. Sect. 7.2) of approx. 1 μW (Privalov, 1989).

3 Theoretical Fundamentals of Differential Scanning Calorimeters

In all DSCs, a temperature difference ΔT – given as a voltage – is the original measurement signal. In almost all instruments a heat flow rate Φ_m (differential heat flow rate) is internally assigned to ΔT. Independent of whether the user obtains ΔT or Φ_m from the respective DSC, knowledge of the functional relation between the measured signal (ΔT, Φ_m) and the quantity searched (the reaction heat flow rate Φ_r consumed/produced by the sample) is important for:

- the time-related assignment of Φ_r to ΔT or Φ_m (investigation into the kinetics of a reaction),
- the determination of partial heats of reaction,
- the evaluation and assessment of the influences of operating parameters and properties of the measuring system with regard to this relation,
- the estimate of the overall uncertainty of measurement.

The relation between Φ_r and ΔT or Φ_m can be derived in varying degrees of approximation to real DSCs. Analytical solutions are possible only for simple boundary and initial conditions and for quasi-steady-states. Numerical procedures and solutions can approximate the actual conditions more exactly, however, without the clarity of the functional relations given by an analytical solution.

Basic considerations in this field are given by Gray, 1968.

To ensure better differentiation from Φ_r, in the following section, ΔT – instead of Φ_m – is assumed to be the measurement signal, i.e. we search the relation $\Phi_r(\Delta T)$. The two quantities ΔT and Φ_m, are strictly proportional, with the exception of the opposite sign.

3.1 The Heat Flux DSC

Three steps of an analytical description of the functional principle of a heat flux DSC will be presented in the following. The results of a numerical calculation will be discussed afterwards.

The Zeroth Approximation

First, the heat flux DSC is represented by a simple linear model (Fig. 3.1).

The following simplifications have been made in the model of the zeroth approximation:

- steady-state (constant) heat flow rates,

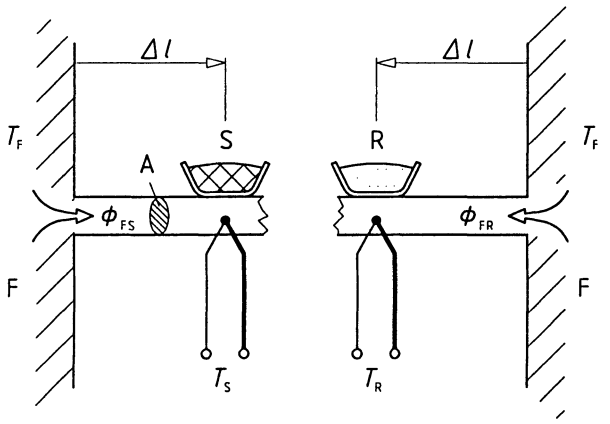

Fig. 3.1. Heat flux DSC (disk-type), model for zeroth approximation (linear model). S sample, R reference sample, F furnace, A cross section of the heat conductor between furnace and S and R, Δl distance between temperature measurement point and furnace

- only the thermal resistance between furnace and sample is taken into account, i. e. no interaction between sample and reference sample,
- with the exception of C_S, C_R (heat capacities of the sample, reference sample), no heat capacities are taken into account,
- sample temperature equal to measured temperature,
- no heat exchange with the surroundings (heat leak).

Figure 3.2 shows the equivalent electric circuit diagram for the zeroth approximation. This diagram serves to understand the interrelations better. From the physical point of view, electric charge transport and heat transport are equivalent processes, and many people find it easier to read electric circuit diagrams than to visualize heat flows in real equipment.

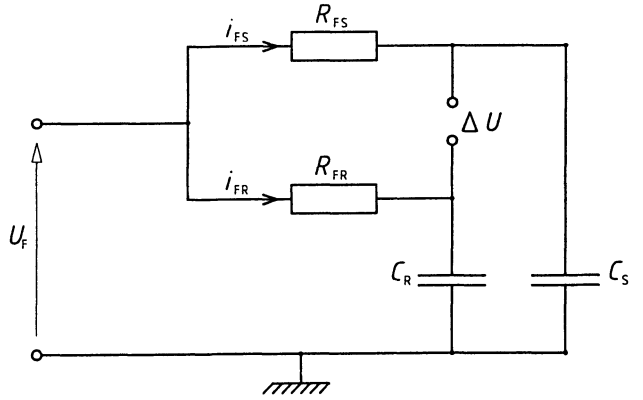

Fig. 3.2. Equivalent electric circuit for the linear model of the heat flux DSC (see Fig. 3.1). C capacitance, R resistance, i current, U voltage. Subscripts: S sample, R reference, F furnace

In absolute values, the Biot-Fourier equation of the (steady-state) conduction of heat reads as follows:

$$\frac{\Phi}{A} = -\lambda \cdot \text{grad}\, T \quad \text{or} \quad \frac{|\Phi|}{A} = \lambda\, |\text{grad}\, T|$$

The amount of the heat flux Φ/A is proportional to the gradient of the temperature; the thermal conductivity λ is the proportionality factor.

In the one-dimensional model referred to above, this equation is reduced as follows for the left-hand and right-hand subsystem shown in Fig. 3.1 (with $T_F > T_S$, T_R in scanning mode):

$$\frac{\Phi_{FS}}{A} = \frac{\lambda\,(T_F - T_S)}{\Delta l} \quad \text{and} \quad \frac{\Phi_{FR}}{A} = \frac{\lambda\,(T_F - T_R)}{\Delta l}$$

In the case of thermal symmetry,

$$\Phi_{FS} = \Phi_{FR}$$

is valid, with $T_S = T_R$.

If a constant (exothermic) heat flow rate ($\Phi_r < 0$)is produced in the sample, T_S increases by ΔT_S, the temperature difference $T_F - T_S$ and thus the heat flow rate Φ_{FS} decreases. When the steady-state (i.e. uniform heating rate) is reached again, for reasons of balance, $\Delta\Phi_{FS}$, the change of Φ_{FS}, must be equal to Φ_r:

$$\Delta\Phi_{FS} = \Phi_r = -\frac{A \cdot \lambda}{\Delta l}\,\Delta T_S$$

Nothing has changed on the side of the reference sample, hence:

$$\Delta T_S = \Delta T_{SR} = T_S - T_R \quad \text{and} \quad \Phi_r = \Delta\Phi_{SR} = \Phi_{FS} - \Phi_{FR}$$

Consequently

$$\Phi_r = -\frac{A \cdot \lambda}{\Delta l}\,(T_S - T_R) = -\frac{A \cdot \lambda}{\Delta l}\,\Delta T_{SR} = -K \cdot \Delta T$$

(measurement signal: $\Delta T = \Delta T_{SR}$)

(Here, $T_S > T_R$, and Φ_r is negative: exothermic effect.)

In this simple steady-state model, K is given completely by the properties of the heat conduction path between the furnace and the samples. This means that in the steady-state, there is direct proportionality between the measurand Φ_r and the measurement signal ΔT. The conditions of constant heat consumption can be achieved when in scanning operation sample and reference sample have different, temperature-independent "heat capacities". A greater amount of heat will always flow into the sample whose heat capacity is higher, in order that the steady-state heating rate is maintained. With $C_S > C_R$ the following is then valid for the difference between the heat flow rates to sample and reference sample:

$$\Delta\Phi_{SR} = -K' \cdot \Delta T_{SR} \quad \text{and} \quad T_S < T_R$$

There is no steady state during sample transitions or reactions; the above approximation does not apply in these cases. Furthermore, C_S and C_R (and thus $\Delta\Phi_{SR}$) change with temperature, but these changes are in many cases rather slow and do not affect the steady-state condition very much.

When there is such a quasi-steady state, the following is valid in approximation:

$$\Delta\Phi_{SR} = \beta(C_S - C_R) \quad \text{and thus} \quad \beta(C_S - C_R) = -K' \cdot \Delta T \tag{3.1}$$

This relation describes the shape of the baseline and is the basic equation to determine the heat capacity C_S. For the empty reference crucible ($C_R = 0$)

$$C_S = -K' \cdot \frac{\Delta T}{\beta}$$

is valid.

When the heat capacity C_R is different from zero (i.e. if $C_R = C_{Ref}$ using a reference material),

$$C_S = C_R - K' \cdot \frac{\Delta T}{\beta}$$

In practice, first a zero line ΔT_0 will be recorded with the crucibles empty (to check the asymmetry of the apparatus) which is subtracted from the measured curves.

For the measurement of heat capacities, see Sect. 6.2.1.

The First Approximation

In the first approximation, non-steady-state processes in the sample are also permitted which manifest themselves as "peaks" of the measured curve. This means that ΔT is not constant in time. For the rest, the simplified arrangement as for the zeroth approximation is used here.

Φ_{FS} is the heat flow rate from the furnace to the sample, $\Phi_r(t)$ the heat flow rate produced inside the sample (reaction, transition). The following balance equation for the heat flow rates is then valid for the sample of heat capacity C_S:

$$C_S \frac{dT_S}{dt} = \Phi_{FS} + \Phi_r \text{ (exothermic: } \Phi_r \text{ negative, endothermic: } \Phi_r \text{ positive)}$$

With $\Delta T = T_S - T_R$,

$$C_S \frac{dT_R}{dt} + C_S \frac{d\Delta T}{dt} = \Phi_{FS} + \Phi_r$$

results.

Accordingly, the following holds for the reference sample ($\Phi_r = 0$ by definition):

$$C_R \frac{dT_R}{dt} = \Phi_{FR}$$

When the difference between the two balance equations is formed, the following is obtained:

$$\Phi_{FS} - \Phi_{FR} = (C_R - C_R)\frac{dT_R}{dt} + C_S \frac{d\Delta T}{dt} + |\Phi_r|$$

The following is valid for the heat flow rates Φ_{FS} and Φ_{FR}:

$$\Phi_{FS} = \frac{(T_F - T_S)}{R_{FS}} \quad \text{and} \quad \Phi_{FR} = \frac{(T_F - T_R)}{R_{FR}}$$

where R_{FS} and R_{FR} are global heat resistances between the furnace and the samples. In the case of thermal symmetry, $R_{FS} = R_{FR} = R$, thus:

$$\Phi_r = -\left(\frac{\Delta T}{R}\right) - (C_S - C_R)\frac{dT_R}{dt} - C_S\frac{d\Delta T}{dt} \tag{3.2}$$

This equation links the reaction heat flow rate Φ_r searched with the measured signal ΔT. The second term takes the asymmetry of the measuring system into account as regards heat capacities of sample and reference sample. The third term considers the contribution of the thermal inertia of the system when a measured signal $\Delta T(t)$ appears. In analogy to the charging or discharging of a capacitor of capacity C, a time constant τ can similarly be defined for the heat flow rates:

$$\tau = C_S \cdot R$$

When ΔT is changed, R is the effective thermal resistance to the "charging or discharging" of the "capacity" C_S. With this resistance and with $dT_R/dt = \beta$, the heating rate; as the reference sample is always in a steady-state heating mode, the following results from Eq. (3.2):

$$\Phi_r(t) = -\left(\frac{\Delta T}{R}\right) - \beta(C_S - C_R) - \left(\frac{\tau}{R}\right)\frac{d\Delta T}{dt} \tag{3.3}$$

The measured signal ΔT is <u>not</u> proportional to the heat flow rate Φ_r at a given moment but delayed with time and thus also distorted ("smeared"). Furthermore, when $C_S \neq C_R$ is valid, the measurement signal is not equal to zero – even if Φ_r is equal to zero and steady-state conditions prevail – but has the value $-R \cdot \beta(C_S - C_R)$ which is the initial deviation after the quasi-steady state has been reached in scanning operation (cf. Eq. (3.1)). This contribution is the measured curve before/behind a peak which is parallel to the abscissa if R, $\Delta C = C_S - C_R$ and β are constant (Fig. 3.3).

In reality, the term $R(C_S - C_R)$ reflects the temperature dependence of the thermal resistance R (in general: of the heat transfer conditions) and of the heat capacities C_S and C_R causing a temperature dependence of the measured curve even without any thermal effect due to the sample. (Equation (3.3) is in principle the so-called Tian equation).

Regarding Eq. (3.3), the conclusions are as follows:

1. When the signal ΔT measured at a given moment is to be assigned to the heat flow rate Φ_r by which it is caused, the 3rd term in Eq. (3.3) must be taken into account (cf. Desmearing, Sect. 5.4).
   R must be determined by calibration (cf. Sect. 4.4); the time constant τ can also be obtained from calibration measurements (cf. below "Higher-order approximations" and Sect. 7.2).

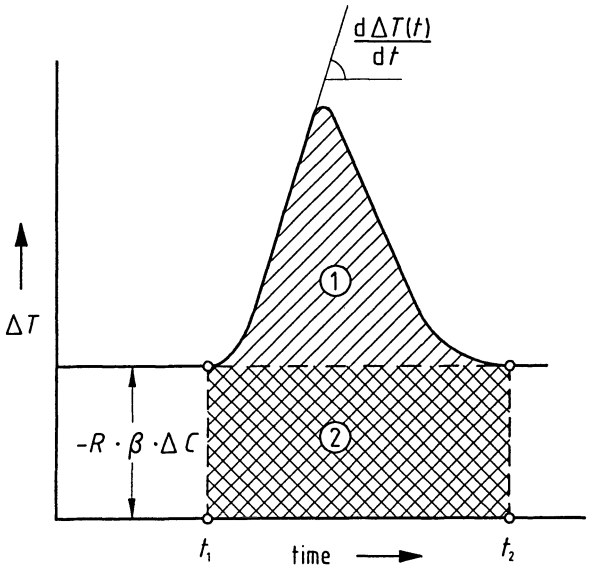

Fig. 3.3. Measured curve of a heat flux DSC (schematic) with heat released inside the sample (exothermic effect).
ΔT measured signal, R thermal resistance between furnace and sample, β heating rate, $\Delta C = C_S - C_R$ difference between the heat capacities of sample and reference sample (here negative, because $C_R > C_S$, ① peak area (exothermic effect); it is a measure of the heat released between t_1 and t_2, ② area below the baseline; it is a measure of the heat required to heat the sample between t_1 and t_2

For $t > t_0$, the solution of the differential Eq. (3.3) for a heat pulse Φ_r at the moment t_0 has the form

$$\Delta T = k_1 \cdot \exp\left(\frac{-t}{\tau}\right) + k_2$$

with $\tau = C_S \cdot R$. Up to the moment $t = t_0$, the solution is the steady-state curve

$$\Delta T = -\beta (C_S - C_R) R$$

For $t \to \infty$, the function $\Delta T(t)$ returns to this curve (cf. Fig. 3.4).

2. For the whole heat of reaction or transition Q_r developed/consumed in the sample, the following balance equation is valid:

$$Q_r = \int_{t_1}^{t_2} \Phi_r(t)\, dt$$

where t_1, t_2 are the beginning and end, respectively, of the peak.

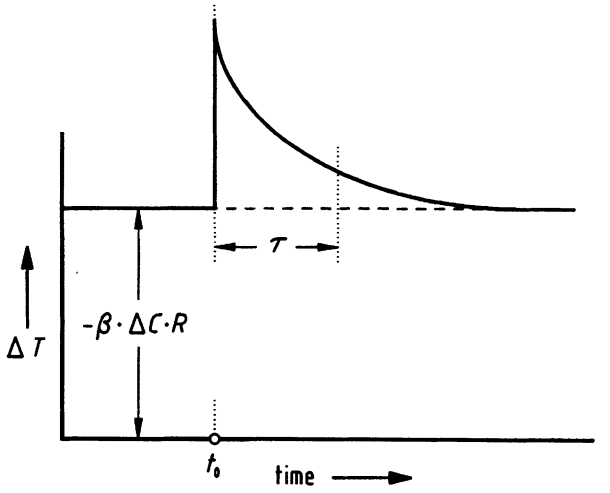

Fig. 3.4. Measurement signal of a heat flux DSC for an exothermic heat pulse at the time t_0 (model of the 1st approximation).
τ time constant; symbols see Fig. 3.3

With Eq. (3.3) inserted, the following is obtained (see Fig. 3.3):

$$Q_r = -\frac{1}{R}\left[\int_{t_1}^{t_2}\Delta T(t)\,dt - \int_{t_1}^{t_2}(-R)\cdot\Delta C\cdot\beta\,dt\right] - \int_{t_1}^{t_2}\frac{\tau}{R}\cdot\frac{d\Delta T}{dt}\,dt \qquad (3.4)$$

The content of the square brackets corresponds to area 1, i.e. the so-called peak area between the measured curve and the (interpolated) baseline (definition see Sect. 5.1).

- When ΔC and R are not temperature- (or time-)dependent, the measured curve outside the peak is a parallel to the abscissa. In this case, $d\Delta T/dt$ is zero before and behind the peak. The contribution of the 3rd term vanishes when integration is carried out over the whole peak,
- in the real case, the 2nd term of Eq. (3.4) is not constant, i.e. the curve before and behind the peak is not parallel to the abscissa. In this case, the 3rd term will not vanish but represents a correction of the values obtained by peak integration.

3. For the partial integration (Fig. 3.5) of the peak between t_1 and t^*, the contribution of the 3rd term must be taken into acount at the point t^*:

$$Q_r(t^*) = \underbrace{-\frac{1}{R}\left[\int_{t_1}^{t^*}\Delta T(t)\,dt - \int_{t_1}^{t^*}(-R)\cdot\Delta C\cdot\beta\,dt\right]}_{\text{partial peak area}} \underbrace{-\int_{t_1}^{t^*}\frac{\tau}{R}\cdot\frac{d\Delta T}{dt}\,dt}_{\text{correction term}}$$

Partial integrations of the peak are necessary for kinetic investigations and to determine the purity (see Sects. 6.2.2 and 6.2.4).

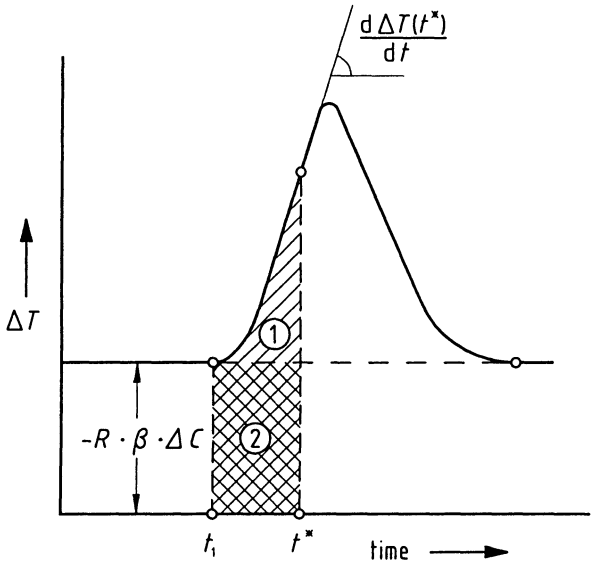

Fig. 3.5. Partial integration of a peak (heat flux DSC, exothermic effect).
$C_R > C_S$, ① partial peak area (between t_1 and t^*), ② area below baseline (between t_1 and t^*);
Symbols see Fig. 3.3

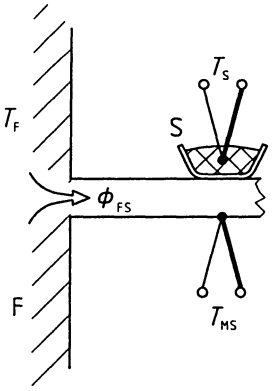

Fig. 3.6. Heat flux DSC (one half), model of the 2nd approximation.
S sample, F furnace, T_{MS} temperature at sample measurement point

Higher-order Approximations

The temperatures of sample and reference sample (assumed here to be homogeneous) are not measured directly. There is a thermal resistance between the temperature measurement points and the respective sample (Fig. 3.6). Depending on the design of the measuring system, the resistance is made up of several parts differing in amount and originating in the transition layers between sample, bottom of the

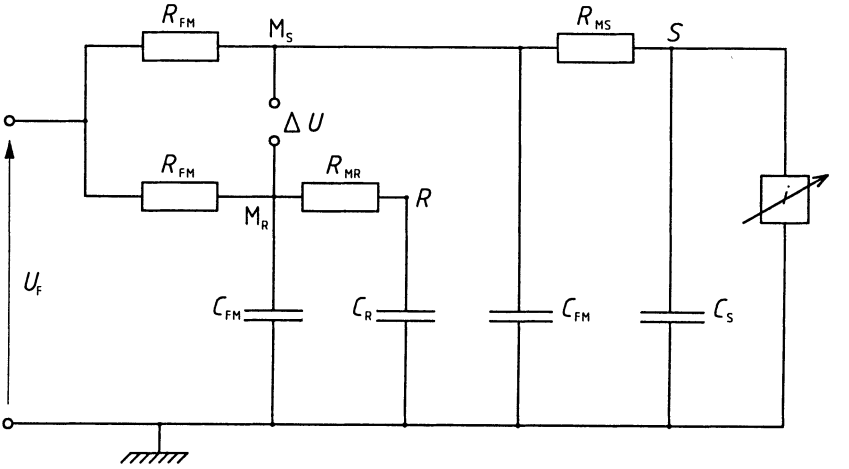

Fig. 3.7. Equivalent electric circuit for the 2nd approximation.
S sample side, R reference side, F furnace, M_S measurement point on sample side, M_R measurement point on reference side. ΔU corresponds to ΔT, U_F corresponds to T_F, i corresponds to Φ_r. R_{FM} thermal resistance between furnace and measurement points M_S, M_R, R_{MS} thermal resistance between sample measurement point and sample, R_{MR} thermal resistance between reference sample measurement point and reference sample, C_S heat capacity of the sample, C_R heat capacity of the reference sample, C_{FM} effective "heat capacity" between furnace and measurement points M_S, M_R. For correspondences between electrical and thermal quantities cf. page 22

crucible and support; there are further resistances between support and temperature sensor. When the sample temperature changes, the temperature measurement point reacts after some delay. The analogue electric circuit diagram of the DSC for this "2nd approximation" is shown in Fig. 3.7. The following is valid for this so-called "thermometer problem":

$$T_{MS} = T_S - \tau_2 \cdot \frac{dT_{MS}}{dt}$$

T_{MS} temperature of the measurement point (e.g. junction of the thermocouple) for the sample
T_S (homogeneous) sample temperature
τ_2 characteristic time constant for temperature balance between sample and temperature measurement point.

In analogy, the following is valid for the reference side:

$$T_{MR} = T_R - \tau_2 \cdot \frac{dT_{MR}}{dt}$$

(τ_2 is to be equal for both sides).

With these equations, the following results for the difference:

$$\Delta T_{SR} = T_S - T_R = T_{MS} - T_{MR} + \tau_2 \left(\frac{dT_{MS}}{dt} - \frac{dT_{MR}}{dt} \right)$$

$$= \Delta T_M + \tau_2 \frac{d\Delta T_M}{dt}$$

($\Delta T_M = T_{MS} - T_{MR}$: measured temperature difference)

The following relation results in analogy to the mathematical procedure of the 1st approximation if we use the above ΔT_{SR} instead of ΔT:

$$\Phi_r(t) = -\frac{1}{R}\left[\Delta T_M + R\,(C_S - C_R)\,\beta + \tau_1 \frac{d\Delta T_M}{dt} + \tau_1 \cdot \tau_2 \left(\frac{d^2 \Delta T_M}{dt^2} \right)\right] \qquad (3.5)$$

In addition to the 1st derivative (slope) of the measured curve $\Delta T_M(t)$, the 2nd derivative (curvature) must be used in the 2nd approximation to reconstruct the heat flow rate converted in the sample; two time constants occur which must be determined. The first time constant τ_1 is determined by the thermal resistance and heat capacity between furnace and temperature sensor. The second time constant is determined by the thermal resistance and the "effective heat capacity" between sample and sample temperature measurement point.

The above-described approximation can be refined as desired: In order that the temperature gradient inside the sample and its influence on the peak shape can be determined, the sample can be considered as having been split up into different layers which are linked with one another by heat-conducting boundary layers. An additional differential quotient in the differential equation and another time constant results for each additional thermal resistance in connection with a heat capacity. The solution of the refined approximation is as follows:

$$\Phi_r(t) = -\frac{1}{R}\left[\Delta T + k_0 + k_1 \frac{d\Delta T}{dt} + k_2 \frac{d^2 \Delta T}{dt^2} + k_3 \frac{d^3 \Delta T}{dt^3} + \ldots\right]$$

In reality, the constants k_i are terms into which the thermal resistances and capacities (and thus the time constants) of the arrangement enter. Calculation of the reaction heat flow rate Φ_r presupposes that all k_i and the measurement signal ΔT and its time derivatives are known. It can be shown (Löblich, 1985) that for practical application, the 2nd order differential equation is a sufficiently good approximation to calculate the true desmeared reaction heat flow rate; the time constants τ_1 and τ_2 must be known for this purpose. For a detailed treatment how to determine the time constants experimentally, see Löblich, 1994.

So far we have only considered the simplified case where it is assumed that no heat exchange takes place between sample and reference sample. This simplification is certainly not permissible for disk-type measuring systems. Figure 3.8 is a more realistic representation of the measuring system of such a calorimeter. When the differential equation is to be set up for this system, it may be convenient to

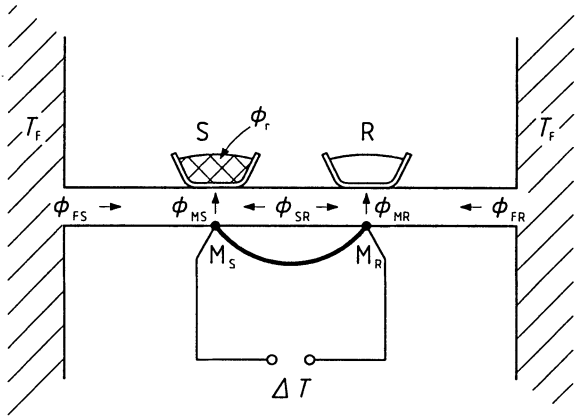

Fig. 3.8. Disk-type measuring system of a heat flux DSC (to calculate the $\Phi_r(\Delta T)$ dependence)
M_S temperature measurement point on sample side, M_R temperature measurement point on reference side, Φ_r heat flow rate produced/consumed by the sample

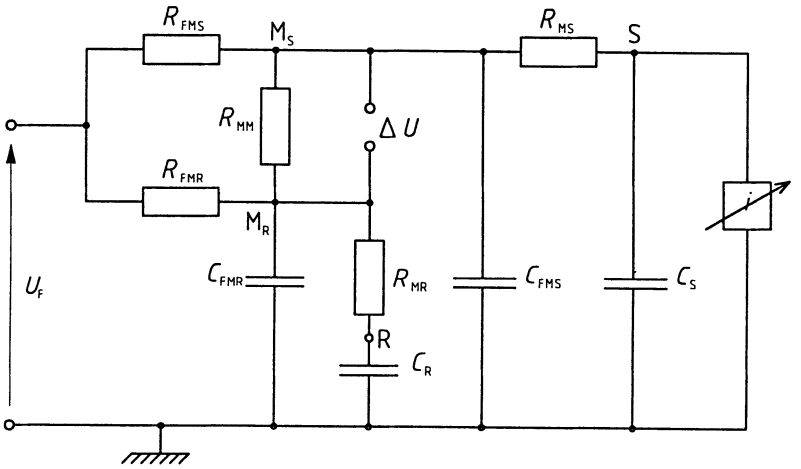

Fig. 3.9. Equivalent electric circuit for the disk-type measuring system according to Fig. 3.8. S sample, R reference sample, M temperature measurement point, F furnace, U voltage, i current, R resistance, C capacitance (cf. legend to Fig. 3.7)

use the analogue electric circuit represented in Fig. 3.9 for the 2nd approximation (Höhne, 1983). In order to formulate the desired differential equation, according to Kirchhoff's laws, the voltage balance and current balance are made up for each loop and each node of the analogue electric circuit. For the circuit of Fig. 3.9, five equations for both voltages and currents are then obtained. On the basis of the laws of the science of electricity, these 10 equations are combined to form a differential

equation and retranslated into the language of heat transport. The result for a symmetric twin design ($R_{FMS} = R_{FMR} = R$, $C_{FMS} = C_{FMR} = C$) is as follows:

$$\Phi_r = -\left(\frac{1}{R} + \frac{2}{R_{MM}}\right)\Delta T - \left[C - C_S\left(1 + R_{MS}\left(\frac{1}{R} + \frac{2}{R_{MM}}\right)\right)\right]\frac{d\Delta T}{dt}$$

$$-R_{MS} \cdot C \cdot C_S \frac{d^2\Delta T}{dt^2} (C_R - C_S)\frac{dT_R}{dt} + C_S \cdot C_R (R_{MS} - R_{MR})\frac{d^2T_R}{dt^2} \quad (3.6)$$

This equation is similar to that of the 2nd approximation (Eq. (3.5)). However, as there is the thermal resistance R_{MM} between sample system and reference sample system, a thermal effect in the sample will also affect the reference side and thus T_R. Only in the steady-state case and at sufficiently large distance from peaks is dT_R/dt equal to the heating rate β, and the second derivative of the reference sample temperature is equal to zero only there. For the steady-state case (st), with

$$\Phi_r = 0 \qquad \frac{d\Delta T}{dt} = 0 \qquad \frac{d^2\Delta T}{dt^2} = 0$$

the following is then valid and characterizes the baseline:

$$\Delta T_{st} = \frac{C_R - C_S}{\frac{1}{R} + \frac{2}{R_{MM}}}\beta$$

When Eq. (3.6) is integrated over the area of a transition peak, with the approximation $dT_R/dt \approx \beta$, the following is valid:

$$\int_{t_1}^{t_2} \Phi_r \, dt = Q_r = \left(\frac{1}{R} + \frac{2}{R_{MM}}\right)\left[\int_{t_1}^{t_2} \Delta T dt - \int_{t_1}^{t_2} \beta \frac{C_R - C_S}{\left(\frac{1}{R} + \frac{2}{R_{MM}}\right)} dt\right]$$

$$= -\left(\frac{1}{R} + \frac{2}{R_{MM}}\right)\int_{t_1}^{t_2} (\Delta T - \Delta T_{st})\, dt$$

This integral describes the peak area between measured curve and (interpolated) baseline. The approximation is the better the smaller the last two summands in Eq. (3.6). From this follows the rule that, when heats of transition are determined with heat flux DSCs, the sample and the reference sample should be as similar as possible ($C_R \approx C_S$, $R_{MR} \approx R_{MS}$).

The factor $(1/R + 2/R_{MM})$ is decisive for the sensitivity of the calorimeter; the greater the thermal resistance of the disk, the higher the peak for a given heat of transition. However, as a result, the time constant increases as well, i.e. the system becomes more inert. In addition, this factor allows the conclusion to be drawn that the ratio of R to R_{MM} plays an important role for the sensitivity. Depending on where sample and reference sample are arranged on the disk, R_{MM} (thermal resistance

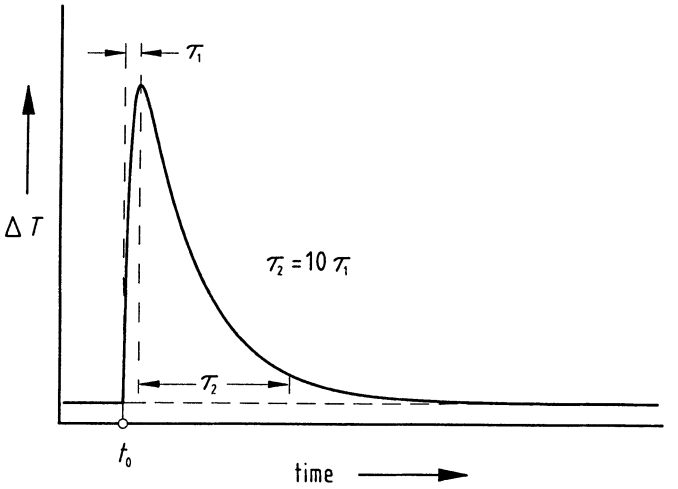

Fig. 3.10. Measured signal ΔT of heat flux DSC for a heat pulse generated in the sample at the time t_0 (sum of two exponential functions with the time constants τ_1 and τ_2)

between sample and reference sample) change, meaning that high reproducibility for the location of sample and reference sample is of great importance for the capability of a DSC to be calibrated.

In the approximation $C_S \approx C_R$ and $R_{MS} \approx R_{MR}$, Eq. (3.6) changes into the 2nd order differential equation stated below:

$$\Phi_r(t) = -K \cdot \Delta T - K_1 \frac{d\Delta T}{dt} - K_2 \frac{d^2\Delta T}{dt^2}$$

The solution of this equation, i.e. the curve $\Delta T(t)$ recorded by the calorimeter, for a heat pulse Φ_r at $t = 0$ is the superposition of two exponential functions:

$$\Delta T(t) = a_1 \cdot e^{-t/\tau_1} + a_2 \cdot e^{-t/\tau_2} \tag{3.7}$$

where there is a complex dependence of the time constants τ_1, τ_2 on the coefficients K, K_1, K_2. Here, τ_1 is determined in approximation by $C_S \cdot R_{MS}$, and τ_2 by $C \cdot R$ (cf. Eq. 3.6). Such a peak, produced by a heat pulse, is shown in Fig. 3.10. The time constant τ_1 essentially determines the ascending, τ_2 the descending part of the curve.

Numerical Simulation

As the equations become increasingly complex and as it is impossible to solve them analytically without introducing simplifications, it is no longer recommended to set up differential equations for calculations, which also cover heat exchange by convection and radiation and include non-linearities due to temperature-dependent thermal resistances and heat capacities. In this case, numerical simulation by the finite-element method (FEM) should be applied. Appropriate computer programs

are commercially available also for personal computers. When the required time and effort are spent, the temperature and heat flow fields and the measured $\Delta T(t)$ curves can be simulated for any complex arrangement and any thermal process inside the sample.

The finite-element method consists in splitting the whole arrangement up into sufficiently small "cells" for which the heat flow rates and the material properties are defined. On the basis of considerations with regard to the energy balance, a system of equations is obtained which is solved by conventional methods. FEM has been applied to a very simple model of a disk-type measuring system and to a commercial disk-type DSC (see Höhne, 1983).

The results are represented in Figs. 3.11 to 3.13. As can be seen, the shape of the peak depends strongly on the test parameters. The position of the peak maximum, for example, changes with the heating rate, the thermal conductance of the sample and with the mass (or heat of transition Q_r) of the sample. The slope of the ascending part is determined by the heating rate and the thermal conductance of the sample. Only the extrapolated peak onset temperature is relatively independent of test parameters. This is why, in addition to the area, this temperature (T_e) is preferred to characterize the temperature of a peak. In contrast to this, the peak temperature maximum (T_p) and the peak width are no values suited to characterize transitions (for definition of the characteristic temperatures, see Sect. 5.1).

Figure 3.14 shows another result of the numerical simulation of the thermal events in a commercial disk-type DSC, namely the DSC signal which is caused by the melting of a small sample of indium.

It has also been possible to show that the calibration factors $K_Q = |Q_r/peak\ area|$ and $K_\Phi = |\Phi_r/\Delta T|$ clearly depend on test parameters (Q_r, λ_{sample}, β) when radiation

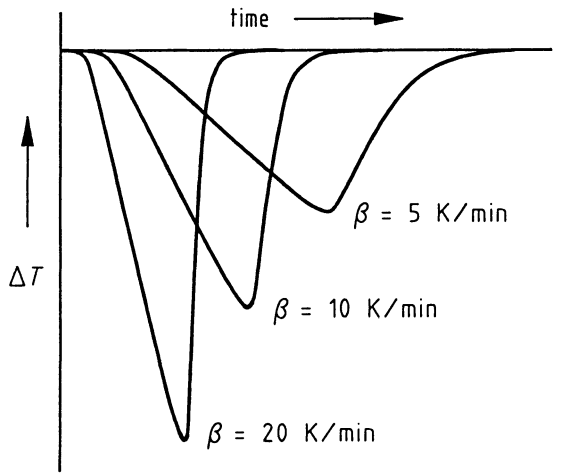

Fig. 3.11. Dependence of the peak shape on the heating rate β, calculated by numerical simulation for a heat flux DSC

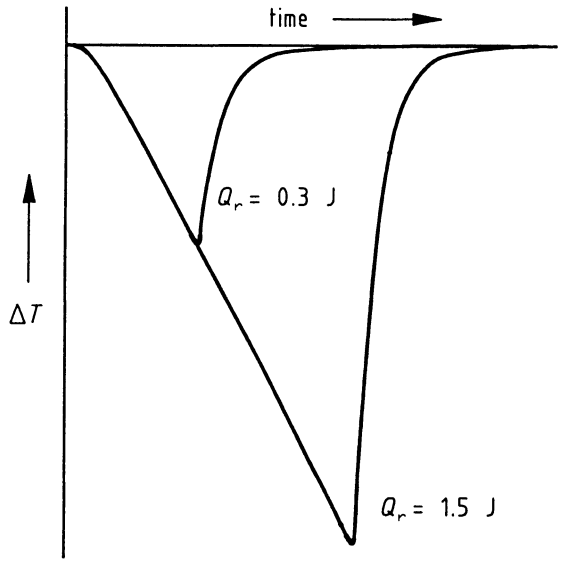

Fig. 3.12. Dependence of the peak shape on the heat of transition Q_r, calculated by numerical simulation for a heat flux DSC (heating rate: 2 K min^{-1})

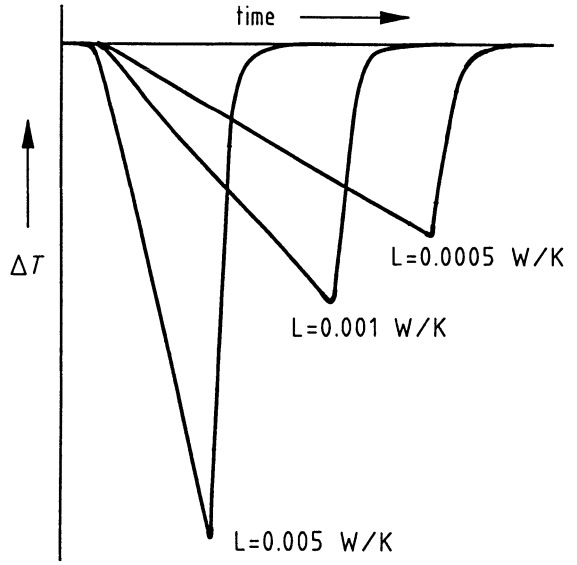

Fig. 3.13. Dependence of the peak shape on the thermal conductance L of the sample, calculated by numerical simulation for a heat flux DSC

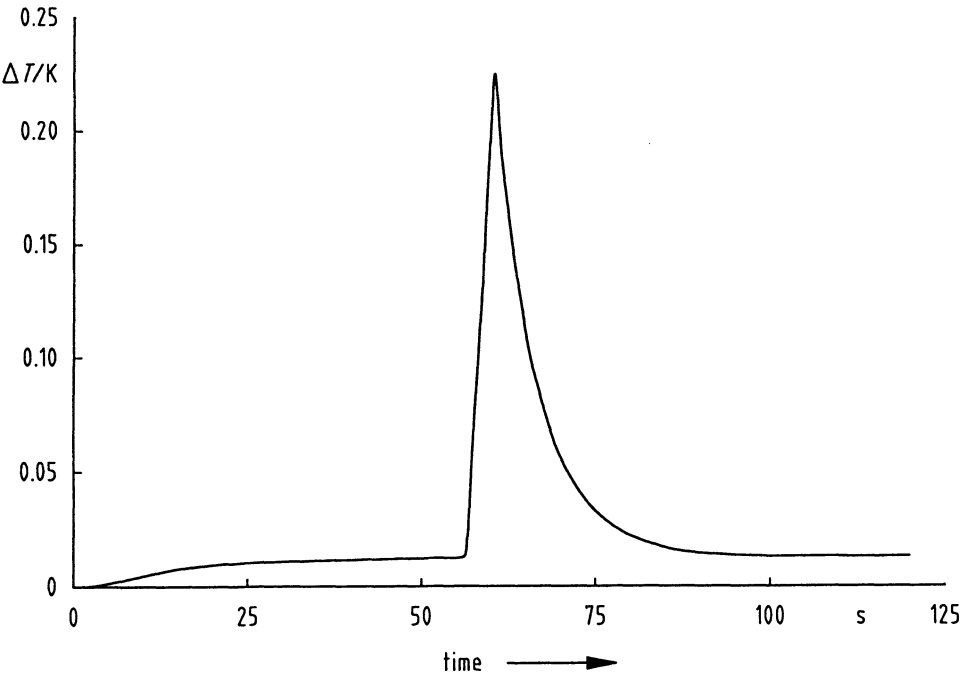

Fig. 3.14. Numerical simulation of the signal (absolute values) generated by the melting of an indium sample in a disk-type DSC (1.38 mg In, 10 K min^{-1})

and convection are included (Höhne, 1983), for an example see Table 3.1. This is a fact which is of importance in practical scanning calorimetry and which *must* be taken into consideration during calibration (cf. Sect. 4.4). The clear temperature dependence of the calibration factor is another conspicuous feature although the temperature dependence of the heat capacities and of the heat resistance of the substances has not been included in these model calculations. The reason is to be found in the intensive radiative heat exchange with the surroundings (heat leak), which is strongly temperature-dependent.

The calibration factor is also strongly influenced by the surface quality (emissivity) of the containers of sample and reference sample.

As far as steady-state reaction heat flow rates are concerned, the above calculations have shown that the calibration factor $K_\Phi = -\Phi_r/\Delta T_{st}$ also depends on the amount of Φ_r (or the difference between the heat capacities, $C_S - C_R$) when radiative exchange is included. In addition, the calibration factors for a peak integration (determination of Q_r) and for steady-state heat flow rates (determination of C_S) are generally not equal.

The difference in the calibration factors K_Φ and K_Q can also be concluded from the following considerations. In a DSC there are always temperature differences between sample and reference sample during the measurement. As a result, the heat exchange between sample and reference sample and the respective environment

Table 3.1. Numerical simulation of a commercial disk-type DSC: Calibration factors K_Φ and K_Q depending on the heat of reaction (ΔQ), emissivity (ε), heating rate (β), density (ρ) and thermal conductivity (λ) of the sample *.
The initial standard parameters (belonging to $K_\Phi = 1$ and $K_Q = 1$) are given in parentheses

Parameter which is varied	*Numerical value of the parameter*	K_Φ	K_Q
ΔQ in J	(0.3965)	1	1
	3.965	1	1.012
	0.03965	1	0.929
ε	0.5 (Al)	1.001	0.915
	0.25 (Ag)	1.001	0.888
β in K s^{-1}	(10)	1	1
	1	1.001	0.930
	0.1	1.004	0.875
	0.01	0.991	0.870
ρ in kg m^{-3}	(7310)	1	1
	73 100	0.998	0.935
	731	1.015	0.885
λ in WK^{-1} m^{-1}	(157)	1	1
	15.7	0.998	1.016
	1570	1.003	0.999

* The parameters have been changed in steps of a factor of 10 only, this is often not realistic but gives an impression of their influence.

varies. As the radiation exchange increases, however, non-linearly with temperature, the overall heat exchange is also non-linearly linked with the temperature difference between sample and reference sample. As a consequence, the measured temperature difference (and thus the measured differential heat flow rate Φ_m) is non-linearly linked with the true heat flow rate into the sample Φ_{true}. This results in the calibration factor K_Φ in the (linearly formulated) Eq. (2.1) becoming a function of the differential heat flow rate Φ_m:

$$\Phi_{true} = K_\Phi(\Phi_m) \cdot \Phi_m \tag{3.8}$$

As the measured heat flow rate Φ_m depends on sample parameters (C_p, mass m) and on the heating rate, K_Φ too, implicitly depends on these quantities. Furthermore, it follows from Eqs. (3.3) and (3.6) that K_Φ is determined by the thermal conduction path and its properties. As these quantities are always a function of temperature, the calibration factor is always also temperature-dependent.

On the other hand, for the determination of the true heat from the peak area, Eq. (2.2) is valid, which is obtained from Eq. (2.1) by integration over the peak. If, however, K_Φ depends on Φ_m this factor is not constant and cannot be placed before the integral, and the integration of Eq. (3.8) yields:

$$Q_{true} = \int(\Phi_{true} - \Phi_{bl,true})\,dt = \int(K_\Phi(\Phi_m) \cdot \Phi_m - K_\Phi(\Phi_{bl}) \cdot \Phi_{bl})\,dt$$

From a comparison with Eq. (2.2) it follows, that K_Q is an integral mean value over the function $K_\Phi(\Phi_m)$ in the region of the peak. As Φ_m may considerably vary during a peak, the difference between K_Φ and K_Q is normally significant (cf. Sect. 4.4.3).

In these cases, a quantitative peak evaluation may lead to results affected by systematic errors, as the calibration factor also undergoes substantial changes.

Summarizing, on the basis of the results of the numerical simulations, the following can be stated for heat flux DSCs:

- For steady-state conditions:

$$\Delta T_{st} = \frac{-(C_S - C_R)}{K_\Phi}\beta$$

is valid (cf. Eq. (3.1)).

With this function for a known heating rate β, the unknown heat capacity C_S can be determined from the measured ΔT_{st}. It must be borne in mind that the calibration constant K_Φ depends on the difference of the heat capacities, $C_S - C_R$.

- For non-steady-state conditions (peak):
  - the shape of the peak changes as a function of heating rate, thermal conductivity, heat capacity and shape of the sample, and of the amount of the heat of transition. As a result, the peak parameters (width, maximum, height) change as well; only the extrapolated peak onset temperature T_e is to a certain degree independent of sample parameters,
  - the calibration factor K_Φ (true heat flow rate/measured heat flow rate) is not constant but a (weak) function of the heat flow rate itself,
  - the calibration factor K_Q (heat of transition/peak area) is not constant but changes more or less with temperature, heating rate and thermal conductivity of the sample as well as with the heat of transition, surface quality (emissivity) and sample location,
  - the calibration factor for peak areas (K_Q) differs from the calibration factor for steady-state heat flow rates.

It is basically recommended that in DSC measurements the best symmetry possible between sample and reference sample be ensured ($C_R \approx C_S$, $R_{MR} \approx R_{MS}$, identical sample containers). The results of the model calculations are confirmed by practical measurements (Sarge et al., 1994).

3.2 The Power Compensation DSC

In ideal power compensation DSCs, each ΔT signal appearing between sample and reference sample would be immediately compensated by a corresponding change in the heating power. The differential heating power required for this purpose would be equal to the differential heat flow rate as the complete electric energy is converted into heat. If the differential heating power was measured and put out, this signal would directly stand for the heat flow rate into the sample which has been sought.

The calibration factor would then be identical to unity and – without "smearing" of the measured signal – $\Phi_r = \Phi_m$ would be obtained. There is, however, no such ideal power compensation DSC. In real power compensation DSCs, the sample is always put into a container and then placed into the heater; at least one heat conduction path and, as a result, at least one time constant τ between the controlled heater and the sample location must therefore be taken into consideration. This leads to a measurement signal Φ_m which is "smeared" in comparison with the processes inside the sample, and a differential equation of at least the 1st order is therefore obtained

$$\Phi_r = \Phi_m + \tau \frac{d\Phi_m}{dt} \qquad (\text{with } \tau \approx C_S \cdot R_{MS})$$

Without exception, commercial power compensation DSCs are instruments in which a temperature difference occurs between sample and reference sample (as is the case with heat flux DSCs). This temperature difference is, firstly, the measurement signal and, secondly, it is used to electrically compensate the measurement effect by means of a proportional controller (cf. Sect. 2.2). However, the proportional control can never completely compensate the measurement effect so that, even in these calorimeters, a ΔT_{SR} remains between the microfurnaces of sample and reference sample, and this in both the steady state and during a peak.

The following is then valid:

$$\Phi_m = -k_{prop} \cdot \Delta T_{SR}$$

with k_{prop} set by the proportional control circuit.

O'Neill, 1964, analyzed the system with a proportional controller; the theoretical analysis of two systems of power compensation DSC, one with P (proportional) and one with PID (proportional, integral and differential) temperature control of the sample microfurnace was presented by Tanaka, 1992.

As different temperatures also result in a different exchange of radiation and convection with the surroundings, conclusions similar to those for heat flux DSCs would have to be drawn. This means that, in principle, what has been stated in the previous section is also valid for power compensation DSCs. However, it applies to a lesser extent as, due to the compensation, the temperature differences are much smaller than in heat flux DSCs. For power compensation DSCs at present commercially available, it is therefore basically to be expected that

- the shape of the peak depends on sample parameters, the time constant(s) being, however, smaller than those of heat flux DSCs,
- the calibration factor is not exactly equal to 1 (i.e. calibration is necessary),
- the calibration factors for steady-state (determination of the heat capacity) and for peak evaluation are not the same,
- the calibration factor depends on the temperature, the heating rate, the thermal conductivity of the sample, the amount of the heat of transition and on the sample location.

Practical measurements have confirmed these assumptions (Höhne, Glöggler, 1989). As had been expected, the effects are, however, substantially smaller than

with heat flux DSCs. When power compensation DSCs are calibrated, this dependence on parameters must be taken into consideration.

When heat capacities are measured (see Sect. 6.2.1), the reference microfurnace very often does not contain a sample. Due to the complex heat transfer conditions in the non-symmetrical DSC measuring system, heat losses then arise which cannot be compensated. These heat losses are different in static and dynamic operation. An analysis shows that the dynamic measurement error can be determined by means of the static losses measured before and after heating (for details, see Poeßnecker, 1993).

Another method to describe the behavior of an apparatus is deduced from the transfer theory, namely the theory of linear response which can be applied if the apparatus in question behaves linearly. This is true if it can be described with the aid of linear differential equations of any order. We have shown in Sect. 3.1 that heat flux DSCs can be described in this way if radiation and convection heat exchange are disregarded.

In the case of power compensated DSC, the situation is more complicated because of the control electronics involved. For the equipment of the Perkin-Elmer Corp. most frequently used, it has been shown recently that this DSC can be considered as a linear apparatus in first approximation (Tanaka, 1992; Höhne and Schawe, 1993; Schawe et al., 1993, 1994). However, any asymmetry between sample and reference side disturbs the linear behavior, and the theory of linear response is strictly speaking no longer valid. This has consequences for desmearing procedures which require linear response, such as deconvolution (Sect. 5.4), in particular in peak regions of a measured curve.

Note:

In contradiction to what has been presumed in Chapter 3, no real DSC is strictly symmetric in its functionality. Even in the empty state, the temperatures of the sample and of the reference cell are not equal so that a residual temperature difference will arise, which may change with temperature during a scan. As a consequence, the empty DSC will produce a measured curve, which is indeed neither zero nor constant with temperature but has an apparatus-dependent shape $\Phi_0(T)$. This zero line, which will mostly be measured with the crucibles in the calorimeter cells empty, is a function, that is additive to the measurement signal which stems from the sample processes. In every real case, this function should first be subtracted from the measured curve before evaluations according to the theoretical considerations can be made. We therefore must insert the term $\Phi_m - \Phi_0$(or $\Delta T - \Delta T_0$) instead of Φ_m (or ΔT) in all formulas used so far, this has been omitted in this chapter for clarity.

4 Calibration of Differential Scanning Calorimeters

There is not, as yet, an international agreement on procedures for the temperature calibration and caloric calibration of DSCs which have been definitely backed up both theoretically and experimentally. The results of investigations in this respect will have to be taken into account in the relevant calibration regulations, and they also show the basic limits set to the reliability of measurements. To what extent DSCs are capable of being calibrated depends on the quality of the DSCs' measuring system, on operational parameters and on the availability of precisely measured calibration materials. Here, the situation is still quite unsatisfactory. Moreover, no complete theory of the DSCs exists, which takes full account of the systematic influences from the instrument and inherent error sources. It should be borne in mind that it is the overall uncertainty of the calibration which yields the smallest possible systematic uncertainty of the measurements.

4.1 Aspects of Quality Assurance

Thermoanalytical instruments, including DSCs, are extensively used by industry in quality assurance systems to warrant trustworthy, reproducible properties of the products, even when we mean products which are the measurement results by which products are characterized. The ISO 9000 series and the EN 45 000 series are the basic standards in the field of quality management and quality assurance. The standard EN 45001 in particular specifies general requirements to be met by test laboratories. It will no longer be sufficient to have technical and scientific competence, this competence must be documented and made apparent to others. DSC methods are used for quality assurance in many ways: for example for the inspection of raw materials, as an accompanying measure in manufacture and for the control of the finished products.

To enable DSC methods to be useful for quality assurance, they, too, must be subject to the requirements of the relevant standards. Calibration of the DSC is an important precondition to fulfil these requirements. Calibration involves the application of reasonable calibration procedures and the use of calibration substances which are – if possible – traceable * to national/international standards. This means:

* Traceability: Property of the result of a measurement or the value of a standard whereby it can be related to stated references, usually international or national standards, through an unbroken chain of comparisons all having stated uncertainties (International Vocabulary of Basic and General Terms in Metrology, 2nd ed.,1994).

to create confidence in the quality of the measured values and to avoid repeat measurements, metrologically sound calibration procedures and traceable calibration substances (Certified Reference Materials) must be developed on the basis of which reliable uncertainty values can finally be assigned to the measurement results.

In the following sections, calibration procedures and materials will be presented which are mainly based on investigations carried out by the German Society for Thermal Analysis (GEFTA). Recommendations for calibrating DSCs and for calibration materials suitable for temperature calibration and caloric calibration are made. They are regarded as a first step in the development of internationally accepted recommendations (temperature calibration: Höhne et al., 1990; Cammenga et al., 1993; caloric calibration: Sarge et al., 1994).

4.2 Thermodynamic Aspects

In the following, reference will be made to some important thermodynamic aspects of calibration. The same considerations are valid for the phase transitions of a pure substance and for chemical reactions.

The quantity assigned to the substance is the *enthalpy difference* ΔH of the phase transition (with T = constant); it is the difference between two variables of state and, consequently, well defined. Inside the calorimeter, it is the *heat of transition* Q which is measured. The relation between heat and enthalpy is given by the first law of thermodynamics and the definition of the enthalpy function:

$$\mathrm{d}U = \mathrm{d}Q + \mathrm{d}W + \sum_i \mathrm{d}E_i \quad \text{(first law of thermodynamics)}$$

$$\mathrm{d}H = \mathrm{d}U + p \cdot \mathrm{d}V + V \cdot \mathrm{d}p \quad \text{(from enthalpy definition)}$$

From this it follows (with $\mathrm{d}W = -p \cdot \mathrm{d}V$):

$$\mathrm{d}Q = \mathrm{d}H - V \cdot \mathrm{d}p - \sum_i \mathrm{d}E_i$$

(U internal energy, W work, E_i various forms of energy)

The enthalpy H of a system is a function of the following variables of state: pressure p, temperature T and composition ξ:

$$H = H(p, T, \xi)$$

The total differential is:

$$\mathrm{d}H = \left(\frac{\partial H}{\partial p}\right)_{T,\xi} \mathrm{d}p + \left(\frac{\partial H}{\partial T}\right)_{p,\xi} \mathrm{d}T + \left(\frac{\partial H}{\partial \xi}\right)_{p,T} \mathrm{d}\xi$$

Calorimetrically, the differential heat which is measured is:

$$\mathrm{d}Q_\mathrm{m} = \left[\left(\frac{\partial H}{\partial p}\right) - V\right]_{T,\xi} \mathrm{d}p + \left(\frac{\partial H}{\partial T}\right)_{p,\xi} \mathrm{d}T + \left(\frac{\partial H}{\partial \xi}\right)_{p,T} \mathrm{d}\xi - \sum_i \mathrm{d}E_i \qquad (4.1)$$

Under the conditions normally prevailing during DSC measurements, the first term can almost always be neglected, even if closed crucibles are used (maximum pressure changes: 1 to 2 bar, $dp \approx 0$). The second term is the heat capacity at constant pressure and constant composition of the (reacting) system:

$$C_{p,\xi}(T) = \left(\frac{\partial H}{\partial T}\right)_{p,\xi}$$

The third term in Eq. (4.1) is the isothermal and isobaric enthalpy change due, for example, to a phase transition ($\Delta H = \Delta_{trs} H$), a mixing effect ($\Delta H = \Delta_{mix} H$) or a reaction ($\Delta H = \Delta_r H$).

Only if $p \approx$ const. and $\sum_i dE_i = 0$ and if the C_p share is known (the correct baseline in the course of a thermal event, cf. Sect. 5.3) is the following (obtained by integration of Eq. (4.1)) valid for the melting of a pure substance:

$$\Delta_{fus} H = Q_{fus}$$

i.e. the heat of melting equals the enthalpy difference only if the above restrictions are valid. A change in the surface already takes place if many small single crystals fuse together and form a big bead of the melting substance. As a result, surface heat is exchanged ($dE_{surface} \neq 0$) and Eq. (4.1) becomes $\Delta Q = \Delta_{fus} H - \Delta_{surface} E$.

Almost the same is valid when deformation energy is exchanged during melting or when there is an interaction between the melted substance and the surface of the sample pan (wetting energy). Though the difference between the heat of fusion $\Delta_{fus} Q$ and the enthalpy difference ΔH is small, these contributions must not be basically ignored. It is furthermore pointed out that ΔH is defined only for the indefinitely great "phase". For smaller phases (small crystals), ΔH depends on the size of the sample grains (crystal size) which means that the specific heat of melting of a fine powder differs from that of a large crystal. (As a result, the temperature of melting changes as well.)

By differentiation of Eq. (4.1), the following is obtained for the heat flow rate under ideal conditions ($p \approx$ const., $\sum_i dE_i \approx 0$).

$$\frac{dQ_m}{dt} = \Phi_m = C_{p,\xi}(T)\frac{dT}{dt} + \left(\frac{\partial H}{\partial \xi}\right)_{p,T}\frac{d\xi}{dt} \tag{4.2}$$

This equation forms the basis for the kinetic evaluation of DSC curves (cf. Sect. 6.2.2.2).

4.3 Temperature Calibration

Temperature calibration means the unambiguous assignment of the temperature "indicated" by the instrument to the "true" temperature.

The "true" temperature is defined by fixed points with the aid of calibration substances. It is reasonable to choose as calibration substances, if possible, the substances used to realize the fixed points of the International Temperature Scale of

1990 (ITS-90). The temperature "indicated" by the instrument must be derived from the measured curves, which usually requires extrapolation to zero heating rate in order to eliminate/minimize the influences of instrument and sample parameters, if possible.

Static methods (thermodynamic equilibrium) are applied to realize the fixed points of the temperature scale. In a DSC, these can be achieved only approximately. As the point of temperature measurement is not the point where the sample is located, a systematic error will always occur in a scanning operation which depends on instrument and experimental parameters. The calibration procedure described in the following takes these special features into account in a general way, independent of the special DSC type (see Höhne et al., 1990).

After calibration has been completed, the potentiometer provided for this purpose will either be adjusted until the temperature indicated corresponds to the true one, or adaptation will be ensured via the internal computer program (in a way usually not apparent to the user), or a graph or table is established showing the relation between the indicated and the true temperatures. In each case, a table should be drawn up which shows the variation of the indicated temperature at different heating rates.

A calibration already carried out by the manufacturer must be checked. Regular calibrations provide important information about the repeatability error and any

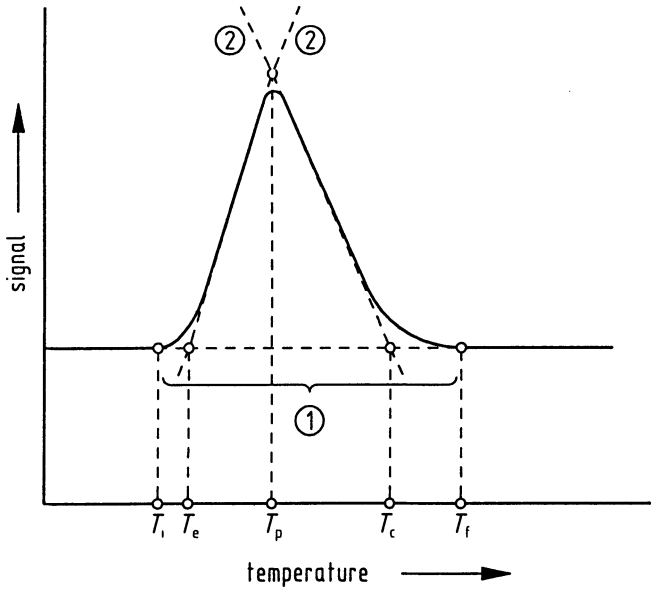

Fig. 4.1. Heat flow rate signal of a DSC during a transition (schematic representation, acc. to Hemminger, 1994).
① baseline (interpolated), ② auxiliary lines, T_i initial peak temperature, T_e extrapolated peak onset temperature, T_p peak maximum temperature, T_c extrapolated peak completion temperature, T_f final peak temperature

long-term systematic variations (drift). (It should be noted that repeatability error is not the same as uncertainty of measurement, cf. Sects. 7.2 and 7.3).

In the case of an endothermic event, the DSC records the heat flow rate signal schematically shown in Fig. 4.1. The section between the initial peak temperature T_i and the final peak temperature T_f is defined as peak (for definitions see Sect. 5.1).

The interpolated baseline is interpolated by various methods between T_i and T_f (cf. Sect. 5.3). The intersection between the auxiliary line and the baseline suffices to fix the characteristic temperature T_e (extrapolated peak onset temperature) which is important here.

4.3.1 Calibration Procedure

- Selection of at least 3 calibration substances (cf. Sect. 4.6.1) which cover the desired temperature range as uniformly as possible (at least 3 in order that nonlinearities can be detected),
- at least two calibration samples of each substance are prepared (for repeat measurements). The sample mass should correspond to that commonly used in routine measurements,
- the transition has to be measured with each calibration sample at at least 5 different heating rates in the range of interest, including the smallest possible one. The second calibration sample of the same substance is also measured at different heating rates (cf. the example below),
- it has to be checked whether there is a significant difference between the characteristic temperatures (especially T_e) obtained at identical heating rates for the first and second calibration sample of the same substance. If necessary, it should be checked whether the temperatures depend on other parameters (mass, location of the sample in the crucible etc.),
- if this is not the case, T_e is represented as a function of the heating rate and the extrapolated value T_e ($\beta \rightarrow 0$) determined for zero heating rate (Fig. 4.2),
- the difference ΔT_{corr} ($\beta = 0$) between the value $T_e(\beta \rightarrow 0)$ obtained in this way and the respective fixed-point value T_{fix} or the value T_{lit} taken from the literature (cf. e.g. Marsh, 1987; Cammenga et al., 1993) is either used to change the instrument calibration according to the manufacturer's instructions or it enters into a calibration table or curve (cf. Fig. 4.3),
- if T_e depends not only on the heating rate but also on other parameters, these dependences should be represented accordingly (location of the sample in the container, position of the sample container in the measuring system, open/closed sample container, sample mass, sample shape (foil, bead), atmosphere, material of sample container etc.).

In each case, a table (or graph) should be made which shows the variation of the indicated temperature (or of that read from the measured curve) in relation to the true temperature at different heating rates (cf. example below).

Temperature calibration has then been completed.

How are the correct temperatures assigned in practice?

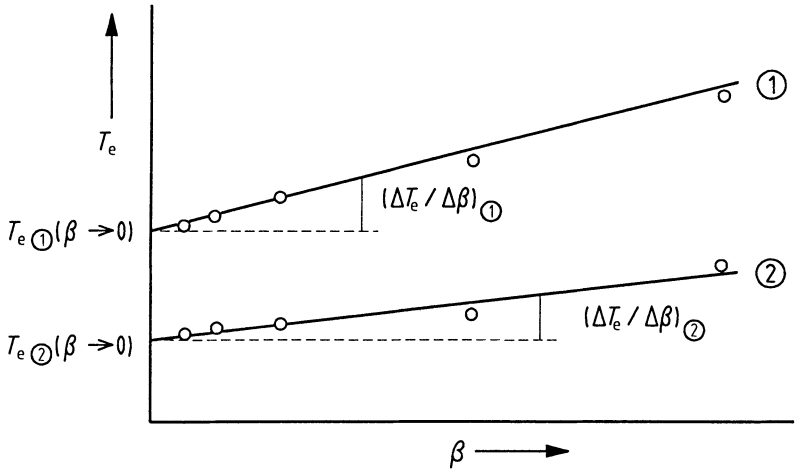

Fig. 4.2. The extrapolated peak onset temperature T_e as a function of the heating rate β, and construction of $T_e(\beta \to 0)$.
$\Delta T_e/\Delta\beta$ variation of T_e with β; ①, ② different calibration substances

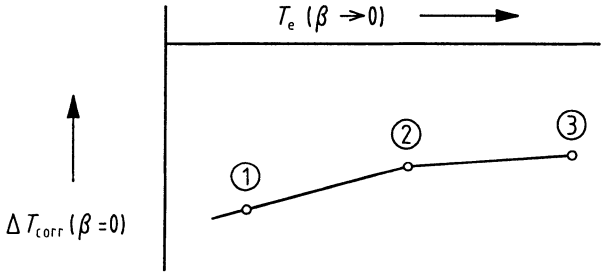

Fig. 4.3. Temperature correction ΔT_{corr} ($\beta = 0$) as a function of the extrapolated peak onset temperature T_e ($\beta \to 0$) for three calibration substances (①, ②, ③).
ΔT_{corr} ($\beta = 0$) is the difference between T_e ($\beta \to 0$) (cf. Fig. 4.2) and the "true" value of the temperature of transition. The curve obtained by means of (at least) three calibration substances shows the corrections to be applied to the measured values T_e ($\beta \to 0$) at different temperatures

1. When the accuracy requirements for temperature measurements are high (e.g. thermodynamic investigations), the substance to be investigated is measured at various heating rates. The desired characteristic temperature (e.g. T_e) is determined by extrapolation to $\beta = 0$ (quasi-equilibrium temperature). The correction ΔT_{corr} ($\beta = 0$) is applied using the proper calibration table or curve (cf. above):

$$T_{true} = T_e\ (\beta \to 0) + \Delta T_{corr}\ (\beta = 0)$$

2. When the accuracy required in the determination of T_e is not so high and/or the process to be investigated depends strongly on the heating rate ("kinetic" pro-

cesses), the value $T_e(\beta \rightarrow 0)$ may be calculated from the mean slope $\Delta T_e/\Delta\beta$ of the $T_e(\beta)$ curve(s) of the calibration substance(s) (cf. above and Fig. 4.2 and example below):

$$T_e(\beta \rightarrow 0) \approx T_e(\beta) - \left(\frac{\Delta T_e}{\Delta \beta}\right)\beta$$

$\Delta T_{corr}(\beta = 0)$ is again taken from the calibration table or curve (Fig. 4.3), so that

$$T_{true} = T_e(\beta \rightarrow 0) + \Delta T_{corr}(\beta = 0)$$

The best thing to do is to start by carrying out two measurements at clearly differing heating rates. Then it is checked whether $\Delta T_e/\Delta\beta$ corresponds with the (mean) slope of the $T_e(\beta)$ curve(s) of the calibration substances. If so, extrapolation to $T_e(\beta \rightarrow 0)$ can be carried out at once. If not, first the heating rate dependence $T_e(\beta)$ must generally be determined as described above.

To simplify the described method, for each heating rate applied, the corresponding overall correction $\Delta T_{corr}(\beta) = \Delta T_{corr}(\beta = 0) - \beta \cdot \Delta T_e/\Delta\beta$ can be listed (cf. example below) so that the "true" temperature can be determined at once:

$$T_{true} = T_m + \Delta T_{corr}(\beta)$$

Here, a distinction by classes of substances (metals, organic substances) must possibly be made.

It is to be expected that, for a certain instrument, $\Delta T_{corr}(\beta = 0)$ will vary with time which is why a recheck should be made about every three months by recalibrating the instrument. The dependence of the extrapolated peak onset temperature $\Delta T_e/\Delta\beta$ on the heating rate is only related to the properties of the sample substance; it remains unchanged for a certain DSC and need not, therefore, be regularly checked.

In order to assign the correct temperature to the individual phases in the case of complex thermal events, with $\beta \neq 0$, an auxiliary line must be drawn at the angle α to the extrapolated baseline. The angle α can be taken from the calibration experiment in which the same heating rate has been applied (Fig. 4.4). The scale division of the axes must be the same in both cases; otherwise the slope of the auxiliary line must be converted. (For more advanced methods of determining characteristic temperatures in the case of endothermic and exothermic events, see Sarge, 1991 and Schawe, 1993).

Uncertainties

Depending on the type of DSC, the minimum repeatability error of the determination of T_e on pure metals amounts to approx. ±0.02 K (sample exactly in the same place in the crucible or measuring system); in the other cases it varies between 0.1 and 0.8 K. An overall uncertainty of measurement of T_e between 0.3 and 1.0 K must be reckoned with. The overall uncertainty of the temperature calibration should in every case be carefully estimated (uncertainty of temperature sensors, uncertainty of the determination of T_e etc.).

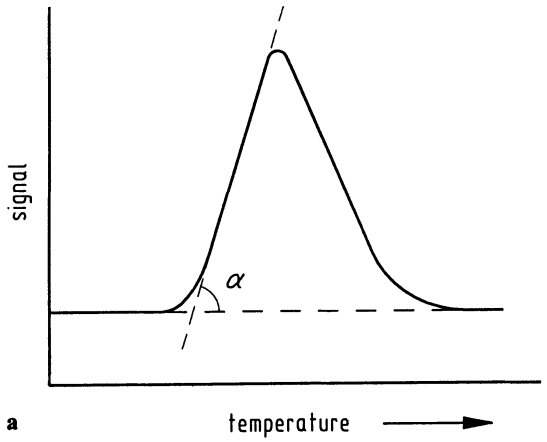

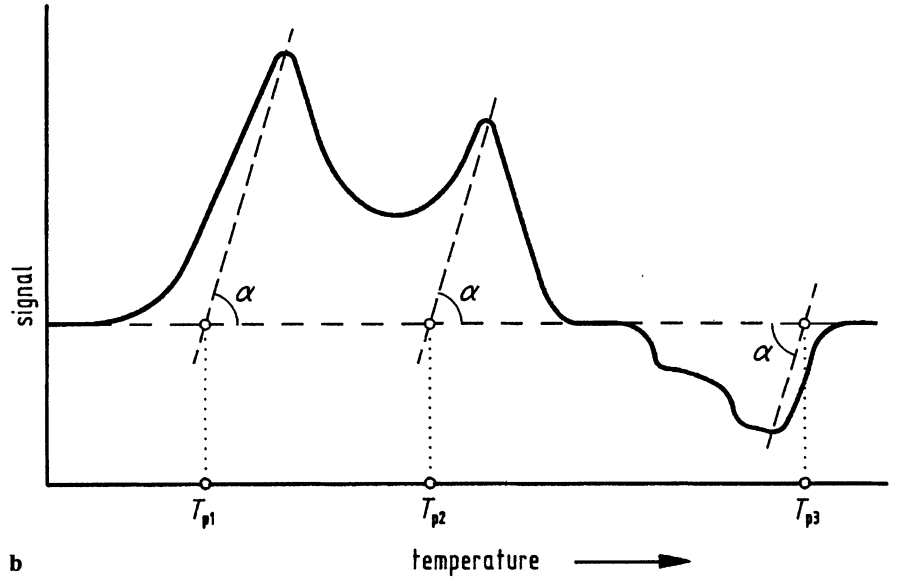

Fig. 4.4. Assignment of the characteristic temperature T_p in complex thermal events.
a Calibration measurement to determine the angle α at a specific heating rate,
b Construction of characteristic peak maximum temperatures T_p of a complex thermal event with the aid of angle α (measurement with the same heating rate as for **a**). In heating operation, due to the thermal lag, each endothermic thermal event in the sample is "indicated" too late, i.e. at too high a temperature. To find the "true" temperature of a characteristic segment of the measured curve in good approximation, a lower temperature must always be assigned instead of the indicated temperature (read at an angle of 90°). This is done with the aid of the angle α. In the case of exothermic events the true temperature can be higher than the measured temperature (cf. T_{p3})

Notes:

1. It has to be checked whether T_e depends on the location of the calibration sample in the sample container (in particular at high temperatures). In the case of power compensation DSCs, due to the isoperibol operation, a temperature profile develops in the bottom plate of the microfurnace which – depending on the sample position – results in an earlier (center) or later (boundary) melting of a calibration sample – and thus in a lower or higher temperature T_e being indicated (Fig. 4.5) (see Höhne, Glöggler, 1989).

   Such effects are also possible in heat flux DSCs, however, to a much lower extent due to the non-isoperibol operation. In cylinder-type measuring systems, above all the dependence on the (vertical) position of the sample in the cylindrical container must be checked.
2. In the case of exothermic events, the sample temperature can be higher than the measured temperature. The amount of this deviation cannot be precisely determined. The assignment of a temperature is therefore useful only at the beginning of the exothermic event.

   The increase in the sample temperature in the course of the reaction can be estimated on the basis of the following considerations:

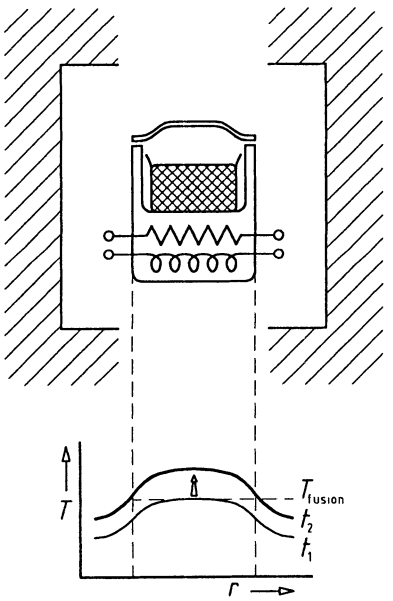

Fig. 4.5. Temperature profile in the microfurnace of a power compensation DSC (schematic). The isoperibol mode of operation (constant ambient temperature) results in a temperature profile in the sample support as shown schematically. During melting of a sample, this temperature profile leads to time-dependent zones of melting (T_{fus} is first reached in the center) and consequently to different extrapolated peak onset temperatures T_e when the radial position (r) of small samples differs (acc. to Höhne, Glöggler, 1989)

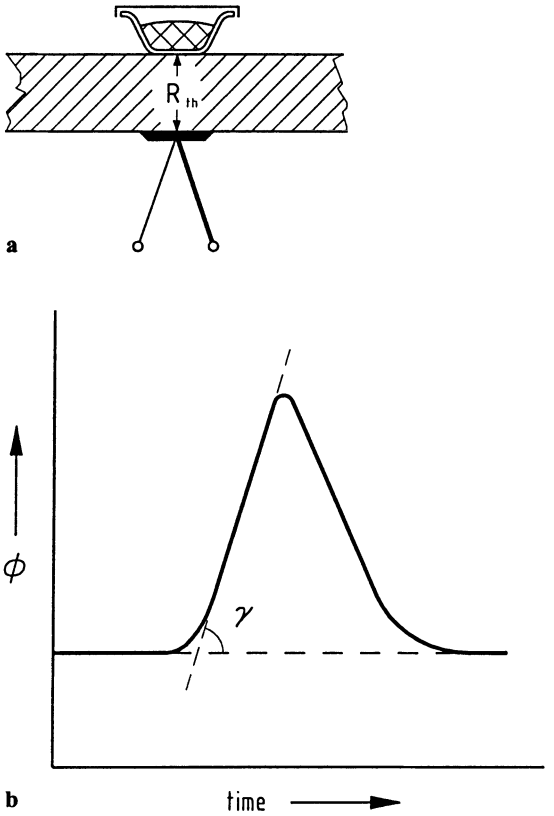

Fig. 4.6. Heat resistance R_{th} between temperature measurement point and sample.
a Diagrammatic view of the sample system,
b Curve measured during melting of a pure substance, Φ heat flow rate into the sample, tan γ ascending slope ($d\Phi/dt$) of the $\Phi(t)$ curve during melting (to calculate R_{th})

If there is a thermal resistance R_{th} between sample (T_S) and temperature sensor (T_M) (Fig. 4.6a, b),

$$T_M - T_S = R_{th} \cdot \Phi_r \tag{4.3}$$

is valid for the difference between the indicated temperature T_M – calibrated as described above – and the sample temperature T_S considered to be homogeneous. When a pure substance melts (calibration, for example), R_{th} can be determined approximately from the slope of the respective heat flow rate curve $\Phi(t)$. From Eq. (4.3), the following results after differentiation (with T_S = constant during melting, $dT_M/dt \approx \beta$ and $\tan \gamma = (d\Phi/dt)_{melting}$):

$$R_{th} \approx \frac{\beta}{\tan \gamma} \tag{4.4}$$

(Experiments at various heating rates will show how well this relation is valid.)

3. In measurements at negative heating rate (cooling), the sample temperature is higher than the indicated temperature. As a result, the correction $\Delta T(\beta)$ from the calibration table or curve must be applied with the sign reversed as compared with heating (see Fig. 4.7), whereas the correction at heating rate zero $\Delta T_{corr}(\beta = 0)$ remains unchanged.

There are no calibration materials so far with well-defined transition temperatures in the cooling mode as the process of undercooling of pure calibration substances is not definitely known. Temperature calibration in the cooling mode is therefore not possible. However, symmetry of the heat transfer phenomena has been generally taken for granted, at least in heat flux DSCs. In the case of power compensation DSCs, the situation is more complicated because of the electronic and control equipment involved. This type of DSC may exhibit asymmetric behavior if the electronic system is not precisely adjusted. Whether or not a DSC behaves symmetrically in the heating and cooling mode can be tested with the aid of substances which show phase transitions without undercooling. The temperature of the phase transition must not be known very precisely; it should only be certain that it is the same in the heating and cooling mode, and that undercooling is below 0.2 K. This is the case for the smectic/nematic transition of certain liquid crystals (see, for example, Höhne et al., 1993). Such a test of three different power compensation DSCs is documented in Fig. 4.8. As can be seen, symmetry due to heating and cooling of the instrument in question is given within the limits of accuracy of the measurements, however, a small deviation from exact symmetry is also apparent. When the electronic system is incorrectly adjusted, the asymmetry of this type of calorimeter can indeed be important

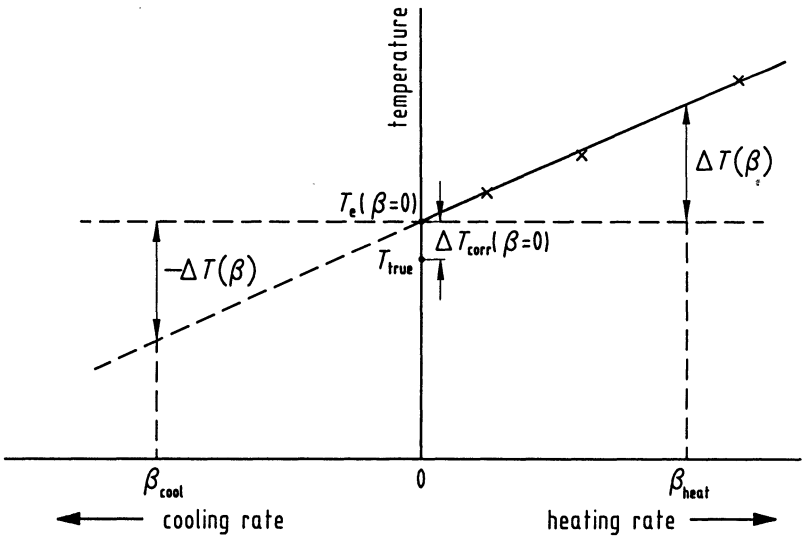

Fig. 4.7. Schematic representation of the temperature corrections in the heating and cooling mode

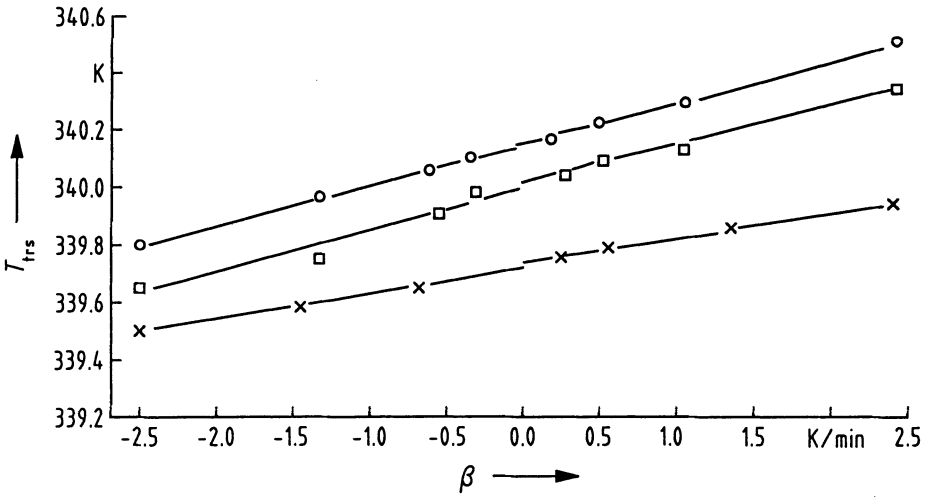

Fig. 4.8. Test of the symmetry of three different power compensation DSCs with respect to the heating and cooling mode using a liquid crystal (acc. to Höhne et al., 1993)

and may lead to errors in the temperature values determined in the cooling mode. In the case of heat flux DSCs (in particular those of the disk-type), the asymmetry need not be detected because of physical reasons. Nevertheless, it is not a mistake to check it as well.

In general, the assignment of the characteristic temperatures of cooling curves is affected by greater uncertainties than in the case of heating curves.

Investigations using liquid crystals as calibration substances are being carried out at present.

4.3.2 Arguments in Support of the Temperature Calibration Procedure

The existing recommendations for the temperature calibration of DSCs (e.g. ASTM E 967-83, ASTM E 794-85) and the specifications of most manufacturers take a standard heating rate (e.g. 10 K min^{-1}) as a basis. This method cannot be recommended since

- different heating rates require different corrections; shifting of T_e is not always linear due to the heating rate (cf. Fig. 4.9),
- the sample temperature is equal to the measured temperature only at zero heating rate; to ensure safe extrapolation to zero heating rate, measurements should be carried out at at least 5 different heating rates (starting with the lowest heating rate),
- the temperature fixed points of the International Temperature Scale are defined for the reference substances in phase equilibrium (i.e. static, zero heating rate).

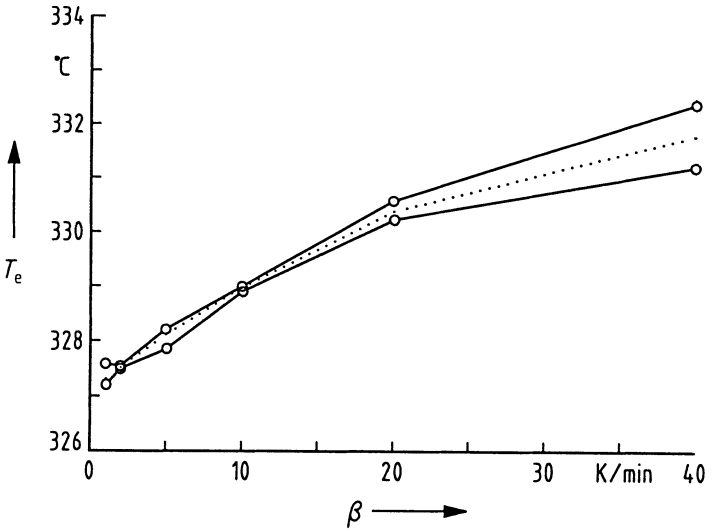

Fig. 4.9. Extrapolated peak onset temperature T_e in °C as a function of the heating rate β (two measurement series of a heat flux DSC with 58 mg of lead).
o—o measured values, ---- curve of average values. The curves show a non-linear dependence $T_e(\beta)$ only towards the highest heating rate and a dispersion of the T_e-values, which depends on β

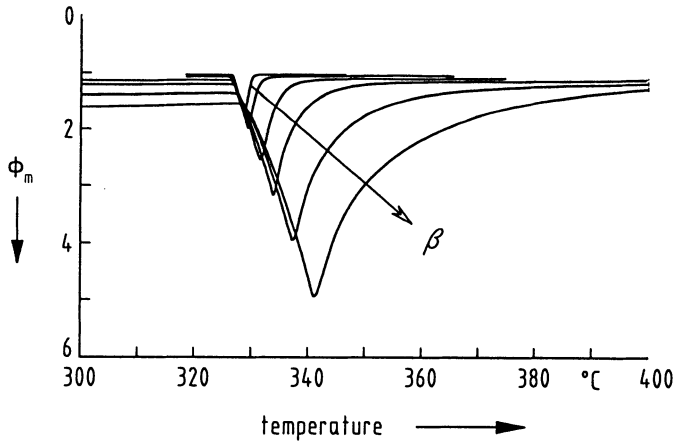

Fig. 4.10. Measured curves showing the peak temperature maximum T_p changing with the heating rate β (heat flux DSC, lead, 58 mg, heating rate β from 5 to 50 K min^{-1}).
Φ_m heat flow rate (arbitrary units). In addition to the shifting of T_p with β, the great changes of T_e and T_f are obvious (for definitions see Fig. 4.1)

Only T_e can be used as a characteristic temperature of a peak to define the DSC's temperature scale (cf. Fig. 4.1), the reasons being the following:

- T_i cannot be determined with the required reliability because of the noise; the same applies to T_f (repeatability error between 2 and 15 K depending on substance, kind of transition etc.),
- T_p and T_c strongly depend on the thermal conductivity, mass and layer thickness (volume) of the sample substance, on the heating rate and the heat transfer from sample to sample container (crucible), which may change due to melting (cf. Fig. 4.10),
- T_e depends least on heating rate and sample parameters (substance, thermal conductivity, mass, layer thickness); any possible effect of melting (heat transfer) should be checked by carrying out various similar experiments with the same calibration sample.

4.3.3 Examples of Temperature Calibration

The results of the temperature calibration of a power compensation DSC according to Sect. 4.3.1 are given as an example. Two samples each (between 2 and 6 mg) of highly pure indium, tin and lead were used (closed aluminium crucibles). The results shown in Tables 4.1 to 4.3 were obtained for the non-calibrated device (cf. Figs. 4.11a to c):

The correction curve shown in Fig. 4.12 has been obtained for the calibration of the device.

Table 4.1 Temperature calibration with indium (cf. Fig. 4.11 a)

sample No.	run No.	heating rate in K min^{-1}	T_e in °C
1	1	10.0	156.21
1	2	10.0	156.16
2	1	10.0	156.25
2	2	10.0	156.21
1	1	5.0	155.81
2	1	5.0	155.91
1	1	2.5	155.65
2	1	2.5	155.67
1	1	1.0	155.64
2	1	1.0	155.65
1	1	0.5	155.52
2	1	0.5	155.65
2	2	0.5	155.53
1	1	0.1	155.49
2	1	0.1	155.20

Results:

$T_e\,(\beta \to 0)$ = 155.523 °C
T_{fix} = 156.5985 °C (ITS-90)
$\Delta T_{corr}\,(\beta = 0)$ = +1.0755 K
$\Delta T_e/\Delta\beta$ = 0.0682 K/(K min^{-1})

Table 4.2 Temperature calibration with tin (cf. Fig. 4.11 b)

sample No.	run No.	heating rate in K min^{-1}	T_e in °C
1	1	10.0	232.35
1	2	10.0	232.18
2	1	10.0	232.06
1	1	5.0	231.81
2	1	5.0	231.69
1	1	2.5	231.54
2	1	2.5	231.41
1	1	1.0	231.33
2	1	1.0	231.22
1	1	0.5	231.28
2	1	0.5	231.12
1	1	0.1	231.26
2	1	0.1	231.12

Results:
$T_e\,(\beta \rightarrow 0)$ = 231.184 °C
T_{fix} = 231.928 °C (ITS-90)
$\Delta T_{corr}\,(\beta = 0)$ = +0.744 K
$\Delta T_e/\Delta\beta$ = 0.103 K/(K min^{-1})

Table 4.3 Temperature calibration with lead (cf. Fig. 4.11 c)

sample No.	run No.	heating rate in K min^{-1}	T_e in °C
1	1	10.0	328.22
1	2	10.0	327.50
1	3	10.0	327.52
2	1	10.0	327.95
2	2	10.0	327.87
1	1	5.0	327.10
1	2	5.0	327.09
2	1	5.0	327.42
1	1	2.5	326.94
2	1	2.5	327.23
1	1	1.0	326.76
2	1	1.0	326.97
1	1	0.5	326.78
2	1	0.5	326.95
1	1	0.1	326.75
2	1	0.1	326.93

Results:
$T_e\,(\beta \rightarrow 0)$ = 326.793 °C
T_{fix} = 327.462 °C (converted from the IPTS-68 to the ITS-90)
$\Delta T_{corr}\,(\beta = 0)$ = +0.669 K
$\Delta T_e/\Delta\beta$ = 0.0997 K/(K min^{-1})

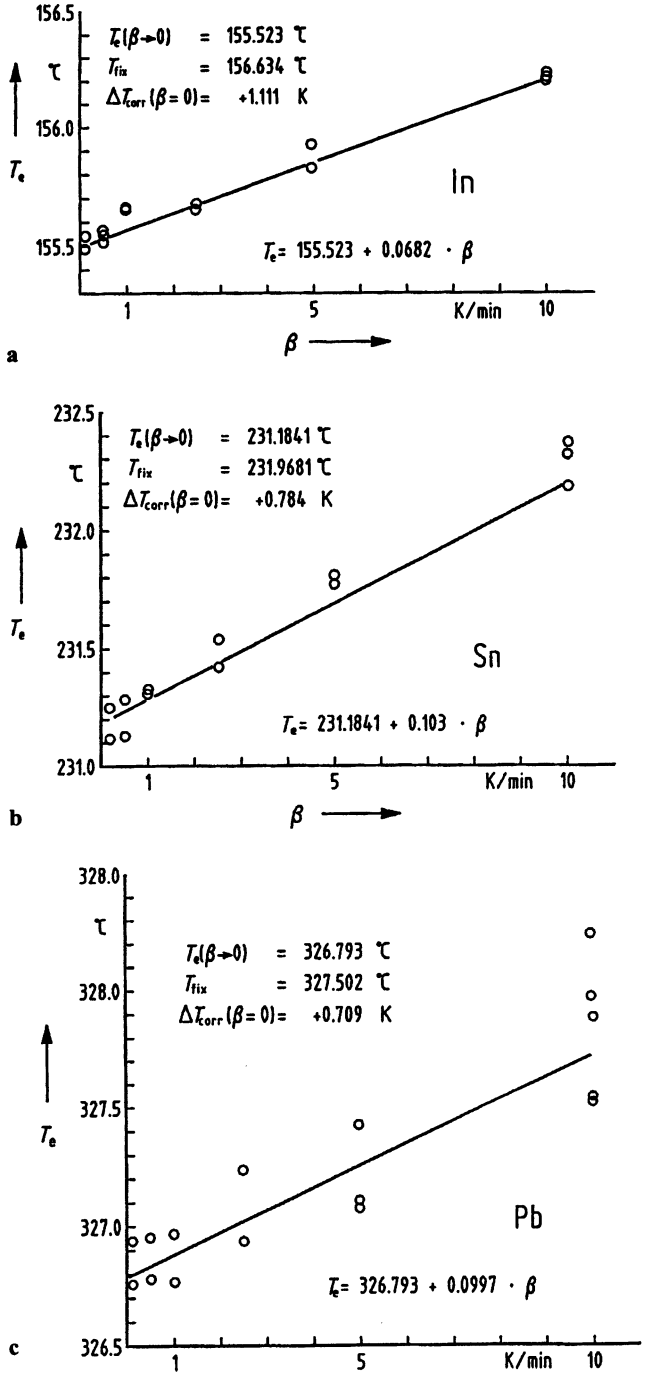

Fig. 4.11. Extrapolated peak onset temperature T_e (in °C) as a function of the heating rate β to determine $T_e(\beta \to 0)$. (Power compensation DSC, two measurement series each with two samples of different mass, closed aluminium crucibles).
a Sample material: indium, **b** Sample material: tin, **c** Sample material: lead. $T_e(\beta \to 0)$ extrapolated peak onset temperature at zero heating rate, T_{fix} fixed-point temperature, i.e. true temperature of melting (ITS-90, in the case of lead converted from the IPTS-68 to the ITS-90), $\Delta T_{corr} = T_{fix} - T_e(\beta \to 0)$ temperature correction

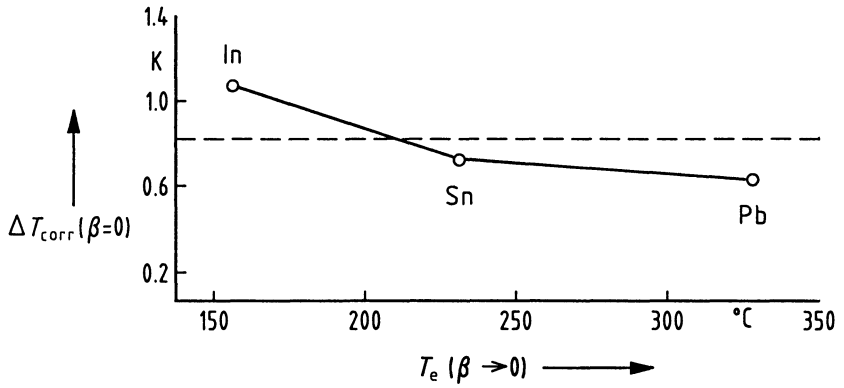

Fig. 4.12. Correction curve for the temperature calibration of a power compensation DSC. The individual corrections $\Delta T_{corr}(\beta = 0)$ have been taken from the results of the calibration measurements shown in Figs. 4.11 a to c.
$\Delta T_{corr}(\beta = 0)$ difference between true temperature (fixed-point temperature) and extrapolated peak onset temperature $T_e(\beta = 0)$ for zero heating rate (for Pb see legend of Fig. 4.11), --- mean value: +0.83 K

In practice, for the purpose of temperature calibration, the potentiometer adjustment will in this case be changed by the mean value of 0.83 K and, if necessary, the shape of the correction curve towards higher temperatures fixed on the basis of another calibration (e.g. with Zn). Different corrections must possibly be applied in different temperature ranges. For many DSCs, the user feeds the results of the calibration measurements (for example, with In and Pb) into the computer which internally converts the temperature scale (slope and position).

After the DSC has been calibrated with the aid of $\Delta T_{corr}(\beta = 0)$, various pure substances are measured at different heating rates and T_e is determined. Table 4.4 is obtained and includes $\Delta T_{corr}(\beta = 0) = T_{lit} - T_e(\beta \rightarrow 0)$, the corrections for the various heating rates calculated from $\Delta T_{corr}(\beta = 0)$ and the slope of the respective fitted line:

$$\Delta T_{corr}(\beta) = \Delta T_{corr}(\beta = 0) - \beta\left(\frac{\Delta T_e}{\Delta \beta}\right)$$

(The values for $\Delta T_{corr}(\beta)$ have in general been rounded to one decimal.)

ΔT_{tot} is defined as $T_{lit} - T_e(\beta)$, i.e. the difference between the "true" temperature T_{lit} and the extrapolated peak onset temperature at a heating rate β.

For this calorimeter there is a linear relation between the shift of T_e and the heating rate β. The gradient $\Delta T_e/\Delta\beta$ of the respective fitted line yields the values given in Table 4.5.

From this, it follows that for this DSC, at a heating rate of 10 K min^{-1}, a mean difference of 0.9 ± 0.3 K results between $T_e(\beta)$ and the true temperature of the transition. Depending on the heat transfer between substance and crucible bottom, the shift may vary between 0.5 and 1.5 K.

Table 4.4 Measurements with various substances to determine $\Delta T_e/\Delta\beta$

Diphenyl ether (phenoxybenzene)

T_e in °C	heating rate in K min^{-1}	$\Delta T_{tot}(\beta)$ in K	
27.05	0.5	−0.19	$T_{lit} = 26.86\,°C$
27.10	1.0	−0.24	$T_e(\beta \to 0) = 26.93\,°C$
27.20	2.5	−0.34	$\Delta T_{corr}(\beta = 0) = -0.07\,K$
27.73	5.0	−0.87	

Gallium

T_e in °C	heating rate in K min^{-1}	$\Delta T_{tot}(\beta)$ in K	
29.92	0.5	−0.16	$T_{lit} = 29.7646\,°C = T_{fix}$
29.97	1.0	−0.21	$T_e(\beta \to 0) = 29.851\,°C$
30.11	2.5	−0.35	$\Delta T_{corr}(\beta = 0) = -0.09\,K$
30.35	5.0	−0.59	
30.94	10.0	−1.18	

$C_{33}H_{68}$ (paraffin) 1st transition

T_e in °C	heating rate in K min^{-1}	$\Delta T_{tot}(\beta)$ in K	
67.35	0.5	0.05	$T_{lit} = 67.4\,°C$
67.36	1.0	0.04	$T_e(\beta \to 0) = 67.3\,°C$
67.47	2.5	−0.07	$\Delta T_{corr}(\beta = 0) = +0.1\,K$
67.66	5.0	−0.26	
68.06	10.0	−0.66	

$C_{33}H_{68}$ (paraffin) 2nd transition

T_e in °C	heating rate in K min^{-1}	$\Delta T_{tot}(\beta)$ in K	
70.98	0.5	0.12	$T_{lit} = 71.1\,°C$
70.98	1.0	0.12	$T_e(\beta \to 0) = 70.91\,°C$
71.10	2.5	0	$\Delta T_{corr}(\beta = 0) = +0.2\,K$
71.27	5.0	−0.17	
71.70	10.0	−0.60	

Benzoic acid

T_e in °C	heating rate in K min^{-1}	$\Delta T_{tot}(\beta)$ in K	
122.28	0.5	0.06	$T_{lit} = 122.34\,°C$
122.23	1.0	0.11	$T_e(\beta \to 0) = 122.22\,°C$
122.34	2.5	0	$\Delta T_{corr}(\beta = 0) = +0.12\,K$
122.46	5.0	−0.12	
122.72	10.0	−0.38	

Table 4.4 (continued)

Indium

T_e in °C	heating rate in K min^{-1}	$\Delta T_{tot}(\beta)$ in K	
156.63	0.5	− 0.03	$T_{lit} = 156.5985\,°C = T_{fix}$
156.67	1.0	− 0.07	$T_e(\beta \rightarrow 0) = 156.53\,°C$
156.80	2.5	− 0.20	$\Delta T_{corr}(\beta = 0) = +0.07\,K$
156.96	5.0	− 0.36	
157.32	10.0	− 0.72	
158.01	20.0	− 1.41	
159.34	40.0	− 2.74	
162.17	80.0	− 5.57	
168.60	160.0	−12.00	

Tin

T_e in °C	heating rate in K min^{-1}	$\Delta T_{tot}(\beta)$ in K	
232.18	0.5	−0.25	$T_{lit} = 231.928\,°C = T_{fix}$
232.21	1.0	−0.28	$T_e(\beta \rightarrow 0) = 232.12\,°C$
232.34	2.5	−0.41	$\Delta T_{corr}(\beta = 0) = -0.19\,K$
232.52	5.0	−0.59	
233.01	10.0	−1.08	

Caffeine

T_e in °C	heating rate in K min^{-1}	$\Delta T_{tot}(\beta)$ in K	
236.30	0.5	−0.20	$T_{lit} = 236.1\,°C$
236.30	1.0	−0.20	$T_e(\beta \rightarrow 0) = 236.24\,°C$
236.36	2.5	−0.26	$\Delta T_{corr}(\beta = 0) = -0.1\,K$
236.67	5.0	−0.57	
236.96	10.0	−0.86	

Lead

T_e in °C	heating rate in K min^{-1}	$\Delta T_{tot}(\beta)$ in K	
237.99	0.5	−0.53	$T_{lit} = 327.462\,°C$
238.00	1.0	−0.54	$T_e(\beta \rightarrow 0) = 327.93\,°C$
238.17	2.5	−0.71	$\Delta T_{corr}(\beta = 0) = -0.47\,K$
238.32	5.0	−0.86	
238.81	10.0	−1.35	

Table 4.5 The dependence of T_e on the heating rate β for various classes of materials (results from Table 4.4)

Substance	$\Delta T_e/\Delta\beta$ in K/(K min^{-1})
Gallium	0.11
Indium	0.07
Tin	0.09
Lead	0.09
Mean value metals	0.09 ± 0.02 *
Diphenyl ether	0.15
Paraffin $C_{33}H_{68}$	0.08
Benzoic acid	0.05
Caffeine	0.07
Mean value organic substances	0.09 ± 0.04 *
Overall mean value	0.09 ± 0.03 *

* standard deviation σ_{n-1}

Separate measurements at different heating rates must be carried out for a substance in order to determine the transition temperatures more accurately.

Note:

The values obtained for T_e in the first measurement of a calibration sample (In, Sn, Pb) are systematically higher than those of the second and all subsequent measurements (at a given heating rate). The reason for this is the heat transfer between the sample and the bottom of the crucible, which strongly improved after the first melting (larger contact area). As a result, T_e is lower. If, for reasons of irreversibility of the process, only the first measurement of a sample can be evaluated, this effect must also be taken into account when the uncertainties of $T_e(\beta \rightarrow 0)$ are estimated.

Another striking feature of the results of the calibration measurements is that the individual T_e of various samples of the same substance are very well situated on a straight line, but that some of the straight lines deviate strongly from one another (e.g. Figs. 4.11 a to c). The reason is that, firstly, the sample containers and thus the heat transfer to the microfurnace are not identical, i.e. each sample encounters different contact points and heat flux conditions, and that, secondly, the location of the sample in the microfurnace of the power compensation DSC clearly influences the T_e of the measured curve. This is obvious from the results shown in Fig. 4.13 (cf. also Höhne, Glöggler, 1989).

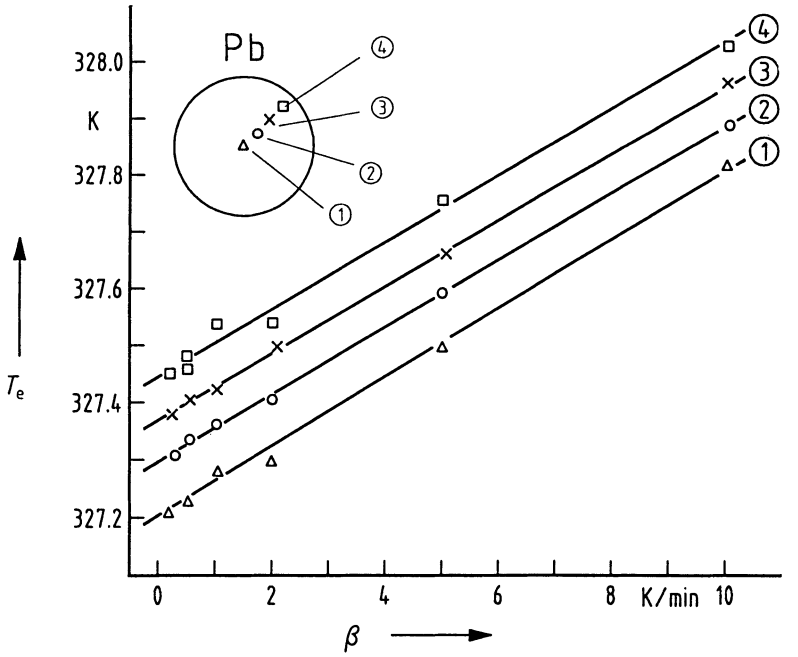

Fig. 4.13 Extrapolated peak onset temperatures T_e of lead (0.2 mg) as a function of heating rate β with the samples in various positions (1 to 4) in the microfurnace of the power compensation DSC (cf. Fig. 4.5, acc. to Höhne, Glöggler, 1989)

4.4 Caloric Calibration

By means of caloric calibration (for a review see Sarge et al., 1994), the proportionality factor between the measured heat flow rate Φ_m and the true heat flow rate Φ_{true} and between the measured exchanged heat Q_m and the heat Q_{true} really transformed is to be determined:

$$\Phi_{true} = K_\Phi \cdot \Phi_m \quad \text{and} \quad Q_{true} = K_Q \cdot Q_m$$

Strictly speaking, Φ_m in this equation should be considered the measured heat flow rate with the instrument zero line (which is constant) already subtracted, but as all correction calculations are usually done using the measured curve Φ_m itself, only Φ_m is used in the following.

This calibration is carried out either as "heat flow rate calibration" in the (quasi-) steady-state

- by electrical heating applying the well-known power,
- by "charging" the known heat capacity of the calibration sample

or as "peak area calibration" by integration over a peak which represents a known heat

$$Q_{true} = \int \Phi_{true}\, dt = K_Q \int (\Phi_m - \Phi_{bl})\, dt$$

- by electrical heating applying the well-known energy,
- by applying the known heat resulting from a phase transition (melting) of a pure substance.

Since $Q_{true} = \int \Phi_{true} \cdot dt$ and $Q_m = \int (\Phi_m - \Phi_{bl})\, dt$, K_Φ and K_Q should be identical which is not, however, the case because in practice – throughout the duration of the peak – K_Φ depends on the temperature T (and therefore also on the time t) and is in addition a function of Φ (cf. Sect. 4.4.3). As a result, the equation $\Phi_{true} = K_\Phi \cdot \Phi_m$ can indeed be integrated but K_Φ must not, however, be placed in front of the integral. As stated already, K_Q is not equal to K_Φ; K_Q is rather a kind of integral mean value of K_Φ over the area of one peak. In practice, the difference between the two calibration factors is between 0.5 and several per cent. Both types of calibration must therefore be carried out separately.

The advantages of the twin principle of DSCs become fully effective only in the case of perfect thermal symmetry of the measuring system. In this case, the measured signal is, however, zero. In real measurements there will always be asymmetries in the temperature field. The effects of such asymmetries are dealt with in Sect. 4.4.3. The conclusion to be drawn for heat calibration is as follows:

The thermophysical behavior of calibration sample and sample to be measured must be as similar as possible. As this is possible only approximately, systematic errors exist which must be estimated and included in the overall uncertainty of measurement (cf. Sect. 7.3).

4.4.1 Heat Flow Rate Calibration

In almost all DSCs commercially available, a heat flow rate signal Φ_m is internally assigned as measurement signal for the actual signal ΔT. (When the measurement signal is put out as a voltage ΔU (for example in mV), the following applies analogously, Φ_m being replaced by ΔU.) The heat flow rate calibration defines the functional relation between Φ_m and the true heat flow rate Φ_{true} consumed or generated by the sample:

$$\Phi_{true} = K_\Phi \cdot \Phi_m$$

(steady state, Φ_m with the zero line – empty crucibles – (definitions see Sect. 5.1) already subtracted).

The proportionality factor (calibration factor, calibration function) K_Φ usually depends on parameters such as temperature and – what is most important – heat flow rate. In some DSCs, K_Φ is made unity by electronic or software means. In these cases, too, the relation between Φ_m and Φ_{true} must be carefully checked.

The heat flow rate calibration can be performed in two ways:

1. Installation of an electric calibration heater in the place of the sample or inside the sample. This method offers the following advantages:
   - the electric power (heating power) can be measured easily and with high accuracy,

- heat flow rates of differing intensity can be generated without the calibration setup being modified,
- the steady state can be adjusted for any period of time desired; the resulting conditions are most similar to those of a C_p measurement,
- the heater can be switched on or off at any temperature desired so that the position of the baseline ($\Phi_{true} = 0$) can also be checked in between (even with a sample placed in the crucible),
- by appropriately presetting the development of the heating power with time, measurement effects (peaks) can be "repeated" (simulated) so that heat flow rates leading to such a peak can be assigned without "desmearing" (see Sect. 5.4),
- the time constant of the measuring system can be easily determined (cf. Sect. 7.2).

The disadvantages of the electrical heat flow rate calibration are the following:

- the heater can hardly be installed in disk-type measuring systems,
- heaters permanently installed in measuring systems are not situated at the sample location; this leads to systematic errors,
- heat fluxes in the wires lead to systematic uncertainties, "heat leaks". (Ensure thermal symmetry of sample and reference side!)

Figure 4.14a shows the electrical calibration in a DSC with cylinder-type measuring system. (Peak area calibration may also be carried out using the peak areas furnished by these measurements; see below.) The resulting calibration curve $K_\Phi(T) = \Phi_{true}(T)/(\Phi_m(T) - \Phi_{bl}(T))$ is represented in Fig. 4.14b; Φ_{bl} is the baseline heat flow rate (Φ_m-curve without electric power).

2. Heat flow rate calibration can also be carried out with a sample of known heat capacity (Fig. 4.15). The following is valid for the heat flow rate absorbed by the sample (without reference sample) in (quasi-) steady state heating mode:

$$\Phi_{true} = C_p \cdot \beta \quad \text{so that} \quad K_\Phi(T) = C_p(T) \cdot \frac{\beta}{(\Phi_m(T) - \Phi_0(T))}$$

(Φ_0: zero line value with empty crucibles.)

The advantages of this calibration method are the following:

- applicable in all DSCs,
- calibration heat flux at the sample location,
- no leads (wires) required.

The disadvantages:

- the calibration cannot be switched off in between, i.e. checking of the baseline (or zero line) is not possible during a run (leads to uncertainties in $\Phi_m - \Phi_0$),
- there is a temperature profile inside the sample (yields "mean C_p").

The calibration substance most frequently used is synthetic sapphire (α-Al_2O_3, corundum), cf. Table 4.9.

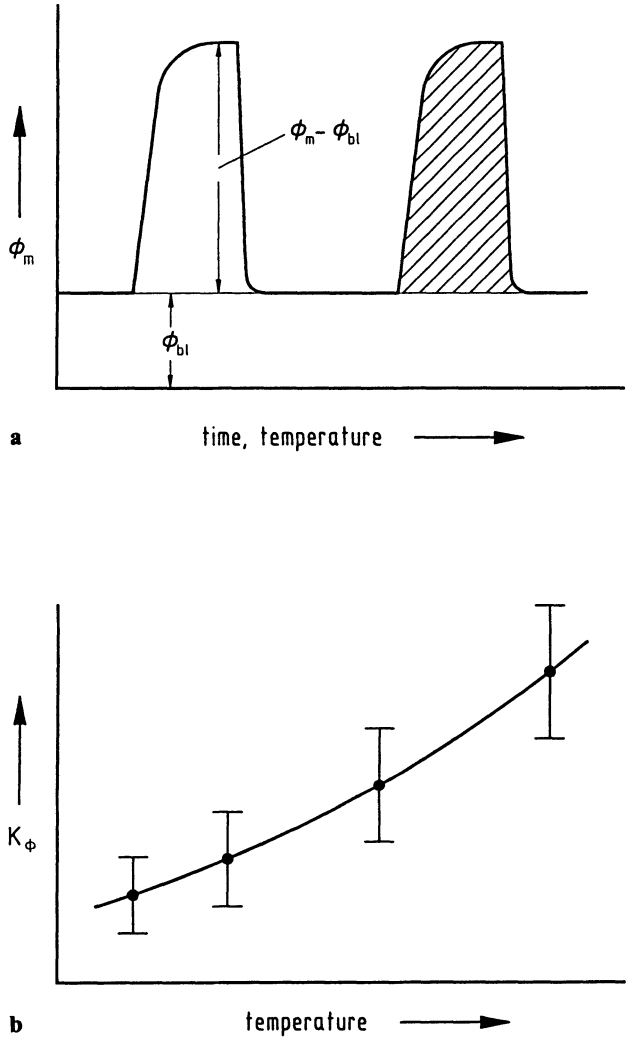

Fig. 4.14. Electrical heat flow rate calibration of a heat flux DSC (cylinder-type measuring system) by means of a built-in heater.
a Calibration peaks generated electrically in isothermal operation or during heating,
b Calibration factor K_Φ (calculated with the data of **a**, schematic) to determine the reaction (real) heat flow rate: $K_\Phi(T) = \Phi_{true}/(\Phi_m(T) - \Phi_{bl}(T))$ (with Φ_{true} as electrical heating power P_{el}), Φ_m measured heat flow rate, Φ_{bl} baseline value of the heat flow rate

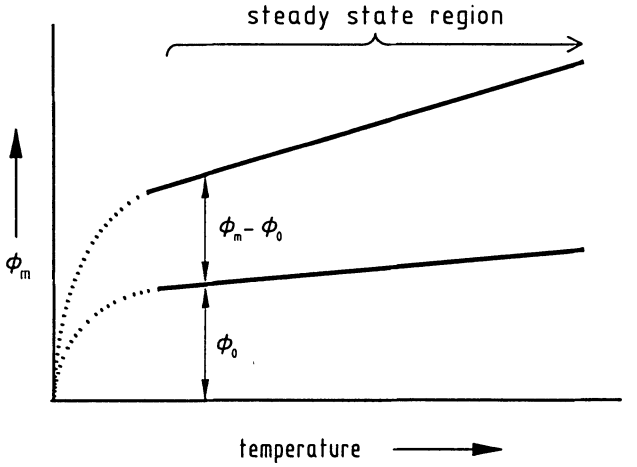

Fig. 4.15. Heat flow rate calibration by means of a known heat capacity C_p.
Φ_m measured heat flow rate, Φ_0 zero line value; calibration factor to determine the true heat flow rate: $K_\Phi = C_p(T) \cdot \beta/(\Phi_m(T) - \Phi_0(T))$

4.4.2 Peak Area Calibration

For peak area calibration, a known heat Q_{true}, dissipated or consumed, is compared with the area of the resulting peak (Figs. 4.16 and 4.17):

$$Q_{true} = K_Q(T) \int_{t_i}^{t_f} [\Phi_m(t) - \Phi_{bl}(t)]\, dt \qquad \text{or}$$

$$Q_{true} = \int_{t_i}^{t_f} [K'_\Phi \cdot \Phi_m(t) - K''_\Phi \cdot \Phi_{bl}(t)]\, dt$$

In principle, $K''_\Phi \neq K'_\Phi$ is valid. Since K_Φ depends on Φ_m and T – which is proportional to time (in all heat flux DSCs and also in power compensation DSCs) –, it cannot be placed in front of the integral. This can be done in a first approximation only if it is assumed that Φ_m and Φ_{bl} are of the same order of magnitude (no dependence on Φ) and the peak width is small (no dependence on T), which is in general the case with phase transitions, not, however, with many polymer transformations.

Integration must be carried out over the whole peak in order that contributions of the 1st derivative of the measurement signal are insignificant.

Peak area calibration can be performed in two ways:

1. If electrical calibration is possible (Fig. 4.16), the advantages connected with electrical heat flow rate calibration (see above) apply analogously to peak area calibration:
   - easy and accurate measurement of the electrically generated heat

$$Q_{true} = -\int P_{el} \cdot dt = -W_{el} = -U \cdot i \cdot \Delta t,$$

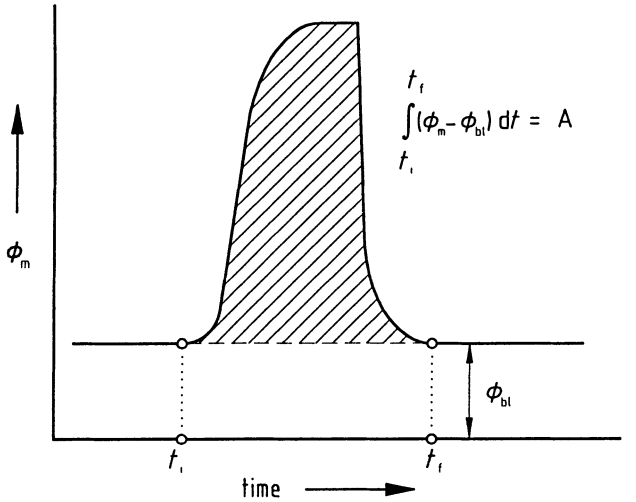

Fig. 4.16. Electrical peak area calibration.
Φ_m measured heat flow rate, t_i, t_f beginning, end of the calibration peak, Φ_{bl} baseline value of the heat flow rate (electric power switched off)

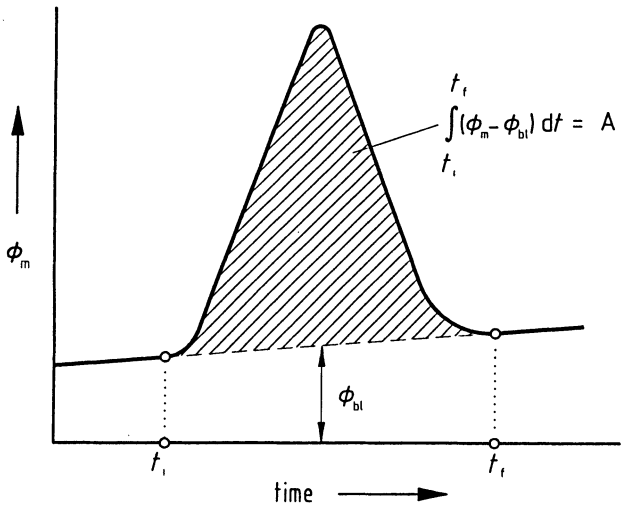

Fig. 4.17. Peak area calibration by means of a known heat of fusion (schematic).
Φ_m measured heat flow rate, t_i, t_f beginning, end of the peak, Φ_{bl} baseline value of the heat flow rate

- peaks of differing size can be produced,
- calibration is possible at any temperature,
- measurement effects (peaks) can be "repeated" (simulated) by appropriately presetting the development of the heating power with time,
- measurement effects (peaks) can be "flanked" during the run by similar calibration peaks.

The disadvantages are the same as those stated in the case of electrical heat flow rate calibration:

- the electric heater can hardly be installed in disk-type measuring systems,
- systematic errors result if heaters are permanently installed (different locations of heater and sample),
- wires give rise to systematic uncertainties (heat leaks).

Care must be taken that electrical calibration is carried out only over a small temperature interval.

2. Peak area calibration of DSCs is usually carried out by means of the heats of melting of pure substances (Fig. 4.17). The advantages of this method are as follows:
   - applicable in all DSCs,
   - calibration heat at the sample location,
   - no wires required,
   - simultaneous temperature and heat calibration is possible with some (selected) calibration materials.

   The disadvantages:

   - calibration possible only at discrete temperatures,
   - no adaptation to the measured peak shape possible,
   - systematic uncertainties due to the special shape of the sample temperature curve $T_S(t)$ during the calibration procedure (melting),
   - uncertainties resulting from the determination of the area (definition of the integration limits and shape of the baseline, cf. Sect. 5.3).

   The calibration procedure for heat flux DSCs is thus as follows:

   - selection of calibration substances which cover the desired temperature range and whose thermophysical characteristic data are similar to those of the sample,
   - weighing-in of such masses which approximately generate a heat effect as is found in normal measurements,
   - adjustment of customary heating rates. (Be careful in the case of calibration substances which melt close to the start temperature: the quasi-steady state must have been reached, the relaxation effects due to the start must have faded; apply lower heating rate if necessary),
   - evaluation of peak (area and extrapolated peak onset temperature T_e),
   - determination of $K_Q(T_e)$, drawing of a calibration curve (establishing a table) or inputting measured data into the apparatus according to the manufacturer's specifications (turning of potentiometer, or by software),

- estimate of the uncertainty of the calibration (uncertainty of the weighing, of the baseline, of the integration limits, of the values for the heat of fusion taken from the literature; the estimated uncertainty from theoretical considerations must be taken into account),
- measurement of the repeatability errors of the calibration factors (or calibration curve). This repeatability error must be clearly smaller than the estimated overall uncertainty of the calibration (see above). The repeatability error is the smallest possible uncertainty of measurement of caloric measurements.

The same calibration procedure is applied to power compensation DSCs, however, in this case, calibration with one calibration material is in general sufficient (e.g. In, cf. Sect. 2.2, 3.2 and Fig. 4.20), as the calibration factor depends on temperature only to a small extent.

4.4.3 Examples of Caloric Calibrations

Calibration Curve

A DSC with cylinder-type measuring system was calibrated with the aid of electric heaters which could be inserted into the sample containers. Only the insert in the sample container was electrically heated; the second insert of the same type placed into the reference container served to establish thermal symmetry.

At regular intervals, heating pulses of defined duration and power were automatically generated over the whole temperature range, the measured signal being put out as an voltage in μV. The peak areas were integrated applying evaluation software. Fig. 4.18 shows schematically the measured curve and the resulting calibration curve.

A heat flux DSC with disk-type measuring system was calibrated with the aid of sapphire (Fig. 4.19).

Differences Between K_Φ and K_Q

When DSCs are calibrated with the aid of the heat of fusion of, for example, metals (peak area calibration) and via the specific heat capacity (heat flow rate calibration), systematic differences occur in practice. This is shown in Fig. 4.20 by the example of a power compensation DSC.

The 1% difference in the case of a power compensation DSC suggests that the difference will be substantially greater for heat flux DSCs. This is confirmed by measurements:

For a heat flux DSC with disk-type measuring system, Fig. 4.21 shows the differences between the average value of a number of heat-of-melting (peak area) calibrations and three (scattering) individual calibrations carried out with the heat capacity of a sapphire sample (heat flow rate calibration).

Dependence on Other Parameters

The repeatability error by which the calibration with a known heat capacity is affected can additionally depend on the sample mass. To give an example, the repeatability error of the calibration of a heat flux DSC with disk-type measuring

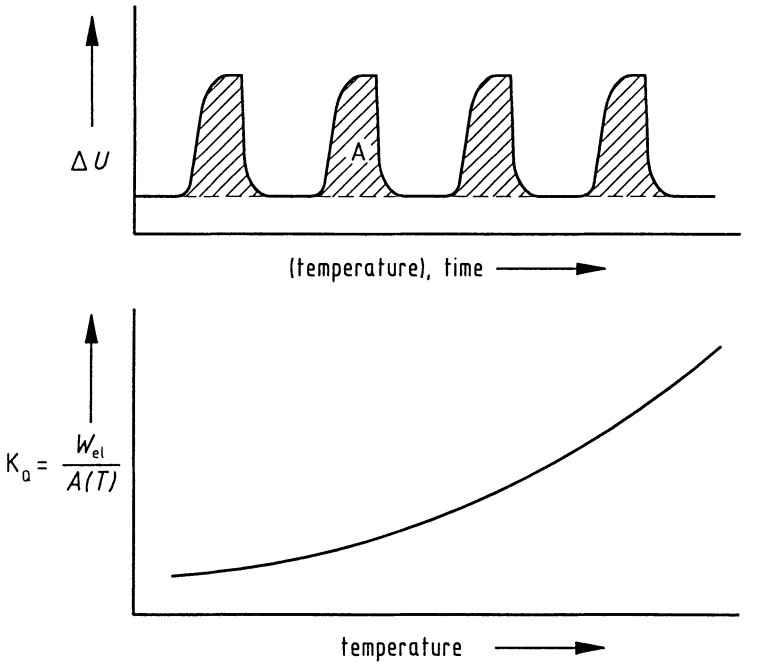

Fig. 4.18. Electrical heat calibration of a heat flux DSC (cylinder-type measuring system with built-in heater, schematic curves).
ΔU measured signal (voltage), K_Q calibration factor for peak area evaluation (in $J\,V^{-1}\,s^{-1}$), A peak area (in V s), W_{el} electrical heating energy (belonging to one peak: $i \cdot \Delta U \cdot \Delta t$). In contrast to Fig. 4.14, the peak areas of the electrical calibration peaks were evaluated here to obtain K_Q. It is also possible to simultaneously determine K_Φ from the electrical heating power

system amounted to 5% when the sample mass was 7 mg; for a sample mass of 27 mg, the scatter decreased to half this amount (Doelman et al., 1977).

Figure 4.22 shows the temperature-dependent systematic difference between the calibration factors, which results when one calibration is carried out with the calibration heater permanently installed (under the bottom of the sample cavity) and the other with the electric heater installed inside the sample (heat flux DSC with cylinder-type measuring system).

The influences of certain parameters (sample mass, heating rate) on the measurement results described in the following, of course, appear analogously during calibration and must be taken into consideration.

For a heat flux DSC with a disk-type measuring system a dependence on the heating rate (Fig. 4.23) resulted for the heat of transition of CsCl.

Figure 4.24 shows the relative dependence of the calibration factor on the heating rate for two different sample masses for a power compensation DSC.

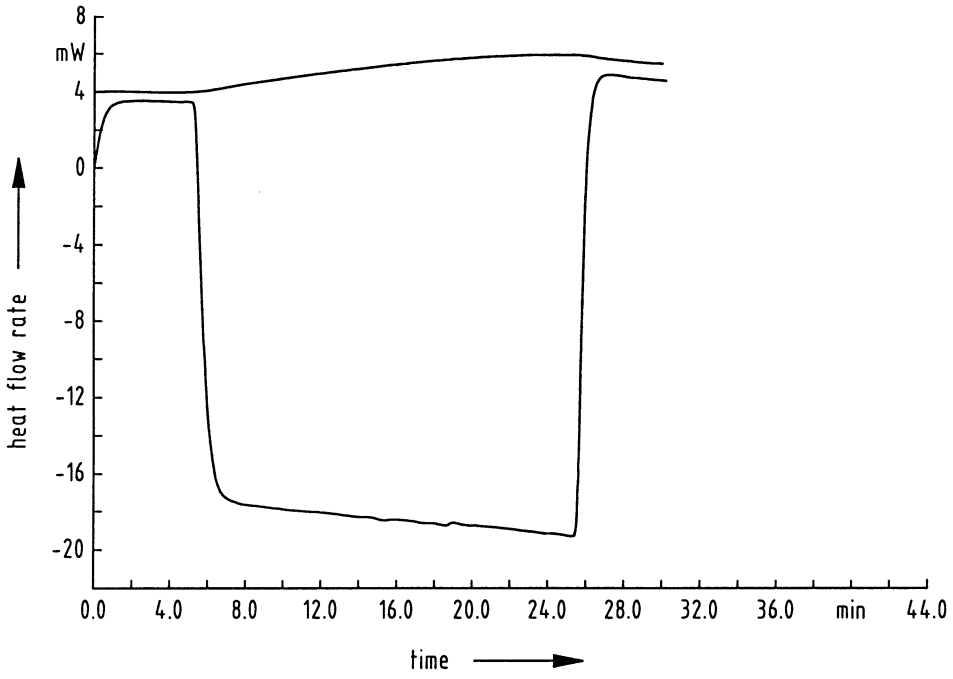

Fig. 4.19. Heat flow rate calibration curve of a disk-type DSC.
Upper curve: Crucibles empty zero line, **lower curve:** 129.6 mg of sapphire, 10 K min^{-1} (acc. to Sarge et al., 1994)

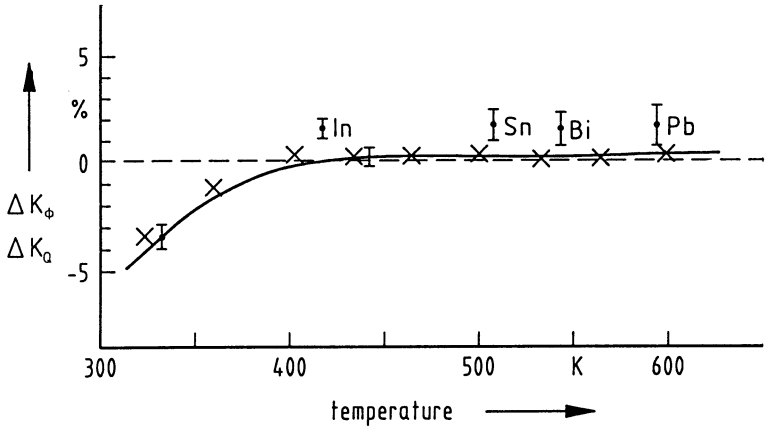

Fig. 4.20 Systematic difference between K_Φ and K_Q in a power compensation DSC. Heat flow rate calibration was carried out with sapphire (solid line) and with copper (crosses); peak area calibration with In, Sn, Bi, Pb (according to Höhne, Glöggler, 1989).
K_Q calibration factor for peak area evaluation, K_Φ calibration factor for heat flow rate measurement, I range of uncertainty of the sapphire measurement (heat flow rate calibration), I range of uncertainty of the heat-of-fusion calibration (peak area calibration)

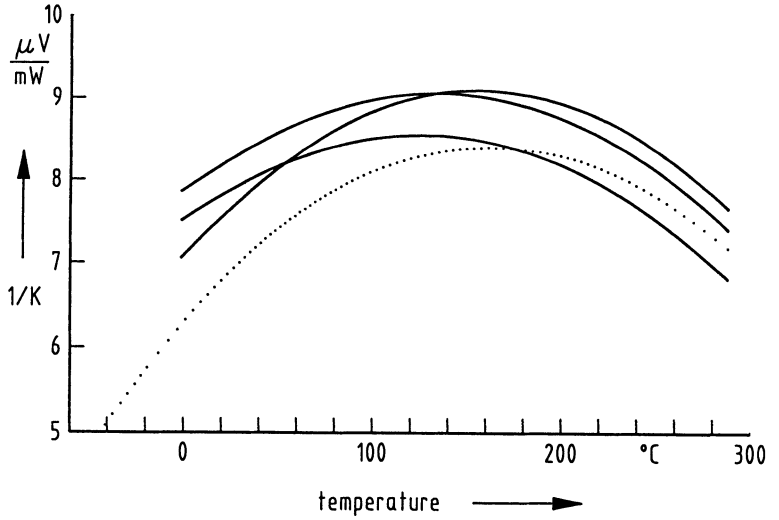

Fig. 4.21. Differences between the heat-of-fusion calibration (peak area calibration) and the calibration by means of a known heat capacity (heat flow rate calibration) (acc. to Sarge, Cammenga, 1985).
K calibration factor, — calibration curve with sapphire (3 measurements at 10 K min^{-1}), ····· average value curve of the calibration with melting samples

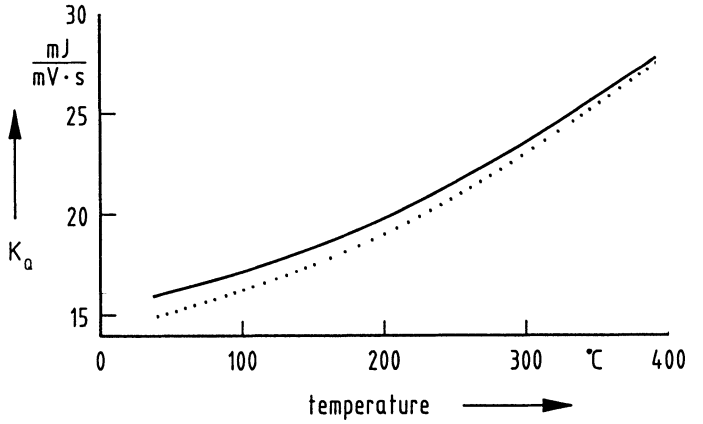

Fig. 4.22. Differences in the electrical peak area calibration of a heat flux DSC with cylinder-type measuring system (acc. to Hemminger, Schönborn, 1982).
K_Q calibration factor for peak area evaluation, — permanently installed calibration heater, below the sample container, ····· miniature heater installed in a copper sample, inside the sample container

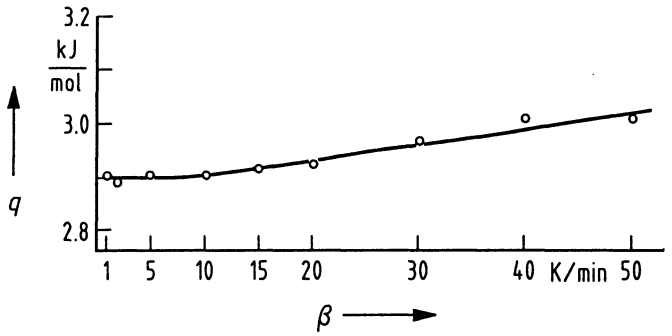

Fig. 4.23. Dependence of the molar heat of transition q of CsCl on the heating rate β for a disk-type DSC (acc. to Breuer, Eysel, 1982)

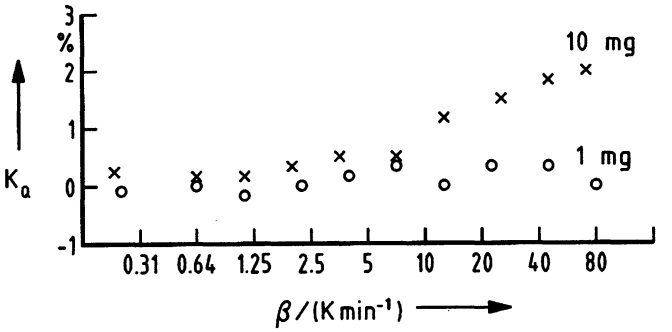

Fig. 4.24 Dependence of the calibration factor K_Q on the sample mass and the heating rate β for a power compensation DSC.
K_Q calibration factor for peak area evaluation (determined by means of the heat of fusion of indium, acc. to Höhne, Glöggler, 1989)

4.5 Conclusions Regarding the Calibration of DSCs

The following conclusions can be drawn from the explanations of Chapter 3 (Theoretical Fundamentals of DSCs), Sect. 4.3 (Temperature Calibration) and Sect. 4.4 (Caloric Calibration).

Temperature Calibration and Temperature Measurement

From among all possible characteristic temperatures which may be assigned to a peak, only the extrapolated peak onset temperature T_e (cf. Fig. 4.1, definition see Sect. 5.1) is relatively independent of sample and test parameters (mass, layer thickness, heat transfer, thermal conductivity and heating rate). This is why only T_e should be used to characterize phase transitions.

T_e should always be corrected to zero heating rate ($\beta = 0$) unless shifting of T_e with the heating rate is the subject of the investigation (for example for kinetic problems). The location of the sample inside the crucible and the calorimetric measuring system is of importance; it should always be the same in precision measurements.

Caloric Calibration and Heat Measurement

Different calibration factors are to be expected for measurements of heats of transition and heat capacities; they must always be determined separately.

It is to be expected that the calibration factor for the heat flow rate depends on the heat flow rate itself (i.e. on the heat capacity of the sample). This must be checked by means of two samples of as different a heat capacity as possible (which must, however, be known).

The reliability of heat capacity measurements by means of heat flux DSCs lies between 5 and 20%; it is 3 to 5% when power compensation DSCs are used. A higher accuracy requires considerable time and effort be spent on the calibration.

When a dual-sample heat flux DSC is used (triple cell DSC, see Sect. 2.1.1), the uncertainty of the heat capacity measurements is lower. A scatter (RMS, see Sect. 7.2) of the calibration factor K_Φ of approx. 1.0 to 1.6% is stated in the literature (see Jin, Wunderlich, 1993).

As regards modulated DSCs, insufficient experimental experience has so far been gained to state reliable figures for the total uncertainty of heat capacity measurements.

Precise heat capacity measurements with heat flux DSCs are possible only if all potential systematic error sources are kept constant by ensuring conditions as identical as possible during the calibration run and measurement run. (Equal mass, equal thermal conductivity, equal heating range, equal heat capacity.)

In the case of peak area calibration, dependence of the calibration factor on the mass of the sample, the heating rate, the peak size, the temperature and on sample properties must be taken into consideration. The respective correlations have to be clarified during calibration and taken into account when the reliability of the results is estimated.

To ensure precise measurements, calibrations prior to the measurements should in principle be as similar to the measurement proper as much as possible. The peak to be measured should be "repeated" (simulated) by electrical calibration if there is the possibility of doing this.

Due to the systematic error sources, a ±5% reliability can be attained when heats of transition are measured with heat flux DSCs. This limit is at ±1% for power compensation DSCs. A prerequisite for a higher reliability is a very elaborate calibration, for example by direct comparison with electric energy.

4.6 Calibration Substances

The requirements to be met by substances to be used for the calibration of DSCs are as follows:

- high (defined) purity (at least 99.999%),
- precisely known characteristic data of the substances,
- non-hygroscopic, insensitive to light, non-toxic,
- no decomposition, chemically stable,
- no reaction with the material of the crucible (see Table 4.8) or with atmosphere,
- negligible vapour pressure,
- grains not too small.

When there are any doubts as to the usability of a substance, i.e. when the risk of persons being injured or equipment damaged cannot be excluded, information should be obtained from experts prior to using such substances.

The following must be observed when calibration samples are prepared:

- clean preparation tools,
- clean crucible,
- no adsorption layers,
- no oxide layers (surface) in the case of metal samples,
- no weighing errors.

4.6.1 Calibration Substances for Temperature Calibration

For the temperature calibration of DSCs, those substances should preferably be used with which the fixed points of the International Temperature Scale of 1990 (ITS-90) are realized*.

Not all substances meet the above requirements. Cadmium, for example, has a high vapour pressure in the liquid state during melting, which may result in injuries to persons and damage to equipment.

The substances used to realize the fixed points of the ITS-90 are listed in Table 4.6 starting with the triple point of neon. These substances have been marked by "ITS-90" (cf. ITS-90, 1990).

Substances which were used to realize the defining fixed points of the International Practical Temperature Scale of 1968 (cf. IPTS-68, 1976) have also been included. (The IPTS-68 was valid until December 31, 1989.) The fixed-point temperatures indicated in the IPTS-68 have been converted to the ITS-90. In addition, al list of secondary reference points was published (Bedford et al., 1984).

To calibrate DSCs in the heating mode, the melting point at zero heating rate ($T_e(\beta = 0)$) is set equal to the solidification (resp. melting) point stated in Table 4.6.

Unfortunately, no suitable fixed-point materials are available for some temperature ranges which is why other substances, too, must be used for the temperature calibration of DSCs. Taking the above criteria into consideration, the German Society for Thermal Analysis (GEFTA) recommends that the substances listed in

* The fixed-point temperatures of metals are associated with the flat part of the temperature-versus-time curve obtained during the slow solidification or melting (in the case of Ga) of very pure metals at a pressure of 101.325 kPa. To calibrate DSCs, it is, however, appropriate to apply the heating mode. (For other calibration substances, cf. Marsh, 1987.)

Table 4.6 Defining fixed points of the ITS-90 and some fixed points of the IPTS-68 (no longer valid) converted to the ITS-90

	T in K	t in °C
Triple point of neon (ITS-90)	24.5561	−248.5939
Triple point of oxygen (ITS-90)	54.3584	−218.7916
Triple point of argon (ITS-90)	83.8058	−189.3442
Triple point of mercury (ITS-90)	234.3156	− 38.8344
Water-ice point	273.15	0.00
Triple point of water (ITS-90)	273.16	0.01
Melting point of gallium (ITS-90)	302.9146	29.7646
Boiling point of water	373.12	99.97
Solidification point of indium (ITS-90)	429.7485	156.5985
Solidification point of tin (ITS-90)	505.078	231.928
Solidification point of bismuth	554.533	271.403
Solidification point of lead	600.612	327.462
Solidification point of zinc (ITS-90)	692.677	419.527
Solidification point of aluminium (ITS-90)	933.473	660.323
Solidification point of silver (ITS-90)	1234.93	961.78
Solidification point of gold (ITS-90)	1337.33	1064.18
Solidification point of copper (ITS-90)	1357.77	1084.62
Solidification point of nickel	1728	1455
Solidification point of palladium	1827	1554
Solidification point of platinum	2041	1768
Solidification point of rhodium	2235	1962
Solidification point of iridium	2719	2446

Table 4.7 are used for temperature calibration. These materials have proved their practical worth, they were carefully tested and cover the temperature range of customary DSCs (Cammenga et al., 1993).

For the compatibility between calibration substances and crucible materials see Table 4.8.

Only the uncertainty of the temperature measurement is decisive for the uncertainty of the calibration when these substances are used. It comprises the pure uncertainty of measurement of the sensors, repeatability errors of the heat transfers in the measuring system and uncertainties in the processing of the analogue signal until it is recorded and evaluated.

4.6.2 Calibration Substances for Heat Flow Rate Calibration

The substances Al_2O_3 and Cu are suitable for heat flow rate calibration purposes. They are chemically stable and the heat capacity is known with an uncertainty of about 0.1% (Tables 4.9 and 4.10).

Table 4.7 Materials recommended for temperature calibration of DSCs (cf. Cammenga et al., 1993)

substance	transition temperature		uncertainty	transition *	ref.**	remarks ***
	T in K	t in °C	ΔT in mK			
Cyclopentane	122.38	−150.77	50	s/s	a	1
Cyclopentane	138.06	−135.09	50	s/s	a	1
Cyclopentane	179.72	− 93.43	50	s/l	a	1
Water	273.15	0.00	10	s/l	b	2
Gallium	302.9146	29.7646		s/l	c	3
Indium	429.7485	156.5985		s/l	c	
Tin	505.078	231.928		s/l	c	4
Lead	600.61	327.46	10	s/l	b	5
Zinc	692.677	419.527		s/l	c	6
Lithium sulphate	851.43	578.28	250	s/s	d	7
Aluminium	933.473	660.323		s/l	c	8
Silver	1234.93	961.78		s/l	c	9
Gold	1337.33	1064.18		s/l	c	9

* s: solid; 1: liquid

** a: Aston et al., 1943, b: Preston-Thomas, 1976 (IPTS-68), c: Preston-Thomas, 1990 (ITS-90), d: Cammenga et al., 1993

*** 1: Only in hermetically sealed crucible. 2: Air-saturated, bidistilled water in hermetically closed crucible. 3: Melt reacts with Al; note that strong undercooling occurs. 4: Melt reacts with Al, Pt. 5: Melt reacts with Pt, oxidizes quickly (use protective gas). 6: Melt (and vapour) react with Al, Pt; high vapour pressure at melting point (approx. 20 Pa). 7: Anhydrate is hygroscopic, thus weigh-in as $Li_2SO_4 \cdot H_2O$. Dehydration takes place from 100 °C, thus turbulent movement of particles in the crucible and high water-vapour pressure (do not use hermetically sealed crucible). Must not melt (change of properties). 8: Melt reacts strongly with Pt. 9: Melt dissolves oxygen, reacts with Pt.

4.6.3 Calibration Substances for Peak Area Calibration

The heats of transition of pure substances for peak area calibration should have been measured with adiabatic precision calorimeters (cf. Appendix 2). Such results are available for only a few substances which fulfill the above requirements (Sect. 4.6). When several independent precise measurements have been carried out on one substance, the ranges of uncertainty stated often do not overlap so that the estimate of the best value and of the overall uncertainty is problematic. Recommended substances are listed in Table 4.11.

The analysis of the relatively large number of measured values of In and Sn obtained by different calorimetric methods allows a minimum uncertainty of about ±0.5% of all values stated in the literature to be assumed (Hemminger, Raetz 1989). When only a few measured values can be used as a basis, these can be affected by substantially greater actual uncertainties as is shown, for example, by the maximum deviations or standard deviations of the values available for Bi (Raetz, 1989).

Table 4.8 Compatibility between calibration substances and crucible materials (according to Cammenga et al., 1993)

crucible material \ calibration substance	Cyclopentane	Water	Gallium	Indium	Tin	Lead	Zinc	Lithium sulphate	Aluminium	Silver	Gold
Corundum, Al_2O_3	□	□	+	+	+	+	+	+	+	+	+
Boron nitride, BN	□	□	+	+	+	+	+	+	+	?	?
Graphite, C	□	□	+	+	+	+	+	+	+	+	–
Silicate glass	+	+	+	+	+	+	?	+	–	×	×
Quartz glass, SiO_2	+	+	+	+	+	+	+	+	–	+	+
Aluminium, Al	+	·	–	+	–	+	–	+	×	×	×
Aluminium, oxidized	+	+	+	+	+	+	+	+	×	×	×
Silver, Ag	+	+	–	–	–	–	–	?	–	×	×
Gold, Au	+	+	·	·	–	–	–	+	–	–	×
Nickel, Ni	+	+	·	·	·	·	·	?	–	+	–
Iron, Fe	+	·	·	+	·	+	–	?	–	+	–
Stainless steel	+	+	·	+	·	+	–	?	–	+	–
Platinum, Pt	+	+	·	·	–	–	–	+	–	–	–
Molybdenum, Mo	+	+	·	?	·	?	·	?	?	?	–
Tantalum, Ta	+	+	?	+	?	?	?	+	–	+	–
Tungsten, W	□	□	·	?	?	·	+	?	·	+	+

+ : No solubility and influence on melting temperature to be expected.
– : Melt dissolves crucible material, greater change of melting temperature.
· : Partial solution processes possible with negligible change of melting temperature.
× : Crucible melts.
? : Compatibility unknown.
□: Combination cannot be realized.

Table 4.9 Heat capacity of α-aluminium oxide (according to Sarge et al., 1994)
Alumina (highly pure $\alpha - Al_2O_3$, synthetic sapphire, corundum)
Molar mass 101.9613 g mol^{-1}

T in K (ITS-90)	c_p in J^{-1} g K^{-1}	$C_{p,\,mol}$ in J mol^{-1} K^{-1}
100	0.1260	12.85
150	0.3133	31.94
200	0.5014	51.12
250	0.6579	67.08
300	0.7794	79.47
350	0.8706	88.77
400	0.9419	96.03
450	0.9976	101.72
500	1.0414	106.19
550	1.0762	109.73
600	1.1042	112.59
650	1.1272	114.93
700	1.1465	116.90
750	1.1630	118.58
800	1.1776	120.07
850	1.1906	121.40
900	1.2026	122.61
950	1.2135	123.73
1000	1.2238	124.78
1050	1.2333	125.75
1100	1.2423	126.66
1150	1.2507	127.52
1200	1.2585	128.32
1250	1.2658	129.07
1300	1.2727	129.77
1350	1.2792	130.43
1400	1.2854	131.06
1450	1.2912	131.66
1500	1.2968	132.23
1550	1.3022	132.77
1600	1.3074	133.30
1650	1.3124	133.81
1700	1.3172	134.30
1750	1.3217	134.77
1800	1.3260	135.20
1850	1.3300	135.61
1900	1.3335	135.97
1950	1.3367	136.29
2000	1.3395	136.58
2050	1.3420	136.83
2100	1.3444	137.08
2150	1.3471	137.35
2200	1.3506	137.71
2250	1.3558	138.24

Table 4.10 Heat capacity of copper (molar mass 63.546 g mol^{-1}) (acc. to Sarge et al., 1994)

T in K (ITS-90)	c_p in J^{-1} g K^{-1}	$C_{p,mol}$ in J mol^{-1} K^{-1}
100	0.2520	16.01
120	0.2867	18.22
140	0.3122	19.84
160	0.3309	21.03
180	0.3447	21.90
200	0.3550	22.56
220	0.3631	23.08
240	0.3699	23.51
260	0.3758	23.88
280	0.3809	24.21
300	0.3850	24.47
320	0.3875	24.63

Table 4.11 Calibration substances for peak area calibration (acc. to Sarge et al., 1994)

substance	T_{trs} (ITS-90) in °C	type of transition *	Q_{trs} in J g^{-1}	uncertainty **
Cyclopentane	−150.77	s/s	69.60	(±0.5%)
Cyclopentane	−135.09	s/s	4.91	(±1.1%)
Cyclopentane	− 93.43	s/l	8.63	(±1.1%)
Gallium	29.7646	s/l	79.88	(±0.9%)
Indium	156.5985	s/l	28.62	(±0.4%)
Tin	231.928	s/l	60.40	(±0.6%)
Bismuth	271.403	s/l	53.83	(±3.9%)
Lithium sulphate	578.28	s/s	228.1	(±4.6%)
Aluminium	660.323	s/l	398.1	(±2.3%)

* s: solid; 1: liquid.
** uncertainties: 2 times standard deviation σ_{n-1}.

Heat flux DSCs have a number of systematic error sources (cf. Sect. 3.1). In our opinion, the reliability of the results obtained with them is therefore of the order of approx. ±5% in routine operation. The uncertainties of the heats of transition indicated in Table 4.11 are therefore sufficient to allow these substances to be used as calibration substances.

Calibration by means of electrically generated heat should be aimed at for precision measurements. In addition, reference is made to the discussion of thermodynamic aspects with respect to the peak area calibration in Sect. 4.2.

The discussion about the suitability of various substances for caloric calibration is at present still going on at the international level. The following complexes of problems are concerned:

- backing-up and redetermination of characteristic data, including an estimate of the uncertainties,
- testing of new substances for their suitability for caloric calibration purposes,
- search for substances suitable for special calibrations, for example polymers (glass transition, heat capacity, special transitions).

5 The DSC Curve

The DSC curve (measured curve) offers quick information on the total measuring process (Fig. 5.1). In addition to the usual measuring effects (C_p changes, transitions, reactions) it can be seen

- whether the predetermined temperature range has been completely covered,
- whether disturbances of the apparatus (mechanical, electrical) occurred,
- whether there were irregularities or unusual shapes of the baseline,
- whether the characteristic temperatures and peak areas lie within the expected range.

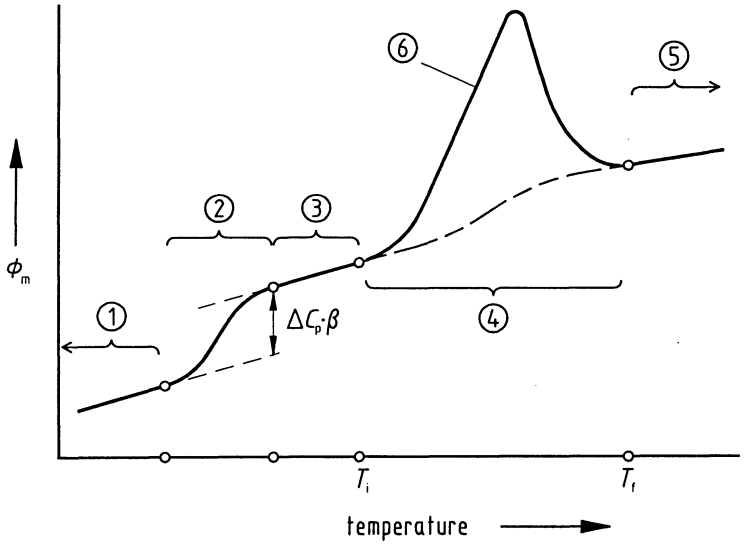

Fig. 5.1. Curve measured by a DSC with step of the baseline (C_p change) and endothermic peak (1st order transition).
ΔC_p change of the sample's heat capacity, T_i, T_f initial peak temperature, final peak temperature, ① initial segment of the measured curve, ② step of the measured curve due to ΔC_p, ③ measured curve, ④ interpolated baseline (between T_i and T_f in the peak region), ⑤ final segment of the measured curve, ⑥ peak (measured curve)

5.1 Characteristic Terms

Some characteristic terms are used to describe a measured curve. They are defined in the following (Fig. 5.2).

- The *zero line* is the curve measured with the instrument empty, i.e. without samples and without sample containers (crucibles), or without samples and with the sample containers (crucibles) empty. It shows the thermal behavior of the measuring system without samples. The smaller the range of variation (repeatability, see Sect. 7.2), the better the instrument,
- the *(interpolated) baseline* is the line which in the range of a peak is constructed in such a way (cf. Sect. 5.3) that it connects the measured curve before and behind the peak as if no heat had been exchanged, i. e. as if no heat (peak) had developed,
- a *peak* in the measured curve appears when the steady state is disturbed by thermally activated heat production or consumption in the sample. Peaks in heat flow rate curves, which are assigned to endothermic processes, are plotted "upwards" (positive direction), as heat added to a system is defined as positive in thermodynamics. A peak begins at T_i (first deviation from the baseline, see below), ascends/descends to the peak maximum/minimum, T_p (see below), and merges into the baseline again at T_f. Only those transitions associated with a heat of transition (e.g. melting) lead to a peak (except for changes in the heat transfer

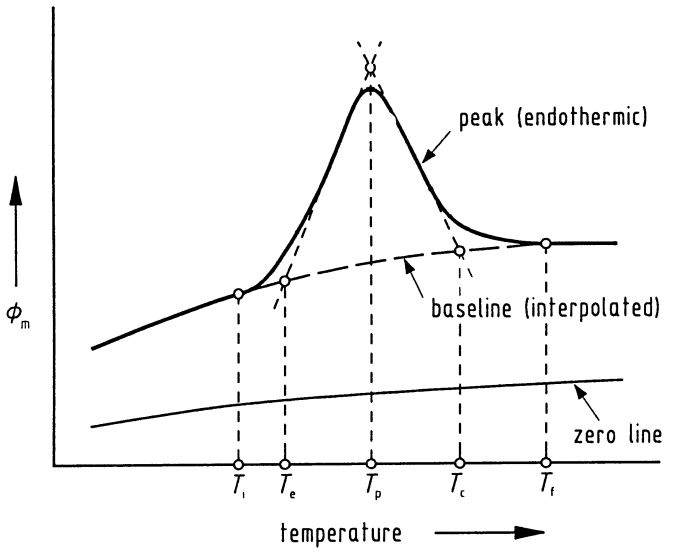

Fig. 5.2. Definition of zero line, baseline, peak and the characteristic temperatures (definitions see text).
T_i initial peak temperature, T_e extrapolated peak onset temperature, T_p peak maximum temperature, T_c extrapolated peak completion temperature, T_f final peak temperature

between the sample and the temperature sensor). Other transitions (e.g. glass transitions) only lead to changes in the shape of the measured curve, for example step changes (see Sect. 6.2.3),

- the characteristic temperatures are defined as follows:
  - T_i *Initial peak temperature*
    Here the curve of measured values begins to deviate from the baseline, the peak begins,
  - T_e *Extrapolated peak onset temperature*
    Here the auxiliary line through the ascending peak slope intersects the baseline. (The auxiliary line is drawn through the (almost) linear section of the ascending peak slope, either as inflectional tangent or as fitted line. The distinction between the two methods is of no significance in practice, as the resulting difference is smaller than the repeatability error of the measurement results.),
  - T_p *Peak maximum temperature*
    This temperature designates the maximum value of the difference between the curve of measured values and the interpolated baseline (not necessarily the absolute maximum of the curve of measured values),
  - T_c *Extrapolated peak completion temperature*
    Here the auxiliary line (see above) through the descending peak slope intersects the baseline,
  - T_f *Final peak temperature*
    Here the curve of measured values reaches again the baseline, the peak is completed.

5.2 Influencing Parameters

In Sects. 4.3 and 4.4, reference has already been made to the influence of some parameters in connection with the calibration. These statements apply by analogy to each measurement.

For highly precise measurements, the baseline must be determined prior to and after the measurements. Temperature and heat calibration must then also be checked at regular intervals (depending on the specific DSC) at least with one calibration substance, e.g. indium. If the DSC shows a distinct tendency towards drifting, a daily test is important.

In this way, information is obtained about drift processes or scatter which cannot be assigned to an exactly known parameter. This information enters into the estimate of the overall uncertainty.

The influencing parameters are listed in the following:

1. The shape of the zero line (without crucibles) is influenced by the heating rate, the kind of purge gas and its flow velocity, likewise by the temperature of the surroundings and by surface properties of the measuring system. If the zero line is measured with the crucibles empty added to this are influences due to unequal masses of the crucibles, differences in the heat transfer between the crucibles and

the furnace, differences between the emissivities of the two crucibles (lids), and influences due to type and material of the crucibles used.

2. Point 1 is also applicable to the shape of the measured curve outside a peak with sample and reference sample placed in the crucibles. In addition, the properties of the reference sample (heat capacity and its temperature dependence) are of importance (differential measurement). In the case of pure C_p changes of the sample (e.g. glass point, Curie point), these changes determine the shape of the measured curve which then contains the desired information. Unfortunately, changes of the measured curve can also take place if the conditions of heat transfer to the sample change abruptly. This type of step changes usually appears statistically and can thus be distinguished from the glass transition of homogeneous samples which always occurs at the same temperature.
3. Point 2 is also applicable to the shape of the measured curve with peak. The peak itself is additionally influenced by
   - the heating rate (cf. Figs. 3.11, 4.10),
   - the thermal conductivity of the sample (cf. Fig. 3.13),
   - the mass and heat capacity of the sample (cf. Fig. 4.24),
   - the structure of the sample (powder, granulates, foil, ...),
   - the thermal resistance between sample and temperature sensor (cf. Reichelt, Hemminger, 1983),
   - the location of the sample in the crucible or measuring system (cf. Fig. 4.13),
   - the kind of gas in the cavity of the measuring system influences the separation (resolution) of closely adjacent peaks (and the calibration).

In addition, attention must be paid to:

- the sample purity,
- the thermal history of the measuring system (cf. Suzuki, Wunderlich, 1984).

Conclusion

Ensure that all the parameters for the measurement are as similar as possible to those for calibration. Use samples of defined state, shape and purity.

5.3 The Baseline and the Determination of the Thermodynamic Functions

The baseline has been defined in Sect. 5.1 (cf. Figs. 5.1, 5.2):

In the region of a peak, the baseline is the curve between T_i and T_f which would have been recorded if all C_p changes (and changes of heat transfer etc. that also influence the baseline) had occurred but no heat of transition had been released. The area between baseline and measured curve is a measure of the heat of transition.

Construction of the Baseline

For 1st order transitions with or without coupled C_p change (and/or change of the heat transport mechanism), the baseline must be constructed (cf. Hemminger, Sarge, 1991). A definite baseline can be constructed only if a pure C_p change

occurs; changes of heat transport conditions in the range of a peak give rise to uncertainties in the shape of the baseline. For certain evaluations (for example kinetics), the measured curve and the respective baseline must possibly be "desmeared" (cf. Sec. 5.4).

1. For *irreversible* transformations without measurable C_p change, the baseline can basically be determined by repeating the measurement with the same sample whose reaction process has come to an end. In these cases, the baseline is interpolated with the help of the measured curve of the 2nd run (example: annealing of lattice defects during recrystallization of a plastically deformed metal). The baseline uncertainty corresponds to the repeatability error of the DSC.
2. For transformations with continuous C_p changes (without changes of the heat transfer conditions), the transformed mass fraction is in principle known for any particular time of the transformation (conservation of mass). Thus, the C_p change coupled to it is also known.
3. Expressed more generally and in a purely formal manner (for example for a non-horizontal measured curve outside the peak), the following is valid: When the degree of reaction $\alpha(t)$ is known (possibly only by approximation), the baseline can be constructed according to van der Plaats, 1984.
   For the change of the slope of the baseline between T_i and T_f, the following is valid in good approximation (see Fig. 5.3).

$$\left(\frac{d\Phi}{dt}\right)_{bl} = (1-\alpha)\left(\frac{d\Phi}{dt}\right)_{T_i} + \alpha\left(\frac{d\Phi}{dt}\right)_{T_f}$$

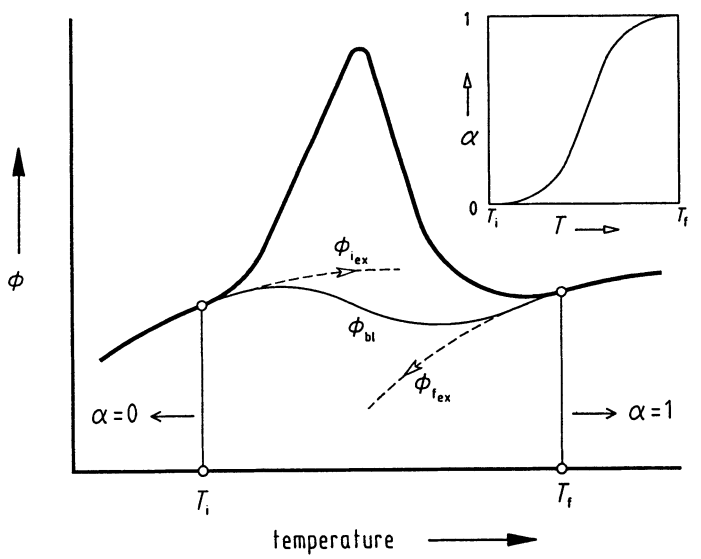

Fig. 5.3. Construction of the baseline taking the degree of reaction $\alpha(t)$ into account (acc. to van der Plaats, 1984).
T_i initial peak temperature, T_f final peak temperature, $\Phi_{i_{ex}}$, $\Phi_{f_{ex}}$ measured curve extrapolated from T_i, T_f into the peak region

That is to say, $\alpha(t)$ determines how quickly the slope of the baseline changes from the slope of the measured curve in T_i (with $\alpha = 0$ for $T < T_i$) in the interval $T_i \leq T \leq T_f$ with $\alpha = \alpha(t)$) to the slope of the measured curve in T_f (with $\alpha = 1$ for $T > T_f$). In the interval between T_i and T_f, the following results by approximation for the functional values Φ_{bl}:

$$\Phi_{bl} = (1 - \alpha)\, \Phi_{i_{ex}} + \alpha \cdot \Phi_{f_{ex}}$$

where $\Phi_{i_{ex}}$ and $\Phi_{f_{ex}}$ are the segments for the measured curve extrapolated into the peak range from the left-hand and right-hand side, respectively. That is to say, $\Phi_{i_{ex}}$ and $\Phi_{f_{ex}}$ are to be calculated as polynomials and extrapolated into the peak range in order that the baseline can be calculated according to the above equation. (When deriving this relation it has been assumed that the difference between the slopes of the measured curves in T_i and T_f is not extreme; otherwise, this should be taken into account as well.)

Integration of the peak area can be carried out at once using the difference between the (desmeared) measured curve and the baseline $\Phi(t) - \Phi_{bl}(t)$.

4. If the heat capacity of the sample changes suddenly by ΔC_S at the transition temperature T_{trs} with a constant sample temperature prevailing during transition (first-order phase transitions), the change in the heat capacity is described by a step function at $T = T_{trs}$. By the "RC-elements" of the measuring system (cf. Figs. 3.7, 3.9), this step function is transformed into an exponential function (of time) (see Hemminger, Sarge, 1991).
5. For transformations showing a jump of the baseline the cause of which is not known and which is not necessarily coupled to the fraction transformed during the reaction (for example spontaneous change of the heat transfer between sample and container), there is no method for finding the "correct" baseline which can be backed up theoretically. Figure 5.4 shows several possible constructions. The peak area very much depends on the selected baseline. For this reason, several possibilities should always be tried out (see Hemminger, Sarge, 1991). The differences in the peak areas (or heat flow rates) appear as systematic uncertainties of the measurements and must be taken into account when the overall uncertainty of measurement is estimated.

The baseline undergoes changes when C_p changes; additional changes may result when:

- the thermal conductivity of the sample changes substantially during transition,
- the thermal resistance (heat exchange conditions) between sample and temperature sensor changes during transition (e.g. during melting),
- the conditions for the heat transfer between sample and surroundings change, for example when the emissivity of the sample changes due to a reaction and the sample is positioned in an open crucible.

When such changes coincide with C_p changes, the uncertainty of how the baseline should be determined generally increases. There is then no method for constructing a "true" baseline.

As emphasized previously, all the theoretical discussions presume a zero line which is at least an absolute straight line. If not, the zero line must first be sub-

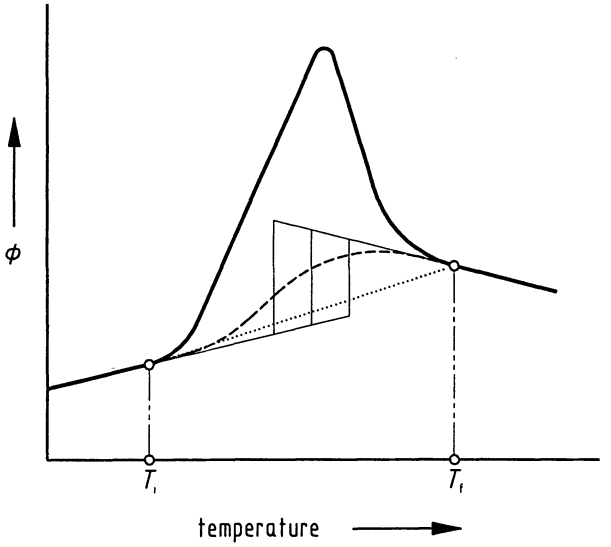

Fig. 5.4. Possible baselines when the reasons for the "baseline jump" between T_i and T_f are not known.
T_i initial peak temperature, T_f final peak temperature, — linear extrapolation into the peak region and jump somewhere between T_i and T_f, – – – constructed by means of an "apparent" transformation function, ···· straight line between T_i and T_f

tracted from the measured curve before the described procedures can be carried out correctly. It is highly recommended that this be done for every measurement. This does not usually require more time and effort to be spent on measurements, as in most cases the zero line does not change very much during a set of measurements if the conditions which influence the zero line (see Sect. 5.2) are kept constant. It is therefore possible to use the same zero line – measured in the morning – for all measurements of the same kind during a working day. Only for highly precise measurements is a separate zero line required in each case and they therefore take twice the time.

Except for a constant factor – namely the heating rate and the mass (see Sect. 2.1.1) – and, of course, the calibration factor, the measured curve with the zero line subtracted is identical with the heat capacity curve. As a consequence, the baseline for its part is proportional to the pure heat capacity of the sample in question. Bearing this in mind, a method can be specified, which allows the latent heat (of a transition or reaction) to be determined from a corrected zero line or a C_p curve without a baseline being constructed.

The procedure will be demonstrated using melting as an example, which is a 1st order thermodynamic transition (Richardson, 1993). Figure 5.5 shows schematically the C_p curve prior to, during and after the transition. The heat capacities $C_{p,s}(T)$ for the solid prior to melting and $C_{p,l}(T)$ for the liquid after transition differ both in their absolute values (at the same temperature) and also in their temperature dependence.

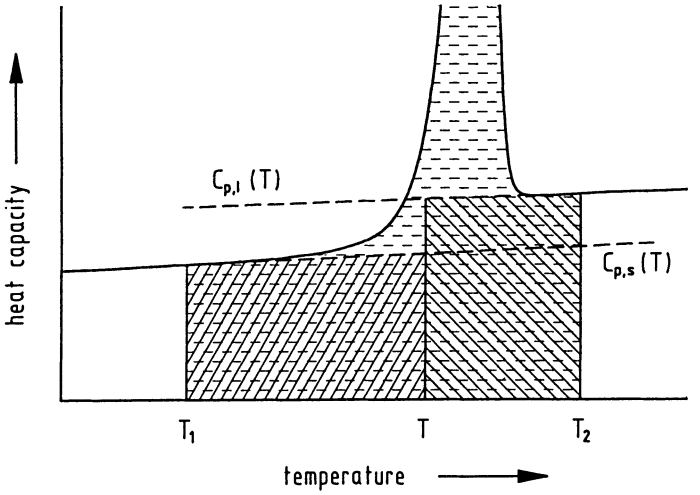

Fig. 5.5. The determination of thermodynamically valid values for the enthalpies of transition (acc. to Richardson, 1993). The limiting temperatures T_1 and T_2 must be chosen well below or above the transition interval.

$\Delta H(T) = Q - A - B$, Q: A: B:

The kind of functional dependence of the heat capacity on the temperature (linear dependence, polynomials of higher order) is unimportant. Extrapolations into temperature ranges that are not directly measurable must, however, be reliable. If this is guaranteed, the heat absorbed over a wide temperature interval can be divided into C_p portions and the isothermal enthalpy of fusion that is of interest. The following is valid (cf. Fig. 6.15):

$$\Delta H(T) = H_l(T) - H_s(T)$$

$$\Delta H(T) = (H_l(T_2) - H_s(T_1)) - H_s(T) - (H_s(T_1)) - (H_s(T_2)) - H_l(T))$$

$$\Delta H(T) = (H_l(T_2) - H_s(T_1)) - \int_{T_1}^{T} C_{p,s}(T)\,dT - \int_{T}^{T_2} C_{p,l}(T)\,dT$$

$$\Delta H(T) = Q - A - B$$

The three quantities Q, A and B can be determined from the measured curve (hatched differently in Fig. 5.5).

Enthalpies of reaction uniquely defined from the thermodynamic viewpoint can be determined analogously; however, this determination presents some special features (cf. Sec. 6.2.2.1) and Figs. 6.13 to 6.16.

At low heating and cooling rates, if necessary after previous desmearing of the measured curve, the entropy change over temperature ranges in which no transi-

tions take place can be determined with sufficient accuracy according to the following equation:

$$\Delta S = \int_{T_1}^{T_2} C_p(T) \frac{\mathrm{d}T}{T}$$

The situation is different if phase transitions are included, in principle these are shifted on the measured curve relative to the true temperature of equilibrium T_{eq} (cf. Sect. 5.4.4). Nevertheless, if in compliance with the above prescription, T_{eq} and $\Delta H(T_{eq})$ are known, the reversibly exchanged entropy of transition can be calculated from the quotient $\Delta H(T_{eq})/T_{eq}$. It is then possible to calculate changes in the entropy and the free enthalpy for arbitrary temperature intervals. If a certain substance exists in several forms, information on their thermodynamic stability as a function of temperature can be obtained.

5.4 Desmearing of the DSC Curve

The user of DSC is usually interested in the heat flow rate into the sample to be investigated or in the related thermodynamic potential function (depending on the temperature), which is either the specific heat capacity $c_p(T_{sample})$ or the enthalpy change $\Delta H(T_{sample})$. The measured curve put out by the calorimeter usually shows the temperature difference between sample and reference support ($T_{MS} - T_{MR}$) as a function of time, or a function proportional to it, which is only a more or less "smeared" representation of the function searched. Degree and quality of this "smearing" differ depending on the type of DSC, and they, moreover, depend on measurement parameters (heating rate, temperature, sample size). The theoretical relations which lead to this smearing have been quantitatively described in Chapter 3 in various approximations.

In many cases the curve measured by the DSC is a sufficiently exact representation of the functions searched, and the desired evaluations can be directly made. When the accuracy requirements are higher, or kinetic evaluation must be performed, the measured curve (and the interpolated baseline) must be corrected and converted prior to their being used to determine the thermodynamic potential function (ΔH) of the sample or its derivative (C_p). This procedure is referred to as "desmearing" and will be described in detail in the following. It should therefore be made quite clear, when individual corrections are required, when they can be dispensed with and which will be the consequences for the uncertainty of the results.

Figure 5.6 schematically shows the relation between the heat flow rate curve recorded by the DSC and the desired potential function for the case of a 1st order endothermic phase transition. Accordingly, desmearing takes place in several steps:

1. Linear transformation of the abscissa (indicated temperatures) in compliance with the results of the calorimeter's temperature calibration, and transformation of the ordinate (indicated heat flow rates) in compliance with the results of the calorimeter's heat flow rate calibration.

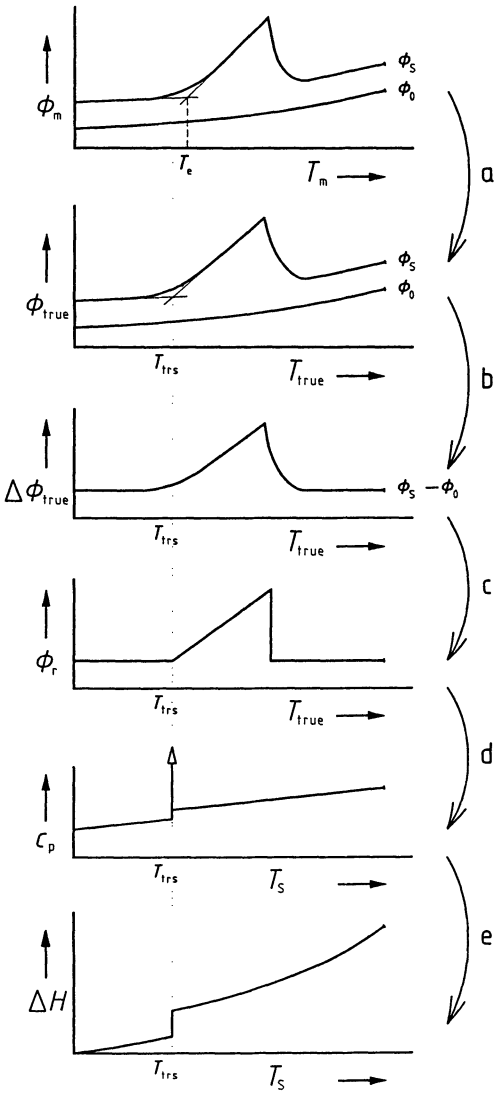

Fig. 5.6. Curve measured by a DSC for a 1st order endothermic transition and its evaluation. **a** Scaling of temperature and heat flow rate axes on the basis of the calibration, **b** Zero line (crucibles empty) subtracted from the measured curve, **c** Desmearing due to influences from the apparatus (thermal lag), **d** Conversion into the heat capacity function, **e** Calculation of the enthalpy function.

Φ_m heat flow rate (measured curve), Φ_S heat flow rate into the sample, Φ_0 zero line heat flow rate, Φ_{true} heat flow rate after calibration, $\Delta\Phi_{true}$ sample heat flow rate Φ_S minus zero line heat flow rate Φ_0, Φ_r reaction heat flow rate into the sample, T_m temperature (measured), T_{true} temperature after calibration, T_{trs} transition temperature, T_S sample temperature, C_p heat capacity of the sample, ΔH enthalpy change

2. Determination and subtraction of the zero line (sample crucibles empty).
3. Mathematical elimination (deconvolution) of the influence which heat transport phenomena inside the DSC (heat flow rate relaxation) exert on the measured curve.
4. Conversion of the heat flow rate function into the specific heat capacity of the sample, i.e. (non-linear) variable transformation of the temperature measured by the DSC into the true sample temperature.
5. Integration leading to the thermodynamic potential function (enthalpy).

The required steps will be described in closer detail in the sections below.

5.4.1 Correction of the Temperature and Heat Flow Rate Indicated

This procedure has already been described in Sect. 4.3, however, for the sake of completeness, reference to it will be made again in the following.

For the correction of the temperature indicated at the heating or cooling rate β, the following is valid.

$$T_{\text{true}} = T_{\text{m}} + \Delta T_{\text{corr}}(\beta) \tag{5.1}$$

$$\Delta T_{\text{corr}}(\beta) = \Delta T_{\text{corr}}(\beta = 0) - \Delta T(\beta)$$

$\Delta T_{\text{corr}}(\beta = 0)$ results from the calibration measurements, and $\Delta T(\beta)$ must either be determined experimentally as it may be different from one sample to the other, or it is determined by approximation from the results of the calibration measurements (cf. Sect. 4.3.1). The above equations describe a shift of the temperature axis scaling of the output measured function, a shift which is different for each heating rate. A simple correction is concerned here which must of course be carried out only if it is significant for the accuracy required for the measurements. The correction of the displayed temperature according to Eq. (5.1) takes only influences from the instrument into account. Samples of great thickness possibly require an additional correction which also considers the temperature profile inside the sample; this correction is described below (Sect. 5.4.4).

The following equations are valid for the correction of the displayed heat flow rate (cf. chapter 3 and Sect. 4.4.1).

$$\Phi_{\text{true}} = K_{\Phi} \cdot \Phi_{\text{m}} \quad \text{or} \quad \Phi_{\text{true}} = -K \cdot \Delta T_{\text{m}}$$

The factors K_{Φ} (or K) are determined by suitable calibration measurements (cf. Sect. 4.4.1). The negative sign in the above equation is not always used consistently; it results from the differing definitions of the sign of ΔT_{m} (measured temperature difference) and Φ_{m}. A linear transformation of the Φ-axis of the measured curve put out, with the form of the function maintained, is, however, only possible if K_{Φ} (or K) is not temperature-dependent in the range of interest. This case is often given only for relatively small temperature ranges (e.g. for a transition peak). In all other cases (above all when the heat capacity is measured over temperature ranges of 100 K or more), the form of the function must be recalculated according to the following equation, the scaling of the T-axis being retained:

$$\Phi_{\text{true}}(T) = K_{\Phi}(T) \cdot \Phi_{\text{m}}(T) \quad \text{or} \quad \Phi_{\text{true}}(T) = -K(T) \cdot \Delta T_{\text{m}}(T)$$

5.4.2 Subtraction of the Baseline

It is not possible to manufacture a perfectly symmetrical DSC in which the differential signal between empty sample system and reference sample system is exactly zero over the entire temperature range. This also applies to the measured curve with the sample crucibles empty (zero line).

To obtain the true heat flow rate into the sample (for example, to calculate the sample's heat capacity), the instrument's asymmetry must be separately determined by a second measurement and the zero line (crucibles empty) subtracted from the signal actually measured.

To correctly determine this zero line, all parameters of the zero line measurement should correspond to those of the actual measurement (with the sample crucible being, however, empty in this case).

The correction of the instrument asymmetry presents the problem that the two measurements can be carried out only one after the other; one must therefore ensure that the DSC's symmetry properties have not changed in the meantime. This is a strict condition which means that high requirements must be met by the calorimeter (cf. Sect. 7.2).

In addition, it is unavoidable that the DSC is opened between the two measurements and the sample crucible changed or moved. This alone can change symmetry properties, which results in the zero line being shifted.

The design of the evaluation software of the DSC computers is normally such that the zero line (empty crucibles) is first subtracted and then the corrections of the temperature and heat flow rate scales (see above) are made. This order is justified only if the scale corrections for the measurement and the baseline are the same. In all other cases, first the correction and then the subtraction must be made. The same is true of all advanced desmearing procedures.

5.4.3 Calculation of the True Heat Flow Rate into the Sample

Owing to the design of the DSC's measuring system, the heat flow rate into the sample cannot be measured directly; the measurement always yields only a heat flow rate at a certain distance from the sample, outside the sample crucible. Due to the finite thermal conductivity of the material between this point of measurement and the sample, the measurement signal is always a smeared representation of the reaction heat flow rate, the kind and degree of smearing depending basically only on the DSC construction.

Good DSCs allow the theory of linear response to be applied to this problem. Using this tool, ways have been found to calculate the true reaction heat flow rate from the measured heat flow rate curve. These methods are generally referred to as *deconvolution* or *desmearing*; they will be described in the following.

Solution of the Differential Equation

For simple cases, the behavior of a calorimeter can be described by normal differential equations.

The mathematical interrelation has already been dealt with in Chapter 3. The desired function $\Phi_r(t)$ can therefore be calculated from the measured function Φ_m (or $\Delta T(t)$ which is linked with Φ_m by the equation $\Phi_m = -k' \cdot \Delta T(t)$), using Eq. (3.6) in the following form:

$$\Phi_r(t) = \Phi_m + a_1 \frac{d\Phi}{dt} + a_2 \frac{d^2\Phi_m}{dt^2} \tag{5.2}$$

Accordingly, the desired function is a simple sum of terms which include the measured function and its derivatives. The coefficients a_1 and a_2 include the time constants τ_1 and τ_2 of the instrument and thus thermal resistances and capacities of the measuring system. Equation (5.2) can easily be realized by an electronic circuit with operational amplifiers. The desmeared signal can then be determined "online" (simultaneously) from the measured signal $\Phi_m(t)$. It is indeed also possible to calculate it from the (stored) function $\Phi_m(t)$ after the measurement has been concluded.

Although the problem is easily solved (mathematically or by electronic means), the determination of the proper coefficients a_1 and a_2 is not so easy in practice. The times constants τ_1 and τ_2 (Eq. (3.7)) can be determined from the measured function of a pulse- or step-like event (cf. Fig. 3.10), but the actual relation to a_1 and a_2 may be more complex than the approximative calculations in Sect. 3.1 possibly predict. There is no other way than to adjust these two coefficients until the results of the desmearing procedure (on-line or calculated) coincide with the original heat flow rate Φ_r inside the sample. The best method to test it is to switch on a constant heat flow rate (for a certain time) with the aid of a built-in electric heater.

Numerical Methods

If the behavior of the DSC cannot be described by simple differential equations within the framework of the required accuracy (e.g. in the case of power compensation DSCs), another method must be applied which has its roots in the theory of linear response. It is valid for all measuring systems which work linearly, that is to say, the measured signal for two distinct pulse-like events in the sample must be the sum (superposition) of the two single functions from each individual event (Fig. 5.7). Another condition is that all measured functions (curves) of various pulse-like events should have the same shape, in other words all these measured functions divided by their peak area (normalizing) must yield the same function, the so-called apparatus (or Green's) function $a(t)$.

If these conditions are fulfilled, the following is valid:

$$\Phi_m(t) = \int \Phi_r(t') \cdot a(t - t')\, dt' \equiv a(t) * \Phi_r(t) \quad \text{(convolution)} \tag{5.3}$$

This equation is valid for all DSCs which work in the above-described linear manner, irrespective of whether a certain approximative formula (such as Eq. (3.6)) is known. Only the "apparatus function" $a(t)$ must be known which can easily be derived from a pulse-like event (usually produced with a built-in electric heater), or by the sudden solidification of a strongly supercooled melt of a pure metal.

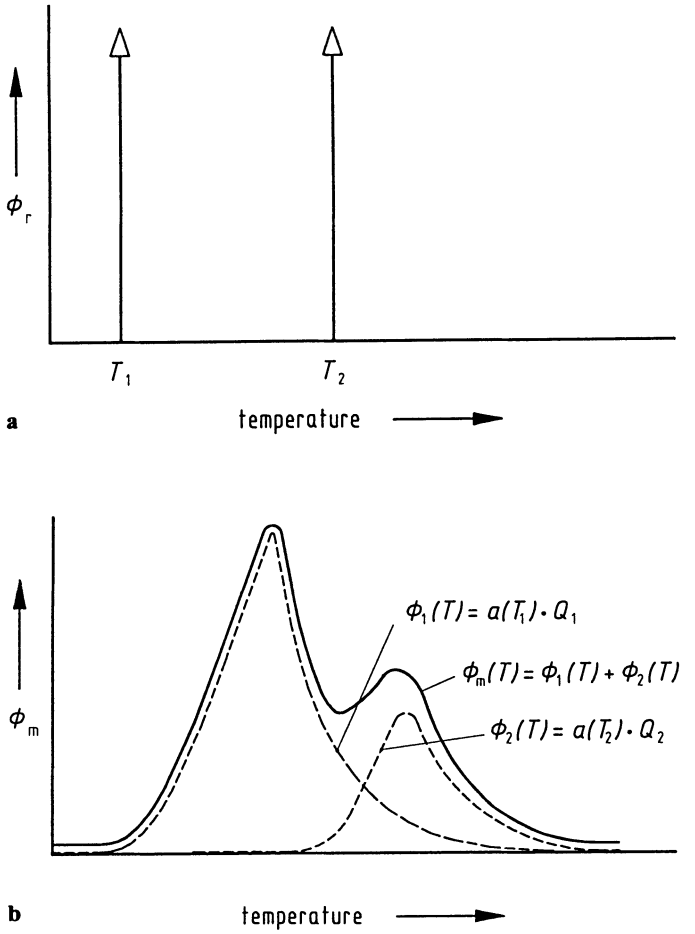

Fig. 5.7. Linear response of a DSC.
a Pulse-like heat events inside the sample at temperatures T_1 and T_2 in the scanning mode, **b** Measured DSC curve, - - - -: hypothetic (measured) curves of the individual events at T_1, T_2, —: recorded (superposed) curve measured for two successive events, Φ_r heat flow rate developed in the sample, Φ_m measured heat flow rate (measured signal), Q heat of the event, $a(T)$ apparatus function of the DSC

The seamy side of this desmearing method, which is also called "deconvolution"* is the rather ambitious mathematics required to solve the integral equation (5.3) for the function of interest $\Phi_r(t)$. There are essentially two methods, the Fourier transform and the recursion method. Both require numerical calculations with a computer.

* Deconvolution is a particular case of "desmearing" carried out by solving the "convolution integral".

The *Fourier transform* represents an integral operation:

$$\mathfrak{F}(f(x)) = 1/2\pi \cdot \int f(y) \exp(\mathrm{i}xy)\, \mathrm{d}y$$

Applied to the convolution integral (Eq. (5.3)), it yields (see textbooks of mathematics):

$$\mathfrak{F}(\Phi_m(t)) = \mathfrak{F}(\Phi_r(t)) \cdot \mathfrak{F}(a(t)) \qquad \text{(convolution theorem)}$$

Thus the convolution product turns into an ordinary product which can be solved for

$$\mathfrak{F}(\Phi_r(t)) = \frac{\mathfrak{F}(\Phi_m(t))}{\mathfrak{F}(a(t))}$$

The desired function is obtained by an inverse Fourier transform:

$$\Phi_r(t) = \mathfrak{F}^{-1}\mathfrak{F}(\Phi_r(t)) = \mathfrak{F}^{-1}\left\{\frac{\mathfrak{F}(\Phi_m(t))}{\mathfrak{F}(a(t))}\right\}$$

This method can be applied in all cases. Today, the Fourier transform is commonly included in the program library of computers. The drawbacks of this procedure lie in its laborious course and abstract nature, since the calculations are performed in Fourier space. Those who lack experience in numerical Fourier transforms are advised to study some "pitfalls" such as the "break-off effect" and the "sampling theorem", both obtained by numerical treatment. Under specific conditions this simulates periodicities and fluctuations which do not reflect any actual processes in the sample. Please refer to the literature for further details (e.g. Bracewell, 1965).

The *recursion method* for solving the convolution integral, Eq. (5.3), starts from the following recursion formula:

$$\Phi_{r_0}(t) = \Phi_m(t)$$

$$\Phi_{r_n}(t) = \Phi_{r_{(n-1)}}(t) + (\Phi_m(t) - a(t) * \Phi_{r_{(n-1)}}(t)) \tag{5.4}$$

The deviation between the "reconvoluted", still inaccurate synthetic function $a(t) * \Phi_{r_{(n-1)}}(t)$ and the measured function $\Phi_m(t)$ is used additively for a simple correction of the approximation.

The recursion formula (5.4) does not converge for all event functions. Abrupt changes and steps (on-off effects and similar phenomena) generate oscillations of the approximation function which diverge rapidly. In the case of the "smooth" curves commonly encountered in calorimetry, the procedure converges quickly and without problems.

The desmeared curve $\Phi_r(t)$ is the basis of any further kinetic evaluation since the result of these procedures strongly depend on the exact shape of the transformed mass fraction, i.e. the reaction heat flow rate function, (see Sect. 6.2.2.2).

It should be noted that every deconvolution procedure increases the noise. The better the resolution in time the higher the noise. Desmearing should therefore be carried out only if it is necessary, i.e. for events (reactions) whose width is in the same order of magnitude as the time constant of the DSC.

Both numerical desmearing procedures can be applied only after the measurements have been concluded (off-line). For the case of a discrete (sampled) function, the convolution integral (Eq. (5.3)) can, however, be represented as a linear system of equations.

$$\Phi_m(t_i) = \Delta t \sum_{k=1}^{i} \Phi_r(t_k) \cdot a(t_{i-k+1}) \qquad (i = 1 \ldots n)$$

which can be resolved for $\Phi_r(t_i)$:

$$\Phi_r(t_i) = \frac{1}{a(t_1)} \left[\frac{\Phi_m(t_i)}{\Delta t} - \sum_{k=1}^{i} \Phi_r(t_k) \cdot a(t_{i-k+1}) \right] \tag{5.5}$$

As can be seen, each value of the desired function can be calculated from the measured points $\Phi_m(t_k)(k \leq i)$ measured before this moment and the stored discrete apparatus function $a(t_i)(i = 1 \ldots n)$. Even with this numerical deconvolution it is then basically possible to calculate and display the desired function online during the measurement.

The problem is that the measured values (and the apparatus function) are not quit exact but noisy, i.e. uncertain, and that the errors enter into the calculation progressively.

In addition, the measured values are small at the beginning of a transformation and the noise fraction is, therefore, relatively high; the initial values of the apparatus function are usually very small which – according to Eq. (5.5) – leads to a very noisy signal $\Phi_r(t_i)$, which in turn results in numerical instabilities which may lead to a "run-time error" of the computer. For these reasons, online deconvolution according to Eq. (5.5) is usually not suitable without special precautions concerning the initial peak region in question. Of course, the calculations can be performed off-line as well, i.e. after the experiment has been finished.

5.4.4 Advanced Desmearing

The desmearing procedures described so far have essentially taken into account the influences from the DSC measuring system and the interaction between sample and instrument. The events inside the sample have not yet been discussed. For a 1st order endothermic phase transition of a pure sample, desmearing as it has been carried out so far furnishes, for example, a deconvoluted measured curve as shown in Fig. 5.8a. When recorded as a c_p function, the 1st order phase transition has, however, the shape according to Fig. 5.8b. Both functions are obviously not alike. To be able to calculate the c_p function from the measured function, the reasons must be known quantitatively which have led to the particular function according to Fig. 5.8a. In the case of an endothermic phase transition, the sample temperature is constant for the duration of the phase transition; as the sample crucible is heated linearly, the heat flow rate into the sample also increases linearly:

$$\Phi_r = L \cdot \Delta T = L \cdot (T_m - T_S)$$

$$\frac{d\Phi_r}{dt} = L \cdot \left(\underbrace{\frac{dT_m}{dt}}_{\approx \beta} - \underbrace{\frac{dT_S}{dt}}_{=0} \right)$$

$$\frac{d\Phi_r}{dt} = L \frac{dT_m}{dt} \tag{5.6}$$

$$\frac{d\Phi_r}{dt} \cdot \frac{dt}{dT_m} = \frac{d\Phi_r}{dT_m} = L$$

(L thermal conductance between sample crucible and sample, β heating rate)

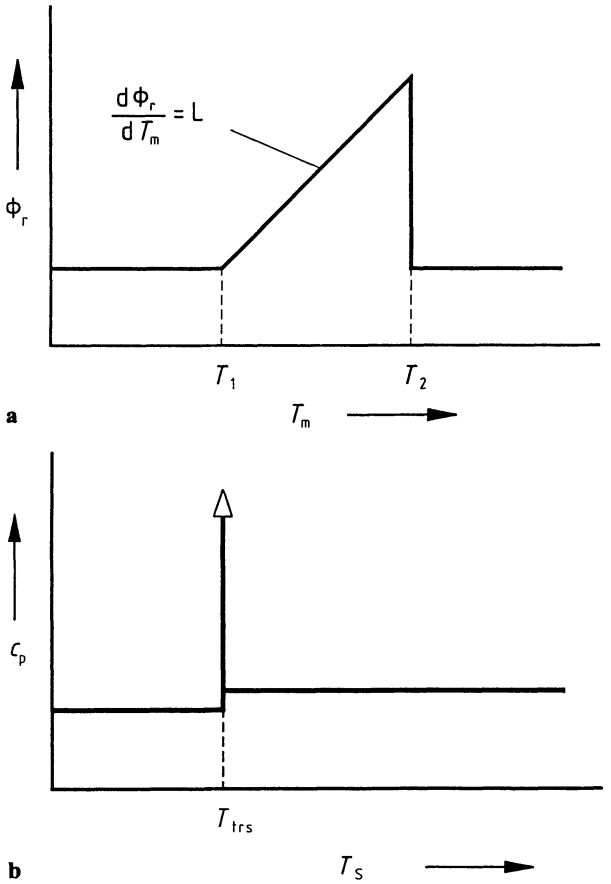

Fig. 5.8. Advanced desmearing in the case of the melting of a pure substance.
a Deconvoluted measured curve, **b** Corresponding $c_p(T)$ function.
Φ_r true heat flow rate into the sample, T_m temperature measured, T_S sample temperature, T_{trs} transition temperature, L thermal conductance between sample crucible and sample, c_p specific heat capacity of the sample, β heating rate

Accordingly, the increase in the heat flow rate depends on the heat transport conditions to the sample and on the heating rate.

In this case, advanced desmearing of the measured curve of a 1st order phase transition consists in simply compressing the abscissa in the range T_1 to T_2 (Fig. 5.8) and dividing the ordinate by the mass and the heating rate. As a result, the triangular peak becomes a δ-peak with the weight factor of the phase transition heat ΔH, and the measurement temperature becomes the sample temperature.

For endothermic transitions of, for instance, impure substances it is to be started from the fact that the rather low heat flow rate at the beginning of the transition is scarcely influenced by the limited thermal conductivity. But if the heat flow rate increases and approaches the magnitude of the phase transition peak, the shape of the measured peak will be smeared more and more. At a certain moment (T_{limit} in Fig. 5.9a) it reaches the heat flow rate limit of the apparatus and the sample temperature falls behind the measured temperature. The limiting factor is the same as for the phase transition of a pure substance, namely the thermal conductance L of the path from the temperature measuring point to the sample. The measured end temperature is not the end temperature of the transition of the sample (Fig. 5.9b). There is a nonlinear connection between these two temperatures which generally cannot be specified.

In the case of impure substances which can be described with the aid of thermodynamics of eutectic multi-component systems, the theoretical shape of the function shown in Fig. 5.9b is known (see Sect. 6.2.4). This allows the true melting curve to be determined from the measured one by calculating along the theoretical curve and comparing the areas which must be equal according to the law of the conservation of energy. Such calculation may be called desmearing as well, but it is far removed from deconvolution due to the theory of linear response.

Another problem is the smearing of the measured curve due to the temperature profile developing in the sample. It is evident that the peak assigned to a transition in a thin sample differs substantially from that in a thick sample. It can be shown by the method of Laplace transformation that the temperature profile in the sample has a parabolic shape and that the mean temperature $\langle T \rangle$ of the sample can be calculated according to the following formula (Hoff, 1991):

$$\langle T \rangle = T_{\text{lb}} - C_p \cdot \rho \cdot \beta \cdot \frac{d^2}{3\lambda} \tag{5.7}$$

T_{lb} being the temperature at the low "hot" boundary of the sample (C_p heat capacity, ρ density, λ thermal conductivity, β heating rate, d thickness).

The second term on the right-hand side of Eq. (5.7) is an additional correction of the temperature scale. In reality both the finite thermal conductivity of the heat path to the sample and the temperature profile of the sample influence the shape of the measured peak. In the case of linearity, the total apparatus function (often called Green's function as well) is the convolution product (Eq. 5.7) of both parts, as these events are connected in series (Höhne, Schawe, 1993). This seems to complicate the desmearing procedure, but fortunately the total apparatus function can be determined in one moment by analysing the switch-on and switch-off behavior

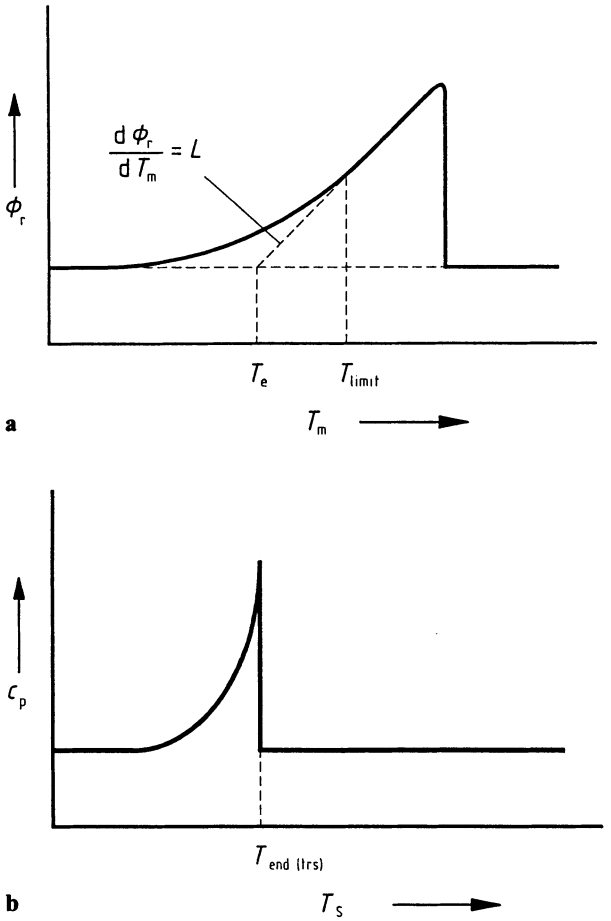

Fig. 5.9. Advanced desmearing in the case of a melting of an impure substance.
a Deconvoluted measured curve, dashed line hypotenuse of a right-angled triangle with the slope L,
b Corresponding $c_p(T)$ function (the temperature scale is not correlated to that of a).
Φ_r true heat flow rate into the sample, T_m temperature measured, T_S sample temperature, T_{trs} transition temperature, T_e extrapolated peak onset temperature, L thermal conductance, c_p specific heat capacity of the sample

of the scanning mode. The starting and ending of a DSC run always implies switching the heating rate from zero to a constant value and vice versa. As a result, the real heat flow rate into the sample should change in a step-like manner, whereas the measured heat flow rate rises with a certain delay (Fig. 5.10). This step response function covers both the heat transport and the sample behavior. By differentiation the impulse response function can be derived from this function (Fig. 5.11), which is the apparatus function in which the investigator is interested. Using this apparatus function desmearing can be carried out as described. Figure 5.12 shows that such a desmearing gives rise to a distinct change in the measured curve in the case

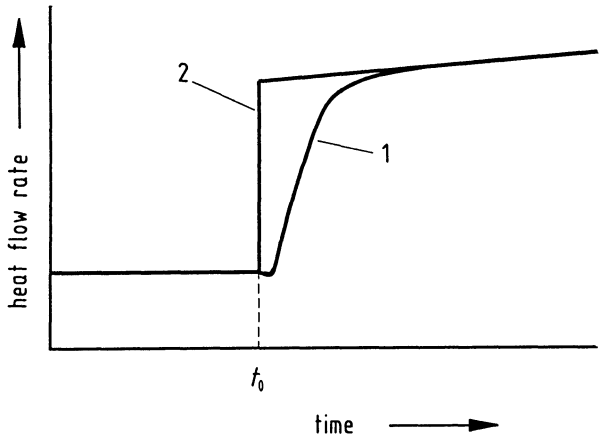

Fig. 5.10. Curve measured with the heating rate switched from zero to β at t_0. 1 measured curve, 2 theoretical heat flow rate into the sample

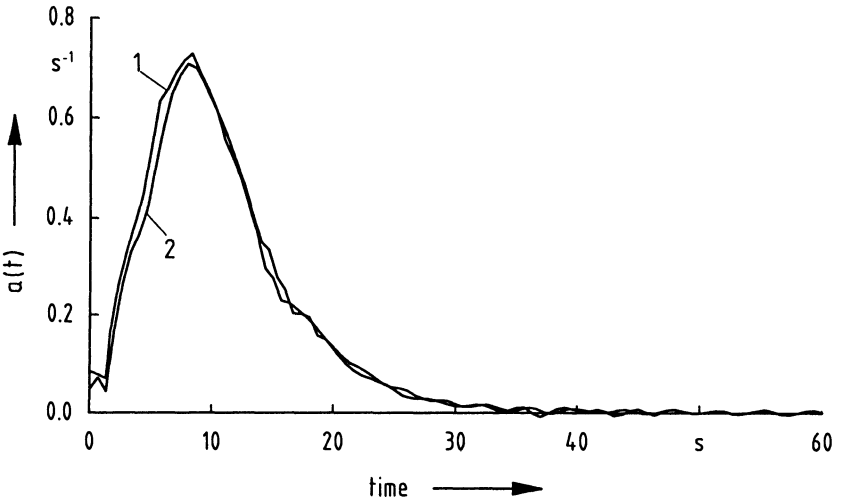

Fig. 5.11. Apparatus function $a(t)$ from step response arising from 1 switch-on, 2 switch-off

of samples with poor thermal conductivity. This may be used as a proof of the influence which the thermal lag and the temperature profile inside the sample exert on the measured curve. An advantage of this method is the easy measurement of the correct apparatus function by only switching from the isothermal to scanning mode and vice versa which is always done in the case of heat capacity measurements (cf. Sect. 6.2.1). Thus the apparatus function in question is always on hand.

The lag between sample and measured temperature due to the thermal resistance between sensor and sample causes an error not only because the shape of a peak is

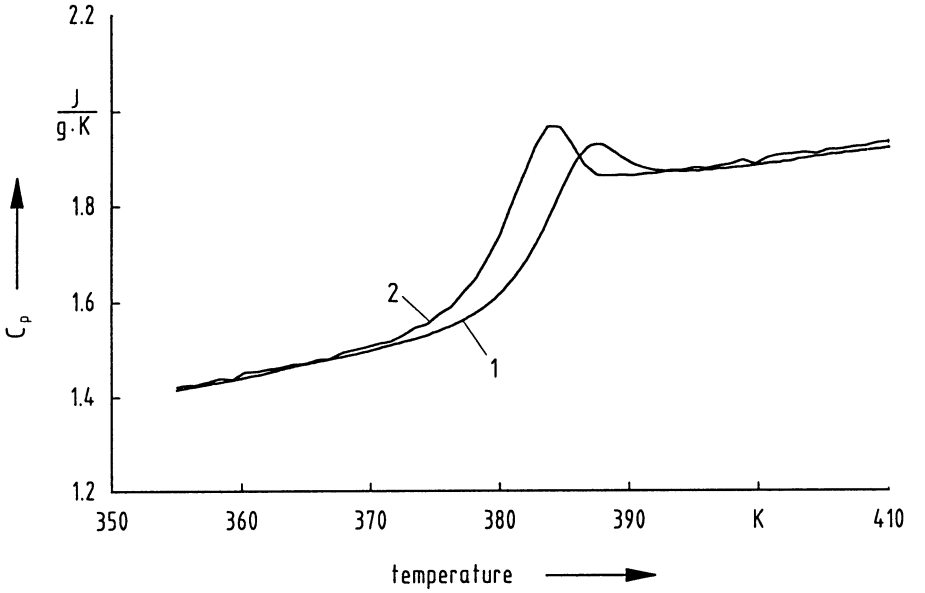

Fig. 5.12. Heat capacity measurement showing a glass transition.
1 measured curve, 2 desmeared curve (10 mg polystyrene, 20 K min^{-1})

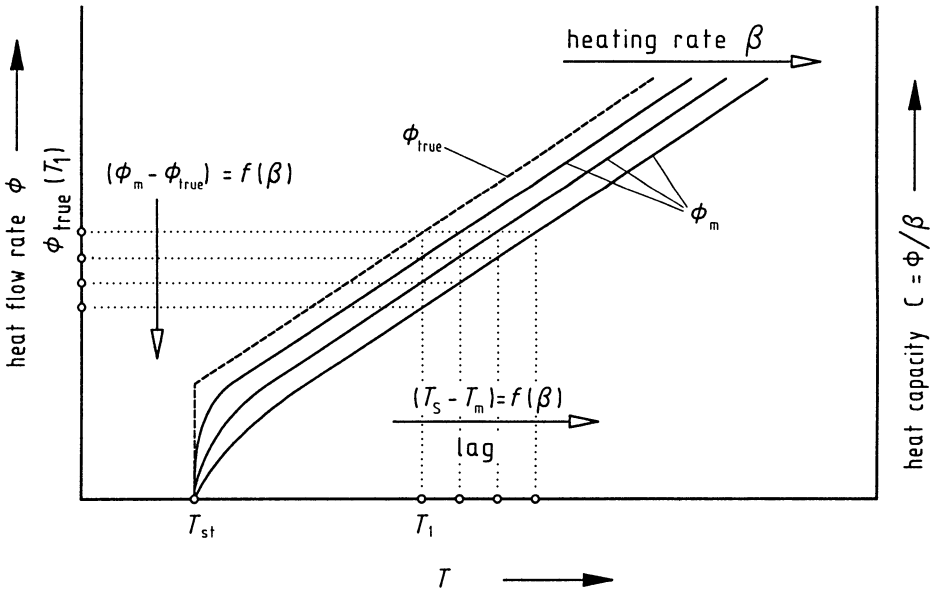

Fig. 5.13. Difference between true and measured heat flow rate (resp. heat capacity) curves. T program temperature, T_{st} starting temperature, T_S sample temperature, T_m measured temperature, Φ_{true} true sample heat flow rate, Φ_m measured heat flow rate

smeared, but also the baseline and the measured curve when pure C_p measurements are performed. Figure 5.13 may serve to explain this "thermal lag" effect: There is in principle a difference between the measured temperature of the sensor and the true temperature of the sample during a scanning run. It increases with the heat flow rate into the sample due to the proportionality of heat flow rate and associated temperature gradient. The heat flow rate for its part depends on the heat capacity of the sample and on the heating rate. As a consequence, the measured curves shift more and more to the right side in Fig. 5.13 with increasing heating rate and heat capacity of the sample.

Due to the proportional relation between heat flow rate and heat capacity of the sample, an analogous relation is valid for the difference between the measured apparent heat capacity (calculated from the measured heat flow rate) and the true heat capacity of the sample. As the sample temperature is lower than the temperature displayed, the heat flow rates (and the heat capacities) displayed are also too low – compared with the true ones – due to the increase in the sample's heat capacity with temperature (see Fig. 5.13).

As the temperature dependence of the heat capacity is normally not very strong, the effect discussed (the *thermal lag*) is not very important. For highly precise measurements (< 1%), it has, however, to be taken into account and, if necessary, it should be corrected by applying the desmearing procedures referred to above. The thermal lag δT itself can be approximately determined (Richardson, Savill, 1975b and Vallebona, 1979) from the heat δQ, which is proportional to the area A between the step function at varying scanning rate and the measured function which is the step response function (i.e. the area between the two functions in Fig. 5.10):

$$\delta T = \frac{\delta Q}{C_{p,\mathrm{S}}}$$

(δT thermal lag in K; A area in J; $C_{p,\mathrm{S}}$ heat capacity of sample in J K^{-1})
With this value, the temperature scale can be corrected for the lag of the sample temperature caused of the finite thermal conductivity and the influences of the sample.

5.4.5 Further Calculations

The desmearing procedures described above furnish the heat capacity-temperature function of the sample, $C_p(T_\mathrm{S})$. An integration must be carried out to obtain the thermodynamic potential function:

$$\Delta H(T) = \int_{T_1}^{T_2} C_p(T)\,\mathrm{d}T$$

Usually, the pressure p is constant in calorimetric experiments and the enthalpy difference $\Delta H(T)$ is obtained from C_p; (see note on ΔH in Sect. 5.3).

If the measurement is carried out at constant volume, in analogy to C_p, first $C_V(T_\mathrm{S})$ is obtained and from this, by integration, the energy difference $\Delta U(T)$ as the

thermodynamic potential function. (This is not very important regarding DSC measurements as the realization of a constant volume is very difficult.)

The time and effort to be spent on desmearing seems to be great and the procedure complex. It should, however, be noted that the individual steps of the desmearing procedure described in this section must be carried out only if the accuracy required for the measurements is higher than the correction to be expected as a result of the respective procedure. For most applications, both deconvolution of instrument influences and the advanced desmearing procedures can be dispensed with; in peak area determination they are absolutely superfluous. They are, however, usually required when, for example, kinetic evaluations or a precise analysis of the phase transition behavior of substances is concerned.

5.5 Interpretation and Presentation of Results

For certain tasks (for example, receiving inspection of materials), by comparison of the measured curve with reference curves, an identification of the sample substance is perhaps possible on the basis of a yes/no decision. This generally concludes interpretation in these cases.

In the normal case, however, interpretation is preceded by the evaluation of the curve in order that data are obtained which are characteristic of the sample substance and/or the transition investigated. The steps of the evaluation are the following:

- desmearing, if necessary (cf. Sect. 5.4),
- determination of the peak area or partial areas after construction of the baseline (cf. Sect. 3.1 "The first approximation" and Sect. 6.2.2.2),
- determination of C_p changes (cf. Sect. 6.2.3),
- estimation of the uncertainties.

The data obtained from the evaluation form the basis of the interpretation. The presentation of uninterpreted measured curves is not very informative. An interpretation can possibly be made only in several steps, for instance by

- variation of the sample parameters (particle size, mass, sample shape, ...),
- variation of operating parameters (heating rate, kind of atmosphere, ...).

The interpretation must correctly describe the effects of the parameters changed. Sometimes, for example with complex reactions, a final interpretation by means of the DSCs is not possible. Other methods must then be applied in addition. Only if the results obtained by all test methods can be interpreted in the same way is it probable that the interpretation is correct. For example, in the case of kinetic investigations in inhomogeneous phases, one should always be aware of the fact that the calculated values are affected by considerable uncertainties.

When DSC results are presented, the following should be stated:

- sample characteristics (mass, purity, structure, ...),
- instrument characteristics (type of DSC),

- test conditions (heating rate, atmosphere),
- the curve originally measured (and a desmeared curve, should desmearing be necessary),
- details of the calibration procedures (materials and their characteristic data),
- details of the evaluation of the measured curve (specification of characteristic temperatures, construction of baseline, peak integration),
- data obtained from the measured curve and the uncertainties by which they are affected,
- basic formula and calculation procedures which are used (e.g. for purity determination),
- interpretation on the basis of the DSC results (taking the uncertainties into account),
- whether the interpretation could be confirmed by variation of the parameters or by other measuring methods,
- comparable results from the literature.

6 Applications of Differential Scanning Calorimetry

The output signal from a DSC, the heat flow rate as a function of temperature, and any derived quantity, such as the heat of transformation or reaction or any change of the heat capacity of the sample, may be used to solve many different problems. The work required to evaluate the measured curve may differ greatly from one case to another. This will become clear from the following text. It will also become obvious that an adequate evaluation may need more effort when the signal to noise ratio is low.

6.1 General Applications Without Sophisticated Evaluation of the Measured Curve

The required information can often be obtained from only a qualitative evaluation of the DSC curve. A simple yes/no-decision is sometimes enough. Quantitative information may not be needed.

6.1.1 Identification of Substances, the Phase Behavior

Such investigations are more meaningful only when they are coupled with other structure-sensitive analytical methods such as hot stage microscopy, infrared spectroscopy and X-ray diffraction. The main advantage of the DSC method lies in the ease and simplicity of operation – in particular both the choice and the rapid change of the required temperatures. This is very important for the investigation of substances with metastable phases. On the other hand there is the disadvantage that it is not possible to carry out experimental manipulations (e.g. nucleation of a supercooled liquid) inside the small and practically always closed crucibles.

If the phase behavior of a sample is reversible, a good practice should always be the evaluation of the second run rather than the first, because only then is there a reproducible heat transfer pass from the sample to the apparatus. Investigations regarding the polymorphism of pharmaceutical substances are especially important, as different modifications or isomers have different rates of solution and thus even different physiological effects on human organisms.

The first example (Fig. 6.1) concerns the melting of acetamide. During the first heating the thermodynamically stable modification (the as received state) melts at about 80 °C. On cooling from the melt the metastable modification crystallizes first

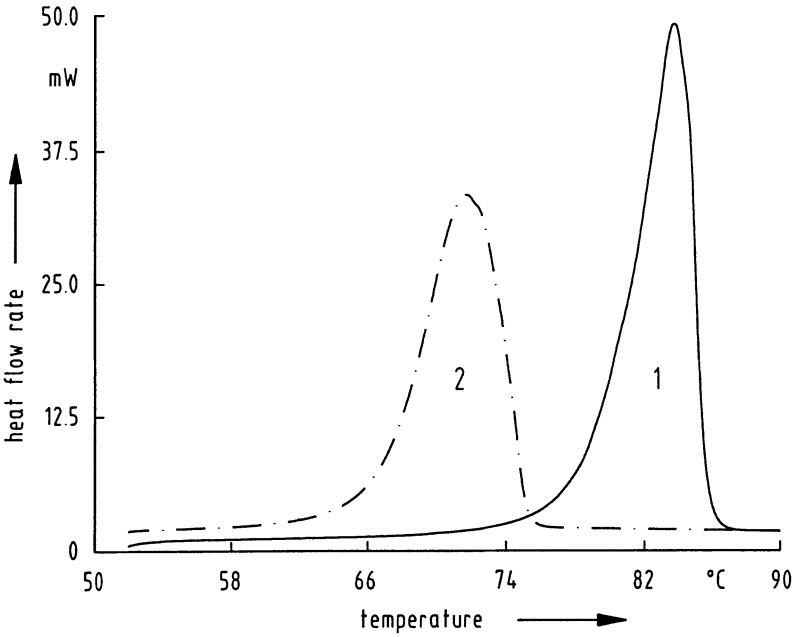

Fig. 6.1. Melting of the thermodynamically stable (curve 1) and of the metastable (curve 2) modification of acetamid

in accordance with Ostwald's step rule. The second run thus shows the melting peak of this metastable modification at about 65 °C. The formation of metastable phases is one of the main problems encountered in the determination of phase diagrams, and this possibility must always be borne in mind to avoid misinterpretation of the observed curves.

Phenylbutazone is another well-known material that shows polymorphism. The stable modification (curve 1 in Fig. 6.2a) melts at about 103 °C. Rapid cooling of the melt yields a glassy phase. On reheating the glass (curve 2) this first recrystallizes to a metastable form at about 35 °C. Subsequent behaviour depends on the heating rates, either melting of the metastable modification at about 93 °C or of the stable structure at 103 °C will be observed. Because the rate of transformation from the metastable to the stable form is low in the solid phase (i.e. <93 °C), only at low heating rates (<1 K min^{-1}) will there be enough time during the experiment for this to occur. At high heating rates (>20 K min^{-1}) the formation of the stable modification does not happen, not even in the liquid phase after the melting of the metastable modification. The corresponding DSC curves are shown in Fig. 6.2b. For better comparison of both curves, curve 2 was also run with a heating rate of 40 K min^{-1} following a preliminary heating to 98 °C at 1 K min^{-1} and recooling to room temperature. At moderate heating rates (ca. 5 K min^{-1}), however, the sample reaches some intermediate state. Any remaining metastable phase that has not transformed during the slow solid state reaction, melts at 93 °C, it then transforms

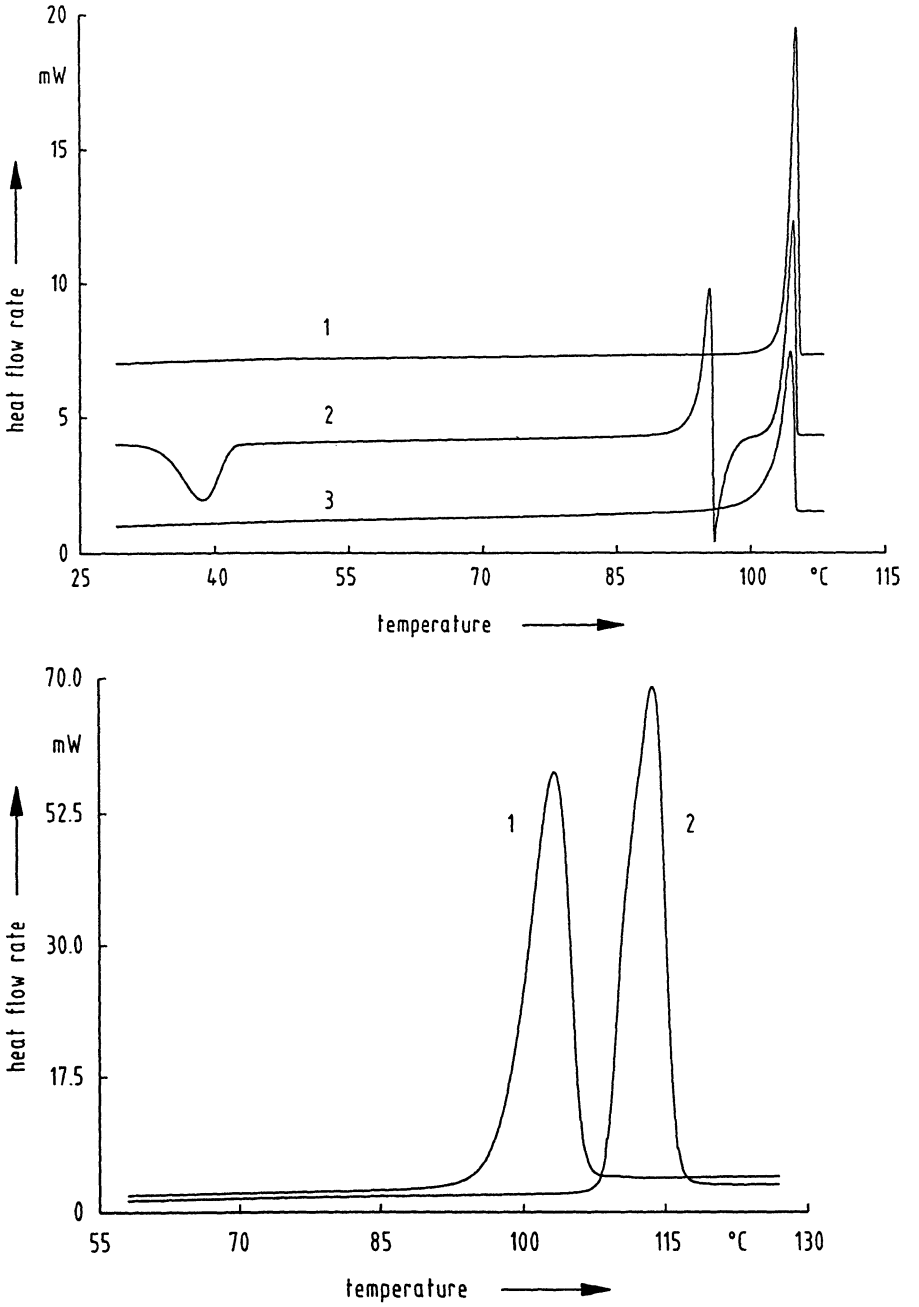

Fig. 6.2. Polymorphism of phenylbutazone.

a 1: first heating run, 2: heating run after quenching from the melt, 3: heating run after reheating the quenched melt up to the end of the exothermic peak at 100 °C (mass: 5.1 mg, heating rate: 5 K min^{-1}),

b two limiting cases in heating the quenched melt, 1: complete melting of the metastable phase during fast heating, 2: melting of the stable phase after previously heating to 98 °C with 1 K min^{-1} (heating rate: 40 K min^{-1})

to the stable modification as an exothermic reaction and finally melts at 103 °C (curve 2 in Fig. 6.2a). This can be proved by quenching the sample immediately after completion of the exothermic reaction (at 100 °C) and reheating it again, when only the melting peak of the stable phase is seen (curve 3).

DSCs are used very frequently for the investigation of polymorphism of substances with liquid-crystalline mesophases. The reliable evaluation of mesophase transitions with small or very small transition energies (sometimes $<0.1\ J\,g^{-1}$) makes great requirements on apparatus and working conditions. An example is the behavior of cholesteryl myristate during heating and cooling (Fig. 6.3). The first peak ($Q = 77.3\ J\,g^{-1}$, $T = 69.0\ °C$) corresponds to the formation of a smectic mesophase. The following two peaks ($Q = 2.5\ J\,g^{-1}$, $T = 77.7\ °C$ and $Q = 1.9\ J\,g^{-1}$, $T = 83.0\ °C$) correspond to the formation of the cholesteric mesophase or the transition into the isotropic melt. All phase transitions are reversible (compare curves 1 and 4). The reason for the narrower peak shape of the first peak of curve 4 ($Q = 76.9\ J\,g^{-1}$, $T = 68.5\ °C$), compared with that of curve 1, is the better heat transfer to the sample after melting. If the cooling run (curve 2) is stopped before the crystalline phase appears, only the two liquid-crystalline phase transitions are observed during the subsequent reheating (curve 3). The heat of transition from the crystalline to the liquid-crystalline mesophase is usually – as in this example – much higher than those of the following mesophase transitions. Further, it can be demonstrated that there are practically no supercooling phenomena for mesophase transitions. The onset temperatures of the heating and cooling runs do not differ from each other

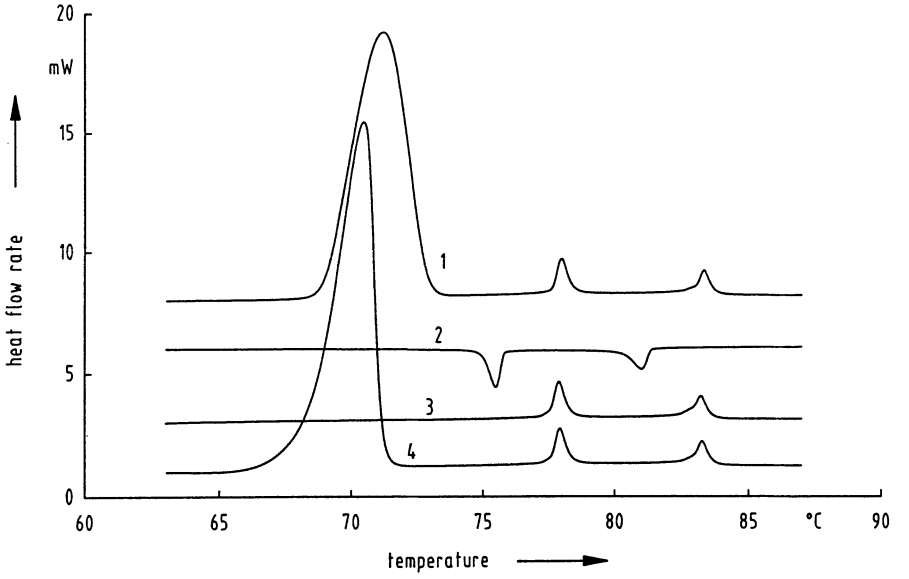

Fig. 6.3. Polymorphism of cholesteryl myristate.
1: first heating, 2: cooling to 60 °C, 3: subsequent heating, 4: heating after cooling from the melt to room temperature (mass: 4 mg, heating and cooling rates: 5 K min^{-1})

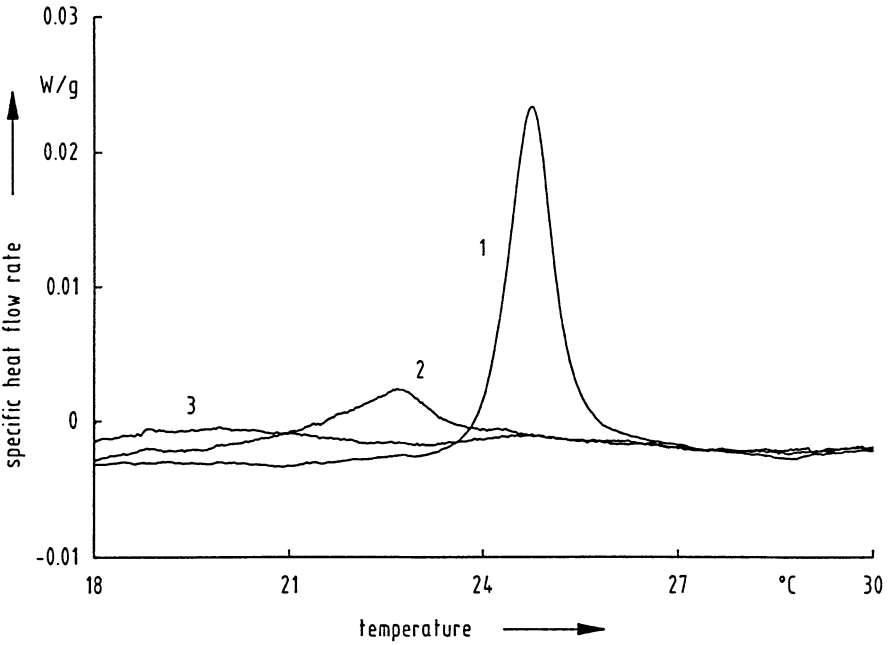

Fig. 6.4. DSC heating curves of the gel-liquid crystalline phase transition of a liposome. 1: 1.75% of dimyristoylphosphatidylcholine (DMPC) in water, 2: after addition of 3% and 3: of 5% of vitamin D3 (mass:15 mg, heating rate: 2 K min^{-1})

after proper correction of the extrapolated onset temperatures to a heating or cooling rate of zero (onset differences of $\Delta T = 0.2$ K and $\Delta T = 0.0$ K for the two transitions). The crystalline phase, however, shows considerable supercooling. It crystallizes at about 30 °C, equivalent to a ΔT of about 40 K.

Besides the pharmaceutical applications already mentioned, DSCs are also used for investigations of stability and of physical and chemical interactions between the active components of drugs. Recently DSC has become increasingly used in both the food industry and biochemistry. As a rule these applications require very high sensitive DSC measurements. One example (Fig. 6.4) shows the transition from gel to liquid crystalline state of a appropriately prepared liposome of 1.75% of dimyristoylphosphatidylcholine (DMPC) in H_2O. The reversible transition (curve 1, $Q = 0.47$ J per g total sample mass, $T_p = 24.6$ °C) corresponds to the change of the hydrocarbon chains from an ordered (crystal-like) to a liquid-like structure. The structural transition of the lipid can be perturbed by molecules which intercalate among the lipid chains and hence hinder the regular packing of the phospholipid molecules into gel-phase structures. This can be realized for instance by addition of the lipophilic vitamin D3. With increasing concentration of vitamin D3 in the liposomes, the peak becomes broader and smaller and the peak maximum shifts to lower temperatures (curve 2: 3% of vitamin D3, $Q = 0.15$ J g^{-1}, $T_p = 22.7$ °C). Addition of more then 5% of vitamin D3 to the DMPC-water lipid (curve 3) causes the disappearance of this peak.

Sometimes melting processes extend over very broad ranges of temperature. For low molar mass substances this may be due to large amounts of impurities (cf. Sect. 6.2.4). For macromolecules this may be caused by the broad distribution of the molar masses or by a distribution of the thicknesses of the crystal-lamellae. The determination of the appropriate baseline and the choice of physically reasonable integration limits for the enthalpy calculation is then very problematic. Mathot, Pijpers, 1983; Mathot, 1984; Mathot, Pijpers, 1989 recommend the use of the heat capacity (C_p) function rather than the normal heat flow rate curve of the sample for evaluation to overcome these difficulties.

Additional problems are found when DSC is used to investigate processes which lead to the production or absorption of gases e. g. dehydrations or oxidations. Here both qualitative and quantitative results are influenced by the experimental conditions – the type and flow rate of the purge gas, geometry of the sample holder, sample preparation and so on. A typical example is the thermal decomposition reaction of calcium oxalate monohydrate. The temperature of the first dehydration peak and the peak width are radically influenced both by the heating rate and the effectiveness of the water vapour transport by the purge gas. Thus every attempt at a kinetic evaluation risks interpreting the transport conditions rather than the kinetics of the decomposition process. The second step in the decomposition of calcium oxalate monohydrate, the elimination of carbon monoxide, to yield $CaCO_3$, is strongly influenced by traces of oxygen in the purge gas because in

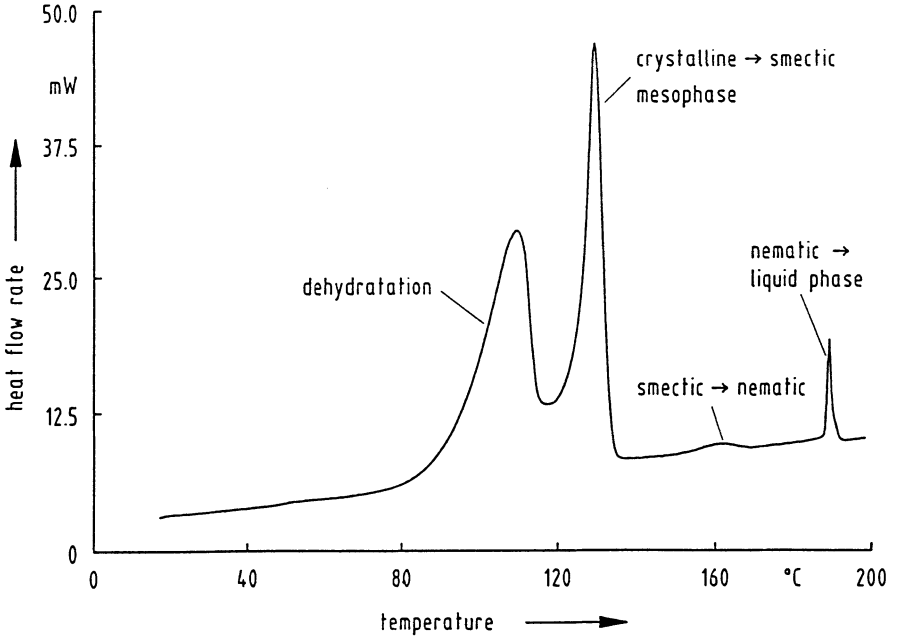

Fig. 6.5. DSC curve of the phase behavior of calcium stearate monohydrate (mass: 3 mg, heating rate: 10 K min^{-1})

presence of O_2 the CO is completely or partially oxidized. The simultaneous coupling of the DSC with thermogravimetry or mass spectrometry is advantageous in these cases.

Another example, the phase behavior of calcium stearate monohydrate is shown in Fig. 6.5. Shape and temperature of the first peak (dehydration) and the separation of it from the second peak are strongly influenced by the effective removal of the evolved water vapour and thus by the experimental conditions (open, partially or completely closed sample crucibles; flow rate and type of purge gas). The three other peaks correspond to the transitions from the crystalline to the smectic phase, from smectic to nematic and finally from nematic to isotropic liquid. Within the homologous series of fatty acids the phase behavior changes both quantitatively (for rather small differences in the chain length) and qualitatively (for larger differences). The DSC method may therefore also be used to solve analytical problems.

6.1.2 Determination of Phase Diagrams

The determination of phase diagrams in the fields of metallurgy and mineralogy was one of the earliest applications of thermal methods. It was one of the decisive reasons for the introduction of Differential Thermal Analysis (DTA, see Appendix 1) at the beginning of the twentieth century.

As an example, the phase diagram of the binary system benzil/acetanilide is shown schematically in Fig. 6.6 together with the DSC curves of the heating runs of the pure components (curves 1 and 7) and of five mixtures including the eutectic (curves 2 to 6). In accordance with the phase diagram benzil and acetanilide are completely miscible in the liquid and immiscible in the solid phase. Pure acetanilide melts at 115 °C, pure benzil at 95 °C. The eutectic, with a mole fraction of about $x_{Ben} = 0.58$, melts at 78 °C. In Fig. 6.6a two different melting pathways (mixtures with $x_1 = 0.1$ and $x_2 = 0.9$ of benzil) are sketched. The measured DSC curve of every mixture shows two events: The first is the peak due to the melting of the eutectic, the subsequent broad endothermic effect is caused by the solution of the remaining solid component in the equilibrium melt (following the pathway along the liquidus curve in Fig. 6.6a). The final point of this peak corresponds to the liquidus temperature according to that mole fraction in the phase diagram. Both the pure components and the eutectic melt at well defined temperatures. These can be determined from the extrapolated peak onset temperatures in the usual way, whereas the determination of the liquidus temperature is not easy. The peak maximum temperature (if necessary corrected for thermal lag, see Sect. 5.4.4) of the second broad peak is a good approximation. In every case slow heating rates ($<2\,K\,min^{-1}$) and small sample masses should be used, to ensure approximate thermodynamic equilibrium at every moment during the experiment and to avoid "smearing" (see Sects. 3 and 5.4) of the DSC curve and thus incorrect temperatures. The heating mode is more suitable for the determination of phase diagrams than the cooling mode, because many organic substances have a tendency to supercool considerably.

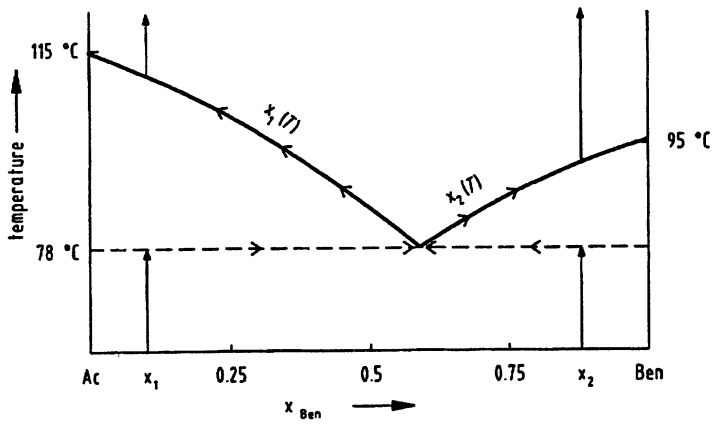

a

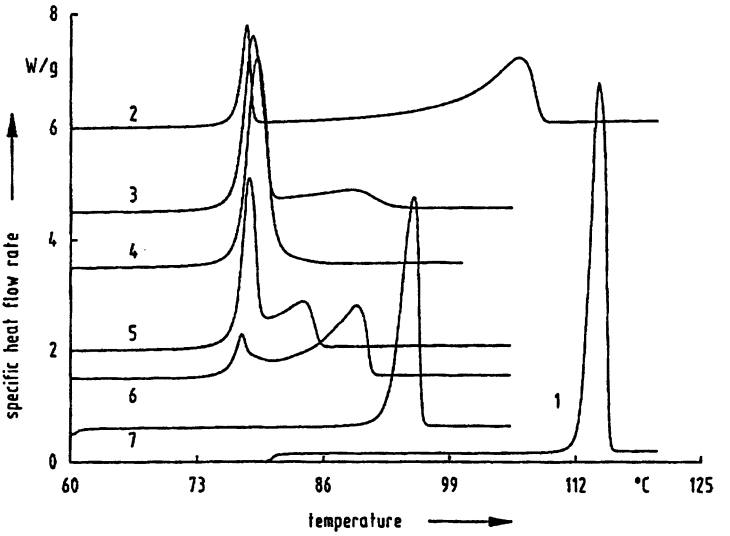

b

Fig. 6.6. The phase behavior of the system acetanilide (Ac) – benzil (Ben).
a Schematic phase diagram of the eutectic system, the arrows mark the course of the melting process for two mixtures with the mole fractions x_1 and x_2,
b DSC curves of the pure components and of five mixtures, 1: acetanilide (x_{Ben}= 0), 2: x_{Ben} = 0.1, 3: x_{Ben}= 0.4, 4: x_{Ben}= 0.578 (eutectic), 5: x_{Ben} = 0.75, 6: x_{Ben} = 0.9, 7: benzil (x_{Ben}= 1)

If the heats of fusion of the pure components are known and the binary system behaves ideally in the liquid phase, the theoretical melting course may be predicted, using the Schröder-Van Laar equation (Brezesinski, Dörfler, 1983; see also Sect. 6.2.4).

The molar heat of fusion of the eutectic $\Delta_{fus}H_{eu}$ can be calculated for ideal eutectic systems (for which the eutectic is a simple blend of microcrystals) using the

normal rule of mixtures:

$$\Delta_{fus}H_{eu} = x_A \cdot \Delta_{fus}H_A + x_B \cdot \Delta_{fus}H_B$$

x_A, x_B mole fractions of the components A and B, $\Delta_{fus}H_A$, $\Delta_{fus}H_B$ molar heats of fusion of the pure components.

For precise calculations $\Delta_{fus}H_A$ and $\Delta_{fus}H_B$ should be converted to the eutectic temperature using Kirchhoff's law.

If this simple additivity holds, the exact composition of the eutectic can be determined by plotting the heats of fusion of the eutectic of different mixtures against the composition. This gives two different straight lines to the right and to the left of the eutectic and the intersection gives the required composition. This procedure is generally also a good approximation for non-ideal mixtures.

For real systems, discrepancies between calculated and experimental eutectic heats of fusion can lead to conclusions regarding the nature of interactions between components. From these differences, the excess functions of entropy, enthalpy and Gibbs energy can be calculated (Rai, Shekhar, 1993). For positive (negative) excess free energy, the attractive interaction between molecules of the same kind is stronger (weaker) than that one between molecules of different components in the mixture.

6.1.3 Safety Aspects

Specific devices for this type of investigation are the reaction or safety calorimeters mentioned in chapter 1. They provide detailed information for the optimization of process parameters, reducing production costs and avoiding safety risks. However, valuable results may be obtained using conventional DTA or DSC (Hentze, 1984). Safety risks in the chemical industry occur when materials, known for their exothermic decomposition reactions, have to be stored for long periods at temperatures, such that the heat evolved is greater than that transferred to the surroundings. Under worst case conditions this may lead to a runaway and subsequent fire or explosion. The direct detection at ambient temperature of the extremely small heat flow rates in question is, in general, not possible with DTA/DSC (exceptions are Calvet calorimeters, cf. Sect. 2.1.2).

Hentze, 1984, avoided this problem by annealing the substance

- at constant temperature and various times
- constant times and various temperatures

and comparing the subsequently measured melting and decomposition peaks with those of a fresh, unannealed sample. In this way quantitative results were obtained for the decomposition kinetics of, for example, p-nitroaniline. Using this procedure it is possible to determine decomposition heats down to 10 mW kg^{-1} at storage temperatures.

Decomposition reactions often react sensitively to traces of foreign materials. With the annealing technique described above, the first detectable decomposition of

azidophenyl acetic acid was determined. In addition the effects of "impurities" of many kinds were investigated. In a similar way the autocatalytic influence of the decomposition products was definitely proved.

Another variant of investigations in the field of safety techniques, suggested by Hentze, 1984, utilizes very slow (0.01 to 0.1 $K\,min^{-1}$) heating of the sample in home-made devices of the DTA type. During the decomposition both heat and pressure are recorded. For the identification of the decomposition products the DTA apparatus is coupled to a mass spectrometer. By this technique the start of the decomposition of p-nitroaniline was observed at about 200 °C, in very good agreement with the corresponding value from annealing experiments.

6.1.4 Characterisation of Polymers by Thermal Analysis; Effects of Origin and Thermal History

Quality control of a material is extremely important both for inspection on delivery and to insure the integrity of manufactured products, this is especially relevant in the plastics industry. Until recently the prime reason for inspection was to ensure continuity of properties if, for instance, the manufacturer, the batch number, or even the manufacturing process, were changed. Now, with the need for recycling used plastics many more questions must be answered, and thermoanalytical methods (DSC, TG, TMA, DMA) have proved very powerful in this respect. The results are easily comprehensible and readily interpreted. This is especially so when plastics of the same chemical nature are recycled for the first time and either analyzed as such or as a mixture with the original plastic. Another important application is the investigation of service failures of plastics.

The DSC curve can be analyzed with respect to the following quantities:

- temperature(s) and step height(s) of the glass transition(s).
  The glass transition temperature reflects the composition of the components, conditions during production, and sometimes also the aging of the plastic product during its use (caused, for instance, by decreasing molar masses and a change of their distribution due to cracking processes by partial oxidation). In heterogeneous or microheterogeneous amorphous blends two or more glass transitions are found, which are characteristic of the individual components. The relative amounts can be estimated by evaluating the respective step heights. Further important information can be taken from the possible existence and intensity of a relaxation peak in the region of the glass transition (cf. Sect. 6.2.3).
- temperatures and heats of fusion, transition and crystallization effects.
  As a rule it is not difficult to identify the components of a plastic mixture, using the characteristic temperatures of the melting peaks. Often even a quite accurate quantitative analysis is possible. Qverlapping peaks can be separated by using appropriate evaluation methods (Opfermann, 1992), since the necessary condition for using such programs – the additive superposition of the respective peaks because of immiscibility in the solid phase – is nearly always fulfilled for plastic mixtures.

A relative (within the type of plastic) degree of crystallinity for semicrystalline products can be obtained very easily (ignoring all precautions described in Sect. 6.1.5) if the area of the melting peak is compared with that of the completely crystalline material of the same type. If a crystallization peak is observed prior to the melting peak, then the crystallization process of the material during production was incomplete. In extreme cases, it is found that for bulk thermoplastic moulded parts the degree of crystallinity varies within the parts, due to uneven cooling rates during moulding.

- onset of thermal and oxidative decomposition.
  To determine this, the plastic is either annealed isothermally in the DSC until the appearance of an exothermic or endothermic signal indicates the beginning of decomposition, or the sample is heated in scanning mode up to this event. By choosing an appropriate gas atmosphere (inert or reactive e.g. oxygen), information is available concerning the thermal or oxidative stability of the material. For these measurements there is always a risk of contaminating the measurement system, so the run should be interrupted immediately after detecting the start of decomposition. However, thermogravimetry is in principle much more suitable for this type of investigation.
- existence and intensity of exothermic reactions peaks.
  The cure of resins and lacquers depends on both the chemistry (including stoichiometry, filler and catalyst content) and on the specific heating procedures. As a result the cured products may differ considerably in their thermal and mechanical properties. This can be demonstrated either by repetition of the experiment under different conditions or by coupling with other methods (IR, GC, NMR, TMA, DMA).

For products containing recycled plastics, most of the above mentioned thermal properties may have changed in a characteristic manner. The observed deviations from the original behavior provide reliable information whether the plastic in question is suitable for the intended application or not.

6.1.5 Determination of the Degree of Crystallinity

DSC is widely used for determination of the degree of crystallinity w_c (weight fraction crystallinity) of semicrystalline polymers. The most simple and obvious possibility is to relate the estimated heat of fusion ($\Delta_{fus}H$) to that of the same polymer but with known crystallinity, provided that this value was determined by an independent method such as X-ray diffraction, Raman scattering, density measurements etc. The determination of the required peak area is problematic, because it is not easy to fix the lower integration limit. The melting of polymers often starts more than 50 K below the maximum temperature of the peak and it is very difficult and rather arbitrary to determine the beginning of this, at first, very slow process on the DSC curve. The situation is made more difficult by the fact that both the degree of the crystallinity and the heat of fusion are dependent on temperature. The use of the heat of fusion measured at higher temperatures yields a value for the crystallinity which is almost certainly too small compared with the value that is actually required

– that at room temperature. Nevertheless, this simple procedure is sufficient for determining relative (within the same type of plastic) crystallinities (e.g. for quality control, cf. Sect. 6.1.4), if one uses fixed integration limits and a fixed reference value for the heat of fusion of the totally crystallized sample.

Mathot, Pijpers, 1983 and 1989, suggest a convenient procedure (Fig. 6.7), which avoids the difficulties mentioned. The heat flow rate after the melting peak, which is proportional to the heat capacity function $C_{p,a}$ of the amorphous (liquid) polymer, is extrapolated to that temperature T, at which the degree of crystallinity $w_c(T)$ is to be calculated. If, in doing so, the experimental curve is not intersected ($T > T^*$, e.g. T_2 in Fig. 6.7), only the area A_1 has to be evaluated. If the extrapolated line intersects the measured curve ($T < T^*$, e.g. T_1 in Fig. 6.7), the area A_2 has to be subtracted from A_1. The heat, corresponding to the areas A_1 (or $A_1 - A_2$), is then divided by the reference value $\Delta_{fus}h(T)$ of a completely crystalline sample at this temperature. For linear polyethylene Mathot, Pijpers, 1983, suggest the following equation for the latter function:

$$\Delta_{fus}h(T) = 293 - 0.3092 \times 10^{-5} \cdot (414.6 - T)^2 \cdot (414.6 + 2T) \quad \text{J g}^{-1}$$

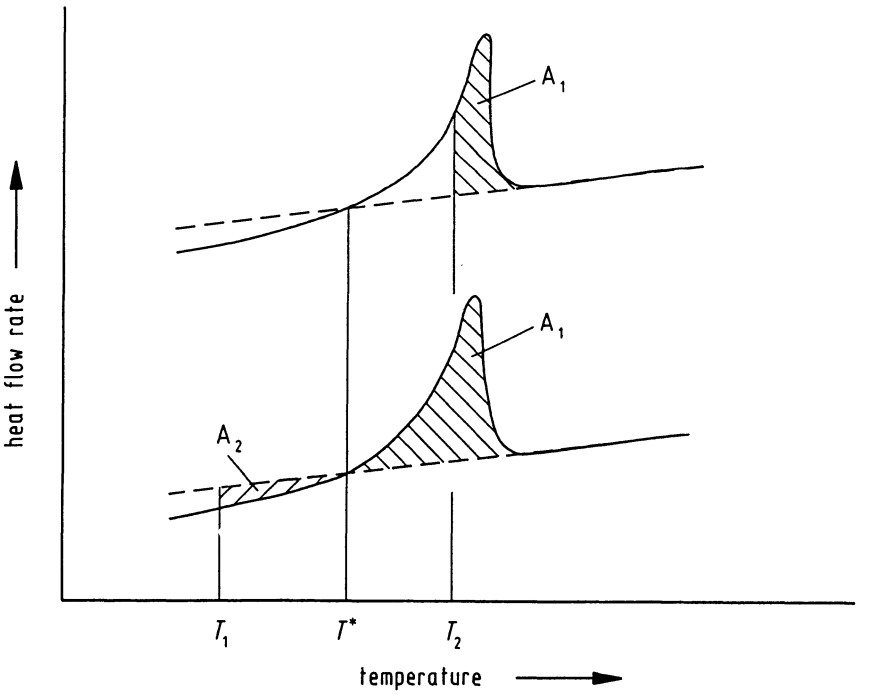

Fig. 6.7. Determination of the degree of crystallinity according to the procedure of Mathot, Pijpers, 1983, at two different temperatures $T_1 < T^*$ and $T_2 > T^*$, where T^* is the temperature of intersection of the extrapolated liquid phase curve and the measured curve (for details see text)

The degree of crystallinity $w_c(T)$ in dependence on temperature is then obtained according to:

$$w_c(T) = \frac{A_1(T) - A_2(T)}{\Delta_{fus} h(T)}$$

Meanwhile the functions $h_a(T)$ for the completely amorphous and $h_c(T)$ for the crystalline form are known for numerous linear macromolecules with sufficient accuracy (Wunderlich et al., 1990).

If the specific heat capacity curve is evaluated from the DSC measurement (see Sect. 6.2.1), a simple integration from T_0 to T of the c_p-curve – and the respective functions of the amorphous and crystalline c_p-function (from literature) – yields the enthalpy difference function $h(T)$ (resp. $h_a(T)$ and $h_c(T)$). This opens a new thermodynamic based calculation of $w_c(T)$, without the necessity of knowing the course of the, often non-linear, baseline in the melting range:

$$w_c(T) = \frac{h_a(T) - h(T)}{h_a(T) - h_c(T)}$$

Of course, the baseline in the melting interval can be calculated too, if a suitable model and the functions $h_a(T)$, $h_c(T)$ and $w_c(T)$ are known for the semicrystalline polymer. The simplest assumption is that the properties of a semicrystalline polymer can be adequately described by a two phase model with only crystalline and amorphous parts. The measuring curve is then calculated according to:

$$c_p(T) = (1 - w_c(T)) \cdot c_{p,a}(T) + w_c(T) \cdot c_{p,c}(T) - (h_a(T) - h_c(T)) \frac{dw_c}{dT}$$

The first two terms correspond to the baseline, the third one describes the temperature dependent change of the degree of crystallinity (the peak). Unfortunately the two phase model fails with some types of polymers, e.g. polyethyleneterephthalate. The baseline can be calculated in such cases by use of improved models, which include a third phase called the 'rigid amorphous phase' (Suzuki et al., 1984, Schick et al., 1985). This phase is thought to exist on the lateral surface of the crystal lamellae and should have a very limited mobility. It follows from this that the rigid amorphous phase does not contribute neither to the thermal glass transition nor to the melting heat of the crystalline part. Nevertheless, the heat capacity of this non-crystallized material can be approximated by that of the crystalline phase.

For some polymers (polydimethylsiloxane, polybutadiene) the rigid amorphous phase is absent and good results for w_c may be obtained for these, if the measured step change of the heat capacity at the glass transition temperature T_g (cf. Sect. 6.2.3) is related to that of the completely amorphous polymer yielding the amorphous amount $w_a = \Delta C_p(T_g)/\Delta C_{p,a}(T_g)$. In this case the degree of crystallinity is $w_c = 1 - w_a$. The completely amorphous state can often be obtained by quenching or ultra-quenching the molten polymer.

6.2 Applications Requiring a Detailed Evaluation of the Measured Curve

All the examples described in this section demand precise measurements and critical, very often special, evaluation procedures of the measured curve. In every case the basis of reliable results is a careful calibration of the DSC (see chapter 4). As a rule, the separately measured zero line (see Sect. 5.1) has to be subtracted from the measured curve before evaluation. In every case, the relationship between uncertainties in the measurements and the quantities to be determined must always be borne in mind.

6.2.1 Measurements of the Heat Capacity

A knowledge of the heat capacity of a material as a function of temperature is the basis for determination of any thermodynamic quantity. The use of normal, not hermetically sealed, DSC crucibles (with a lid which rests on the sample and may be lightly closed by crimping), always gives the heat capacity C_p at constant pressure. The situation is somewhat more complicated if one uses hermetically sealed crucibles or the special crucibles which are available for pressures up to the order of a hundred bar. In addition to the condensed phases, the heat capacity of which is required, sealed crucibles always contain a gaseous phase. In this case it makes no difference whether this phase is composed of air or of gaseous reaction products. Strictly speaking, neither C_p nor C_V are obtained because the thermal expansion of the sample cannot be prevented and the pressure of the gas changes. However, the pressure dependence of the heat capacity of condensed phases is very small and as the change of pressure in the sealed crucibles is generally small, the measured heat capacity is nearly the same as that at normal pressure.

In the following of this section the suffix "p" will be omitted so that C is the heat capacity at constant pressure C_p and c the corresponding specific (per mass unit) quantity c_p for the sample (subscript S) or reference (subscript R).
According to Sects. 3.1 and 3.2 the basic equation for heat capacity determination

$$\Delta\Phi_{SR} = \Phi_S - \Phi_R = C_S \frac{dT_S}{dt} - C_R \frac{dT_R}{dt} = (C_S - C_R) \cdot \beta$$

is valid both for heat flux calorimeters and for power compensating DSCs. As the true heating rates of the sample and the reference material are not accessible by the experiment, they must be replaced by the average heating rate β. If the heat capacity C_R is known, C_S can be determined easily and quickly from the measured differential heat flow rate $\Delta\Phi_{SR}$. Several variants of the experimental procedure are known, four widely used techniques will be discussed.

6.2.1.1 The "Classical" Three Step Procedure

The procedure is illustrated in Fig. 6.8. The temperature-time curve during an experiment is outlined in the lower figure and the response of the calorimeter is shown above. The three steps are:

1. Determination of the heat flow rate of the zero line $\Phi_0(T)$, using empty crucibles (of equal weight) in the sample and the reference sides. The temperature program should only be started when the isothermal heat flow rate at the starting temperature T_{st} has been constant for at least one minute. If the DSC is computer controlled, this can easily be automated by checking the differences between the current average value of the heat flow rate and that one minute ago with allowance for a predetermined drift level. The scanning region between T_{st} and T_{end} can be 50 to 150 K in modern calorimeters. At the isothermal end temperature T_{end} the above computer check must be repeated. For the evaluation procedure all three regions of the curve are needed. The zero line reflects the (inevitable) asymmetry of the DSC.
2. A calibration substance (Ref) of known heat capacity C_{Ref} is placed into the sample crucible (S), whereas nothing is changed on the reference side (R). Using the same experimental procedure as for the zeroline, the following is valid:

   $$c_{Ref}\, m_{Ref}\, \beta = K_\Phi(T)\, (\Phi_{Ref} - \Phi_0)$$

   $K_\Phi(T)$ is a temperature dependent calibration factor (cf. Sect. 4.4.1).
3. The calibration substance (Ref) in crucible S is replaced by the sample (S). In analogy to the equation above we get:

   $$c_S\, m_S\, \beta = K_\Phi(T)\, (\Phi_S - \Phi_0)$$

   The specific heat capacity c_S (at a given temperature) can be calculated by a simple comparison of the heat flow rates into the sample and into the calibration substance as illustrated in Fig. 6.8:

   $$c_S = \frac{\Phi_S - \Phi_0}{\Phi_{Ref} - \Phi_0} \cdot \frac{m_{Ref}}{m_S}\, c_{Ref}$$

   The calibration factor $K_\Phi(T)$ need not, therefore, be known explicitely. If the condition $m_S c_S \approx m_{Ref} c_{Ref}$ holds, the experimental conditions are very similar to those of the second step. Many of the possible sources of error for DSC measurements then tend to have at least partial compensation.

For the previous and the following considerations it is always assumed, that the same crucible has been used on the sample side. If during the second and third step different crucibles must be used, crucibles of the same kind with nearly the same mass (m_{cr}) should be used. It is possible to make routine measurements using crucibles of different masses if allowance is made for the different thermal responses according to:

$$c_S = \frac{\Phi_S - \Phi_0}{\Phi_{Ref} - \Phi_0} \cdot \frac{m_{Ref}}{m_S}\, c_{Ref} + \frac{m_{cr,Ref} - m_{cr,S}}{m_S}\, c_{cr}$$

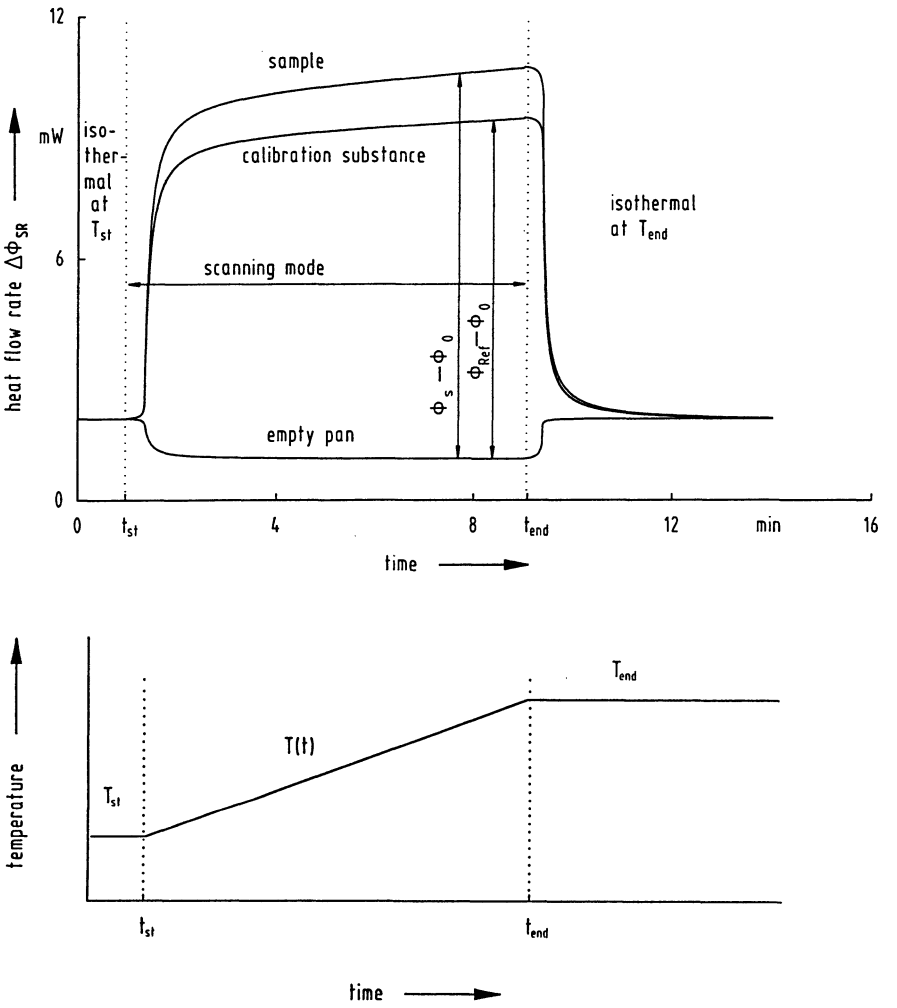

Fig. 6.8. The conventional three-step technique for the determination of heat capacity.
a schematic course of measurement,
b the temperature change during the run.
T_{st} start temperature at time t_{st}, T_{end} end temperature at time t_{end}, Φ_S, Φ_{Ref}, Φ_0 heat flow rates into sample, calibration substance and empty crucible respectively, $\Delta\Phi_{SR}$ differential heat flow rate between sample and reference crucible

The specific heat capacity of the crucible material is needed only as a correction. Those for common crucible materials are known with sufficient accuracy. Omitting the correction results in an error < 1%, if the masses of all crucibles (of Al) differ by less than 0.03 mg for a sample mass > 10 mg (specific heat capacity > 0.5 J g^{-1} K^{-1}).

Sources of error:
Ideal and real conditions during the recording of the zero line and measured curve of the sample are compared in Fig. 6.9. Three differences are obvious:

i The quasi steady-state conditions in the scanning and final isothermal regions are not reached immediately after changes in the scanning program but with a certain delay.
ii The measured heat flow rate (with zero line subtracted) may be smaller than the ideal (theoretical) one.
iii The isothermal levels at t_{st} and t_{end} differ from each other (and may often have non-zero values).

These discrepancies result from the finite thermal conductivity of the path between temperature sensor and sample and from the limited thermal conductivity of the sample itself (cf. Sects. 5.4.3 and 5.4.4). The sample operates both as a heat capacity and as a heat resistance with respect to the thermal surrounding (Poeßnecker, 1990). The signal is therefore a summation of the heat flow stored in the sample and that which passes through it (heat leak). (Of course, it always appears as the differential heat flow rate between sample and reference sides).

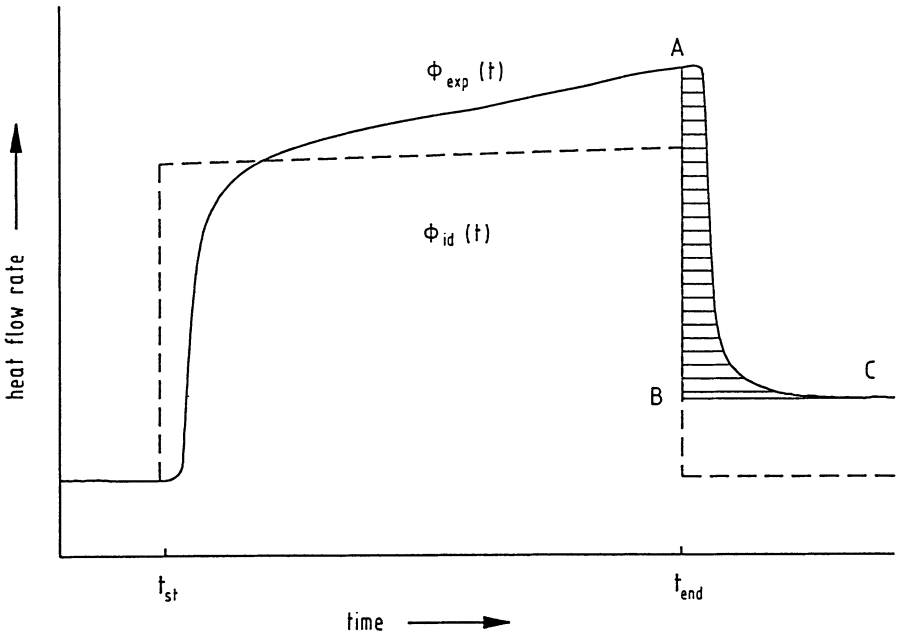

Fig. 6.9. Idealized (dashed line) and real (solid line) curves during a heat capacity measurement.
Curve section AC: delay of the heat flow rate due to restricted heat transfer between sample and sensor, hatched area ABC: the product of thermal lag δT and heat capacity of the sample

In the following the causes of the three above-mentioned deviations from ideal behaviour are considered in detail and possibilities for their correction are given.

i The smearing of the measured heat flow rate curve during the beginning of the scanning region reduces the steady state temperature range over which calculations are valid. The initial unusable temperature range can be estimated by $\Delta T = 5$ to 10 times $\beta \cdot \tau_{eff}$. The effective time constant τ_{eff} results from a coupling of the time constants for the sample and apparatus. As a rule the influence of the apparatus is predominant. The time constants of modern DSCs may vary from 2 to 10 s. For thicker samples with poor thermal conductivity (e.g. polymers) the influence of the sample may dominate τ_{eff}.

ii As discussed in Sect. 5.4.4, the sample temperature is always lower (higher) than the program temperature during the heating (cooling) mode. The measured heat flow rate Φ_m always differs from the true value Φ_{tr}. Assuming the worst conditions (large samples, high heating or cooling rates, large heat capacity, bad thermal contact between crucible and sample holder), the difference between both temperatures may be more than 10 K. This temperature error δT (the thermal lag) can be estimated (see. Sect. 5.4.4) from the heat δQ, which is proportional to the area ABC in Fig. 6.9. This procedure gives a reasonable approximation even for thick samples and/or those with poor thermal conductivity. Although there is still a rather large temperature gradient in such samples, there is a marked reduction in the overall temperature error after correction for thermal lag (Hanitzsch, 1991). As an example the Curie temperatures of Ni (sample mass ca. 250 mg) differed by10 K for the original heating and cooling runs, whereas the difference was reduced to 3.6 K after using this temperature correction method. For a particular sample mass and heating (or cooling) rate the differences between true and measured heat flow rates are influenced by the thermal conductivity of the sample and by the heat transfer resistance between sample and sample holder. The heat transfer resistance can be minimized by proper sample preparation and by correct positioning of the sample in the DSC. It is essential to ensure completely flat bases for the crucibles, uniform sample thickness, size and position.

Thermal conductivity effects can be partially compensated if the calibration substance has a heat capacitiy and a thermal conductivitiy similar to that of the sample. Thermal conductivities of common calibration substances fall in the following order (values in W $cm^{-1} K^{-1}$):

Cu (4.01) > Pt (0.72) > sapphire disk (0.34) > powdered α-Al_2O_3

According to a GEFTA (German Society for Thermal Analysis) recommendation (Sarge et al., 1994) Pt is only partly suitable, because heat capacities are not known to the required accuracy ($\lesssim 0.5\,\%$). If one uses copper, oxide layers on the surface and oxygen in the gaseous phase must be excluded.

The best general method for the correction of all effects due to finite thermal conductivities is to use the special desmearing procedure described by Schawe, Schick, 1991 (cf. Sect. 5.4).

iii The isothermal levels at T_{st} and T_{end} (resp. t_{st} and t_{end}, cf. Fig. 6.8b) for zero line, calibration run and measurement differ from each other by amounts which depend on the type of calorimeter, T_{st} and T_{end} and the temperature interval in between. The offset of the isothermal levels must be corrected to zero before the heat capacities are calculated. The correction is only meaningful if almost comparable conditions for all heat conduction pathes can be assumed for the three successive runs (zero line, calibration substance, sample). However, Poeßnecker, 1990, has shown by a detailed theoretical treatment of the heat transfer in a power compensated DSC that measurements with large differences in the offsets of the isothermals should always be rejected. The heat flow rates of the isothermals at T_{st} and T_{end} should not differ more than 5% of the difference between the heat flow rates in the isothermal and the scanning region.
If it is assumed (but cf. Sect. 6.1) that the change of the isothermal heat flow rates with temperature can be approximated by a straight line $\Phi_{iso}(T)$ within sufficiently small temperature intervals, the offset correction is very simple. Fig. 6.10 demonstrates the procedure. If $\Phi_{iso,st}$ and $\Phi_{iso,end}$ are the heat flow rates of the initial isothermal and the final isothermal, the following is valid:

$$\Phi_{iso}(t) = \Phi_{iso,st} + \frac{\Phi_{iso,end} - \Phi_{iso,st}}{t_{end} - t_{st}} (t - t_{st})$$

The corrected experimental heat flow rates $\Phi_{corr}(t)$ are then obtained from:

$$\Phi_{corr}(t) = \Phi_{exp}(t) - \Phi_{iso}(t)$$

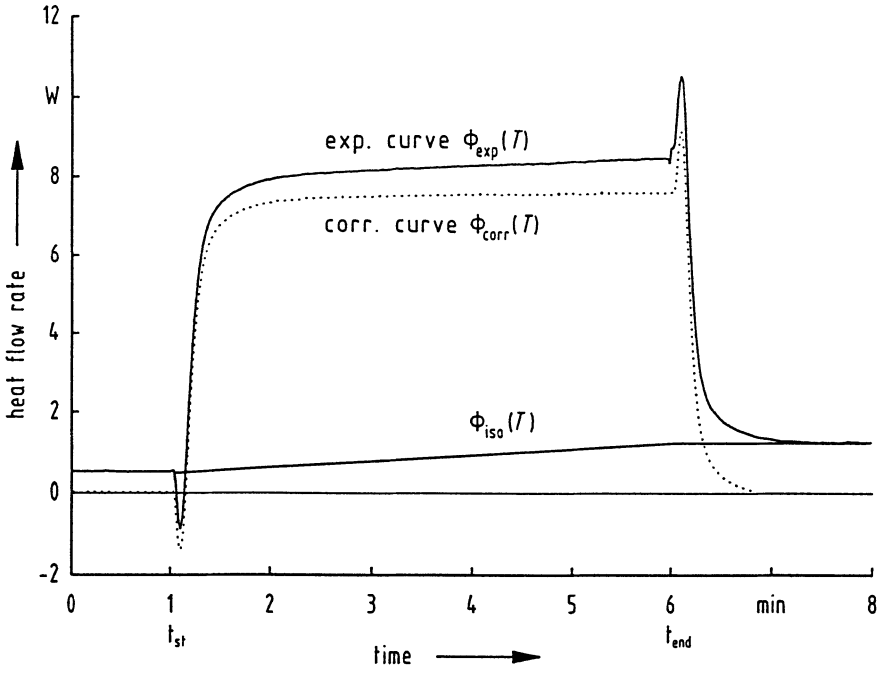

Fig. 6.10. Correction of the experimental heat flow rate curve Φ_{exp} for different isothermals

6.2.1.2 The "Absolute" Dual Step Method

The second step in the C_p measurement procedure (the calibration run, cf. Sect. 6.2.1.1) is not necessary, if the temperature dependent calibration factor $K_\Phi(T)$) is truly constant with time. Then the careful calibration of the heat flow rate within the required temperature interval need only be done once. The heat capacity of the sample can then be calculated as follows:

$$c_S = \frac{K_\Phi(T) \cdot (\Phi_S - \Phi_0)}{\beta \cdot m_S}$$

This method obviously saves time compared with the procedure in Sect. 6.2.1.1. A disadvantage is that conditions of thermal symmetry between sample and calibrant are lost and with them the partial compensation of errors.

The dual step method is always a good technique for the investigation of samples with high thermal conductivities. The comments of Sect. 6.2.1.1 regarding errors and their corrections remain valid for this procedure.

An interesting possibility is to attempt to set up experimental conditions for the sample run which are very similar to those for the zero line run. For this purpose the sample is put into the correct crucible S and a reference substance c_{Ref} is placed in the correct crucible R on the reference side. The (differential) signal $\Delta\Phi$ will approach that of the zero line Φ_0 when $C_S \approx C_{Ref}$. The sample specific heat capacity is then given by:

$$c_S = \frac{m_{Ref}}{m_S} c_{Ref} + \frac{K_\Phi(T) \cdot (\Delta\Phi - \Phi_0)}{\beta \cdot m_S}$$

At first sight this is a fascinating idea because the accuracy of the heat capacity measurements should come close to that of the calibration substance. However, the quality of the measurements is markedly influenced by possible differences in the thermal conductivities and the heat transfer conditions of both substances (or runs). Unfortunately it is very difficult or nearly impossible to recognize these influencing factors and to correct them because:

- Conditions for heat transfer may be poor, although rather small offsets of the isothermals may conceal this and even suggest high-quality measurements.
- Thermal lag cannot be corrected by the simple procedure outlined in Sect. 6.2.1.1. In addition, desmearing has not so far been carried out under these conditions.

6.2.1.3 A Variation of the Classical Technique

Precise measurements of the heat capacity using DSCs require rather narrow temperature intervals – not exceeding 100 to 150 K – otherwise nonlinearities in the temperature dependence of the isothermals cannot be neglected. However, heat capacities are usually required over much larger ranges of temperature. The region of interest must then be divided into smaller intervals. In this case the two conventional procedures (cf. Sects. 6.2.1.1 and 6.2.1.2) are cumbersome,

because empty (for zero line) and sample crucibles must be exchanged several times. The measuring time is increased and errors result from the inevitable lack of reproducibility in conditions for heat transfer. A better procedure was suggested by Hanitzsch, 1991 (see Fig. 6.11). The temperature range of interest is scanned three times, first with empty crucibles, then with the calibration substance and finally with the sample. After each run the subsequent cooling after a heating run (or the subsequent heating after a cooling run) to the start temperature T_{st} is interrupted every 50 to 100 K to get several isothermal heat flow rate levels. The intermediate isothermal levels are recorded. Fig. 6.11a explains this procedure for the case of a calibration with synthetic sapphire. The program temperature and the heat flow rate into the sample are plotted as function of time. Analogous curves are obtained for the empty pan and the sample run. From the heat flow rates of the initial, end and intermediate isothermals a polynomial of third or higher order can be calculated, which describes the generally existing curvature of the temperature dependence of the isothermals to a very good approximation:

$$\Phi_{iso}(t) = a_0 + a_1 t + a_2 t^2 + a_3 t^3$$

Fig. 6.11b shows the isothermal reference line (here Φ_0), the experimental and the corrected (due to the procedure of Sect. 6.2.1.1) heat flow rate curves. The calculation of the heat capacities is then analogous to the three step or dual step technique.

If the calibration factor $K_\Phi(T)$ is independent of the temperature – this is a good approximation for Perkin-Elmer power compensation DSCs – the calculation of the heat capacities can be further simplified and the required time reduced (Hanitzsch, 1991). If deviations of the calibration factor from unity are known from a preceding run and these deviations have been included in the hardware of the apparatus or the software, the quantity $K_\Phi(T)$ as third unknown is cancelled in the following two equations:

calibration run:

$$K_\Phi(T)\,(\Phi_{Ref} - \Phi_0) = \beta \cdot (m_{Ref} \cdot c_{Ref} + (m_{cr,Ref} - m_{cr,0})\,c_{cr})$$

measuring run:

$$K_\Phi(T)\,(\Phi_S - \Phi_0) = \beta \cdot (m_S \cdot c_S + (m_{cr,S} - m_{cr,0})\,c_{cr})$$

The specific heat capacity c_S is then obtained without need for the zero line Φ_0;

$$c_S = \frac{\Phi_S - \Phi_{Ref}}{m_S \cdot \beta} + \frac{m_{Ref} \cdot c_{Ref}}{m_S} + \frac{(m_{cr,Ref} - m_{cr,S})\,c_{cr}}{m_S}$$

The third term of this equation can be neglected if the masses of the empty crucibles $m_{cr,S}$, and $m_{cr,Ref}$ differ by no more than ±0.03 mg. The comments of Sect. 6.2.1.1 regarding errors and their corrections remain valid for this procedure.

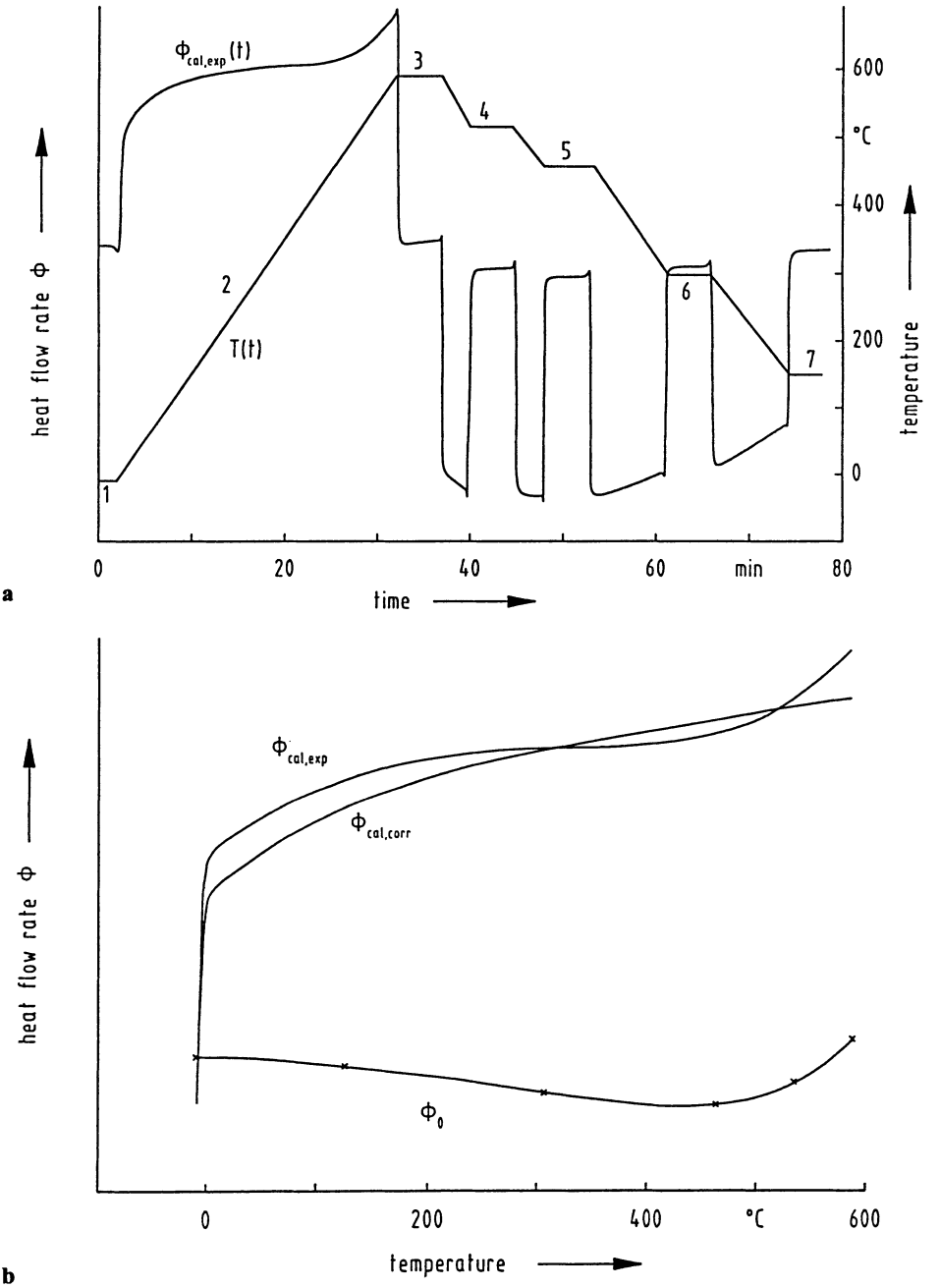

Fig. 6.11. Modified procedure for the determination of heat capacity for non-linear changes in the isothermals between the start and end of a run (acc. to Hanitzsch, 1991).
a program temperature $T(t)$ and heat flow rate $\Phi_{cal,exp}(t)$ during a calibrating run with synthetic sapphire, 1: initial isothermal at T_{st}, 2: scanning part of the heating run, 3: final isothermal at T_{end}, 4 to 7: intermediate isothermals during subsequent cooling to T_{st},
b $\Phi_{cal,exp}$ measured calibration heat flow rate, Φ_0 calculated polynomial fit of the isothermals (3–7 and 1) measured on cooling, $\Phi_{cal,corr}$ with Φ_0 corrected calibration heat flow rate

6.2.1.4 A Discontinuous Procedure

The techniques described so far allow a large temperature range to be covered in one long run. This gives a continuous heat capacity-temperature curve. An alternative procedure is to measure exchanged heats (areas). Thus the total temperature range must be divided into narrow intervals (Fig. 6.12) which are successively scanned with isothermal periods in between (Flynn, 1974; 1993). Depending on the temperature interval the procedure corresponds to Fig 6.12a or 6.12b. The operation must then be repeated with empty crucibles. If T_i and ΔT represent the initial temperature and the temperature interval respectively, the average specific heat capacity for the j-th temperature interval between $T_{j-1} = T_i + (j-1)\,\Delta T$ and $T_j = T_i + j\,\Delta T$ can be calculated from the heat Q_j, which is proportional to the area enclosed by the sample and zero runs:

$$\langle c_S(T_j)\rangle = \frac{K_Q(T_j) \cdot Q_j}{\Delta T \cdot m_S}$$

It is very important, that the isothermal periods are long enough to attain steady state conditions. These times differ according to the type of calorimeter. The isoperibolic Perkin-Elmer DSC, for example, needs 1 to 3 minutes, the longer times are needed for samples that are large and/or have poor thermal conductivity.

By analogy with Sect. 6.2.1.2, the empty reference crucible may be replaced by a crucible containing a calibration sample. The "Δ" in the symbol $\Delta(Q_j)$ of the following equation is used to emphasize this. If all crucibles, both on the sample and reference side, are assumed to have the same mass, we obtain:

$$\langle c_S(T_j)\rangle = \frac{K_Q(T_j) \cdot \Delta(Q_j)}{\Delta T \cdot m_S} + \frac{m_{Ref} \cdot c_{Ref}}{m_S}$$

This discontinuous technique replaces the disadvantage of the determination of absolute values of the heat flow rates from the continuous method with the advantage of the integration method for heat determination. A further advantage is that no correction for thermal lag is required but the temperature calibration must be very precise. If the ΔT-intervals are in the range of 1 to 2 K the calculated average value $\langle c_S(T_j)\rangle$ reproduces the searched value $c_S(T_j)$ sufficiently. The interval may be increased to 5 or 10 K when there is a low temperature dependence of the heat capacity.

The discontinuous procedure has been little used so far. Possible reasons for this are:

- Long measurement times are needed. To determine the heat capacity over 100 K with the continuous procedures of Sects. 6.2.1.1 to 6.2.1.3 requires 30 to 60 min at a heating rate of 10 K min^{-1}. In contrast the discontinuous technique takes 400 to 600 min for ΔT-intervals of 1 K.
  This time can, however, be reduced to 150 to 75 min if a 1 K interval is measured every 5 or 10 K only. This is perfectly acceptable when heat capacities are only slowly changing functions of temperature. The measurement time then becomes comparable with that of the other techniques.

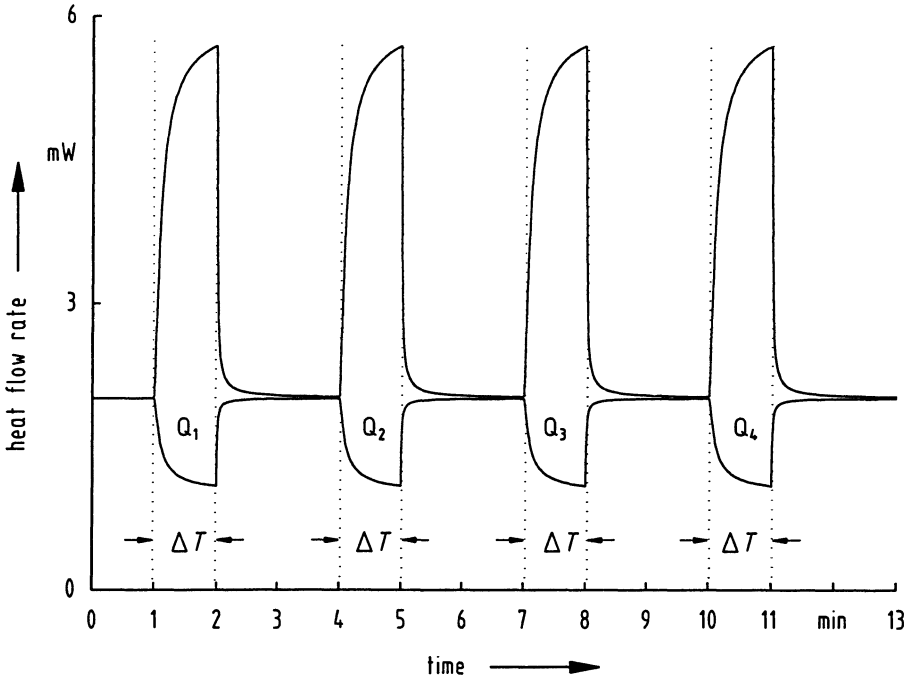

a

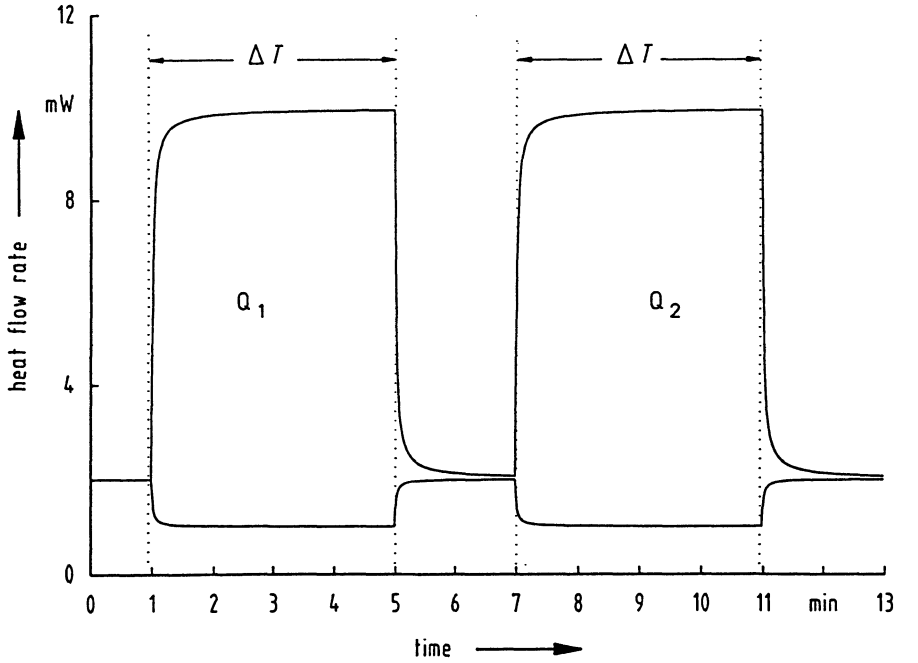

b

Fig. 6.12. Discontinuous method for the determination of the heat capacity.
a small temperature intervals ΔT, the heat flow rate does not reach the steady-state,
b larger temperature intervals ΔT, the heat flow rate comes to a steady-state

- If adequate software is not available a major effort must be put into the evaluation of data.
- The accuracy of heat capacities measured in this way is not higher than for those determined using the continuous technique. For normal sample masses (10 to 20 mg), temperature intervals of 1 K and specific heat capacities of 0.5 $J\,g^{-1}\,K^{-1}$, the heats to be determined are only in the order of 5 to 10 mJ. This is comparable with the area of the fusion peak of indium samples with masses of 0.15 to 0.3 mg. Unfortunately, minor errors in determination of the isothermal heat flow rates, which are unavoidable, affect the results of the c_p determination much more than is the case for In fusion peaks.

6.2.1.5 Determination Using the Dual Sample DSC

In a dual sample DSC (cf. Sect. 2.1.1) two samples can be analyzed simultaneously in the same thermal environment. It becomes possible to measure the heat capacity of a sample in a single run (Jin, Wunderlich, 1993). An empty crucible is placed in the reference position and the two sample crucibles contain the sample and the calibrant (Ref) respectively. The advantage of a single-run experiment, beside time savings, results from reduction of systematic experimental errors (e.g. due to thermal fluctuations of the signal), compared with the two or three successive runs necessary with a normal DSC. Assuming ideal symmetry of the cells and exact sample placement (within ± 0.2 mm e.g. using an autosampler), the temperature-dependent calibration factors $K_\Phi(T)$ should be identical for both sample cells. The $C_S(T)$ function of the sample would then immediately result from the ratio of the heat flow rates into the sample and into the calibration sample.

In reality there are asymmetries in the measuring system and it is essential to determine the different $K_\Phi(T)$ factors for both sample positions. Taking into account all possible sources of error (asymmetry of the measuring system, temperature lag, non-linear temperature calibration, heating rate differences between sample and reference), the uncertainties (RMS, see Sect. 7.2) of all measurements (using standard samples of sapphire, selenium, aluminum, quartz, polystyrene, and sodium chloride with well known data from adiabatic calorimetry) were estimated to be <1 % at temperatures above 300 K, <3% below 200 K, and <2% between 200 and 300 K (Jin, Wunderlich, 1993).

6.2.1.6 General Precautions for the Minimization of Errors

Calculation of heat capacities following the procedures of Sects. 6.2.1.1 to 6.2.1.3 needs true heat flow rates into the sample (the difference between recorded signal and the zero line). The zero line cannot be obtained simultaneously, but only after the sample crucible has been replaced once (or several) times. In doing so the original geometry between sample, crucible and temperature sensors can never be reproduced perfectly. It follows that changes in the conditions for the heat transfer, which cannot be immediately detected, are responsible for the great difficulties in

obtaining precise heat capacities. In order to limit the uncertainties to values smaller than 3 to 5% during routine operation, the following precautions are advisable:

- very careful sample preparation to optimize thermal contacts at all interfaces,
- sample and calibrant should have similar heat capacities and, if possible, similar thermal conductivities,
- temperature intervals no longer than 100 to 200 K for a single run. Larger temperature ranges should be divided into smaller intervals. For isoperibolic DSCs the initial and end isothermals are nonlinearely connected (due to asymmetries of radiation losses) and this tendency increases at higher temperatures. This must be borne in mind when selecting a propriate temperature interval. Differences in the observed heat capacities in overlapping temperature regions clearly reflect the uncertainties of the experiments,
- comparison of heating and cooling runs,
- an effective program of operation. The essential zero line and calibration runs should be carried out before and after the, perhaps multiple, sample runs under the same conditions,
- constant line voltage,
- constant purge gas flow,
- preheating of the calorimeter (including, if possible, the sample) to at least 10 to 15 K above the maximum temperature of the following measurement in order to stabilize the system, optimize the heat transfer conditions, and remove adsorbed moisture or retained solvent,
- for low temperature operation, prevention of any condensation of water from the atmosphere or of volatile components of the sample on the cold surroundings of the measuring system,
- constant room temperature (for precise measurements),
- in the case of isoperibolic DSC, very good temperature control of the isoperibolic surroundings, which influences the long-time stability of the recorded signal to a great extent. If, for instance, the DSC has been heated to a high final temperature during the zero line run and the stabilization of the temperature of the sample holder surroundings has not been sufficient, the following sample run would give a different isothermal. The same happens if the experiment is started before the isothermal baseline has reached a steady state (cf. Sect. 6.2.1.1).

Detailed considerations can be found in papers of Richardson, 1989; Suzuki, Wunderlich, 1984; Poeßnecker, 1990, and Flynn, 1993.

6.2.1.7 Typical Applications of Heat Capacity Measurements

- Calculation of the reaction enthalpies from the measured heat capacities of reactants and products using Kirchhoff's law:

$$\Delta_r H(T_2) = \Delta_r H(T_1) + \int \sum_i (\nu_i \cdot C_{m,i}(T))\, dT$$

$\Delta_r H(T_1)$, $\Delta_r H(T_2)$ molar reaction enthalpies at T_1 und T_2; $C_{m,i}(T)$ molar heat capacitiy of the i-th component; ν_i stoichiometric factor of the i-th component (positive for products, negative for reactants).

- Refined models for the description of the melting of polymers over broad (>100 K) ranges of temperatures require heat capacities of the amorphous and crystalline fraction in this region.
- Characterization of the glass transition process (cf. sect. 6.2.3) requires heat capacity functions for the non-equilibrium glassy amorphous and the equilibrium liquid state. Most such applications need only the change of the heat capacity with temperature. Thus for commonly used polynomials of the type $C(T) = a_0 + a_1\ T + a_2\ T^2 + \ldots$ or $C(T) = a_0 + a_1\ T + a_2\ T^{-2}$, a_0 is not needed. It is generally found that a linear approximation (all $a_i > a_1$ are zero) is sufficient.
- Very important from the theoretical point of view is, on the one hand, the comparison of theoretical and measured heat capacities and, on the other, the calculation of the thermodynamic potential functions $S(T)$, $H(T)$, $F(T)$ and $G(T)$.

For polymers numerous reliable experimental heat capacity results are available and these have been collected in a data bank (Wunderlich, 1990). The majority of these are DSC measurements and generally refer to relatively high temperatures (>200 K). Values at lower temperatures (as close as possible to 0 K) must be measured using high-performance adiabatic calorimeters.

The main microscopic cause of the measured macroscopic heat capacity of solids is the vibrational motion. It is thus possible to calculate the heat capacity of solid polymers if the vibrational spectra are known. According to the procedure of Wunderlich and co-workers (Lau et al., 1984; Wunderlich, 1990; Roles, Wunderlich, 1993) the spectra may be approximately separated into group and skeletal contributions. The former are obtained from infrared and Raman spectra. The latter can be approximated by Tarasov-functions, the characteristic parameters for which are obtained by fitting the experimental heat capacities at low temperatures, when the group vibrations are not yet excited.

The result of the calculation is C_V, the molar heat capacity at constant volume. To compare with the experimental C_p a relation between both quantities is needed. The thermodynamically exact conversion

$$C_p - C_V = T \cdot V \cdot \gamma^2/\chi$$

cannot often be used because neither the thermal expansivity γ nor the compressibility χ are known. A good approximation is to use a modified Nernst-Lindemann equation (Roles, Wunderlich, 1993).

$$C_p - C_V = 3R \cdot A_0 \cdot C_p^2 \cdot T/(C_V \cdot T_{fus}^0)$$

T_{fus}^0 equilibrium fusion temperature; A_0 empirical constant (for many polymers: $A_0 = 3.9\ 10^{-3}\ \mathrm{K\,mol\,J^{-1}}$).

When the heat capacity functions $C_p(T)$ are known from as near as possible to 0 K, the thermodynamic functions $H(T)$, $S(T)$, $F(T)$ and $G(T)$ can be cal-

culated as normal:

$$H(T) = H_0 + \int_0^T C_p(T)\,\mathrm{d}T \qquad S(T) = S_0 + \int_0^T \frac{C_p(T)}{T}\,\mathrm{d}T$$

$$F(T) = U(T) - T \cdot S(T) \qquad G(T) = H(T) - T \cdot S(T)$$

Low temperature DSC measurements of C_p are not possible and for this technique only changes in these functions can be calculated.

6.2.1.8 Heat Capacity Measurements with Temperature Modulated DSC

Recently, "modulated" ("oscillating", "dynamic") DSCs has become available (Reading et al., 1994). In this type of calorimeter, the common DSC principle has been modified to the extent that a (small) sinusoidal (or other periodic) term is added to the linear temperature-time function:

$$T(t) = T_0 + \beta \cdot t + A_T \sin \omega t$$

It has been shown (Wunderlich et al., 1994) that this type of DSC allows the heat capacity of the sample to be determined in one run. The easiest way is to determine it in the isothermal mode from the differential amplitude A_Δ (from sample and reference sensors), the amplitude A_T, the angular frequency ω, the thermal conductance L (between sample sensor and sample) and the heat capacity of the empty crucible C_0:

$$C_S = A_\Delta / A_T \sqrt{(L/\omega)^2 + C_0^2}$$

In principle it is also possible to determine the heat capacity of the sample in the same way from the non-isothermal, modulated scanning run, but in this case a horizontal zero line must be guaranteed. Care must be taken that the proper calibration is carried out, i.e. the determination of the effective thermal conductance L (in $\mathrm{W\,K^{-1}}$). With this proviso, heat capacities can be measured with this type of calorimeter with an error of 1% and better. This is one of the reasons why modulated (oscillating, dynamic) DSC is of considerable interest at present.

Another theoretical approach proceeds from the definition of a complex heat capacity function, which exist in the case of time dependent processes (e.g. the glass transition) and can be measured with the aid of temperature modulated DSC. As this approach is rather new, and a brief explanation is difficult, the reader is referred to the original literature (Jung et al., 1992; Schawe, 1995).

6.2.2 The Investigation of Reactions

The results of such investigations are the (temperature dependent) heat of reaction and the kinetics of the reaction. A definition of the true reaction mechanism (not just a formal mathematical fitting), the so called kinetic analysis, is a far more difficult problem. Any kinetic analysis demands a knowledge of the conversion rates as function of the progress of reaction. This is expressed as the extent of reac-

tion ξ or the degree of reaction α. Whatever the aim, interpretation assumes that both the initial and the final state of the reaction are unambiguous and well-defined. Without this information results will be, at best, semi-quantitative.

6.2.2.1 Determination of Heats of Reaction

The aim is to determine a thermodynamically well defined reaction enthalpy. If a subsequent kinetic analysis is planned, the calculation of a similarly well defined conversion-time curve is of equal importance. Because of the limited precision of DSCs minor effects due, for example, to changes in pressure, stress or surface contributions may be neglected. The following simplified equation is then obtained for the measured heat flow rates in a DSC :

$$\left(\frac{dQ}{dt}\right)_p = \Phi_m = C_{p,\xi}(T) \cdot \frac{dT}{dt} + \left(\frac{\partial H}{\partial \xi}\right)_{T,p} \cdot \frac{d\xi}{dt}$$

$C_{p,\xi}(T)$ is the heat capacity of the system at constant pressure and at constant extent of reaction. The partial molar reaction enthalpy $\Delta_r H = (\partial H/\partial \xi)_{T,p}$ is nearly always replaced by the average reaction enthalpy $\langle \Delta_r H \rangle$, which is independent of the instantaneous composition of the system. The Kirchhoff equation

$$\left(\frac{\partial C_{p,\xi}}{\partial \xi}\right)_{T,p} = \left(\frac{\partial \Delta_r H}{\partial T}\right)_{p,\xi} = \sum_i (\nu_i \cdot C_{p,i})$$

describes the relation between the change of the heat capacity of the reacting system and the temperature-dependent reaction enthalpy. Here the ν_i are the stoichiometric numbers and $C_{p,i}$ the partial molar heat capacities of reactants and products.

Reactions may be carried out isothermally or non-isothermally (in scanning mode or following a special temperature programm). Advantages and disadvantages are discussed in detail in Sect 6.2.2.2.

Reactions in the Isothermal Mode

Here, the sample is heated as rapidly as possible from a temperature at which the system is inert (often room temperature) to the reaction temperature. The "drop in" technique (cf. Appendix 2) may also be used – the sample is dropped into the preheated calorimeter. The end of the reaction is indicated by a constant heat flow rate Φ_{end}. Extrapolation of this Φ_{end} to the start yields the baseline of the reaction peak. As there is no heat capacity contribution in the isothermal mode, the relation between the heat produced or consumed and the average reaction enthalpy is very simple:

$$Q_m(t) = \int_0^t (\Phi_m - \Phi_{end})\, dt = \langle \Delta_r H \rangle \int_0^\xi d\xi$$

The only uncertainty is due to possible drift in the signal. The caloric error for a typical sample mass of 10 mg and a heat production of 360 J g^{-1} is less than 1%, if

drift during a one hour reaction is less than 10 μW. For long-term reactions drift must therefore be comparable with the short time noise (cf. sect. 7.2).

If a reaction is investigated at several temperatures (essential for a kinetic analysis), the temperature dependence of the reaction heat is also obtained. Alternatively, if the $C_p(T)$ functions of reactants and products are known, $\Delta_r H(T)$ may be calculated by means of the Kirchhoff equation.

The main problem with isothermal measurements results from the ill-defined behaviour of the signal following the initial introduction of the sample. Even for DSCs with very short time constants this time amounts to at least 10 to 15 s. Most of this error can, however, be eliminated by subtracting the measured curve of a second run with the same (now reacted) sample and exactly the same conditions. Nevertheless, minor differences may remain because of the different thermal conductivities of products and reactants and because heat transfer conditions may change during the reaction.

In order to check the completeness of the reaction, the sample is often heated to higher temperatures. However, this is only useful if side reactions or shifts of chemical equilibria at higher temperatures can be excluded. If additional reaction has been detected, the clear assignment of a reaction heat to a definite temperature may be lost.

Reactions in the Scanning Mode

In principle, the correct evaluation corresponds to that already discussed in Sect. 5.3. However, the situation is more difficult, because it cannot be assumed that reactants and products have almost constant heat capacities owing to the large temperature interval of the reaction (100 K and more). In contrast to phase transitions, which follow a zeroth order reaction law, chemical reactions do not terminate at, or shortly beyond, the reaction peak maximum. To complicate matters, the reaction products may have a glass transition within the reaction region. In addition, the glass temperature of the original reactants may shift into this temperature range. As a typical example, the curing of an epoxide resin is shown in Fig. 6.13 (Richardson, 1989). The reaction starts immediately after the glass transition of the reactants at A and is finished at B. (In the following it is always assumed that the zero line has no curvature or has been subtracted and that changes in heat transfer conditions can be neglected). Reaction enthalpies may be determined in the following ways (in the first case only the heat flow rate curve has to be measured, all other methods require C_p measurements).

Method 1: A linear baseline is drawn between the points A and B (Fig. 6.13). This simple and widely used procedure is only an approximation. It is better the smaller the heat capacity difference between reactants and products. The validity of this assumption can be decided very easily by comparing the original run with a rerun on the reacted material. Both curves should then fit at A and B. As can be seen from Fig. 6.14b, this is not true for this system, even after allowance for the glass transition.

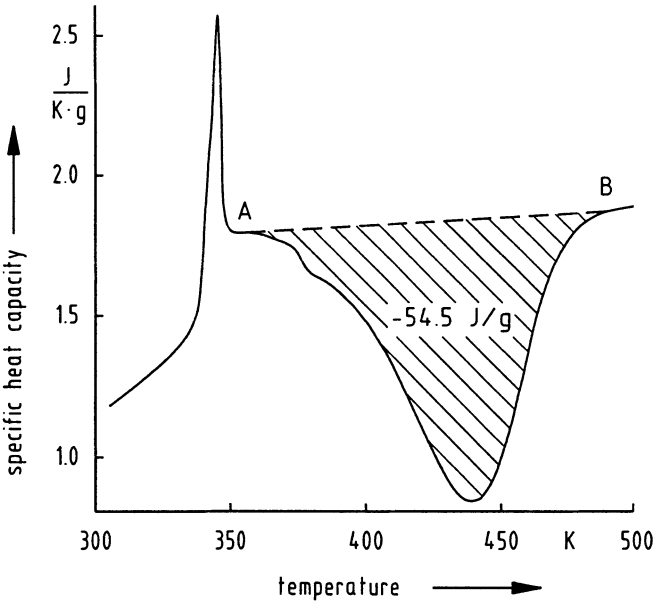

Fig. 6.13. Curing of an epoxide resin (acc. to Richardson, 1989) and the procedure mostly used to determine the heat of reaction. The linear baseline between start (A) and end (B) of the reaction ignores all possible changes in heat capacity

Method 2: If the temperature dependent change of the heat capacity $C_{p,\xi}(T)$ of the reacting system cannot be neglected, but the heat capacities of reactants and products are known over the relevant temperature range (and there are no glass transitions), then the baseline can be calculated by iterations similar to those of case 3 in Sect. 5.3. Method 1 above gives the zeroth approximation to the extent of reaction function $\xi(T)$. The heat capacities of the products can easily be obtained from the rerun on the fully reacted sample. If the first run of the reaction mixture can be started at least 30 K before the reaction starts, the heat capacity of the reactants may be determined from this interval. Extrapolation into the reaction temperature range is generally accurate enough. Otherwise, the heat capacities of all components of the reaction mixture must be measured separately and the C_p function calculated using simple mixing rules.

After subtraction of the baseline constructed in this way from the measured curve, an average heat of reaction is obtained (the term reaction enthalpy should be avoided, the quantity has no thermodynamic significance) for the temperature range between T_1 and T_2. Improvements relative to method 1 are only found if the heat capacity functions are known with sufficient precision (uncertainties $< 1\%$). Obvious improvements in the definition of the baseline should result from the use of "modulated" ("oscillating", "dynamic") DSC (cf. Sect 6.2.1.8). By this method it is possible to get both the heat flow rate curve (which is proportional to the actual

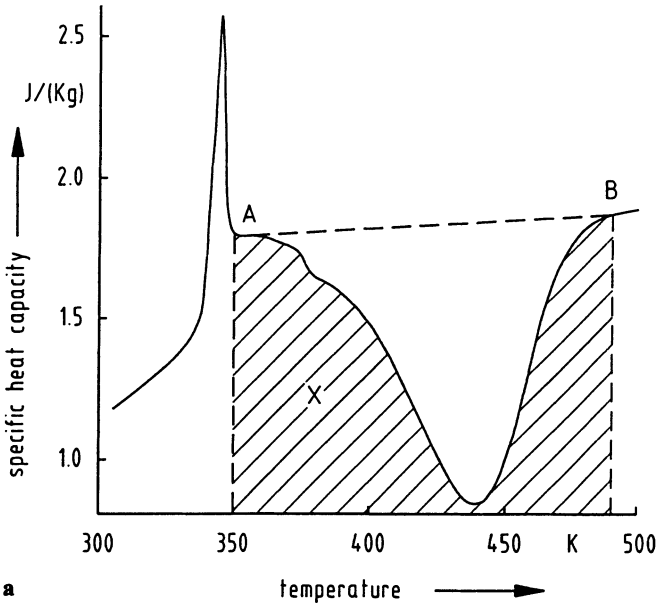

a

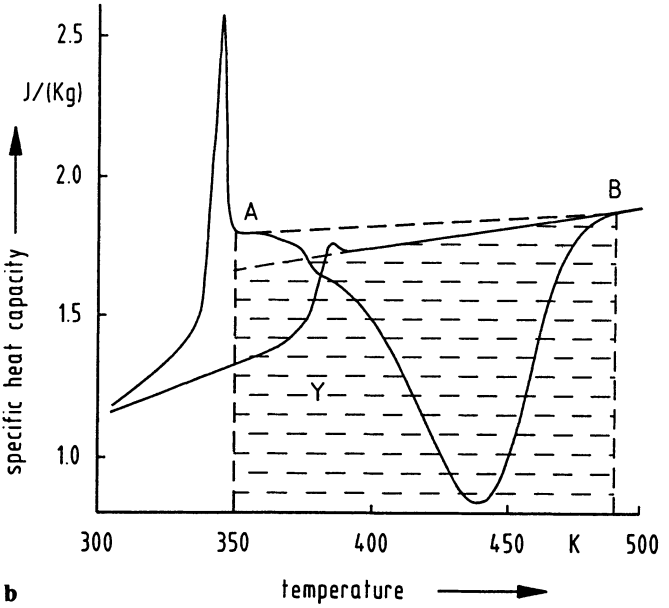

b

Fig. 6.14. The thermodynamically correct determination of the specific heat of reaction (acc. to Richardson, 1989); for details see text.

a 1st run curve,

b 1st and 2nd run curves.

Hatched areas extended to $c_p = 0$; $\Delta h(350\,\mathrm{K}) = X - Y = h_{\mathrm{products}}(350\,\mathrm{K}) - h_{\mathrm{reactants}}(350\,\mathrm{K}) = -44.7\,\mathrm{J\,g^{-1}}$

reaction rate) and the heat capacity function of the reacting mixture from the same run.

The extent of reaction function $\xi(T)$ can be obtained from the ratio between partial heats (up to a certain temperature) and the overall heat of the reaction.

Method 3: Many of the above problems and difficulties can be avoided by integration of the C_p curves (Richardson, 1989; 1992b; Flynn, 1993). The specific reaction enthalpy $\Delta_r h\ (T_1)$ at the starting temperature T_1 (e.g. 350 K) may be determined in a thermodynamically correct way even if a glass transition occurs within the temperature range of the reaction. From the procedure of Fig. 6.14 it follows that

$$\Delta_r h\ (T_1) = h_l\ (\mathrm{P}, 350\ \mathrm{K}) - h_l\ (\mathrm{R}, 350\ \mathrm{K})$$

The reaction enthalpy at temperature T_1 (i.e. $\Delta_r h(T_1)$) is obtained as difference between the areas X and Y. The baseline is not necessary in this case, because only differences are needed:

$$\Delta_r h\ (T_1) = X - Y = ((h_l\ (\mathrm{P}, 490\ \mathrm{K}) - h_l\ (\mathrm{R}, 350\ \mathrm{K})) - (h_l\ (\mathrm{P}, 490\ \mathrm{K}) - h_l\ (\mathrm{P}, 350\ \mathrm{K}))$$

The enthalpy subscript l represents the liquid state of the reactants R and the liquid-like or rubbery state of the products P. The difference h_l(P, 490 K) – h_l(R, 350 K) corresponds to the experimental quantity, the area X, defined by the lines at T_1, T_2, $c_p = 0$ and the reaction curve. The horizontal hatched area Y follows from the rerun on the reacted sample.

$$Y = h_l\ (\mathrm{P}, 490\ \mathrm{K}) - h_l\ (\mathrm{P}, 350\ \mathrm{K}) = \int_{350\ \mathrm{K}}^{490\ \mathrm{K}} c_{p,l}\ (\mathrm{P})\ \mathrm{d}T$$

If the glass transition of the products is above T_1, as is the case in Fig. 6.14, $C_{p,l}$ must be extrapolated as shown. Without this extrapolation another result would be obtained:

$$\Delta_r h'\ (T_1) = h_g\ (\mathrm{P}, 350\ \mathrm{K}) - h_l\ (\mathrm{R}, 350\ \mathrm{K})$$

The procedure can also be extended to the determination of reaction enthalpies at any temperature T between T_1 and T_2 (Richardson, 1992b; cf. also Sect. 5.3). At first a possible glass transition is disregarded. One obtains:

$$\begin{aligned}\Delta_r h\ (T) &= h\ (\mathrm{P}, T) - h\ (\mathrm{R}, T) \\ &= (h\ (\mathrm{P}, T_2) - h\ (\mathrm{R}, T_1)) - (h\ (\mathrm{P}, T_2) - h\ (\mathrm{P}, T)) \\ &\quad - (h\ (\mathrm{R}, T) - h\ (\mathrm{R}, T_1))\end{aligned}$$

or:

$$\Delta_r h\ (T) = X - \int_T^{T_2} c_p(\mathrm{P})\ \mathrm{d}T - \int_{T_1}^{T} c_p(\mathrm{R})\ \mathrm{d}T = X - Z$$

This procedure is schematically shown in Fig. 6.15. The areas X and Z are hatched horizontally and vertically respectively. A simple rearrangement of the last equation

gives:

$$\Delta_r h\,(T) = X - \int_{T_1}^{T_2} c_p(\mathrm{P})\,\mathrm{d}T + \int_{T_1}^{T} (c_p(\mathrm{P}) - c_p(\mathrm{R}))\,\mathrm{d}T$$

$$= \Delta_r h\,(T_1) + \int_{T_1}^{T} (c_p(\mathrm{P}) - c_p(\mathrm{R}))\,\mathrm{d}T$$

It is clear from Fig. 6.15 that this procedure is a direct application of the Kirchhoff equation. An enthalpy-temperature diagram (Fig. 6.16) is especially clear and instructive. Here, for the sake of simplicity, temperature independent heat capacities are assumed. The enthalpies are then linear functions of the temperature. The diagram also recognizes that both reactants and products may be in the glassy (curves $H_g(\mathrm{R})$ and $H_g(\mathrm{P})$) or liquid (curves $H_l(\mathrm{R})$ and $H_l(\mathrm{P})$) state. A reaction usually proceeds at a measurable rate only when the reactants are in the liquid state (above glass transition $T_g(\mathrm{R})$). Further, the glass transition of the products ($T_g(\mathrm{P})$) is very often somewhere between T_1 and T_2. A formal (Flynn, 1993) and thermodynamically correct procedure yields four different reaction enthalpies and four different ξ values at each temperature (see Fig. 6.16):

glassy reactants	→ glassy products	$\Delta_r H$ = bd, ξ = bc/bd
glassy reactants	→ liquid (rubbery) products	$\Delta_r H$ = be, ξ = bc/be
liquid reactants	→ glassy products	$\Delta_r H$ = ad, ξ = ac/ad
liquid reactants	→ liquid (rubbery) products	$\Delta_r H$ = ae, ξ = ac/ae

Only the final case has any meaning for kinetic studies.

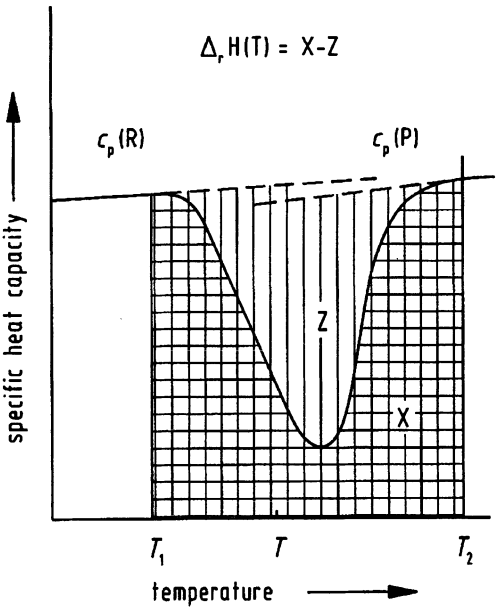

Fig. 6.15. The thermodynamically correct determination of a reaction enthalpy (acc. to Richardson, 1992b); for details see text

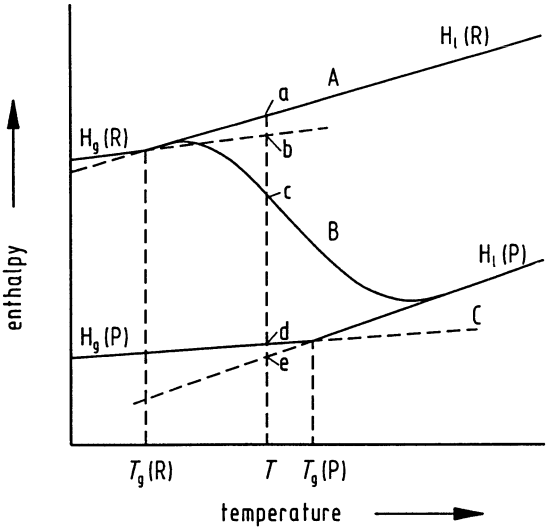

Fig. 6.16. The determination of reaction enthalpies from an enthalpy-temperature diagram; for details see text.
A: integral of $C_p(T)$ for the reactants, B: integral of $C_p(T)$ for the reaction mixture, C: integral of $C_p(T)$ for the products

Rarely, e.g. where there is a possibility of side or decomposition reactions, the heating should be stopped at a temperature at which such disturbing reactions can still be excluded. The reaction should then be completed isothermally at this temperature. Baselines are needed for both the scanning and isothermal parts of the reaction (Richardson, 1989). However, it may be more convenient to carry out all the reaction in the isothermal mode.

6.2.2.2 Kinetic Investigations

6.2.2.2.1 Introduction and Definitions

As mentioned in Sect. 4.4, the assignment of the time dependent heat flow rates to defined reactions lead to kinetic data. The true aim of a *kinetic analysis* is an evaluation of the correct reaction mechanism: this is fully defined, if the sequence of all elementary steps is known as are the activation parameters for each of these. A large body of experimental data has then been reduced to a few equations which describe the relevant process, so reliable predictions are possible. For example, the influence of variations in the activation conditions can be described together with the effects of changes in the composition of the reacting systems. Much time and effort is required to reach this points and supplementary investigations are essential. If the evaluation of a given system is limited only to a mathematical description of the reaction by formal kinetic parameters (overall rate equation, overall

activation parameters), less effort is clearly required. However, the possibility of predicting reaction rates for systems with another composition is then much restricted or almost impossible.

Every quantitative kinetic analysis starts with the determination of an unbroken sequence of concentration-time data. Using DSC gives a direct measurement of the rate of conversion versus time. The rate of reaction law for the overall or the elementary reaction may then be formulated as usual:

$$r = \frac{1}{V} \cdot \frac{\mathrm{d}\xi}{\mathrm{d}t} = \frac{1}{\nu_i} \cdot \frac{\mathrm{d}c_i}{\mathrm{d}t} = f(c_\mathrm{A}, c_\mathrm{B}, \ldots, p, T)$$

At constant temperature and constant pressure and postulating a simple mechanism one obtains:

$$r = \frac{1}{V} \cdot \frac{\mathrm{d}\xi}{\mathrm{d}t} = \frac{1}{\nu_i} \cdot \frac{\mathrm{d}c_i}{\mathrm{d}t} = k(T) \cdot c_\mathrm{A}^{n_\mathrm{A}} \cdot c_\mathrm{B}^{n_\mathrm{B}} \cdot \ldots$$

$k(T)$ is the rate constant; the exponents n_A, n_B, ... are the partial orders of the respective reactants in the rate law. They are generally not identical with the stoichiometric coefficients. Their sum is equal to the overall reaction order n. As a rule the experiment does not provide the concentrations of the respective components themselves, but rather quantities (or changes of these quantities with respect to time) which are proportional to the concentrations or to the concentration changes. With DSCs, the change in concentration of a component at time t may be obtained from the measured heat flow rate, but only unambignously, if

- the heat of reaction is independent of the extent of reaction,
- the overall reaction is an elementary reaction, i.e. only one heat-producing reaction exists,
- the initial and final states of the reaction are known.

It is clear from these restrictions that, in general, a kinetic evaluation of DSC measurements is only meaningful if supplemented by results from other analytical methods (e.g. from IR, UV, NMR, MS, GC, HPLC etc.).

Using thermoanalytical methods for the investigation of kinetic problems, the concentration of the reactants are frequently replaced by the degrees of reaction $\alpha = \xi/\xi_{\max}$, in particular if reactions in heterogeneous systems are investigated. For simple n-th order reactions in the case of equimolar mixtures one obtains:

$$\frac{\mathrm{d}\alpha}{\mathrm{d}t} = k(T) \cdot c_0^n \cdot (1-\alpha)^n$$

For any other mechanism a general conversion function $f(\alpha)$, dependent on the special type of the homogeneous or heterogeneous reaction, is introduced:

$$\frac{\mathrm{d}\alpha}{\mathrm{d}t} = k(T) \cdot f(\alpha)$$

$\mathrm{d}\alpha/\mathrm{d}t$ is measured in units of reciprocal time, α ranges from 0 to 1.

Using the DSC in the scanning mode at a constant rate ($\beta = dT/dt = \text{const}$), the term $d\alpha/dt$ will be replaced by the term $\beta\, d\alpha/dT$ (minor self-heating of the sample during the exothermic reaction is neglected).

Usually the temperature dependence of the rate constant $k(T)$ is described by the empirical Arrhenius equation or by the Eyring equation, which follows from the activated complex theory:

$$\text{Arrhenius:} \quad k(T) = A \cdot e^{-E_A/RT}$$

$$\text{Eyring:} \quad k(T) = \frac{k_B \cdot T}{h} \cdot e^{\Delta S^{\ddagger}/R} \cdot e^{-\Delta H^{\ddagger}/RT}$$

k_B is the Boltzmann constant, h the Planck constant.

The Arrhenius parameters (A preexponential factor, E_A activation energy) and the Eyring parameters ($\Delta S^{\ddagger}$ activation entropy, $\Delta H^{\ddagger}$ activation enthalpy) are related to one another by (for condensed systems):

$$\Delta H^{\ddagger} = E_A - R \cdot T \qquad \Delta S^{\ddagger} = R \cdot \ln \frac{A \cdot h}{e \cdot k_B \cdot T}$$

The Eyring activation parameters are more suitable for the understanding of relations between the structure of the reactants and the reactivity (Heublein et al., 1984). DSC methods are widely used to solve kinetic problems because of the simple and fast sample preparation and the wide range of experimental conditions – much information is produced in a short time. The technique, by contrast with many other methods, immediately gives a series of "reaction rates" as a function of the degree of reaction α. The methodology is quite general and it is immaterial whether the reactions investigated come from inorganic, organic or macromolecular chemistry. Continuing advances in instrumentation and data treatment facilitate refined calculations. However, these are only meaningful after consideration of specific aspects due to sample preparation, some peculiarities of the DSC method, data sampling and the processing of the raw data.

6.2.2.2.2 Experimental Preconditions for a Reliable Kinetic Analysis

1. Sample Requirements

- After the introduction of the sample into the DSC the amount of reaction should be negligible prior to the attainment of a stable steady state. If this is not the case it must be determined separately and allowance made for this effect.
- The reaction mixture must not react with the material of the crucibles nor should there be any catalytic influence.
- Samples with an appreciable vapour pressure must be loaded into special sealable crucibles. Errors due to the effect of pressure on the measured C are usually insignificant. Much larger errors can occur because of changes in the concentration of a volatile component, for example a catalyst, used in very low concentrations, could be partially in the gaseous phase outside the reac-

tion mixture. The change in the concentration in the reaction mixture can be allowed for to a sufficient approximation, if the vapor pressure of the volatile component and the volume of the gaseous phase are known.

- Multiple measurements should always be made (with the same operation parameters) to check on the experimental repeatability. In addition some spot checks on other independently prepared reaction mixtures of the same composition should be carried out in order to exclude accidental errors during sample preparation. If the mixture is reactive at room temperature, loaded crucibles should be stored in liquid nitrogen.

2. *Features Peculiar to DSC Methods*

- The reaction mixture in the small and sealed crucibles of a DSC cannot be stirred. The results can, therefore, only be partially interpreted if concentration gradients occur during the reaction, or if there are transport processes to the gaseous phase (e. g. the decomposition of hydrates).
- It is not possible to add solid or liquid components to the reaction mixture after closing the crucibles.
- To apply these results to technical processes (e.g. to predict behavior in a reactor) the very different conditions must be recognized and, in particular, allowance made for heat transfer effects.

3. *Data Aquisition and Processing*

- If one needs in addition to the $\alpha(t)$ function also that of the rate of conversion $\mathrm{d}\alpha(t)/\mathrm{d}t$ for a kinetic analysis, the baseline must be determined first (according to the method 1 or 2 in Sect. 6.2.2.1) and then subtracted from the measured curve. It is also possible to proceed from method 3 in that section. In every case the measured reaction heat Q_m must be checked and, if necessary, corrected with respect to the final degree of conversion actually reached. This correction must be made whatever the reason for the cessation of reaction – perhaps caused by a great increase in viscosity (vitrification) or coming to an equilibrium state. All subsequent kinetic analyses are incorrect if this modification is omitted. Otherwise the calculated $\alpha(t)$ is not related to the thermodynamic degree of conversion but to an apparent final state that is specific to the individual experiment. If the correct heat of reaction Q_∞ can be related to only one heat-producing reaction, the resultant overall $\alpha(t)$ curve is the true normalized degree of reaction function, independent of any model considerations. Similarly the normalized rate of conversion follows from the current heat flow rate:

$$\alpha(t) = \frac{Q_t}{Q_\infty} \quad \text{and} \quad \dot{\alpha}(t) = \frac{\mathrm{d}\alpha}{\mathrm{d}t} = \frac{\Phi(t)}{Q_\infty}$$

- In general, however, several reactions contribute to the measured heat flow rate. An evaluation is then possible only with respect to a certain model. If the overall reaction is made up of, say, n reactions, all contribute to the measured heat flow rate and their reaction heats can be treated as parameters and determined as such by variation procedures. It is obviously much better to deter-

mine as much supplementary information as possible (for the optimum case of $n-1$) for the individual heats of reaction by changes in the DSC conditions or other measurements, e.g. temperature dependent spectroscopic investigations of equilibrium states etc.
- The experimental curve has to be desmeared (Sect. 5.4) before any evaluation if there are significant changes in the heat flow rates at time periods which are comparable with the time constants of the calorimeter.
- The true sample temperature may differ from that measured by the thermometer which is outside the sample, because of the limited thermal conductivity of the sample and its surroundings. This is especially true for larger sample weights and higher reaction rates. Strictly speaking, even "isothermal" reactions proceed non-isothermally. The true sample temperature can be calculated if the instantaneous heat generated by the reaction is related to the heat exchanged with the calorimeter (this is limited by the overall thermal relaxation time constant of sample and calorimeter). For example, with very fast light-activated reactions there are sometimes heat generation rates of 100 mW and more leading to temperature corrections greater than 10 K even for calorimeters with small time constants.
- Assuming that absolute and random errors for the measured signal are independent of time, the relative errors of the measured reaction rates increase at the end of the reaction. Therefore, efficient software should weight the data appropriately.
- Correct calibration of the DSC is essential – the temperature scale, the heat flow and the scanning rates.
- Changes of the sample volume during the reaction (e.g. up to 8% decrease in volume during epoxide amine curing reactions are possible) have to be considered, irrespective of whether subsequent calculations are made as functions of concentration or degree of reaction.

In much of the literature it is unfortunately not clear whether the above aspects have been considered. For example, a kinetic analysis of non-isothermal crystallization may have serious flaws if published heat flow rate curves are without proper baselines. Again, if high heating or cooling rates (up to 40 K min^{-1}) are used, leading to large changes in heat flow rates, it is rare to find that curves have been desmeared prior to analysis.

6.2.2.2.3 Isothermal or Non-isothermal Reaction Mode?

Classical techniques of chemical kinetics normally operate in the (quasi-) isothermal mode. By contrast, it is very convenient to make kinetic studies by DSC using the scanning mode. Both modes are possible in DSC and have particular advantages and disadvantages (Flammersheim, 1988). They complement each other and should not be regarded as alternatives.

Advantages and disadvantages of the isothermal mode.
- A simple and immediate interpretation of the measured curve is possible because of the complete decoupling of the two variables, temperature and time, if the

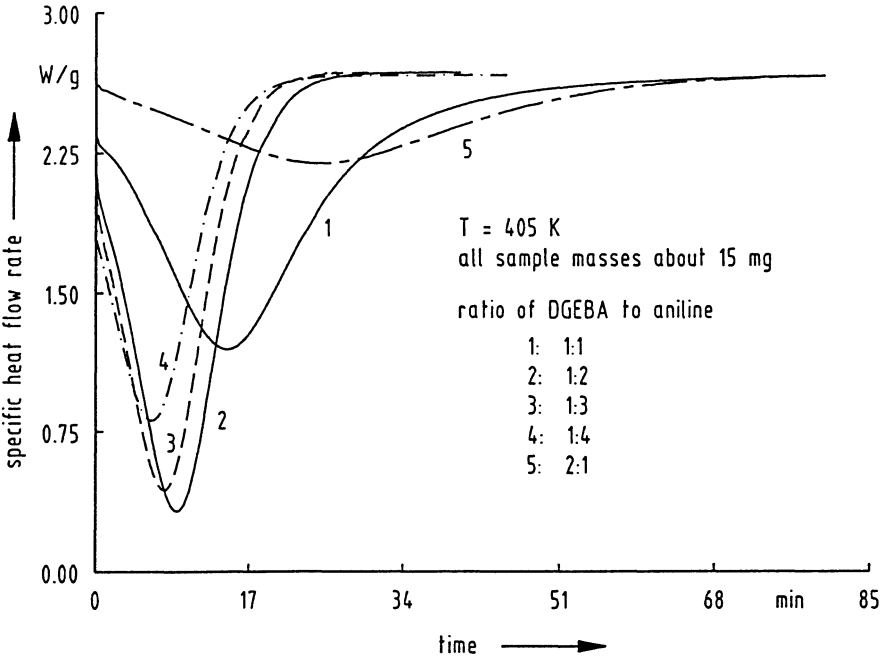

Fig. 6.17. Isothermal reaction curves for the polyaddition of aniline and bisphenol-A-diglycidyl ether (DGEBA) in mixtures with different stoichiometry

minor changes of the sample temperature during the reaction can be neglected. This method is especially useful when searching for the most probable reaction mechanism. Two examples will illustrate this:

During the polyaddition reaction of aniline and the diglycidylether of bisphenol-A (DGEBA) the maximum conversion rate is found at non-zero degrees of reaction (Fig. 6.17). This can only be due to autocatalytic and/or consecutive reactions. Furthermore it is obvious that not only the ratio of the concentrations of both reactants has substantial consequences but also that equal excess concentrations of amine or epoxide differ greatly in their effects. This is a very important pointer to the possible reaction mechanism.

The second example (Fig. 6.18) is the polyaddition reaction of a mixture of the two isomers 2,2,4-trimethylhexamethylene diisocyanate and 2,4,4-trimethylhexamethylene diisocyanate (TMDI) with 3,6-dioxaoctane-1,8-dithiol (TGDT) in presence of varying concentrations of a catalyst. As expected, the initial conversion rate is proportional to the catalyst concentration but the increase in the slope of the leading edge of the reaction peak in direct proportion to the concentration of catalyst is unusual. This can only be explained if one assumes a direct coupling of catalysis and autocatalysis (cf. Sect. 6.2.2.2.8).

- The baseline follows unambiguously by extrapolating the measured heat flow rate after the complete reaction, assuming that all parameters, which can influence the measurement directly or indirectly (e.g. the temperature of the

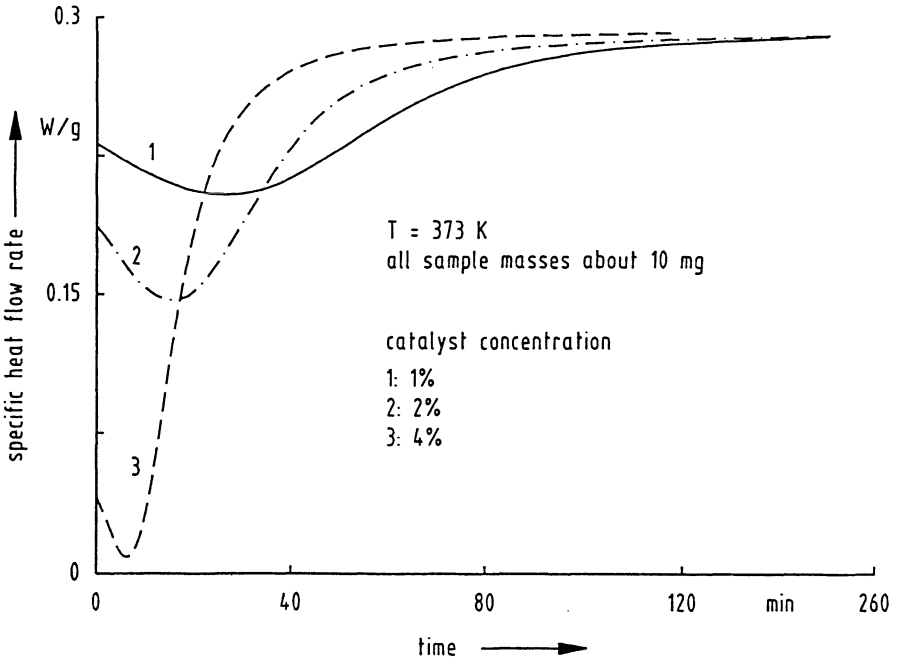

Fig. 6.18. Isothermal reaction curves for a stoichiometric system of trimethylhexamethylene diisocyanate and 3,6-dioxaoctane-1,8-dithiol with pyridine as a catalyst. The change in the reaction rate on the leading edge of the peaks shows direct coupling of catalysis and autocatalysis

surroundings) are sufficiently constant. Demands on the apparatus can be considerable, depending on the reaction time in question. Above all the long-time drift of the signal should not be greater than the short-time noise. The standard controls offered by the manufacturers of commercial DSCs are not generally sufficient. For instance, for a Perkin-Elmer DSC it is necessary to control the temperature of the isoperibolic block to better than ± 0.01 K (by adding of a controlled Peltier cooling device or a cryostat with circulation of the coolant) and stabilize the room temperature to ± 0.2 K, for to come to optimum conditions, i.e. to a caloric error below 1%.

- The reaction can be allowed to take place at low temperatures such that decomposition or side reactions can be avoided.
- The main disadvantage, already mentioned in Sect. 6.2.2.1, is that the initial phase of the reaction cannot be measured precisely, as the steady state conditions are disturbed on introduction of the sample. The solution given, using the difference between the reaction curve and the fully reacted rerun, for kinetic analysis, is only partially successful. A better solution is to always choose sufficiently low reaction temperatures so that unavoidable errors are minimized to values which do not influence model calculations. In addition, smearing of the heat flow rate data and deviations of the sample temperature from that of

the isothermal surroundings are so small that the experimental data need not be corrected.
- Isothermal measurements need more time than scanning runs, because reaction isotherms must be recorded at a minimum of five different temperatures that are as widely separated as possible.

Advantages and disadvantages of non-isothermal measurements.
- Scanning measurements need less time than isothermal experiments but construction of the proper baseline may be a problem.
- The measurement can be started at temperatures well below that of the beginning of the reaction, so steady state conditions of the DSC are ensured. Unfortunately, reactions may go to completion, even at low heating rates, at such high temperatures that secondary reactions cannot be neglected (this is especially relevant for organic reactions).
- The kinetic parameters can, in principle, be obtained from a single measurement, if the reaction mechanism is known. The experimental data cover such a wide temperature/concentration/time regime, that reliable results concerning the mechanism are possible. Unfortunately it is not clear from the shape of the curve what type of reaction is involved and this is a drawback when searching for the most probable reaction mechanism.

6.2.2.2.4 Thermal Activation of the Sample or Activation by High Energy Radiation

Reactions that are studied in the DSC are normally thermally activated. The wide range of experimental conditions (scanning rates, temperature range, possibility of more complicated procedures with intermediate annealing phases) is responsible for the extensive use of this technique.

Many reactions, however, can also be started by radiation with sufficiently high energy. The investigation of such reactions in a "Photo-DSC" (cf. Sect. 2.2) has considerable value for the optimization of process control parameters and this is especially true for those polyaddition and polymerization reactions that give materials with widespread uses.

A typical example of a light-activated measurement is shown in Fig. 6.19. It is often found, even in the case of absolutely symmetric radiation conditions on both the sample and the reference side, that the baselines change during the dark and the illumination phase, as in the figure. Simple subtraction of a second curve measured with the same procedure but with the reacted substance removes this effect. Light-initiated reactions, using conditions in the DSC which come close to those used in practice, are always extremely fast. The apparatus (or Green's) function, which is needed for the subsequent desmearing (deconvolution, see Sect. 5.4), is obtained easily and is sufficiently precise if, after the completed reaction, the response of the sample to a light flash is recorded (Flammersheim et al., 1991). If it were not for the fact that the heat produced during the chemical reaction is evolved inside the sample, but during the light flash it is mostly a surface effect, this response would be an ideal apparatus function for the sample properties in question. The dashed line in

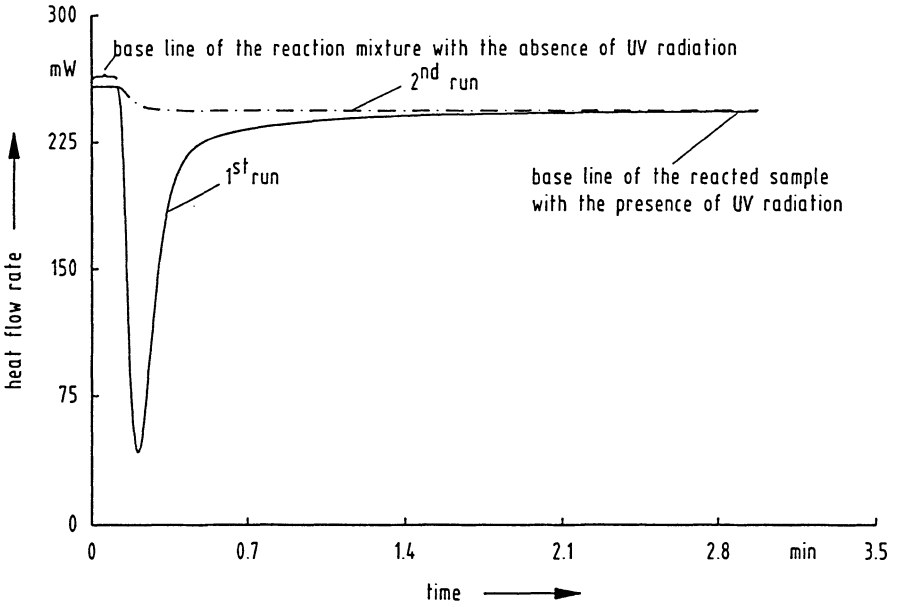

Fig. 6.19. 1st and 2nd run for the photopolymerization of a multifunctional acrylate at room temperature.
(photoinitiator: 1 % 2,2-dimethoxy-2-phenylacetophenone (benzyldimethylketal), light intensity: 5 mW cm^{-2} at 365 nm)

Fig. 6.20 corresponds to the deconvoluted curve. The solid curve is the original measured curve after subtraction of the baseline (2nd run) from Fig. 6.19.

The kinetic evaluation of light-activated reactions has so far only been partially succesful because the true reaction course is overshadowed by additional influences:

- Irradiation of the initiator causes a time dependence of the concentration of the initiating radicals but this effect can be easily corrected if the kinetics of the decomposition are known.
- Samples have finite thickness (0.1 to 0.4 mm). It follows from the Beer-Lambert law that there is a varying light absorption and hence a gradient of the reaction rates within the sample. However, the calorimeter always records an overall heat flow rate. As result of this rate gradient there is a corresponding concentration gradient of the reactive component. An exact solution of the subsequent system of differential equations is only possible for drastically simplified boundary and initial conditions (Shultz, 1984).
- The situation may be made more difficult by the increasing viscosity of the mixture during the reaction, which nearly always is carried out at room temperature. As a result, the reaction may be incomplete (Klemm et al., 1985). For example, at room temperature phenyl glycidyl ether (PGE) reacts completely during cationic polymerization induced by irradiation of diaryliodonium salts, whereas the

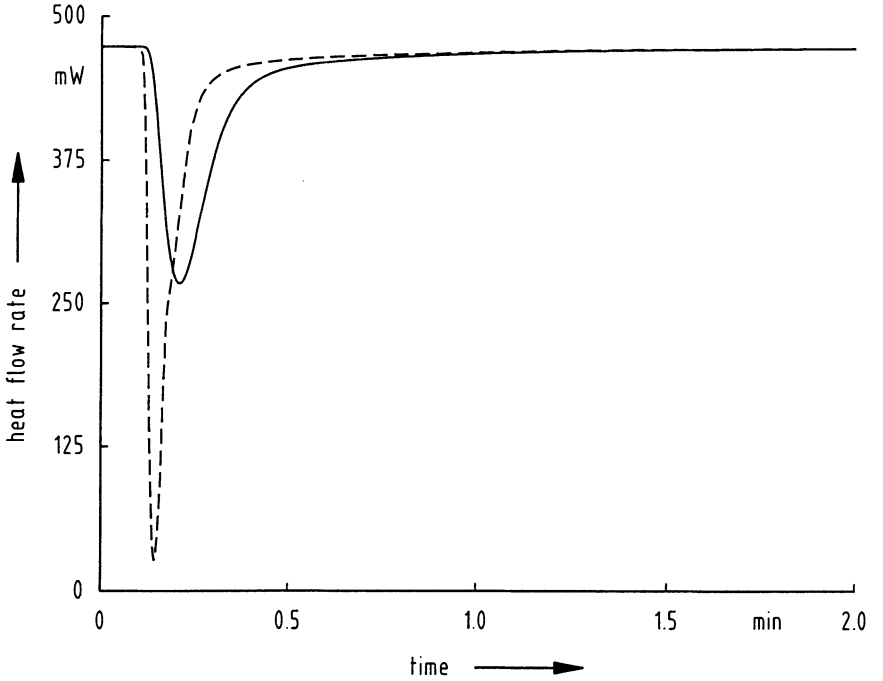

Fig. 6.20. Baseline corrected experimental (solid line) and desmeared (dashed line) curves for the photoinduced reaction of Fig. 6.19

reaction of DGEBA stops at about 50 to 55% conversion (Klemm et al., 1985). In this case, a kinetic analysis is impossible and even the estimation of the final degree of reaction is difficult because of missing or insufficiently reliable experimental information from other analytical methods. To solve the problem, it was supposed in this special case, that the same heat is produced during the reaction of the oxirane ring both for PGE and DGEBA.

The experimental situation can be improved if extremely thin (<0.1 mm) samples are used with the lowest possible concentrations of photoinitiator. If diffusion limitations are small during the whole reaction, as in the case of the reaction of PGE, one then finds a simple first order rate law with respect to the monomer.

The advantages that lead to the application of DSCs for investigation of light-activated reactions are essentially the fast, reliable and quantitative collection of data that reflect the effects of those parameters which influence the conversion rate:

- type of monomer,
- type and concentration of solvents, photoinitiators and inhibitors,
- wavelength and intensity of the radiation used.

6.2.2.2.5 Remarks on the Influence of Different Phases

Reactions in Homogeneous Systems

In this case both reactants and products are in a homogeneous (generally liquid) phase during the whole reaction. Solvent-free systems are normally investigated, because of the higher reaction heat per unit volume of sample. The measured heat flow rate curves are a reliable basis for subsequent kinetic analyses. The classic approaches of kinetics for homogeneous systems may be used without restriction. To some extent this also holds when reactants and products are completely or partially immiscible, the reaction is virtually irreversible and the products have no autocatalytic influences.

Many reactions can be described within a wide range of degrees of reaction by simple n-th order rate laws

$$r = k(T) \cdot (1 - \alpha^n)$$

or by laws, which in addition allow for catalytic and autocatalytic effects

$$r = k(T) \cdot \alpha^m \cdot (1 - \alpha^n)$$

Non-integer exponents m and n suggest complex reaction mechanisms and the converse, integer exponents, do not automatically imply a simple mechanism.

Reactions in Heterogeneous Systems

During a chemical reaction of this type the reactants may always exist in different phases (liquid-solid, solid-solid) or the system may change due to the development of new phases and/or the vitrification of polymerizing components. Although open to criticism (Flynn, 1990) (and in the absence of any obviously better approach) reactions of this type are normally treated using procedures that are formally similar to those for homogeneous systems. In addition to this very fundamental problem there are numerous additional sources of error connected with sample preparation and measuring conditions. In particular, if the gaseous phase is important in the reaction, there is always the risk that the analysis interprets the kinetics of transport through the sample rather than the reaction mechanism. Heat flow rate curves are frequently difficult to analyze without help from other analytical methods (especially temperature programmed X-ray diffraction, hot stage microscopy, thermogravimetry and possibly mass spectroscopy and gas chromatography).

It is typical of heterogeneous reactions that very different events such as nucleation, growth and diffusion can occur simultaneously and successively. A review and a critical judgement of the most frequently used rate laws is given by Brown et al., 1980.

6.2.2.2.6 Evaluation of Overall Rate Laws and Formal Kinetic Parameters

The primary aim of kinetic investigations is the determination of adequate rate laws. For technological purposes an adequate description of even a complex reaction by a mathematical model is often sufficient. Of course, reliable predictions are then only possible within the often very narrow limits of the data sets included into the

evaluation. The physical and chemical use of such rate laws is severely restricted and – if it has any value whatever – it must be done very carefully. An overall rate law may give a good description over a certain range of reaction, because the rate reacts very sensitively to those parameters which are present in the rate law. It may be insensitive with respect to those parameters, which do not appear explicitly (e.g. stoichiometry of the reaction, solvents, catalysts, packing efficiency for heterogeneous samples, flow rate and type of the purge gas). A rate law can often be found by systematic trial and error, this is a result of possible simplifications that may sometimes be made to the rather complicated differential equations that describe the true reaction mechanism. In spite of this, a determination of the overall rate law may be a useful first step in finding the reaction mechanism.

The risk of using overall rate laws for the description of the reaction is that it may possibly hinder further advances towards the true mechanism. For instance, the validity within a certain range of conversion may be taken as confirmation of a postulated, but often too simple, model. Deviations over other ranges of conversion are then interpreted within the framework of that model only. A typical example is the following equation (Sourour, Kamal, 1976), which is often used in the polymer chemistry literature to describe the epoxide amine polyaddition reaction. For stoichiometric reactions it reads:

$$\frac{d\alpha}{dt} = k_1 \cdot c \cdot (1-\alpha)^n + k_2 \cdot \alpha^m \cdot (1-\alpha)^n$$

The chemistry of the reaction is thus reduced to a simple rate law containing catalytic and autocatalytic steps. c is the concentration of a catalyst, n and m are formal reaction orders and k_1 and k_2 are the rate constants of the catalyzed or autocatalyzed reaction.

With $n = 2$ and $m = 1$ this equation was originally derived by Smith, 1961, as the most probable reaction model for the epoxide amine system on the basis of all experimental results available at that time. However, solvent-free reactions can only be described by this equation up to conversion degrees of about 0.6, equivalent to a degree of polymerization of only 2. There have been numerous attempts to retain this simple rate law but any connection with the chemistry of the process is completely lost. If the detailed chemistry of the complex process is unimportant, the value of any further corrections to this equation simply reflects the better fit that results from any increase in the number of parameters. It is hardly surprising, therefore, that the rate law of Sourour, Kamal, 1976, has become independent of the original reaction and that it is used to describe quite different reactions in polymer chemistry.

To describe epoxide amine reactions to higher degrees of reaction, n and m are taken as fitting parameters alone, sometimes even as temperature dependent ones (Ryan, Dutta, 1979; Chung, 1984; Keenan, 1987). The term "reaction order" is then meaningless. The data can still only be fitted, even after such corrections, up to degrees of reaction of about 0.9 and an additional correction is introduced: it is suggested that there is a change from kinetic control to diffusion control at higher conversions (Barton, 1980; Huguenin, Klein, 1985). At first sight this seems an obvious

correction and a review of the most important literature, to 1984, has been given by Barton, 1985. Whether the assumption of a diffusion-controlled reaction is justified, can and should be experimentally checked by choosing the experimental conditions in such a way that diffusion control is extremely unlikely. For example, the reaction can be carried out in solvents or at temperatures well above T_g but the most convincing approach is to use low-molar mass, monofunctional model systems. In this way it has been shown (Klee et al., 1990) that diffusion control is not the best way to correct for the failure of the above equation.

Three general methods have been developed for the determination of kinetic parameters:

- The starting point is the procedure of Borchardt, Daniels, 1957, which needs both the concentrations (in DSC, the degrees of reaction) and the corresponding conversion rates. To evaluate simple rate laws of the form

  $$f(\alpha) = (1 - \alpha)^n$$

  it is especially useful to proceed from the logarithmic form:

  $$\ln\left(\frac{d\alpha}{dt}\right) = \ln A + n \cdot \ln(1 - \alpha) - \frac{E_A}{RT} + (n - 1) \cdot \ln c_0$$

  Today multiple nonlinear regression software from all calorimeter manufacturers allows one to estimate the best values for n, $\ln A$ and E_A by evaluation of a single data set from one scanning experiment. Various choices are offered for $f(\alpha)$ (simple rate laws, rate laws including autocatalytic steps, typical rate laws for the kinetics of reactions in heterogeneous systems). It must always be remembered that the analysis of a single curve can give results that could be misunderstood – a reliable decision between possible reaction models is rarely possible (Opfermann et al., 1991). Moreover, preconceived ideas for a certain reaction mechanism can often be confirmed by data fitting over a particular range of the degree of reaction.
- If an integrated form of a rate law is used

  $$\int_0^\alpha \frac{1}{f(\alpha)}\, d\alpha = g(\alpha) = k(T) \cdot \int_0^t dt$$

  only a few conversion/time data points are needed to calculate the activation parameters. Evaluation of isothermal experiments gives no problems when the rate law is known. A review of important cases can be found in the literature, e.g. Hemminger, Cammenga, 1989. For scanning experiments using

  $$\int_0^\alpha \frac{1}{f(\alpha)}\, d\alpha = g(\alpha) = \frac{A}{\beta} \int_0^T e^{-E_A/RT}\, dT$$

  there are difficulties because an exponential integral cannot be solved analytically. A solution is to use integral tables as calculated, for example, by Doyle, 1961. The importance of integral procedures has decreased considerably with developments in computer technology.

– Freeman, Carroll, 1958, used the logarithmic equation for n-th order reactions in a form based on differences between neighboring data points

$$\Delta \ln\left(\frac{d\alpha}{dT}\right) = n \cdot \Delta \ln(1-\alpha) - \frac{E_A}{R} \cdot \Delta\left(\frac{1}{T}\right)$$

A graph of $\Delta \ln(d\alpha/dt)$ versus $\Delta \ln(1-\alpha)$ (for constant increments of $1/T$) yields the reaction order and activation energy. This analysis is very sensitive to experimental errors and this is particularly true for the procedure of Ellerstein, 1968, in which the last equation is differentiated once more.

If the evaluation shows a significant dependence of the activation parameters on the degree of reaction, this is an unmistakable sign that the reaction mechanism has at least two elementary steps.

6.2.2.2.7 Determination of the True Reaction Mechanism

Including the results of other analytical methods, the system of differential equations for the suggested reaction mechanism is formulated and solved. Latest developments in numerical analysis (Opfermann et al., 1991) allow one to determine the optimized parameters even for complicated systems of differential equations. An analytical solution is not necessary and there is no longer any need for simplifications. The result is the correct order of reaction and optimized activation parameters for each elementary step in the reaction mechanism.

Satisfactory agreement between calculated and experimental curves, including the use of statistical tests, is decisive in the acceptance or rejection of a specific reaction model. The success of such decisions is strongly influenced by suitable experimental conditions. For scanning measurements, at least three different heating rates should be used (Opfermann et al., 1991). If analysis assumes the validity of the usual rate laws for the kinetics of homogeneous systems (solid state or surface reactions are negligible), maximum information follows from careful design of experiments. It is essential to investigate the effects of different stoichiometries, catalyst and solvent concentrations and possibly added intermediates or reaction products. Of course, this is often difficult because of the small volume of sample and the low heat flow rates involved. An evaluation from only one measured curve has no value even if there is an excellent fit of the experimental data.

Current software packages allow the systematic inspection of up to 10 to 15 assumed rate laws both for homogeneous and solid state reactions. Combinations of several steps (simultaneous or consecutive reactions) are possible. However, the most powerful procedure is to dispense with trial and error and instead formulate the most probable system of differential equations using the input routine of the software (Flammersheim et al., 1993). If the rates of reversible reaction steps are found to be much higher than those of subsequent reactions, the former can be replaced by chemical equilibria.

Of course, a complicated reaction mechanism can often be simplified if certain elementary reactions have very different rates and sometimes if equilibria are involved, a much simpler rate law than describes the overall reaction. In contrast to

rate laws which result from systematic trial and error, the simpler rate law obtained in this way is based on the true reaction mechanism and may thus be reliably extrapolated to different reaction conditions. Even here, they must be tested by spot check measurements within the framework of the model used.

6.2.2.2.8 Selected Examples

1. Example

Photochemically produced molten *cis*-azobenzene converts into the *trans* form above room temperature in a well-defined 1st order reaction. The activation parameters have been found to be $\ln(A/s^{-1}) = 27.7$ and $E_A = 103.6\,kJ\,mol^{-1}$ (Eligehausen et al., 1989). By contrast with the situation for temperature and caloric calibration, there are so far no internationally recommended test reactions for kinetic investigations. The use of this well-known reaction could be a first step in this direction, to test individual calorimeters, the sample preparation technique and the evaluation procedure.

The conversion of *cis*-azobenzene is only a 1st order reaction in the liquid phase. Before each measurement the solid substance ($T_{fus} = 71.6\,°C$) must be rapidly melted and quenched to the starting temperature (35 °C). Minor reaction at this stage has no influence on the subsequent calculation of the kinetic parameters. The true baseline of this non-isothermal measurement should be constructed using the heat capacities of *cis*- and *trans*-azobenzene, according to method 2 of Sect. 6.2.2.1. However, this is not possible because the liquid *cis*-azobenzene cannot be supercooled sufficiently to measure $c_p(T)$ down to temperatures below the start of the isomerization reaction and a straight baseline must be used. This is a good approximation because the differences between a calculated sigmoidal baseline (from literature c_p-values) and the straight line are very small. An approximate (because of different thermal conductivities) but adequate desmearing is possible using the crystallization peak of molten *trans*-azobenzene as the apparatus function. The correction is small because the isomerization is rate determining even at the highest used heating rates. A precise temperature correction to zero heating rate values for all heating runs is very important.

Fig. 6.21 shows the excellent agreement between experiments and calculations using multiple-curve analysis by non-linear regression. All curves from runs at five heating rates and at four isothermal temperatures have been included in the calculations (that for the lowest temperature is not shown in the figure). If minor self-heating of the sample because of the limited heat exchange with the calorimeter is allowed for, no systematic differences are found between the single-curve and the multi-curve analysis. In addition, the same activation parameters are found even at higher heating rates ($40\,K\,min^{-1}$). Assuming a fixed reaction order of $n = 1$ the procedure gives activation parameters of $\ln(A/s^{-1}) = 27.8 \pm 1$ and $E_A = 102.8 \pm 2.7\,kJ\,mol^{-1}$, in good agreement with Eligehausen et al., 1989.

2. Example

The radical polymerization of a monofunctional monomer is a simple 1st order reaction, if a number of ideal conditions can be assumed (reactivity of the macro-

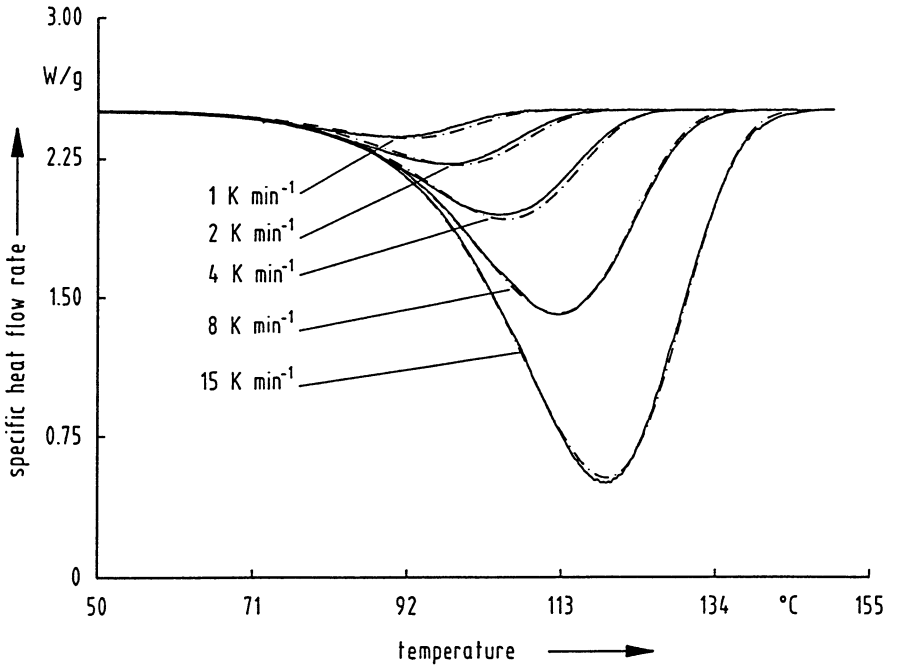

a

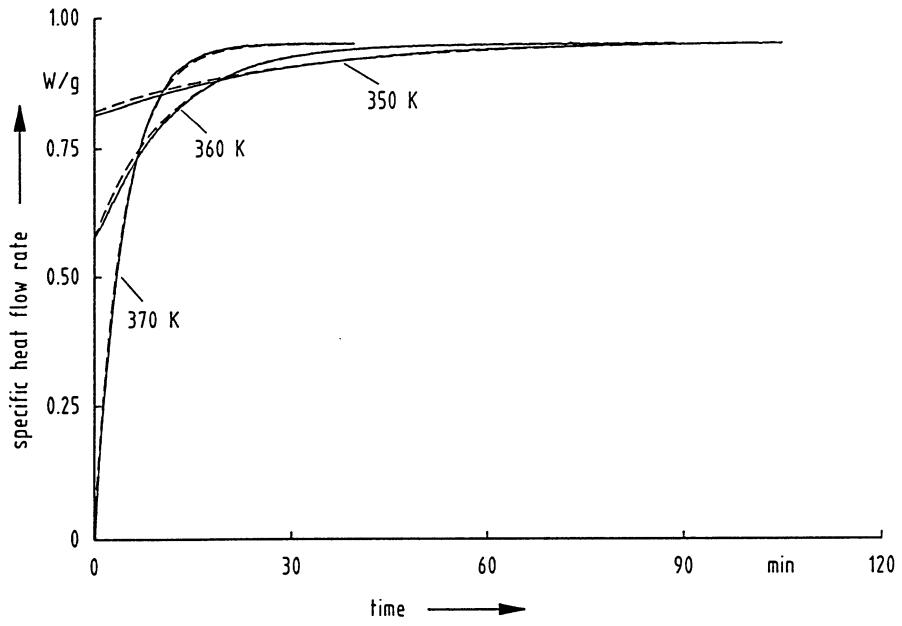

b

Fig. 6.21. Measured (solid lines) and calculated (dashed lines) curves for the *cis-trans* isomerization of azobenzene in the liquid phase.
a in scanning mode at different rates,
b in isothermal mode at different temperatures

radicals is independent of the chain length, approximately constant radical concentration during the whole reaction, bimolecular chain termination reactions). Under these circumstances, the rate of concentration change is proportional to the concentration of the monomer (c_M) as follows:

$$-\frac{dc_M}{dt} = k_{pro} \cdot \left(\frac{\Gamma \cdot k_{ini}}{k_{ter}}\right)^{1/2} \cdot c_I^{1/2} \cdot c_M$$

The quantity Γ is the yield of radicals due to the thermal homolysis of the initiator (I) (e. g. 2,2'-azodiisobutyronitril (AiBN) or dibenzoylperoxide), k_{pro}, k_{ter} and k_{ini} are the rate constants of the chain propagation, chain termination and initiation, respectively. If the thermal initiator is replaced by a photoinitiator, like benzoin methyl ether or 2,2'-dimethoxy-2-phenyl acetophenone (benzyldimethylketal), the analogous overall rate law reads :

$$-\frac{dc_M}{dt} = k_{pro} \cdot \left(\frac{\Gamma \cdot I_{abs}}{k_{ter}}\right)^{1/2} \cdot c_M$$

Here Γ is the quantum yield of the initiator, I_{abs} is the radiant power absorbed by the sample. In contrast to polyfunctional acrylates, for which cross-linking reaction starts immediately (Fig. 6.19), monofunctional methacrylates (methyl-, ethyl-, propyl-, butyl-) follow the simple 1st order law up to degrees of reaction of 0.3 to 0.6 (dependent on the chemical nature during both thermal and light-induced polymerization). After this stage the so-called gel or Trommsdorff-Norrish effect dominates, this is recognizable by increasing reaction rates despite decreasing monomer concentrations (Malavašič et al., 1986). This is also valid (Fig. 6.22) for the

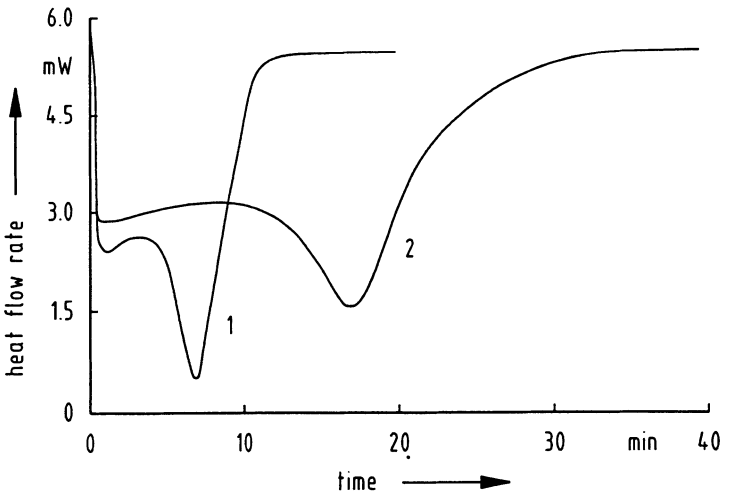

Fig. 6.22. Light-initiated (1) and thermally activated (2) polymerization of DOMA. (curve 1: λ = 365 nm, I_0 = 0.35 mW cm^{-2}, T = 298 K, 1 % 2,2-dimethoxy-2-phenylacetophenone as photoinitiator; curve 2: T = 343 K, 1 % 2,2-azodiisobutyronitril as initiator)

polymerization of (2,2-dimethyl-1,3-dioxolan-4-yl)methylmethacrylate (DOMA) (Flammersheim, Klemm, 1985). There are no qualitative differences between curves 1 and 2. In both cases the change of reaction rate with time is small enough during the entire reaction that desmearing is not necessary. Spectroscopic investigations on the soluble reaction product verify the complete reaction of the acrylate double bonds, whereas the dioxolane ring remains intact under these experimental conditions. Up to a degree of reaction of 0.3, the rate law is 1st order. Knowing the activation term $(\Gamma k_{ini} c_I)^{1/2}$ or $(\Gamma I_{abs})^{1/2}$, the overall rate constant gives the ratio $k_{pro}/k_{ter}^{1/2}$. During the gel effect this ratio is formally dependent on the degree of reaction reached. In contrast to the nearly unhindered chain propagation reactions of the small monomer molecules, the chain termination reactions of the growing macroradicals are increasingly hindered in the more and more viscous matrix. The result is a pronounced dark reaction after switching off the light during the polymerization (Fig. 6.23). The first run was interrupted at $\alpha = 0.35$. After the dark reaction was complete the same sample was once more radiated and the light switched off again at a overall degree of reaction of 0.8 (curve 2). To get a better comparison the second curve is shifted to the origin of the time scale in Fig. 6.23. As a result, the relative extent of the dark reaction is proportional to the degree of reaction at that

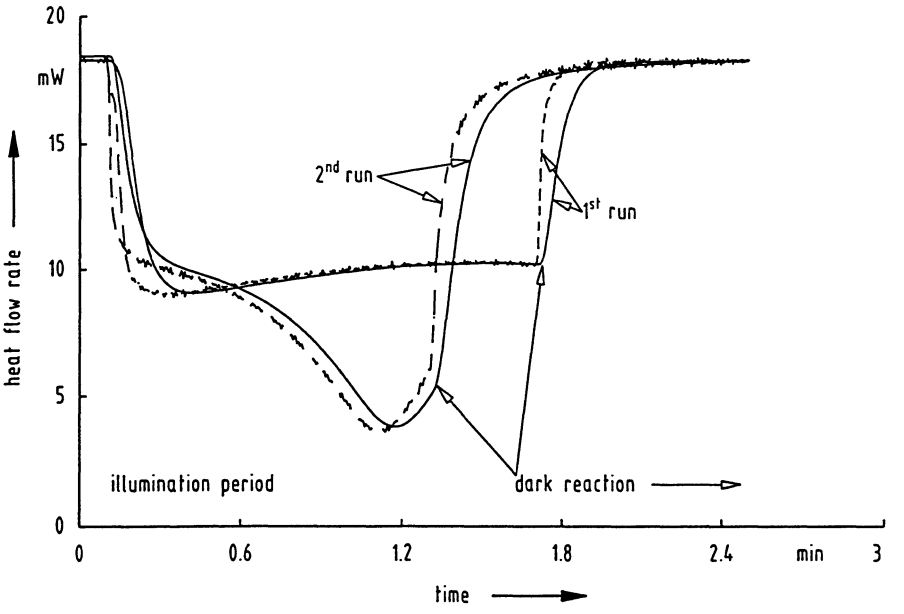

Fig. 6.23. Photopolymerization of DOMA with interruption of the radiation at reaction degrees of 0.35 and 0.80 (arrows). Both curves are consecutive runs of the same sample, but the second curve is shifted to the same origin of the time scale.
Solid lines: measured curves, dashed lines: desmeared curves ($\lambda = 365$ nm, $I_0 = 3.5$ mW cm^{-2}, $T = 298$ K, 1% 2,2-dimethoxy-2-phenylacetophenone as photoinitiator)

moment at which the light was interrupted. The rate of the dark reaction (missing activation by ΓI_{abs}) is described by:

$$-\frac{c_M}{\frac{dc_M}{dt}} = \frac{k_{ter}}{k_{pro}} \cdot t - \frac{c_{M_0}}{\frac{dc_{M_0}}{dt}}$$

If the ratio $k_{pro}/k_{ter}^{1/2}$ is determined from the measured curve immediately before the light is interrupted and, following this, the ratio k_{ter}/k_{pro} from the dark reaction (last equation) the rate constants k_{ter} and k_{pro} result from the combination of these. Though desmearing is not necessary during the illumination period with normal light intensities, the evaluation of the dark period signal is meaningless without it, especially if the dark reaction is performed at low conversions (because of the very rapid decrease of the heat flow rate due to a large k_{ter}/k_{pro} ratio). The picture shows this effect very clearly. The linear relation between $-c_M/(dc_M/dt)$ and t (see the last equation) is only found from the desmeared signal (k_{ter}/k_{pro} is about 310 at $\alpha = 0.35$ and about 11 at $\alpha = 0.80$). Measurement of this reaction in DSCs is only possible if their time constants are lower than 2 to 4 s.

3. Example

The formation of polythiolcarbamates from diisocyanates and dithiols cannot be described by a simple rate law even if autocatalytic effects are included. All discussion of the most probable reaction mechanism must account for the following experimental observations (cf. also Fig. 6.18):

- The initial reaction rate is proportional to the concentration of the catalyst (pyridine, picoline, lutidine, collidine).
- The reaction includes autocatalytic steps.
- Catalysis and autocatalysis are directly coupled.
- Isocyanate and dithiol are not equivalent in the stoichiometry of the reaction mixture.
- A possible partial diffusion control can be excluded under the experimental conditions used.
- The existence of dithiol/catalyst, diisocyanate/catalyst and product/diisocyanate/catalyst complexes could be proved using spectroscopic methods (NMR, UV, IR). Further, the equilibrium constants of the first two complexes could be determined.
- The apparent activation energy, which follows from the temperature dependence of the overall reaction rate, is unusually low.

Following the general recommendations given above, reaction curves for a given system (dithiol, diisocyanate, catalyst) including variations of stoichiometry, temperature and catalyst concentration have been made for the non-linear regres-

sion analysis. The most probable reaction mechanism is (Flammersheim et al., 1993):

$$S + K \underset{k_{-1}}{\overset{k_1}{\rightleftharpoons}} SK \quad (1)$$

$$I + K \underset{k_{-2}}{\overset{k_2}{\rightleftharpoons}} IK \quad (2)$$

$$IK + S \xrightarrow{k_3} P + K \quad (3)$$

$$IK + P + S \xrightarrow{k_4} 2P + K \quad (4)$$

(S dithiol, K catalyst, I isocyanate, P product, IK and SK complexes of the catalyst with I and S).

In this scheme SK (step 1) is a nonreactive and IK (step 2) a reactive complex. Step 3 corresponds to the normal catalytic reaction between IK and the dithiol, step 4 represents the much rarer combination of catalysis (via IK) and autocatalysis (via P). An impression of the quality of this model is given in Fig. 6.24, which com-

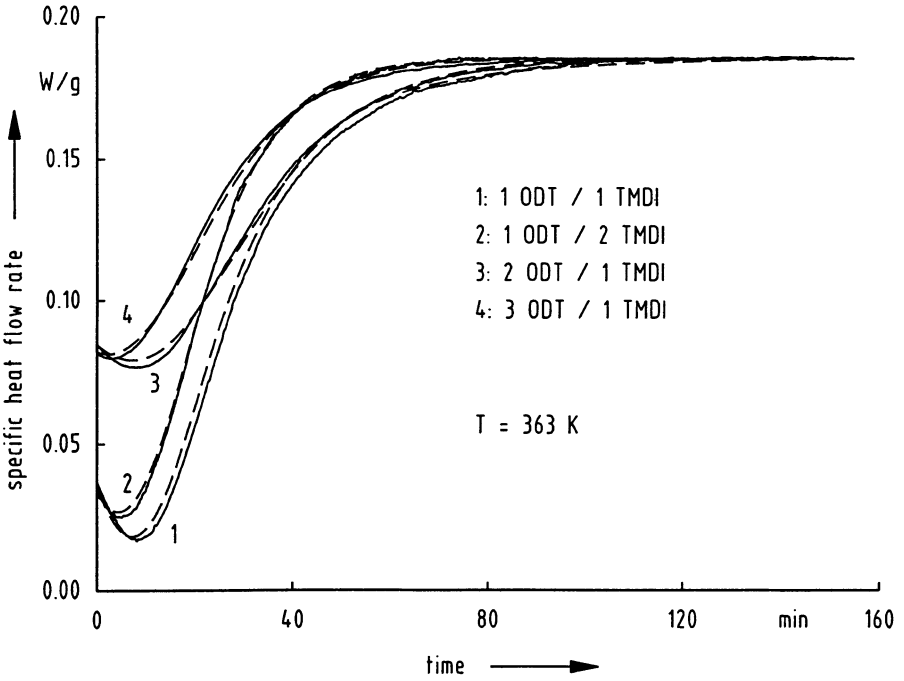

Fig. 6.24. Comparison between measured (solid lines) and calculated (dashed lines) reaction isotherms of the system TMDI/ODT/3,5 lutidine. For exact compositions see text

pares measured and calculated isotherms for the system TMDI/octane-1,8-dithiole (ODT)/3,5-lutidine (concentrations are given in the table).

Component concentrations for the reactions of Fig. 6.24

Stoichiometric ratio ODT/TMDI	curve number	concentrations in mol l^{-1}		
		ODT	TMDI	3,5-lutidin
1:1	1	4.881	4.870	0.477
1:2	2	3.142	6.359	0.561
2:1	3	6.834	3.225	0.361
3:1	4	7.709	2.343	0.439

The calculated activation parameters for this system are

$$E_A = 43.5 \pm 2 \text{ kJ mol}^{-1} \text{ and } \ln (A/\text{l mol}^{-1}\text{s}^{-1}) = 8.27 \pm 0.25 \text{ for step 3}$$

$$E_A = 44.7 \pm 3 \text{ kJ mol}^{-1} \text{ and } \ln (A/\text{l}^2 \text{ mol}^{-2}\text{s}^{-1}) = 7.94 \pm 0.45 \text{ for step 4.}$$

The enthalpies and entropies of reaction are

$$\Delta_r H = -10.5 \pm 1 \text{ kJ mol}^{-1} \text{ and } \Delta_r S = -35 \pm 3 \text{ J K}^{-1} \text{ mol}^{-1} \text{ for SK}$$

$$\Delta_r H = -32 \pm 3 \text{ kJ mol}^{-1} \text{ and } \Delta_r S = -94 \pm 11 \text{ J K}^{-1} \text{ mol}^{-1} \text{ for IK.}$$

The already mentioned very low apparent activation energy of the overall reaction follows from the coupling of the exothermic formation of IK with an reaction energy of -32 kJ mol^{-1} during the reversible step 2 and the consecutive reactions which have normal activation energies of about 45 kJ mol^{-1}.

The formulation of step 4 as triple impact reaction is extremely unlikely and it should be replaced by the two following steps:

$$\text{IK} + \text{P} \underset{k_{-5}}{\overset{k_5}{\rightleftharpoons}} \text{PIK} \tag{5}$$

$$\text{PIK} + \text{S} \xrightarrow{k_6} 2\text{P} + \text{K} \tag{6}$$

The fit to the experimental curves is just as good as without this extension, correlation coefficients are generally higher than 0.998. However, it is impossible to calculate kinetic parameters for the coupled reactions (5) and (6).

This demonstrates a typical situation in calculating optimized model parameters for more complicated reaction mechanisms. The number of model parameters is very often so large that although an excellent fitting of the experimental curves is possible, the parameters in question (rate constants, equilibrium constants) are rather uncertain. In general the reasons for this are experimental (noise and uncertainty of the measured quantities) rather than mathematical. Improvements may be expected, not from additional DSC experiments, but from other analytical methods. For the present, therefore, although the elementary reaction steps (5) and (6) must be favoured, reliable kinetic parameters remain unavailable (the ratio of

both rate constants is also unknown). Their replacement by step (4) is a necessary consequence. The situation is analogous for the determination of the equilibrium constants for the reactions (1) and (2) in the above scheme. The calculation provides only mean equilibrium constants. Formally, it should be possible to optimize the products, concentration times activity coefficient, instead of the concentrations to get the thermodynamic equilibrium constants (in the sense that these are independent of the composition of the system). Of course, this fails because the parameter set is now twice as large and yields meaningless equilibrium constants.

6.2.3 The Glass Transition Process

6.2.3.1 The Phenomenology of the Glass Transition

Indirect C_p measurements intended to provide information regarding the glass transition are much commoner than direct determinations of the temperature dependent heat capacity (cf. Sect. 6.2.1). The best experimental procedure and an unambiguous interpretation of the results is not possible without basic information about the nature of the glassy state and the transition process between glassy (amorphous) and liquid states.

Most materials can be obtained in the glassy state by suitable treatment. Inorganic systems have been known since ancient times, they are responsible for the name of this state of matter. However, from the DSC point of view, organic glasses and, especially, macromolecular glasses are of special importance.

Typical values for the temperature ranges of the transition are 10 K for low-molar mass glasses, 20 to 50 K for most of the organic polymeric glasses and 100 K or more for silicate network glasses. The glass transition is characterized by an appropriately defined glass transition temperature T_g. Within the transition region many macroscopic properties, which may have great practical importance, change their values (viscosity, dielectric and especially mechanical properties). Each of these could form the basis of an experimental determination of T_g. With DSCs, the glass transition is detectable by a step change of the heat capacity Δc_p on heating or cooling. Both the temperature and magnitude of this event are important. Observed values of Δc_p range from 0.1 to 2 $J\,g^{-1}\,K^{-1}$. Fig. 6.25 shows a typical DSC curve for a linear, high-molar mass epoxide-amine polyadduct which was first cooled at the rate shown and then immediately reheated.

For polymeric glasses the temperatures of the transition range from −100 to 300 °C whereas the corresponding range for silicate glasses is from 500 to 1000 °C. Polymeric glasses are thus more suitable for DSC measurements than inorganic glasses. For polymer chemists and materials scientists a knowledge of the glass transition temperature is at least as important as is the melting temperature.

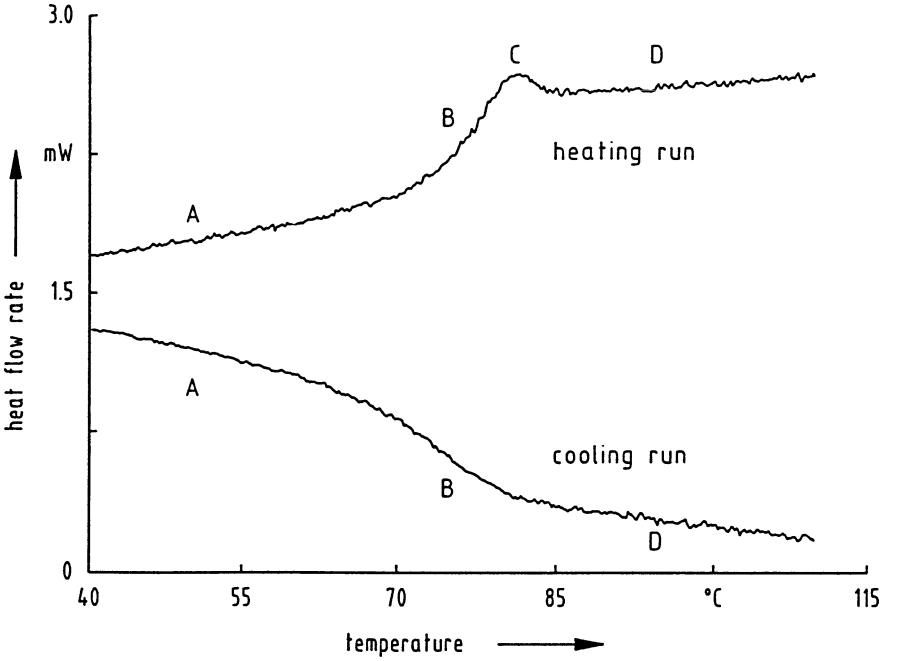

Fig. 6.25. Typical DSC curves for an amorphous polymer in the glass transition region. A: glassy non-equilibrium state, B: glass transition region, C: "relaxation peak", D: equilibrium liquid state (sample: linear epoxide-amine polyadduct, heating and cooling rate: 5 K min^{-1})

6.2.3.2 The Nature of the Glass Transition and Consequences for DSC Measurements

Problems result from the fact that the glassy (or vitreous) solid is, thermodynamically, far from equilibrium. The formation and behavior of a glass are exclusively kinetic events. There are only formal similarities between the C_p-change at an "ideal" glass transition and at a thermodynamically well defined second order transition. Only the liquid (or rubbery) state at the high temperature end of the glass transition is at equilibrium and thermodynamics is valid without any restrictions in this region. Here any external (experimental) influence is slow compared with the mobility of the internal degrees of freedom which thus always are in equilibrium. Equilibrium thermodynamics can also be applied if the internal degrees of freedom react very slowly, in this case the system is in a frozen (vitrified) state with respect to external influences. This is true for temperatures well below the glass transition. The heat capacity function can, therefore, be determined (see Sect. 6.2.1) for both ranges without any restrictions. During the glass transition, changes of both the intrinsic and the measurement variables occur on the same time scale, the measured quantities become time-dependent, and classical thermodynamics is no longer valid. The system passes through a sequence of non-equilibrium states during heating or cooling. The typical asymmetric shape of the glass transition curve (an extensive tail on the low temperature side and a fairly abrupt end at high

temperatures) is due to a distribution of the intrinsic variables which vitrify (or devitrify) over a wide range.

A special problem when investigating the glass transition (key word: relaxation phenomena) is caused by the effect of the previous history of the glass on the thermal behavior. The system has, so to speak, a memory of its thermal history. This is important not only for theoretical investigations but also for practical DSC measurements of the glass transition.

Essential conclusions are:

- In contrast to the measurement of equilibrium transitions, it is not possible to get 'equilibrium' values of the characteristic quantities T_g and Δc_p by extrapolation to zero heating or cooling rates: these quantities are determined by the thermal history (scanning rates and annealing times). If, for instance, the cooling rate is changed by an order of magnitude T_g will change by 3 to 20 K depending on the material in question. For flexible polymers the magnitude is generally 3 to 5 K, whereas it is 15 to 18 K for the considerably stiffer borosilicate network glasses. By contrast Δc_p shows much less dependence on thermal history.
- Characterization of glasses by DSC measurements (Fig. 6.25) is mostly carried out in the heating mode because this is practicable even for those heat flux DSCs, having relatively sluggish furnaces. A heating run is also advantageous when it is important to characterize the "as received" glassy state (e.g resulting from particular cooling or anealing procedures or chemical reaction). It must be remembered that, on heating, the original glassy state can change at temperatures as much as 50 K below the transition region (for instance, if the heating rate is slower than the previous cooling rate). T_g then depends on the heating rate. To sum up, values for T_g (and to a lesser extent Δc_p) are only meaningful with respect to the chosen experimental conditions and – as will be pointed out later – in the context of the particular definition of the "glass transition temperature".
- If the glass sample to be investigated is formed only by cooling from the liquid, a cooling run is indeed better for its characterization. Problems due to the coupling of vitrification and devitrification processes (occuring during heating) are avoided. Cooling runs, therefore, immediately reflect – possibly after desmearing of the experimental curve – the kinetics of the vitrification. The cooling rates must not be too low ($\geq 5\ \mathrm{K\,min^{-1}}$) for a reliable determination of the rather small changes of the heat capacity. This may sometimes be difficult because of the large inertia of many DSC furnaces in the cooling mode.
- In addition the measured curve of the glass process is falsified by the limited heat transfer between sample and temperature sensor (cf. sect. 5.4.4). Correction of these influences is important, because larger sample masses (10 – 20 mg) and larger scanning rates (10 or 20 $\mathrm{K\,min^{-1}}$) are used in practice. For this purpose the advanced desmearing with the aid of the step response function (cf. Sect. 5.4.4) is very advantageous.
- Thermal lag can be determined using the following methods.

  1. Determination as explained in the Sects. 5.4.4 and 6.2.1.1 (Figs. 5.10 and 6.9).
  2. Placing a small piece of indium both on the bottom and in the middle of the sample and noting the difference between the extrapolated onset temperatures

from the In fusion peaks which corresponds to the thermal lag. Attention must be focused on a good thermal contact between the indium and the sample.

3. A temperature correction suggested by Hutchinson et al., 1988. This method appears to be problematical, however, as it already presupposes the validity of one of the models which describes the glass process (Kovacs et al., 1979).

A disadvantage of all of these corrections is that only an average lag is obtained and thus can be corrected.

6.2.3.3 Definition and Determination of the Glass Transition Temperature T_g

6.2.3.3.1 Conventional Glass Transition Temperatures

The main parameters used to characterize the glass transition are shown in Fig. 6.26. For many applications it is important to know the temperature range $T_{g,i}$ to $T_{g,f}$ over which the substance vitrifies on cooling, or devitrifies on heating. Unfortunately, the practical determination of these temperatures is problematic, there are large errors in their definition and it is difficult to give clear instructions for their measurement. The situation is improved if clearer, more chararacteristic temperatures

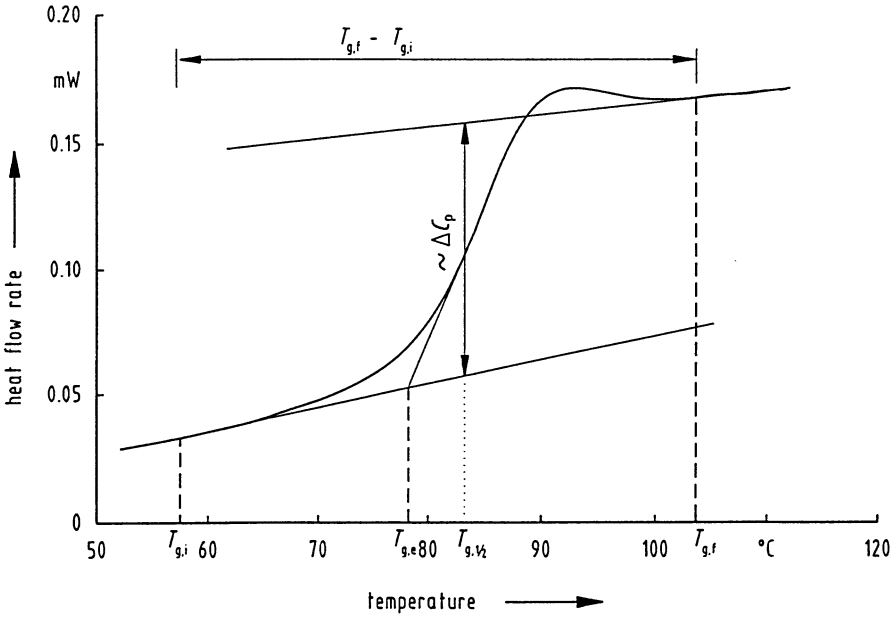

Fig. 6.26. Definition of the most frequently used conventional quantities for characterization of the glass transition.
$T_{g,e}$: extrapolated onset temperature, $T_{g,1/2}$: half-step temperature, ΔC_p: C_p-change at the half-step temperature, $T_{g,i}$ and $T_{g,f}$ initial and final temperatures of the glass transition, $T_{g,f} - T_{g,i}$ temperature interval of the glass transition

from the transition region are used. These are the extrapolated onset-temperature $T_{g,e}$ (analogous to the peak onset temperature) and the half-step temperature $T_{g,1/2}$ related to the C_p change (the temperature at which C_p is midway between the extrapolated heat capacity functions of the glassy and liquid state). The use of the latter is more meaningful as this temperature is better related to the second characteristic quantity of the glass transition, the C_p change. A third definition, the temperature of the inflection point of the glass transition curve is seldom used.

Under certain circumstances glass transition temperatures defined in this way may be used without restriction to compare experimental data:

1. All investigations are made in cooling mode at the same rate.
2. If evaluation must be done on heating runs, the sample must be previously cooled from the liquid at a fixed rate.

$T_{g,e}$ and $T_{g,1/2}$ can both easily be obtained from routine measurements, this is the reason for the nearly exclusive use of these pragmatically defined glass transition temperatures up to now. A repeatability error of ± 1 K is acceptable in practice. For heating runs the following practical and frequently used procedure is recommended:

- The sample is heated to a temperature at least 15 to 30 K above T_g.
- Short (5–10 min) annealing at this temperature in order to establish thermodynamic equilibrium and erase the "memory" (with respect to its thermal history) of the system.
- Rapid programmed cooling (or quenching) to a temperature at least 50 K below the glass transition.
- Immediate reheating at constant rate (10 or 20 K min^{-1}). These rates lead to relatively high temperature errors (3 to 10 K) and, in addition, a broadening of the transition, on the other hand problems caused by relaxation processes during the transition are avoided. The thermal history can be obtained quantitatively by comparison of the original run with the rerun under the same conditions.

Neither $T_{g,e}$ nor $T_{g,1/2}$ make any allowance for the nonequilibrium nature of the glass transition. This is especially striking (Fig. 6.27), if the glass transition is accompanied by "enthalpy relaxation peaks". These appear on heating curves as endothermic events at the high temperature end of the glass transition range. Their height may be comparable with those of the melting peaks of crystalline materials (Petrie, 1972). For the example shown in Fig. 6.27 the glass annealed 70 h at 68 °C has $T_{g,e} = 89.1$ °C, $T_{g,1/2} = 87.3$ °C whereas the quenched glass has $T_{g,e} = 81.6$ °C, $T_{g,1/2} = 85.1$ °C. This use of $T_{g,e}$ and $T_{g,1/2}$ to characterize the glass process gives the paradoxical result that a slowly cooled or annealed glass seems to have a higher glass transition temperature than a rapidly cooled one. In addition $T_{g,e}$ and $T_{g,1/2}$ react to the thermal history in a different manner.

$T_{g,e}$ and $T_{g,1/2}$ are not useful for theoretical treatments of the kinetics of the glass process, this is also true for certain relationships between T_g and other properties (e.g. T_g as function of the molar mass or as a function of the degree of conversion in a reacting system).

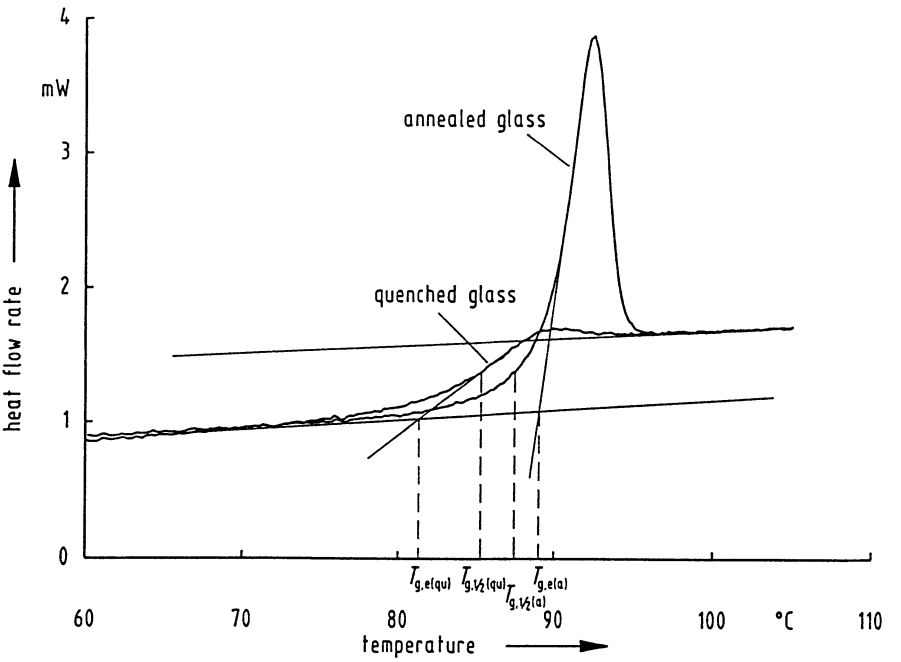

Fig. 6.27. DSC heating curves for an annealed (or slowly cooled) (a) and a quenched (qu) glass showing the paradoxical result that the conventional glass temperatures of the quenched glass seem to be lower than those of the annealed glass, for details see text. $T_{g,e}$ extrapolated onset temperature, $T_{g,1/2}$ half-step temperature

6.2.3.3.2 The Thermodynamically Defined Glass Transition Temperature

The "glass transition", although a kinetic phenomenon, can be unequivocally defined thermodynamically. This uses the so-called *fictive temperature* $T_{g,fic}$ first introduced by Tool, 1946. $T_{g,fic}$ is a well defined quantity that reflects the current structural state of the glass to be characterized.

The concept of the fictive temperature was considerably extended by Narayanaswamy, 1971, Moynihan et al., 1976, and de Bolt et al., 1976. An analogously defined "thermodynamic" or "enthalpic" T_g-temperature, based on the specific information of a DSC, was introduced by Flynn, 1974, Richardson, Savill, 1975a, and Richardson, 1976. In the following section this thermodynamically defined temperature $T_{g,fic}$ is shown as T_g without the additional suffix.

To understand the definition of T_g, the enthalpy versus temperature diagram (Fig. 6.28) will be discussed. Heat capacity functions for the glass and liquid can be described approximately by straight lines within a temperature range of 50 to 100 K. The enthalpy functions are then slightly parabolic curves. For simplicity, curvature of the enthalpy functions is neglected in this figure, in other words C_p is assumed to be temperature independent. Depending on the cooling rate, the sample vitrifies (changes from H_l to H_g) at different temperatures. The lower the cooling

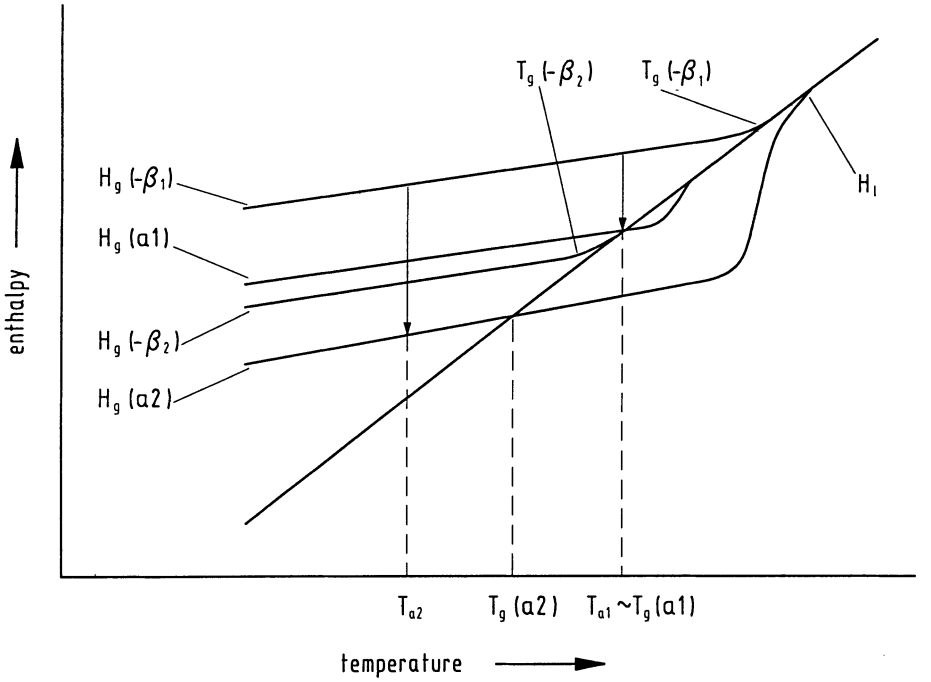

Fig. 6.28. Schematic enthalpy-temperature curves for the glass transition of an amorphous sample at different cooling rates ($-\beta_i$) and subsequent heating after isothermal annealing at T_{ai}, for details see text. H_g enthalpy of the different non-equilibrium glassy states, H_l enthalpy function of the equilibrium liquid state, $T_g(-\beta_i)$ glass transition temperatures on different cooling ($|\beta_1| > |\beta_2|$), $T_g(a_i)$ glass transition temperatures on heating after different annealing schedules

rates ($-\beta$) during this process the lower are the vitrification temperatures ($T_g(-\beta_1)$) or $T_g(-\beta_2)$). The enthalpy functions $H_g(-\beta_1)$ and $H_g(-\beta_2)$ characterize the two respective glasses. For simplicity it is further assumed that all enthalpy functions are parallel, in other words that the heat capacities of the glassy state are assumed to be independent of the conditions during vitrification (although very precise measurements (Gilmour, 1977) show slight differences). If the glass is annealed at temperatures down to, at most, 50 K below the vitrification temperature, the mobility of the frozen states is still so large that internal degrees of freedom are not totally frozen and can relax towards equilibrium. During this process the H_g-function approaches the (extrapolated) H_l-function (Petrie, 1972; Peyser, 1983; Cowie, Ferguson, 1986; Agrawal, 1989). The figure shows this for two annealing temperatures T_{a1} and T_{a2} of a glass, which was obtained at a cooling rate $-\beta_1$. At T_{a1} the annealing time was sufficient to reach the equilibrium enthalpy value of the liquid at that temperature, whereas this was not the case at T_{a2}. Reheating of the annealed glass then proceeds along the enthalpy lines $H_g(a1)$ or $H_g(a2)$. From the theoretical point of view, the glass should devitrify exactly when the enthalpy line of the glass crosses that of the liquid but the transition from H_g to H_l is not sharp. To determine the intersection of enthalpy curves for the glassy and liquid states therefore requires

the extrapolation of these curves from temperatures, which are clearly above or below that of the transition region. The point of intersection, obtained in this way, defines the thermodynamic glass transition temperature T_g. Tool, 1946, called this temperature the *fictive temperature*, because during heating nothing happens at that point. Hence T_g cannot be located directly on the measured curve, instead, on heating, the system progresses further along the H_g-curve (superheating effect). This is more pronounced the better the glass has been annealed (i.e. after annealing at T_{a2} it is far more intensive than after annealing at T_{a1}). This is the reason for the paradoxical values, mentioned earlier, for the pragmatically defined $T_{g,e}$ or $T_{g,1/2}$ temperatures, when comparing slowly cooled (or annealed) and quenched glasses. Superheating ends only at temperatures well above T_g, the return to the equilibrium curve is now rapid and produces the so-called relaxation peak. The reason for the superheating effect is the drastically decreased mobility in the glassy state, which parallels the slow enthalpy decrease during annealing.

If the enthalpy definition (Flynn, 1974; Richardson, Savill, 1975a, and Richardson, 1976; Moynihan et al., 1976) is used, T_g can easily be calculated from DSC measurements.

The procedure in question (Richardson, Savill, 1975a; Richardson, 1976) is explained in Fig. 6.29. We start with the definition, the equality of $h_g(T)$ and $h_l(T)$

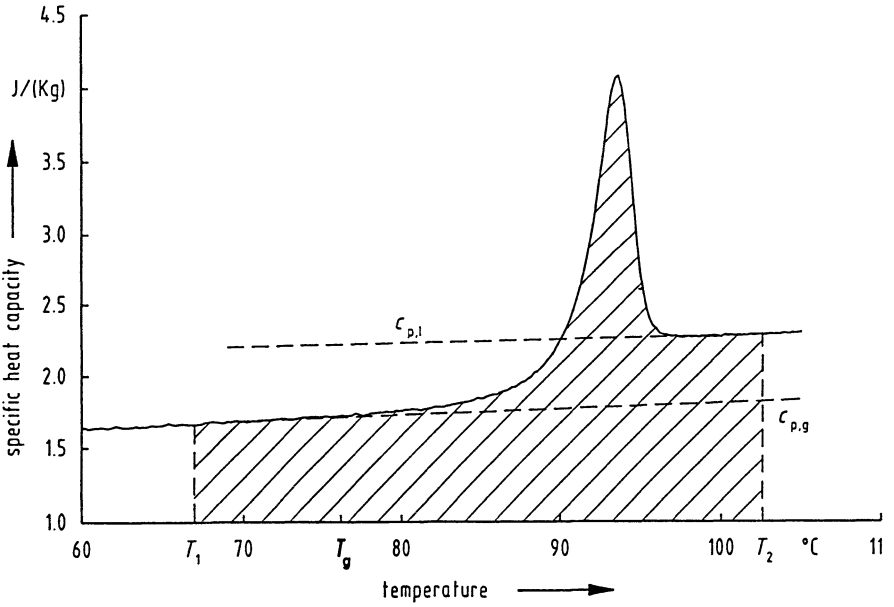

Fig. 6.29. Determination of the thermodynamic glass temperature from DSC heating curves with a „relaxation peak" (Richardson, Savill, 1975a; Richardson, 1976).
$c_{p,g}$ and $c_{p,l}$ are the (extrapolated) specific heat capacity functions of the glass and liquid, respectively, T_1 and T_2 are the integration limit temperatures in the glassy and liquid state, respectively, the hatched area (extended to $c_p = 0$) corresponds to the difference $h_l(T_2) - h_g(T_1)$. For details see text

at T_g. The enthalpies $h(T)$ for the glass and liquid are obtained by integration of the corresponding c_p-functions, which can always be approximated by linear equations:

glass: $c_{p,g} = a + b \cdot T$ and $h_g(T) = a \cdot T + \frac{1}{2} b \cdot T^2 + P$

liquid: $c_{p,l} = A + B \cdot T$ and $h_l(T) = A \cdot T + \frac{1}{2} B \cdot T^2 + Q$

The integration constants P and Q are not known but $Q-P$ may be obtained from the difference $h_l(T_2) - h_g(T_1)$, the hatched area in Fig. 6.29, a directly accessible experimental quantity:

$$h_l(T_2) - h_g(T_1) = A \cdot T_2 - a \cdot T_1 + \tfrac{1}{2} B \cdot T_2^2 - \tfrac{1}{2} b \cdot T_1^2 + (Q - P)$$

T_1 and T_2 are convenient arbitrary temperatures that must be chosen to be below and above the glass transition region (i.e. in the glassy and in the liquid state, respectively). Using $Q - P$ from the above equation the desired glass temperature is obtained by solving the quadratic equation:

$$\tfrac{1}{2}(B - b) \cdot T_g^2 + (A - a)\, T_g + (Q - P) = 0$$

Fig. 6.30 shows an equivalent, graphical procedure (Moynihan et al., 1976) for determining T_g. From the enthalpy definition it follows that:

$$\int_{T_g}^{T_2} (c_{p,l}(T) - c_{p,g}(T))\, \mathrm{d}T = \int_{T_1}^{T_2} (c_p(T) - c_{p,g}(T))\, \mathrm{d}T$$

where $c_p(T)$ is the experimentally determined curve and $c_{p,g}(T)$ and $c_{p,l}(T)$ are the (linearily extrapolated) specific heat capacities of the glass and liquid, respectively, the integration limits T_1 and T_2 have the same meaning as those in the last figure. It must be guaranteed, however, that T_1 (on heating) and T_2 (on cooling) are definitely in the steady state region of the DSC. The lower limit of the left hand side integral, the thermodynamic glass temperature T_g, must be determined so that the integrals on both sides are equal. In other words, the area between T_1 and T_2 and the (extrapolated) c_p curves of glass and liquid (the left side integral) must be equal to that between the experimental curve and the (extrapolated) c_p curve of the glass (the right side integral). The two areas are hatched differently in Fig. 6.30.

It is clear from the equation above that absolute values of heat capacities are not required for calculating T_g. It is sufficient to know c_p differences and this is also the case for the Richardson and Savill procedure. Nevertheless, their changes with temperature must be determined very precisely. This demand can only be fulfilled if the repeatability of the experimental curve is very good (for the same thermal history) and if a sufficiently large temperature range (more than 50 K on each side of T_g) is available for extrapolation.

An error estimation was done by Richardson, Savill, 1975a: for a typical Δc_p of 0.3 J g^{-1} K^{-1} an uncertainty of 0.3 J g^{-1} for the enthalpy change would result in a temperature uncertainty of ± 1 K. For total enthalpy changes of about 100 J g^{-1} and caloric errors of ± 1%, the determined T_g would be uncertain to ± 3 K and this is not acceptable in practice. Fortunately, some errors tend to compensate each other in both procedures. For instance, an incorrectly extrapolated $c_{p,l}$ curve (Fig. 6.30)

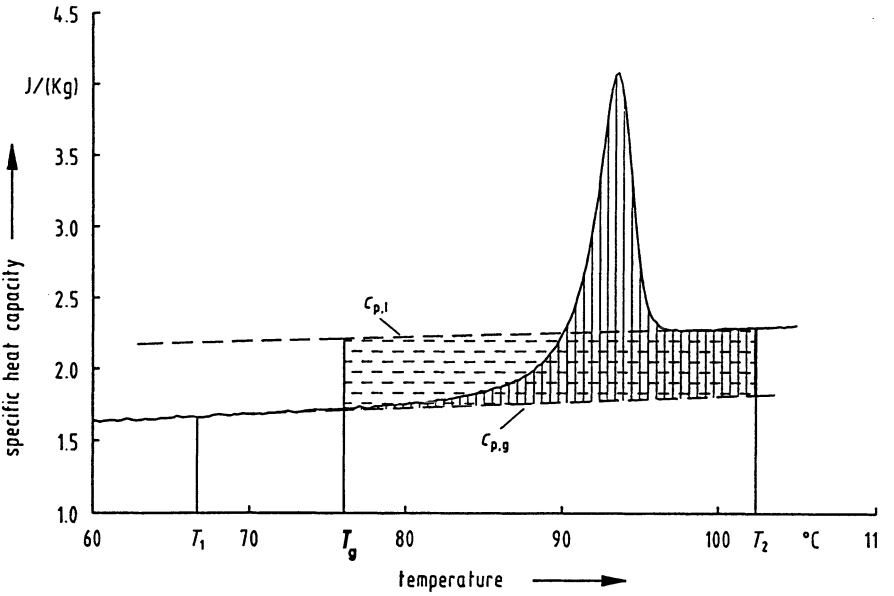

Fig. 6.30. Construction to determine the thermodynamic glass temperature T_g, which is defined by the equality of the different hatched areas (for other quantities see Fig. 6.29)

has the same influence on both hatched areas, but the same only holds to a limited extend for the extrapolation of $c_{p,g}$. T_g cannot, therefore, be determined to better than ± 0.5 to ± 1 K with this method during routine measurements. However, this is not the reason why the thermodynamic T_g is so rarely used in practice – ± 1 K is adequate for many investigations of common T_g relations.

In fact, the sparsity of thermodynamic T_g data has mainly been due to a lack of suitable programs in manufacturers software. The situation is now changing rapidly and "fictive temperatures" ($T_{g,fic} \equiv T_g$) can be calculated for most instruments. This is fortunate because for theoretical investigations of the kinetics of the glass processes the situation is clear: only the thermodynamically defined glass transition temperature reflects unambiguously the thermal history and all the other conditions during the formation of the investigated material. T_g is thus the central quantity for all kinds of relaxation studies. The aim of such investigations is to reproduce the behavior of the glass in the transition region, i.e. in the case of DSC measurements to reproduce the course of the function $c_p = c_p(T)$ precisely. As the changes in T_g, caused by different thermal histories, may only be of the order of a few tenths K, T_g has to be determined at least with that precision.

To minimize the errors in determining T_g,

- all error sources, associated with the determination of c_p (cf. Sect. 6.2.1) must be borne in mind and carefully excluded.
- the sample should remain untouched in the apparatus during all experimental manipulation even for (often time consuming) annealing experiments. Annealing

the sample outside the apparatus almost always yields unsatisfactory results because heat transfer conditions are not exactly reproducible after replacing the sample in the DSC.

The values for the glass transition temperatures obtained from DSC measurements need not necessarily agree with those of other methods. Discrepancies are caused by the different influences of the particular technique on the relaxation of the intrinsic variables (Duncan et al., 1991). A formal conversion, taking into account the various experimental influences, can be made using the (modified, if necessary) equation of Williams, Landel, Ferry (WLF) (Williams, 1955). Principal differences must be attributed to different interactions between the method in question and the relaxation time spectrum of the intrinsic variables.

In studies of this kind it is indeed important to ensure that experimental errors have really been minimized and that any direct influence of the apparatus on the results is at least understood, if not avoidable. To illustrate this problem, in Fig. 6.31 the T_g values (open symbols) of polystyrene (determined as explained here) for different cooling (circles) and subsequent heating (triangles) runs at different rates are shown (Schawe et al., 1996). As can be seen, there is a significant difference between the results of heating and cooling obtained at a particular rate. In addition, this difference increases with the heating (or cooling) rate in question. From the theoretical point of view, there should not be any difference between the thermodynamic

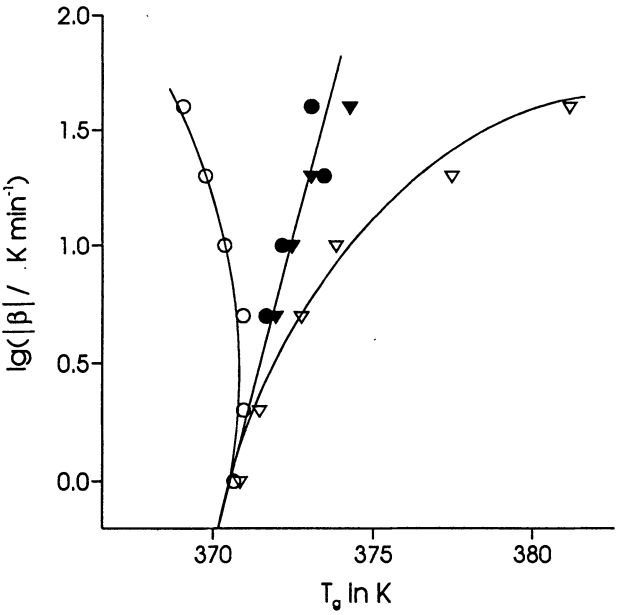

Fig. 6.31. Thermodynamic glass transition temperature T_g of polystyrene from DSC measurements as a function of heating or cooling rate. (Circles: cooling mode; triangles: heating mode; open symbols: as measured, solid symbols: desmeared, acc. to Schawe et al., 1996)

glass transition temperature measured in the heating and cooling mode if the sample has been cooled with the same rate before the heating run. The glass transition should only depend on the procedure according to which the sample has been transformed from the liquid state to the glassy state. The differences measured result from the smearing effect due to the heat transfer path and the temperature profile inside the sample (cf. sect. 5.4) which causes a lag of the sample temperature relative to the measured one. Thus the experimental glass temperatures are no fictive or thermodynamic ones, though determined as such. If the step response desmearing procedure described in Sect. 5.4.3 is applied and the glass transition temperature determined accordingly, the result is quite different (solid symbols in Fig. 6.31). Now the corrected values from the cooling and heating experiments almost superimpose. Furthermore, there is clearly a systematic change in T_g with the cooling rate (1.9 K per decade). This figure is comparable with the corresponding value from the activation plot of mechanical or dielectrical measurements carried out on the same sample. Nevertheless, absolute values are shifted half a decade with respect to dielectric results if one calculates an effective frequency from the cooling rate in question and this agrees with modulated temperature DSC measurements (Schawe, unpublished).

Although the DSC method is very convenient for the characterization of the glass transition, it is not very sensitive. If the c_p changes are small and take place over a broad temperature interval (as, for instance, is the case for lightly crosslinked polymers), the evaluation of the DSC curve is difficult and uncertain. Dynamic mechanical or dielectric measurements are then more suitable.

6.2.3.4 Applications of Glass Transition Measurements

Many important applications of DSC measurement in the glass transition region are connected with polymer research, these are:

- theoretical investigations concerning the thermokinetics of the glass transition. The quantitative description and modelling of relaxation phenomena implies either the determination of enthalpy changes (Petrie, 1972; Cowie, Ferguson, 1986; Agrawal, 1989; Montserrat, 1992; Hay, 1992) or of the thermodynamic glass transition temperature (Moynihan et al., 1976; Stevens, Richardson, 1985). An understanding of the relaxation processes is not only of theoretical interest for physicists but also allows a better access to physical aging phenomena in glassy, polymer materials (Struik, 1978; Cowie, Ferguson, 1986; Pérez et al., 1991). Quantitative descriptions of the phenomena are often based on scanning experiments alone (Kovacs, 1963; Kovacs, Hutchinson, 1979; Moynihan et al., 1976; Ramos et al., 1984; Hutchinson, Ruddy, 1988; Hutchinson, 1990; 1992; Chang, 1988). However, some aspects of glassy behavior can be better studied following various isothermal annealing schedules (Petrie, 1972; Cowie, Ferguson, 1986; Agrawal, 1989; Montserrat, 1992; Hay, 1992). In this method the enthalpy difference between the annealed glass and the quenched glass is determined and evaluated using the empirical Williams-Watts function.
- T_g as one of the most important properties of amorphous materials. For production of new materials with defined properties, the prediction of the glass tran-

sition temperature is a natural necessity. Predictions can be based on group contributions (Becker 1976; 1977; 1978; Wunderlich, 1978). Possible discrepancies between calculated and experimental T_g values may then contribute to a better understanding of the relations between structure and properties of a specific material. Similar investigations concerning the correlation between structure and the caloric information (Δc_p of the glass transition) are still rare to find.

- finding of relations between T_g and caloric quantities of the glass or the glass process (Becker, 1976; Batzer, 1982; Wunderlich, 1990).
- relations between molar mass and glass transition temperatures of polymers. The most widely used equations are those of Fox, 1950:

$$T_g = T_{g,\infty} - \frac{A}{M_n}$$

and Überreiter, Kanig, 1952:

$$\frac{1}{T_g} = \frac{1}{T_{g,\infty}} + \frac{A'}{M_n}$$

where $T_{g,\infty}$ is the glass transition temperature of a polymer with infinite number average molar mass and A and A' are constants for certain broad classes of materials. Both equations can be used for high-molar mass polymers but that of Ueberreiter and Kanig is much better for oligomeric glasses. If, in such investigations, the glass transition temperature must be determined from heating runs, the thermodynamic T_g should always be used. All other (empirical) T_g's are unsuitable because of the inevitable relaxation processes on heating (Agrawal, 1989; Aras, Richardson, 1989).

- investigation of polymerization reactions. T_g is often more sensitive to the progress of a polymerization than is the heat production. This is especially true towards the end of the reaction where the heat production is low and barely detectable, whereas a distinct change of T_g may be observed (Mijovic, Lee, 1989; Wisanrakkit, Gillham, 1990; Hale et al., 1991), for instance, if the crosslink density increases. As typical example DSC curves for an epoxide-amine system, which has reacted different times at 160 °C, are shown in Fig. 6.32.

  It is generally not possible, and in any case it would be far too time-consuming, to determine the degree of reaction only from the changes of T_g during polymerization. In addition the difficulties mentioned in determining exact T_g values would result in very uncertain results for any kinetic analysis. The situation is even more complicated because the glass transition for reacting systems may often be overlapped by the reaction heat flow and thus not precisely determinable.

  A "calibration curve" must be determined connecting the degree of reaction (obtained by another method such as an IR technique or, for soluble polymers, determination of the molar mass) with the T_g values obtained by DSC measurements, nearly identical experimental conditions should be chosen for the different methods. The empirical function $T_g = f(\alpha)$, obtained this way, is not related to a specific reaction model but it can be calculated if some assumptions

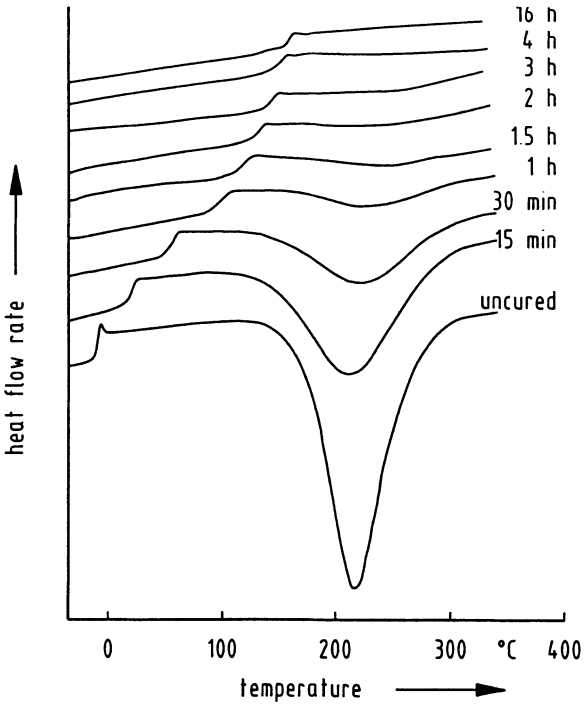

Fig. 6.32. DSC measurements of an epoxide cured at 160 °C for the times shown: the glass transition temperature increases with extent of reaction (acc. to Wisanrakkit, Gillham, 1990)

are fulfilled: for instance, the Fox-Flory model can be used to describe the linear (L) polyaddition reaction:

$$T_g = T_{g,0} + \alpha \cdot ((T_{g,\infty})_L - T_{g,0}) = T_{g,0} + \Delta T_{g,L}$$

$T_{g,0}$ and $(T_{g,\infty})_L$ are the limiting values of the glass transition temperatures for the monomer mixture and the linear polymer with infinite molar mass, respectively. As early as 1970 Horie et al. tried to extend these considerations to reactions which give crosslinked polymers. In this case T_g shows a more pronounced rise, due to the increasing crosslink density, than is the case for linear polyaddition:

$$T_g = T_{g,0} + \Delta T_{g,0} = T_{g,0} + \Delta T_{g,L} + \Delta T_{g,\nu}$$

The relation between $\Delta T_{g,\nu}$ and the crosslink density ν is complex and the separation of ΔT_g into $\Delta T_{g,L}$ and $\Delta T_{g,\nu}$ may not be possible but Min et al., 1993, were successful. They found by NIR measurements that in the system bisphenol-A-diglycidylether (DGEBA) and 4,4'-diaminodiphenyl-sulfone (DDS) the reaction of the primary amine hydrogens only increases the molar mass of the linear polymer whereas that of the secondary amine hydrogen is responsible for crosslinking. Hence the total degree of reaction α can be separated into one part α_L for the linear polymerization and another part α_ν for the crosslinking reaction.

Both parts can be individually obtained from the experiment. If $T_{g,\infty}$ represents the glass transition temperature of the completely reacted and crosslinked polymer, the following is valid:

$$T_g = T_{g,0} + \Delta T_{g,L} + \Delta T_{g,v} = T_{g,0} + \alpha_L((T_{g,\infty})_L - T_{g,0}) + \alpha_v(T_{g,\infty} - (T_{g,\infty})_L)$$

- Investigation of enthalpy relaxation as a function of the degree of cure. Polymers heated for the first time after their production often show very large "relaxation peaks" (Sect. 6.2.3.3.2) which cannot be reproduced by any subsequent thermal manipulation (Montserrat-Ribas, 1992). The reason for this exceptional relaxation behaviour is not yet known. The shape and intensity of the relaxation peak reflect somehow the specific conditions of the polymer forming process and so far it has not been possible to decode this kind of "memory".
- The glass transition temperature of copolymers, blends and polymers containing plasticizers. The influence of plasticizers on T_g of polymers or the glass transition behavior of blends have often been investigated (Fox, 1950; Couchman, Karasz, 1978; Chee, 1985; Kalachandra, Turner, 1987; Braun et al., 1988; Brekner et al., 1988; Tsitsilianis, Staikos, 1992; Pomposo et al., 1993). Homogeneous blends have only one T_g transition, whereas heterogeneous blends show the separate glass transitions of the components with Δc_p values correlated with their relative masses. The glass transition temperature of an ideal homogeneous system of two components can be calculated from their T_g values and mass fractions w_i by the Fox equation (Fox, 1950):

$$\frac{1}{T_g} = \frac{w_1}{T_{g_1}} + \frac{w_2}{T_{g_2}}$$

or by the Karasz equation (Couchman, Karasz, 1978):

$$\ln T_g = \frac{w_1 \cdot \Delta c_{p1} \cdot \ln T_{g_1} + w_2 \cdot \Delta c_{p2} \cdot \ln T_{g_2}}{w_1 \cdot \Delta c_{p1} + w_2 \cdot \Delta c_{p2}}$$

Possible interactions between the components may have very different effects depending on the composition of the system in question. Several equations have been suggested to describe the influence of molecular interactions on T_g with the aid of up to three additional parameters (Podešva, Procházka, 1979; Braun et al., 1988).

Relaxation experiments are helpful for deciding the sometimes difficult problem of whether a polymer blend is homogeneous or heterogeneous (Jorda, Wilkes, 1988; Tsitsilianis, Staikos, 1992). Following their proposals, a clearly detectable relaxation peak formed during the annealing of the sample is used as an "amplifier" for glass transitions, which otherwise only can be detected with difficulty. In this way glass transitions can even be detected which are only a few degrees apart from one another and which would normally overlap to give one broad transition and thus imply a homogeneous product. As an example Fig. 6.33 shows the DSC curves of one homogeneous and two heterogeneous glasses before and after annealing. The two heterogeneous blends differ in the amount of both copolymer components. After annealing the homogeneous sample shows only one

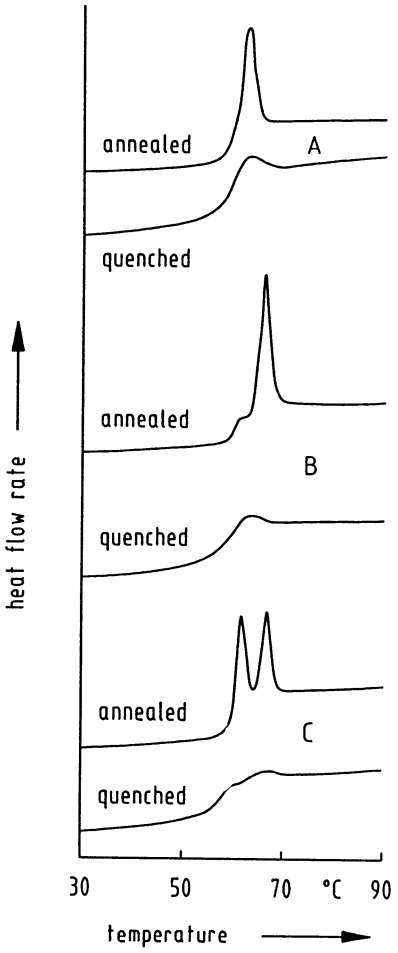

Fig. 6.33. DSC curves of a homogeneous (A) and two heterogeneous (B, C) blends which have been quenched from the melt or annealed a few K below T_g for 14 days. The relaxation peak(s) of the annealed samples clearly show that blends B and C are phase-separated (acc. to Jorda, Wilkes, 1988)

non-structured relaxation peak, whereas the heterogeneous ones possess two separated relaxation peaks, though the DSC curves of the unannealed glasses show no signs of heterogenity.

- the glass transition of semicrystalline polymers. The inverse correlation between the glass transition and melting process has been investigated (Schick et al., 1985; 1989). It is often found that the sum of the amounts of amorphous material (determined from Δc_p) and of crystalline material (determined from the heat of fusion) is lower than expected for a two phase model. In these cases there must be a third phase (called "rigid amorphous"), which shows neither amorphous (glass transition) nor crystalline (melting) behavior. In addition, correlations have been found (Okui, 1990) between the glass transition temperature and other characteristic temperatures, e.g. the melting temperature or the temperature of the maximum crystallization rate.

6.2.4 Purity Determination of Chemicals

The theory of purity determination using DSC is based on the thermodynamics of two-component systems. The simplest and most widely used theory presupposes an eutectic mixture of ideal behavior. For this case we find in textbooks of chemical thermodynamics that the mole fraction x of one component (defined here as the pure one) can be calculated as follows:

$$\ln x = \frac{1}{R} \int_{T_{trs}}^{T} \frac{\Delta H(T)}{T^2} \, dT \tag{6.1}$$

(R, gas constant: 8.31441 J mol^{-1} K^{-1}; $\Delta H(T)$: phase transition enthalpy at temperature T of the pure component in question, T_{trs}: phase transition temperature of this completely pure component).

In the case of a negligible temperature dependence of the phase transition enthalpy, eq. (6.1) is reduced to

$$\ln x = \frac{\Delta H}{R}\left(\frac{1}{T_{trs}} - \frac{1}{T}\right) \quad \text{or} \quad x = \exp\left(\frac{\Delta H}{R}\left(\frac{1}{T_{trs}} - \frac{1}{T}\right)\right) \tag{6.2}$$

This equation serves to calculate eutectic phase diagrams and the melting behavior of slightly impure materials. If a change is made to the mole fraction of the (eutectic) impurity $x_{imp} = 1 - x$ and $\ln(1 - x_{imp})$ approximated (for small values of x_{imp}) by $-x_{imp}$ and the product $T_{trs} \cdot T$ by T_{trs}^2, we obtain:

$$x_{imp}(T) = \Delta H \frac{T_{trs} - T}{R \cdot T_{trs}^2} \tag{6.3}$$

This is the well-known van't Hoff equation which relates the decrease in the melting temperature of the impure component to the amount of impurity involved. In principle, any melting of an eutectic mixture starts at the eutectic temperature and ends at the temperature T which is related to the composition of the mixture via Eq. (6.3) (see Fig. 6.34) and may serve to determine the amount of impurities. The theoretical heat flow rate curve of eutectic mixtures can be calculated: the result is shown in Fig. 6.34 for different concentrations. With increasing impurity, the melting peak becomes lower and lower and less sharp. In reality, for small amounts of impurity, the eutectic melting peak and the starting of the main peak are hardly visible on the DSC curve. The measured curve (Fig. 6.35) is also smeared due to the finite thermal conductivity (cf. Sect. 5.4) so that it differs considerably from the theoretical shape (Fig. 6.34). The end temperature of the peak cannot be determined with the required accuracy and the concentration of the impurity must therefore be determined in a different way.

The software in commercial DSCs usually starts from the assumption that, during the melting process, the instantaneous mole fraction of the mixture at the temperature T (along the eutectic curve, cf. Fig. 6.6a) relative to the initial com-

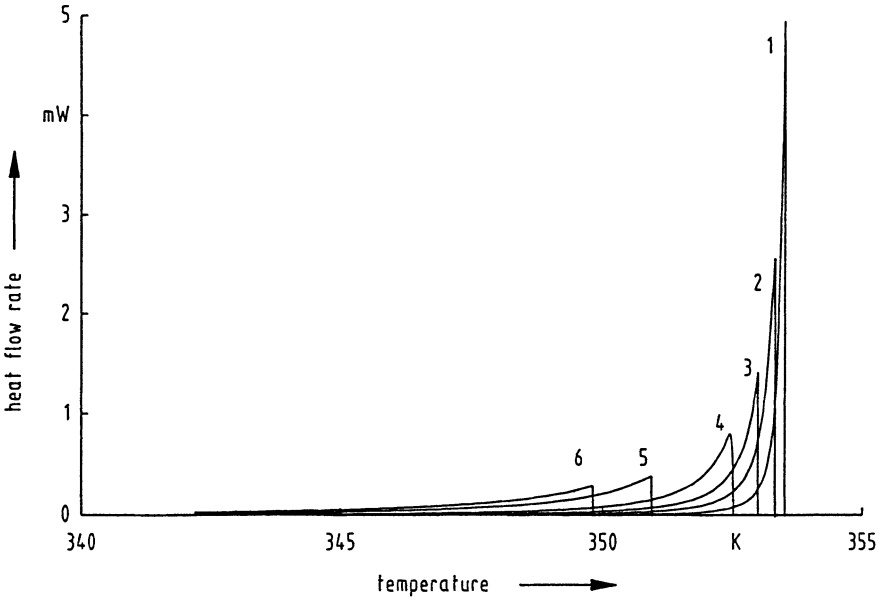

Fig. 6.34. Theoretical melting peaks, normalized to unit area (1: 0.20%; 2: 0.55%; 3: 1.05%; 4: 2.03%; 5: 4.67%; 6: 6.65% impurity)

position is the same as the relation between the heat of fusion used up to that temperature and the total heat:

$$\frac{x_{\text{imp}}(T)}{x_{\text{imp}}} = \frac{Q_T}{Q_\infty} \equiv F(T) \tag{6.4}$$

The right-hand side of this equation is the quotient of the partial peak area up to the temperature T and the total peak area if smearing effects are disregarded. For this quotient, the abbreviated form $F(T)$ (relative partial area) is often used. Inserting Eq. (6.4) into (6.3) furnishes an equation according to which the impurity x_{imp} can be determined from the slope of a plot of the temperature versus $1/F(T)$ which should be a straight line. In practice this is not the case because of the difficulty in deciding when melting actually starts and the limited heat transfer to the sample. Commercial software generally corrects the measured values in such a way that a straight line is obtained in the plot. This is of course only an approximation to correct for deviations from experimental and theoretical shortcomings (e.g. the smearing effects), nevertheless it is widely used. To avoid larger errors, small sample masses and low heating rates should be used for purity determination. However, the signal will then be noisy and the partial areas cannot therefore be detected very precisely.

Recently Bader et al., 1993, presented a new method which determines the impurity from the shape of the measured curve at the start of the melting process, just

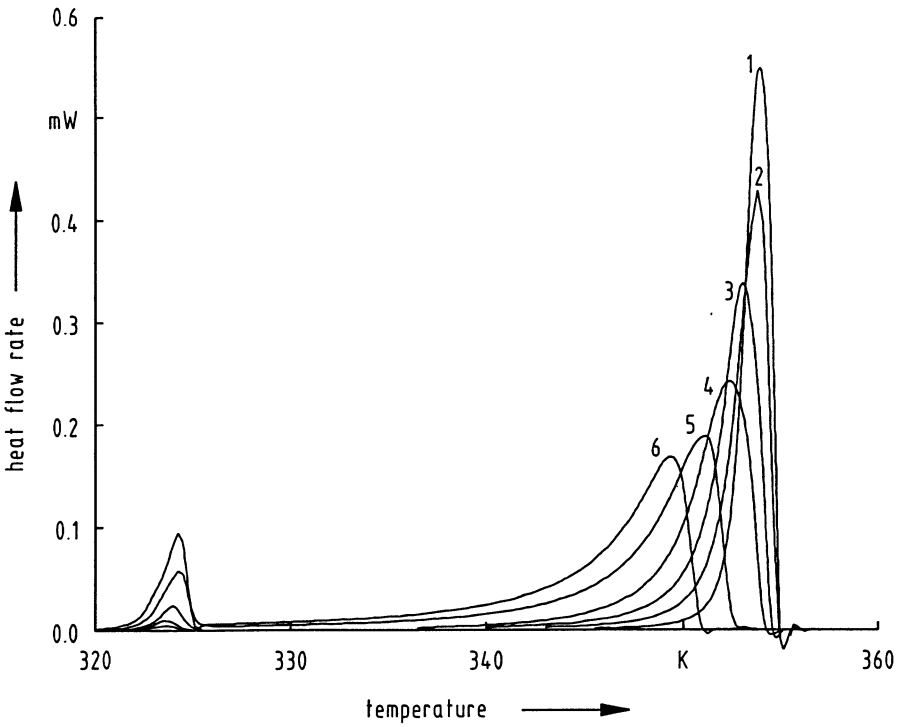

Fig. 6.35. Real melting peaks measured in a DSC and normalized to unit area (impurities as in Fig. 6.34)

behind the eutectic point where the heat flow rates are still small and falsification due to smearing low. In principle, the shape of the melting peak is determined from the phase diagram of an ideal mixture of two components and can be calculated from Eq. (6.1) or (6.2) (cf. Fig. 6.34). If the equation in question is solved for x as a function of temperature and the (normalized) heat flow rate at the respective temperature, a straight line should be obtained which intersects the ordinate at the value of the purity of the sample and drops to 1.0 at the maximum temperature of the peak (Fig. 6.36). The same type of plot can be calculated from the heat flow rates (normalized and with the baseline subtracted) of the measured curves (Fig. 6.35), it is shown in Fig. 6.37. The result does not come up to what had been expected because of the difficulty of precisely determining the baseline and thus the beginning of the peak. It has, however, been shown (Bader et al., 1993) that some minor parameter variations (well below the uncertainty of the measurement) correct the problem satisfactorily (Fig. 6.38). Further details of this special method are not given here, as it has not yet been accepted by the manufacturers and the user may be unable to implement it in his computer himself. The interested reader is referred to the original publication. The advantage of using the shape at the start of the melting peak (rather than the end temperature or the partial areas procedure) for evaluation is the

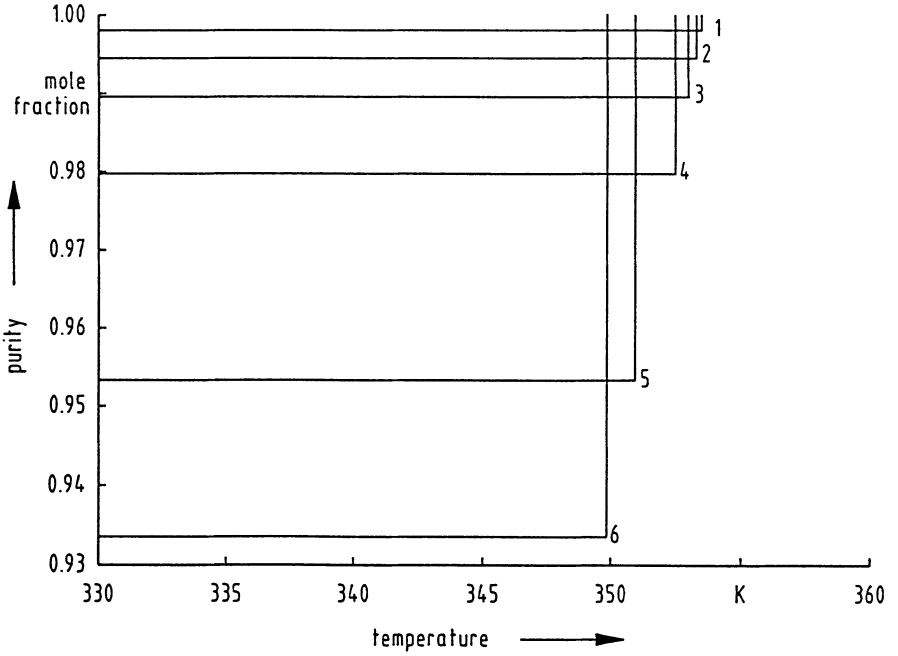

Fig. 6.36. "Purity function" from theoretical melting peaks of Fig. 6.34

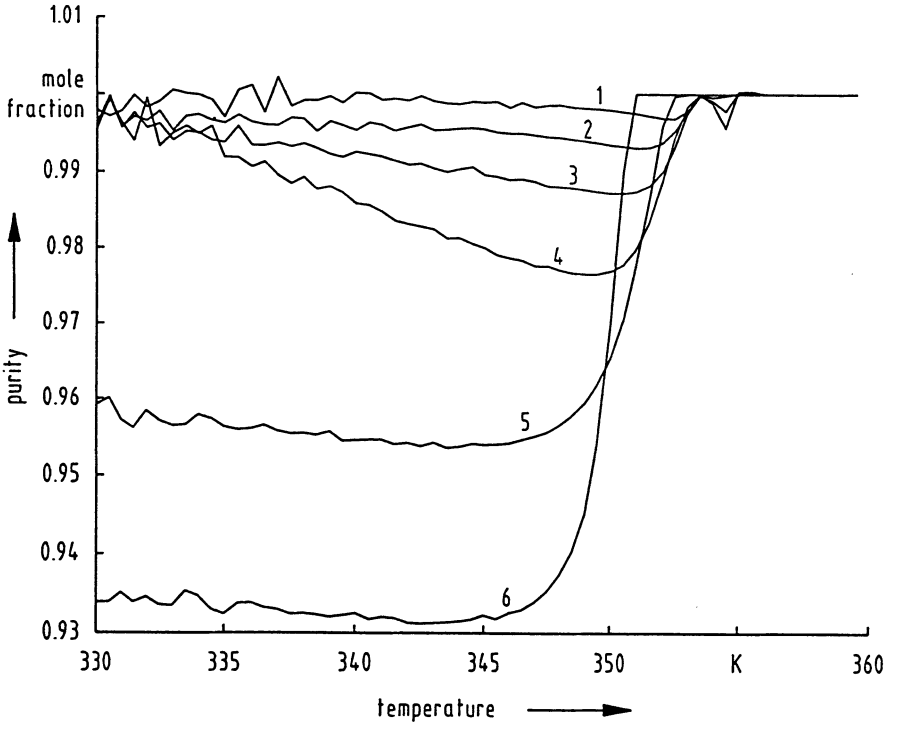

Fig. 6.37. "Purity function" from measured melting peaks of Fig. 6.35

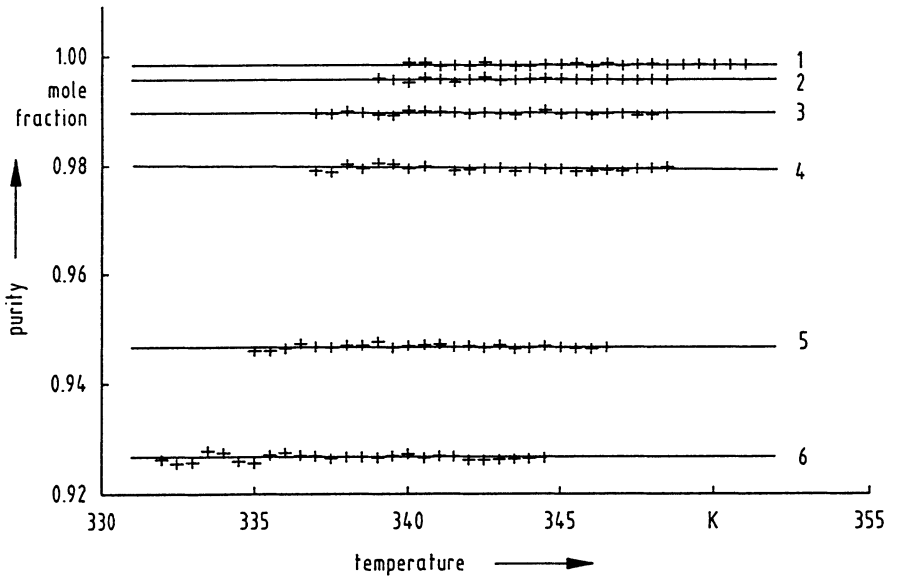

Fig. 6.38. Corrected "purity function" of measured melting peaks from Fig. 6.35 (impurities as in Fig. 6.34)

negligible falsification due to smearing of this part of the curve. This permits the use of larger heating rates and sample masses which increases the signal-to-noise ratio and the accuracy of the measurements.

From the example given it follows that the accuracy of all purity evaluations is largely influenced by the smearing of the measured curve, as the results are calculated in one way or the other from the shape of the peak. Bearing in mind that most theories of purity determination start from the assumption of eutectic mixtures, which is actually only one special case, the accuracy of every determination of purities by DSC should be considered to be a rather limited approximation to the truth. Nevertheless, it is convenient and therefore often used in quality control.

7 Evaluation of the Performance of a Differential Scanning Calorimeter

The DSC furnishes information on temperature and heat flow rates (resp. heat). Whether it is suited to solve the respective problem depends on the efficiency of the instrument. The characteristic data of the DSC which describe the instrument unambigously must therefore be known. They allow a decision to be taken as to whether the DSC will be suitable for the intended use, and they also make a comparison with other DSCs possible.

A distinction can be made between:

1. the characterization of the complete instrument,
2. the characterization of the measuring system,
3. the characterization of the results of a DSC measurement.

7.1 Characterization of the Complete Instrument

The following serves to characterize the DSC instrument as a whole:

- measuring principle (heat flux or power compensation DSC),
- temperature range,
- potential heating rates and temperature-time programs,
- usable sample volume,
- atmosphere (gases which may be used, vacuum, pressure).

7.2 Characterization of the Measuring System

In this section characteristic terms are presented which may be used to describe the efficiency of a DSC measuring system. Instructions how to determine the numerical values are suggested. The characteristic terms in question are the following:

- the noise,
- the repeatability,
- the linearity,
- the time constant.

- The *noise* of the measured signal (given, for example, in μW) is indicated in different ways (see Fig. 7.1):
  - as peak-to-peak noise (pp): maximum variation of the measured signal in relation to the mean signal value,

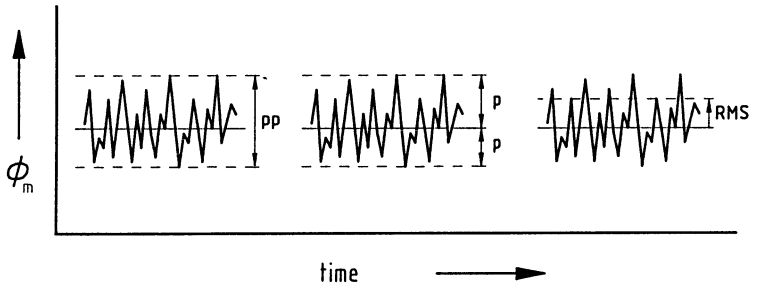

Fig. 7.1. The various definitions of noise (acc. to Hemminger, 1994).
pp peak-to-peak noise, p peak noise, RMS root-mean-square noise, Φ_m measured heat flow rate

- as peak noise (p): maximum deviation of the measured signal from the mean signal value,
- as root-mean-square noise (RMS): root of the mean value of the squared instantaneous deviations of the measured signal from the mean signal value.

These three definitions of noise are statistically dependent on one another; in general, the following is valid: p = 0.5 pp; for a sine-shaped measurement signal, the RMS noise is equal to 0.35 pp noise; for a statistical random signal, the RMS noise is about 0.25 pp noise.

The noise of the DSC and DTA instrument depends on the heating rate, the temperature and on other parameters (e.g. atmosphere). The signal-to-noise ratio is decisive for the smallest heat flow rate detectable ("heat flow rate resolution"or "detection limit" of the DSC). This threshold for the heat flow rate determination amounts to about 2 to 5 times the noise (cf. Wies et al., 1992).

It is often expedient to indicate the sample volume- or sample mass-related noise (for example in $\mu W\ cm^{-3}$ or $\mu W\ g^{-1}$) which allows the smallest detectable heat flow rate to be estimated for a given sample.

The noise (so called "short-time noise") can be measured:

- In the desired operating mode (isothermal or scanning mode at a specified heating rate) and at the temperature of interest, the measured signal is amplified to such a degree (most sensitive measuring range) that the noise is clearly recognizable.

  The mean variation (pp, p or RMS) of the signal over a period of about 1 min furnishes the respective (short-time) noise (for example in μW) (with the amplification factor taken into account, if necessary).

  The isothermal noise should be the smallest noise possible (compare the scanning noise of the zero line). It gives an impression of the disturbances from the environment to which the sensors are subject. It determines the maximum possible signal-to-noise ratio.

- The *repeatability* indicates the closeness of the agreement between the results of successive measurements of the same kind carried out with a specific instrument

(acc. to International Vocabulary of Basic and General Terms in Metrology, 1984).

DSCs can be characterized by the repeatability by measuring a significant DSC quality (e.g. extrapolated peak onset temperature, peak area, course of the zero line etc.) several times under the same conditions on samples of the same kind. Examples:

- The repeatability of the zero line is determined by measuring 4 or 5 zero lines over the whole temperature range at medium scanning rate and superimposing the curves. The temperature-dependent range of the deviation from the "mean" zero line (absolute or in %) gives the repeatability.

  This ± range of scatter gives an impression of the uncertainty of the heat flow rate calibration and is the systematic part of the uncertainty when an absolute heat flow rate must be determined that is related to the zero line (for example when c_p is measured).
- The repeatability of the peak area and of the baseline is determined by measuring for example the peak area caused by the melting of a pure metal several times under the same condition. (Either only repeat measurements without moving the sample crucible or with replacing the crucible after each run). The curves with the peaks and the baselines constructed for each peak are superimposed. The ± range related to the mean area shows the repeatability of the peak area (heat of fusion) determination. A separate baseline repeatability can be determined (acc. to the procedure with the zero line, see above). The repeatability of the peak area (taking the baseline repeatability into account) furnishes the calibration uncertainty of the peak area (heat) calibration which is the smallest uncertainty for heat measurements.

When the repeatability is given as a ± range (scatter), it must be stated which measure is used: the standard deviation, the maximum deviation or another characteristic value.

Note:

The *reproducibility* describes the closeness of the agreement between the results of measurements carried out on a sample using different instruments in different laboratories (round robin, interlaboratory comparison). The absolute or percentage deviation of the mean value of the results of an instrument from the total mean value is a measure of the reproducibility. Low reproducibility may point to *systematic errors of measurement* (see below) of certain instruments.

- The *linearity* of a DSC shows the relation between the measured heat flow rate Φ_m (signal) and the true heat flow rate Φ_{true} or between the measured heat Q_m (or peak area A) and the true heat Q_{true}: $\Phi_{true} = K_\Phi \cdot \Phi_m$ or $Q_{true} = K_Q \cdot Q_m$.

  The respective proportionality factor K depends on parameters, e.g. the temperature, the mass of the sample, the heating rate etc.

  To determine the linearity means to measure the dependence of the respective K on parameters and to represent this function graphically, i.e. to show $K_\Phi = \Phi_{true}/\Phi_m$ or $K_Q = Q_{true}/Q_m$ as a funtion of a parameter. An ideal linearity means K = const.

Examples:

- The temperature dependence $K = K(T)$ is determined by caloric calibration (cf. Sect. 4.4). In some DSCs, this dependence is linearized electronically or by means of the pertinent software. This apparent ideal linearity is of course affected by the full uncertainties of calibration and interpolation.
- The dependence of the factor K_Q on the mass of the sample ($K_Q = K_Q(m)$) is determined by measuring the peak areas related with the melting of, for example, indium samples of different mass, with the other parameters unchanged (Fig. 7.2).

Note:

With decreasing mass, the minimum heat of fusion can be assessed which can be distinguished with reasonable accuracy from the noise and the baseline uncertainty.

The linearity can be tested with regard to, for example,

- the scanning rate,
- the sample position in the crucible,
- the surface-to-volume ratio of the sample.

- The *time constant* τ of the DSC measuring system is the time interval in which – after a stepwise change of a constant heat flow rate which is produced at the place of the sample – the measurement signal reaches the new final value up to the e-th part (i.e. up to 63.2%). In other words, if a constant heat flow rate that

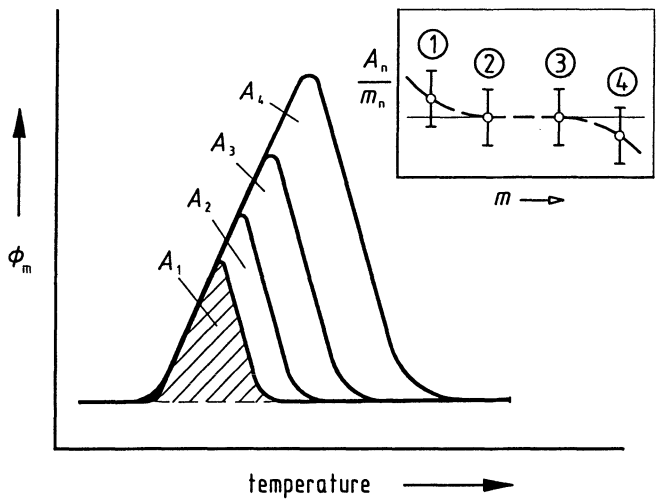

Fig. 7.2. Linearity (acc. to Hemminger, 1994).
Φ_m measured signal (heat flow rate), A_1 to A_4 peak areas, belonging to sample masses m_1 to m_4 ($m_1 < m_2 < m_3 < m_4$). In the partial figure: ratio A_n/m_n with the range of uncertainty of the area determination, ---- deviation from ideal linearity (here only found for very small ① and very big ④ sample masses)

causes a signal $\Phi_{m,0}$ is switched off, the signal drops down to $\Phi_{m,0}/e$ (36.8%; i.e. it decreases by 63.2%) after the time interval τ (Fig. 7.3). The time constant determines to what degree two successive thermal events (peaks) are recorded clearly separated from each other (resolution with time). Knowledge of the time constant is important for the desmearing of DSC curves (see sect. 5.4.).

The time constant can be determined as follows (cf. Ulbrich, Cammenga, 1993; Löblich, 1994):

- When an electric calibration heater can be is installed, a constant heat flow rate, $\Phi_{m,0}$, is switched on until a constant measurement signal is obtained; after switching-off of the heater, the descending curve is evaluated according to Fig. 7.3 or evaluated analytically:

$$\Phi(t) = \Phi_{m,0} \cdot \exp(-t/\tau)$$

$$\frac{d\Phi}{dt} = -\frac{\Phi}{\tau}$$

so for any time t^* we get

$$\tau = -\frac{\Phi(t^*)}{\frac{d\Phi}{dt}}$$

t^* should not be too close to the switching-off time because other, smaller time constants (τ_2, τ_3 etc.) may then be superimposed on the maximum time constant τ_{max} (see below).

- When no calibration heater can be installed, the descending section of a peak is evaluated by the "tangent method" when a pure substance is melted (cf.

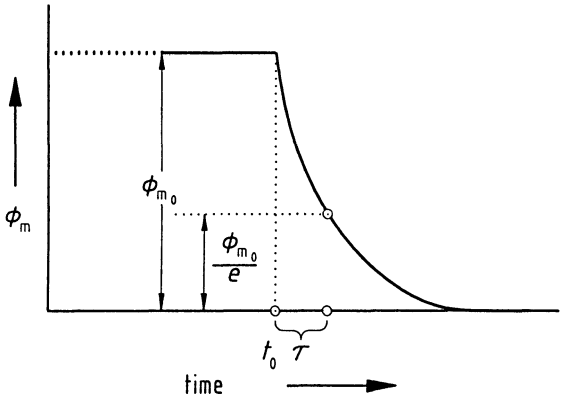

Fig. 7.3. Determination of the time constant τ (acc. to Hemminger, 1994).
After a constant measurement signal $\Phi_{m,0}$ has been reached, the constant heating current is switched off at the time t_0. After the time interval τ, the measurement signal $\Phi_{m,0}$ has dropped to $\Phi_{m,0}/e$

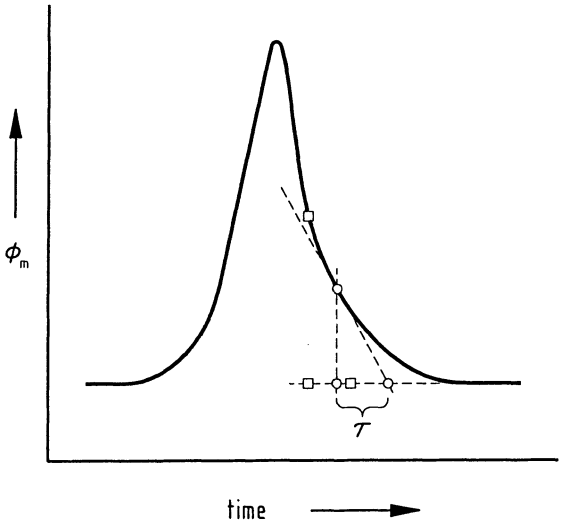

Fig. 7.4. Determination of the time constant τ from the melting peak of a pure substance (acc. to Hemminger, 1994)

Fig. 7.4). Several tangents are plotted to the descending section and the time constants $\tau_1 \ldots \tau_{max}$ are graphically determined from the intersections with the linearly interpolated baseline. Towards the end of the descending curve, a constant value (Δt between t^* and the intersecting tangent baseline) results: the (greatest) time constant τ_{max} which describes the thermal inertia of the measuring system in good approximation.

- From the measured curve, at the moment of the (usually sudden) solidification of the (supercooled) melt of a pure substance (procedure as above).

- It is sometimes important to know the *sensitivity* of a DSC measuring system. This quantity gives the relation between the change of the measurement signal and the change of the measured quantity that creates the signal. In DSC systems the measured quantity is a change in the heat flow rate $\Delta\Phi$, for example in μW, the signal output is an electric voltage ΔU, for example in μV, so the sensitivity is given in $\mu V\ \mu W^{-1}$.

7.3 Characterization of the Results of a Measurement

The quality of measurement results must be evaluated prior to their being used in calculations (purity, kinetics etc.) and interpreted. This evaluation is made on the basis of the data characterizing efficiency of the measuring system (cf. Sect. 7.2).

Terms describing the quality of measurement results (cf. International Vocabulary of Basic and General Terms in Metrology 1984, 1994):

- the *accuracy* describes how well the result of a measurement approximates the "true" value. The accuracy is determined by *random* (unforeseeable, uncorrelated) and *systematic errors* of measurement. With the conditions of measure-

ment unchanged, systematic errors are constant; they may comprise known and unknown components.

Known systematic errors (deviations) are allowed for in the measurement result as *corrections*. The uncertainty of these corrections, unknown systematic errors and random errors must be estimated. The standard deviation is an estimate of the random errors.

- The *total uncertainty of measurement* indicates a range of values in which the true value of the measurand lies with high probability. The total uncertainty is often referred to as accuracy (more precisely: inaccuracy); it is not identical with the repeatability or the reproducibility (cf. sect. 7.2).

All the relevant quantities should be carefully evaluated and taken into account when the uncertainty of a measured value is estimated. Statement of the uncertainty enables the reader or colleague to judge the rank of the investigations published.

Example (see Fig. 7.5):

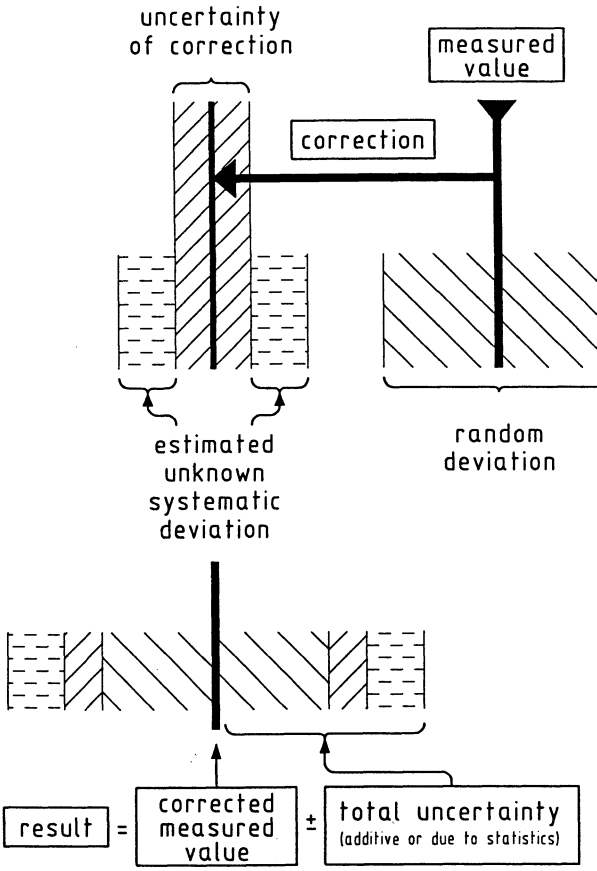

Fig. 7.5. Diagram to describe the relation between the terms "result of a measurement", "measured value" and "total uncertainty" (cf. text)

Result of a measurement = measured value (e.g. mean value of a series of measurements) (100 μW)
+ known systematic error (correction) (−10 μW)
Overall uncertainty { + uncertainty of the correction, estimated (±1 μW)
+ unknown systematic error, estimated (±2 μW)
+ random error (e.g. twice the standard deviation) (±4 μW)
= 90 μW ±7 μW (additive total uncertainty)

(taking no account of the error propagation or the like).

7.4 Check List for DSCs

The following check list serves to collect the essential characteristic data of a DSC. It may be used to

- ask the manufacturers for the values,
- establish a guide-line when characteristic data are measured in one's own laboratory or in the manufacturer's laboratory,
- compare different types of DSCs,
- compare the DSCs data with the values which required to investigate a problem.

Manufacturer:	
Type of measuring system:	☐ heat flux disk-type
	☐ heat flux cylinder-type
	☐ power compensation
Special features:	.....
Sample volume (standard crucible):	..... mm^3
Atmosphere (vacuum?, which gases? pressure?):	.....
Temperature range:	from ..... to ..... °C or K
Scanning rates:	from ... to ... K min^{-1} steps: ... K min^{-1}
Zero line repeatability:	from ± ..... μW (at ..... °C)
	to ± ..... μW (at ..... °C)
Peak area repeatability:	± ..... % (at ..... °C)
Total uncertainty for heat:	± ..... % (at ..... °C)
Extrapolated peak onset temperature repeatability:	..... K (at ..... °C)
Total uncertainty for temperature:	± ..... K (at ..... °C)
Scanning noise (pp) at ..... K/min:	from ± ..... μW (at ..... °C)
	to ± ..... μW (at ..... °C)
Isothermal noise (pp):	from ± ..... μW (at ..... °C)
	to ± ..... μW (at ..... °C)
Time constant with sample:	..... s
Additional facilities:	.....

Appendix 1

Comparison of Heat Flux Differential Scanning Calorimeters and Differential Thermal Analysis Instruments

The measured signal generated in DTA instruments is the temperature difference ΔT between sample and reference sample. The measuring system comprises temperature sensors and a suitable holder or support to fix the temperature sensors and the sample containers mechanically. A defined, constant and good thermal contact must be established between temperature sensors and sample containers. Strict repeatability of the measuring system over the whole temperature range must be ensured; the system's properties are reflected in the shape of the zero line (i.e. curve measured with the measuring system empty or with empty crucibles).

Depending on the desired measurement temperature, sample volume and sensitivity, a choice can be made from among various DTA measuring systems. In the following, the two contrasting basic types – the *block-type measuring system* and the *measuring system with free-standing crucibles* – will be described.

DTA: The Block-type Measuring System

The following is characteristic of this type of measuring system (cf. Fig. A1.1):

- The temperature difference ΔT is measured directly in the sample substances. As a result, the temperature sensors are subject to the attack by the sample and reference sample substance.
- The duration (resolution with time) and the height (sensitivity) of the measured signal are determined by the thermal resistance between sample substance and block, sample substance and temperature sensor and by the properties of the block material.
- The duration and height of the measurement signal and as its shape also depend on the location of the temperature sensor in the sample substance and on the (changing) thermophysical properties of the sample substance. A quantitative evaluation of the heat in question is therefore impossible.

The generally high sensitivity and the rapid, almost instantaneous "response" to sample reactions are advantages of this measuring system.

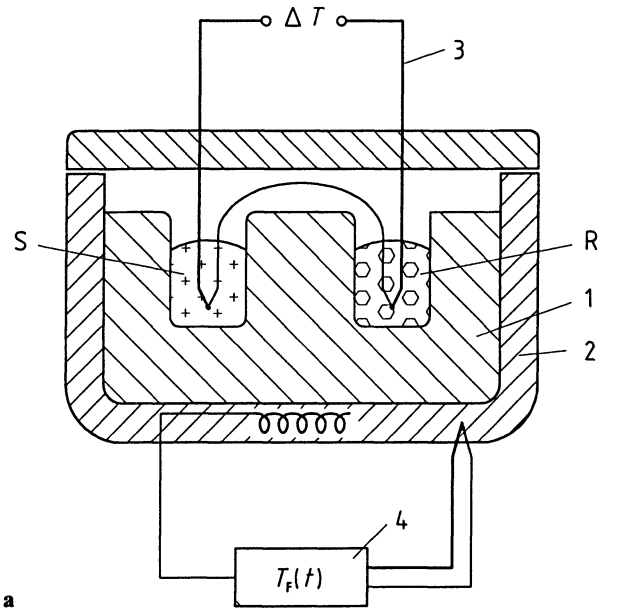

a

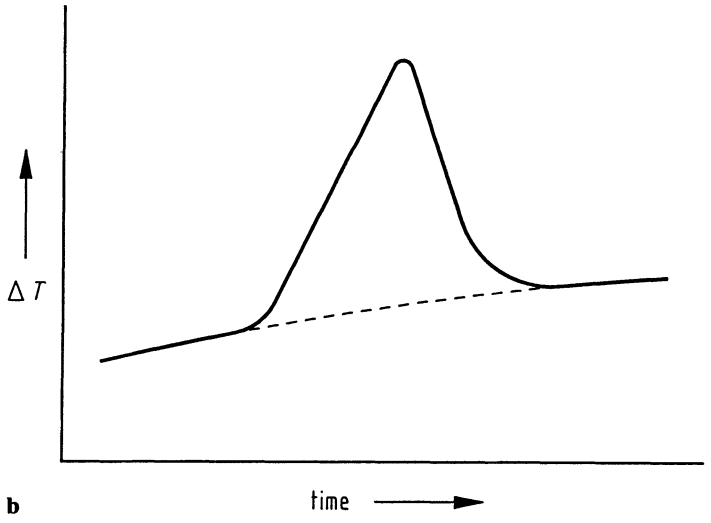

b

Fig. A 1.1. **a** Instrument for Differential Thermal Analysis (DTA) with block-type measuring system,
b Schematic measured curve $\Delta T(t)$ (exothermic transition).
1 "block" with cavities to take up sample and reference sample substance, 2 furnace, 3 differential thermocouple, 4 programmer and controller, S sample substance, R reference sample substance, T_F furnace temperature

DTA: Measuring System with Free-standing Crucibles

This measuring system (Fig. A1.2) is more frequently used in DTA instruments than the block-type measuring system. A characteristic feature is that free-standing sample crucibles are put over the protective tubes of the thermocouples for the purpose of ΔT measurements. The thermocouple junction is in thermal contact with the bottom of the crucible.

The following is characteristic of this type of measuring system:

- The thermophysical properties of the sample substance affect the height and shape of the measured curve only slightly. The peak shape is, to a large extent,

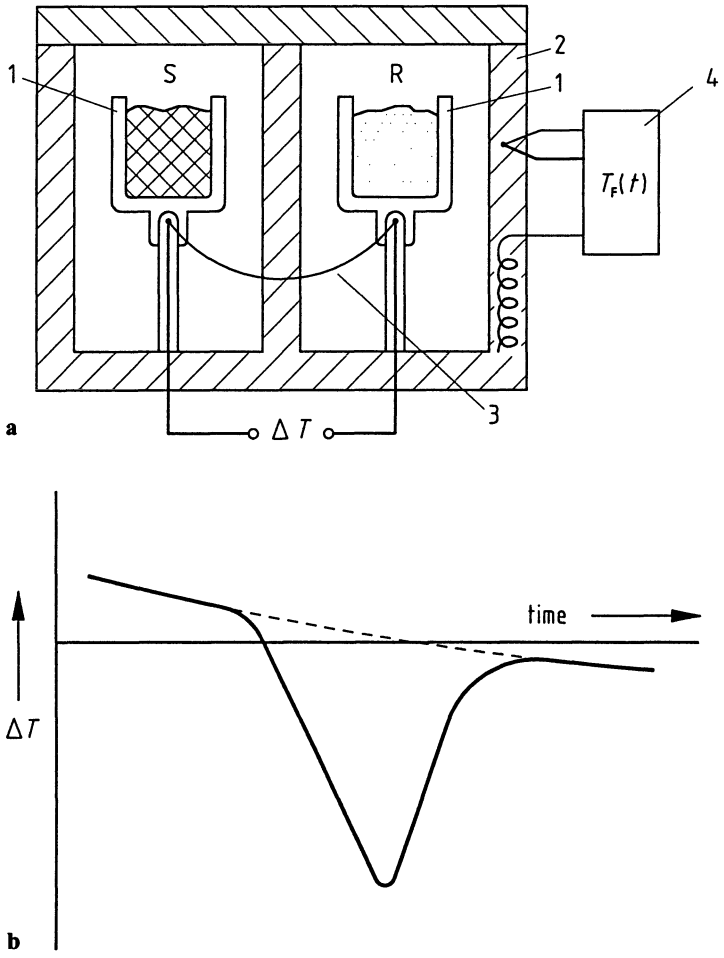

Fig. A 1.2. **a** Instrument for Differential Thermal Analysis (DTA), measuring system with free-standing crucibles,
b Schematic measured curve $\Delta T(t)$ (endothermic transition).
1 crucible, 2 furnace, 3 differential thermocouple, 4 programmer and controller, S sample substance, R reference sample substance, T_F furnace temperature

determined by the containers, this allows a semi-quantitative evaluation of the heat in question from the peak area.
- Depending on the problems to be solved and the mass and structure of the samples, a choice can be made from among a great number of container types (crucibles), among them "poly-plate" crucibles, micro-crucibles worked out from the thermocouple bead, crucibles for "self-generated atmosphere" and others.
- The high flexibility as far as the usability of different furnaces is concerned (temperature ranges), the adjustment of different gas atmospheres (including vacuum) and the usability in instruments for simultaneous thermal analysis.

In other types of DTA instruments, sleeves containing the sample substance are placed on the thermocouple junctions which are either unprotected or covered by thin tubes. With this the attempt is made to have the advantages offered by direct, undelayed temperature measurement, without having to put up with the unfavourable effects of the block material (resolution, sensitivity) or the (isolated) individual crucibles (delayed, "smeared" temperature measurement).

Heat Flux DSC

In contrast to the majority of the DTA instruments of rather simple design, DSCs should be capable of being calibrated for heat measurement. An unambiguous and repeatable assignment of the measurement signal proper, ΔT, to the measurand $\Delta\Phi$ must be ensured ($\Delta\Phi = \Phi_{FS} - \Phi_{FR}$, differential heat flow rate from the furnace to the samples). The DSC should be suitable for the investigation of different substances and transitions under different test conditions. This is why the properties of the measuring system may depend as little as possible on the sample properties, the type of transition and on test parameters (e.g. heating rate).

Within certain limits, these requirements can be fulfilled in good approximation when the temperature field of the measuring system does not primarily depend on sample properties but on the properties of the measuring system itself which are given by its design.

This *dominance of the measuring system*, which is essential for DSCs, follows from the fact that – compared with the sample – the measuring system is made up of solid parts and has defined heat conduction paths. The sample reaction can then be regarded as a small disturbance of the steady-state temperature field established during heating. As this disturbance must be small, the measured signal itself, ΔT, will also be small. As a consequence, the noise of the whole measuring set-up must be low to allow the sensitive measurement of heat flow rates.

In all DSCs the calibration factor depends on instrument and sample parameters. This leads to systematic error sources, and the uncertainty of the result is, therefore, much larger than the repeatability error of the measurements. Very careful calibration, with the sample parameters adjusted, is, therefore, necessary.

Appendix 2

Calorimetry – a Synopsis

A great variety of calorimeters serve to measure heats and heat capacities in various fields of application.

In the following, a classification system for calorimeters and a couple of examples of different types of calorimeters will be presented.

The aim is to give a structured survey of the whole field of calorimetry which may help to better recognize and evaluate the advantages of and limitations to the DSCs which result from their mode of operation.

Classification

In a classification system, calorimeters are arranged in groups according to particular characteristics. Various classification systems are reasonable and practicable (cf. Hemminger, Höhne, 1984; Rouquerol, Zielenkiewicz, 1986). It may sometimes be difficult to arrange calorimeters in proper order in a relatively simple system, and such a classification may even be impossible. Classification systems covering the entire field of calorimetry tend to become very sophisticated, an end in itself and rather useless for practical applications. When thermodynamical principles of heat exchange or the aspect of how the caloric signal is formed are taken as a basis for classification, the result will always be that a certain number of calorimeters are characterized satisfactorily well whereas additional explanations or auxiliary definitions are required for others. Nevertheless, a classification system is useful to show basic principles of calorimetry. It should be based on existing instruments and open to future developments. In the following, a simple system for practical use will be developed which will suffice to discuss characteristic features and error sources by groups.

Criteria for the classification are the following:

1. *The principle of measurement*
   - 1.1 Measurement of the energy required for compensating the heat to be measured (heat-compensating calorimeters).
   - 1.2 Measurement of the temperature change of a substance due to the heat to be measured (heat-accumulating calorimeters).
   - 1.3 Measurement of the heat flow rate between sample and surroundings due to the heat to be measured (heat-exchanging calorimeters).

2. *Mode of operation*
   - 2.1 isothermal
   - 2.2 isoperibol
   - 2.3 adiabatic

   } static modes

   - 2.4 scanning of surroundings
   - 2.5 isoperibol scanning
   - 2.6 adiabatic scanning

   } dynamic modes

3. *Construction principle*
   - 3.1 Single calorimeter
   - 3.2 Twin or differential calorimeter

Most of the calorimeters can be classified by the above-mentioned criteria. All combinations of the criteria 1, 2 and 3 are, of course, not possible as some of the criteria are incompatible.

Calorimeters which are used today will be presented in the following according to this classification. As the classic calorimeters will be dealt with only briefly, reference will be made to the literature for further information on construction details, error sources, methods for the evaluation of the measured values, and ranges of application of these instruments. The DSCs, however, are treated in closer detail in several sections of this book (see chapters 2 and 3).

Examples of Calorimeters

The aim of this section is to give the reader an idea of the variety of calorimeters offered in addition to DSCs. This will help to better classify the range and potentialities of the DSC methods in comparison with different calorimetric methods.

Heat-compensating Calorimeters

In the case of this calorimetric method, the effect of the heat to be measured is "suppressed", i.e. temperature changes of the sample or of the calorimeter's measuring system, or temperature differences in the measuring system due to the caloric effect are compensated. For this purpose, an equally high, well-known amount of energy, with the sign reversed, is added.

Possibilities: Compensation of the heat to be measured with the aid of the "latent heat" of a phase transition (e.g. ice calorimeter) or with electric energy (Joule's heat or Peltier's cold). The compensation by means of reversible expansion or compression of an ideal gas was described by Ter Minassian, Milliou, 1983.

It is an advantage of all compensating methods that the measurements are carried out under quasi-isothermal conditions and that heat leaks do not, therefore, represent important error sources. Moreover, in the case of electric compensation, no calibrated temperature sensor is required for the measurement but only a sensitive thermometer which controls the compensation power of a controller so that the temperature remains constant.

1st example: "Ice calorimeter"

1. Compensation of the heat to be measured by latent heat
2. Isothermal
3. Single calorimeter

A warm sample placed in an ice calorimeter (Fig. A 2.1) transfers its heat to a 0 °C ice jacket. As a result, a certain mass of ice (to be determined) melts. In the case of the ice calorimeter according to Lavoisier, de Laplace, 1784, the melted water was weighed, whereas Bunsen, 1870, determined the change of the ice/water ratio on the basis of the change in the volume of the whole mixture (density difference of ice and water). The measurements which Ginnings and Corruccini carried out at the National Bureau of Standards (NBS) during the late forties were counted among the important applications of an ice calorimeter. They measured heat with an uncertainty of about 0.02%, the temperature of the sample at the moment of its being dropped into the calorimeter lying between 100 °C and 600 °C.

The liquid to gaseous phase transition was also made use of ("boil-off" calorimeter), in particular since in this case the difference between the density of both phases – and thus the sensitivity – is by two or three orders of magnitude higher than in solid to liquid transitions.

Phase transition calorimeters are relatively simple to construct and allow precise measurements to be performed. A disadvantage is that measurements can be carried out only at one temperature, i.e. at the temperature of transition of the respective calorimeter substance.

The quantity to be determined is the transformed mass of calorimeter substance (ice, liquid); the heat of transition must be known. (In general, the calorimeter is calibrated electically.)

2nd example: "Measurement of heats of solution"

1. Compensation of the heat to be measured with the aid of electric energy
2. Isothermal
3. Single calorimeter

A container filled with water is equipped with a stirrer, a controllable electric heater and a sensitive thermometer (Fig. A 2.2). At constant temperature, an endothermically solving salt is added. The heater is adjusted so that the temperature of the liquid remains constant. The supplied electric energy is then equal to the heat of solution of the salt (Brönsted, 1906).

Expressed more generally, the following is valid:
In calorimeters of this type, the heat to be measured is compensated by Joule's heat or with the aid of the Peltier effect. This is done in that a sensitive thermometer activates the compensation control circuit so that, if possible, no temperature change due to reaction heat takes place. As the Peltier power for the compensation

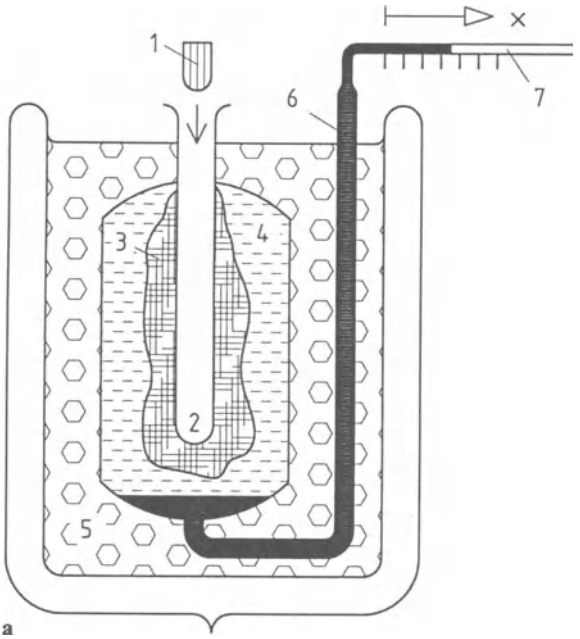

a

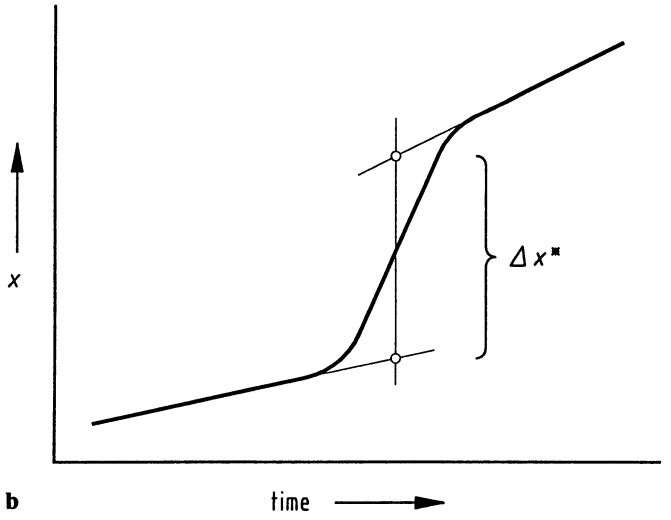

b

Fig. A 2.1. **a** "Ice calorimeter" (Bunsen, 1870),
b Measured curve (acc. to Hemminger, 1994).
1 sample, 2 sample container (receiver), 3 ice, 4 water, 5 ice-water mixture, 6 mercury, 7 capillary tube, x position of the mercury meniscus.
The displacement Δx^* of the meniscus is proportional to the heat Q exchanged with the sample (positive for an endothermic effect). Δx^* is determined taking the "preperiod" and the "postperiod" into account

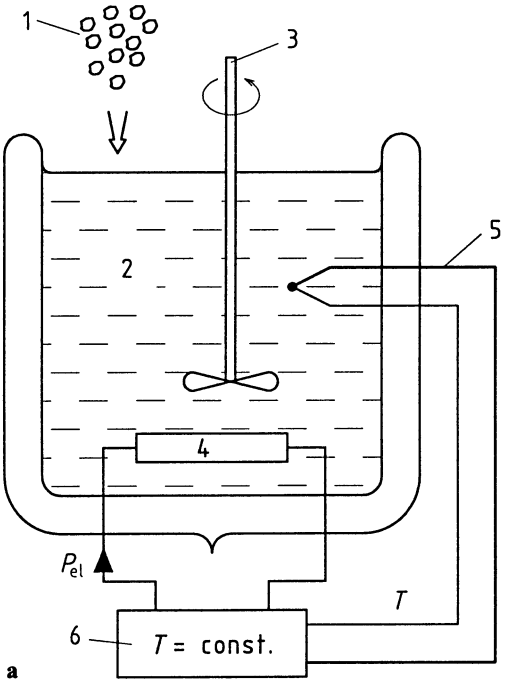

a

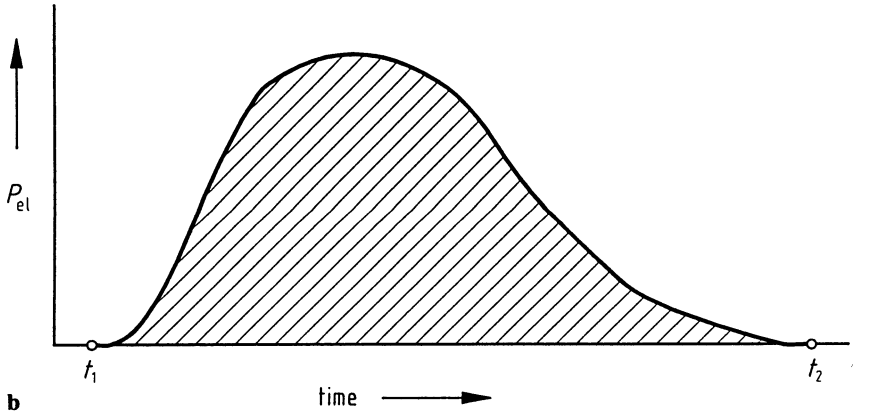

b

Fig. A 2.2. **a** "Compensation calorimeter" (Brönsted, 1906),
b Measured curve (acc. to Hemminger, 1994).
1 sample (salt), 2 water, 3 stirrer, 4 electric heater, 5 temperature sensor, 6 controller, P_{el} electric heating power.
The area below the measured curve $P_{el}(t)$ corresponds to the compensation heat and (at constant temperature) also to the endothermic heat of solution Q of the sample substance, which has been searched:

$$Q = \int_{t_1}^{t_2} P_{el}(t)\, dt$$

of exothermic effects cannot be measured with sufficient accuracy, the calorimeter substance (e.g. water) is generally cooled with constant Peltier power and at the same time heated with equally high Joule's heat (controlled). To compensate an endothermic effect, the heating power is increased in order to keep the temperature of the calorimeter substance constant. When an exothermic effect is to be compensated, the heating power is decreased with the Peltier power remaining unchanged (see for example Christensen et al., 1968). These calorimeters do not attain the strictly isothermal state of phase transition calorimeters, as the difference between actual and set temperature value must be non-zero in order that the electrical power control is activated. In addition, temperature control is delayed by the heat transfer processes, and it is very difficult to obtain spatially homogeneous temperature fields by electric heating.

The advantages of these quasi-isothermal calorimeters consist in the simple and very precise measurement of the electric compensation energy and the possibility of using highly sensitive sensors to measure temperature changes; these sensors must not, however, be calibrated.

This is done in that a sensitive thermometer activates the compensation control circuit so that, if possible, no temperature change due to reaction heat takes plase.

3rd example: "Adiabatic scanning calorimeter"

---

1. Compensation of the heat to be measured with the aid of electric energy
2. Adiabatic scanning
3. Single calorimeter

In these calorimeters (Fig. A 2.3), the temperature program is preset. So much electrical heating power is supplied to the sample as is necessary to comply with the given temperature program. (In practical application, the electrical heating power required for sample heating is often preset and the resulting heating rate measured.) Heat losses are minimized by adapting the temperature of the surroundings as well as possible to the temperature of the sample (or sample container) (adiabacy). Calorimeters of this type allow the heat capacity to be measured with high accuracy (uncertainty $\leq 0.1\%$) (cf. 4th example of heat-accumulating calorimeters).

The following is valid for the heat capacity $C(T)$:

$$C(T) = \frac{P_{el,1} - P_{el,2}}{\dfrac{dT}{dt}} \qquad (dT/dt\text{: preset})$$

or

$$C(T) = P_{el}\left(\frac{1}{\left(\dfrac{dT}{dt}\right)_2} - \frac{1}{\left(\dfrac{dT}{dt}\right)_1}\right) \qquad (P_{el}\text{: preset})$$

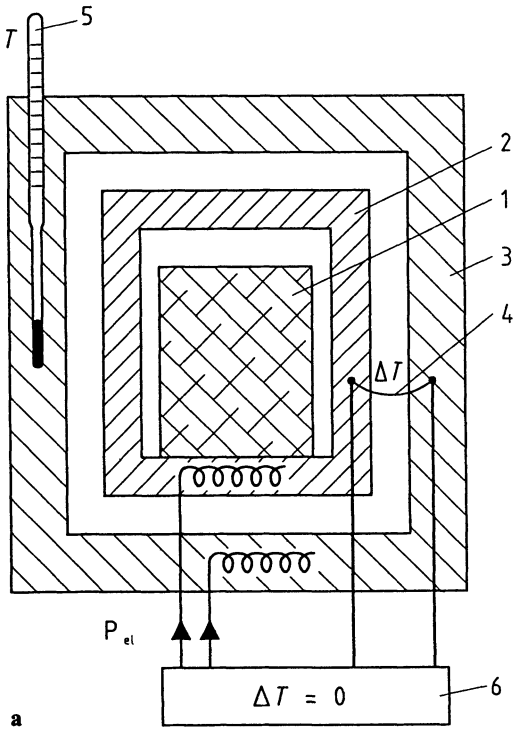

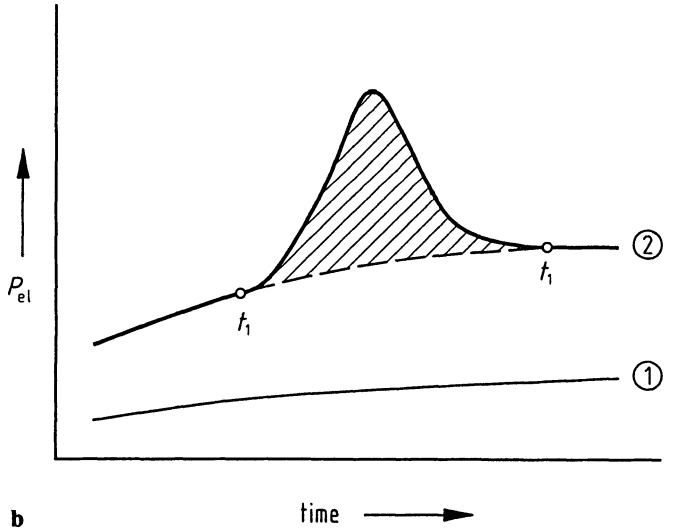

Fig. A 2.3. **a** "Adiabatic scanning calorimeter".
1 sample, 2 sample furnace, 3 heatable (adiabatic) shield, 4 temperature difference sensor, 5 temperature sensor, 6 programmer and controller, P_{el} electrical heating power. When there is a variation of the temperature with time $T(t)$, $P_{el}(t)$ is controlled so that $(dT/dt)_1 = (dT/dt)_2$ (outside the peak),
b Measured curve (acc. to Hemminger, 1994). ① curve measured with the calorimeter empty, ② curve measured with the sample placed in the calorimeter, sample transition between t_1 and t_2 (peak)

① run with the calorimeter empty
② run with the sample placed in the calorimeter

$P_{el} = i \cdot U$	electrical heating power
dT/dt	heating rate at the respective moment
$C(T)$	comprises the heat capacities of sample and container. The heat capacity of the empty container is determined by separate measurement.

When in a 1st order transition (e.g. melting of a pure metal) the sample temperature remains constant during transition in spite of the fact that heating power is continued to be supplied, the heat of transition is directly determined from the integral of the heating power over the transition time ($Q_{trs} = \int i(t) \cdot U(t)\, dt$).

The adiabatic shield guarantees quasi-isothermal conditions while the heat to be determined is compensated with the aid of electric energy.

Calorimeters of this type are used for the accurate, absolute and direct measurement of heat capacities and heats of transition (cf. for example Nölting, 1985; Kagan, 1984; an extension to a low-temperature turn system has been described by Rahm, Gmelin, 1992).

4th example: "Power compensation DSC"

---

1. Compensation of the heat to be measured with the aid of electric energy
2. Isoperibol scanning
3. Twin calorimeter

The temperature of the sample surroundings remains constant (isoperibol). The calorimeter (Figs. 2.4, 2.5) comprises two identical measuring systems (twin principle), one containing the sample, the other the reference sample. The temperature difference between the two systems is measured. In 1st approximation, disturbances from the surroundings have the same effect on both measuring systems and therefore cancel out with respect to the temperature difference. The individual sample supports (microfurnaces) are heated separately so that they comply with the given temperature-time program. When there is ideal thermal symmetry between the two measuring systems, the same heating power is required for sample and reference sample. When additional heat is released or consumed during sample transition (exothermic or endothermic process), the sample's heating power is regulated by means of a proportional controller so that the electric heat supplied is decreased or increased by just the amount as has been generated or consumed during the exothermic or endothermic transition process. The measured signal is the temperature difference ΔT (deviation from the set value) to which the compensation heating power ΔP is proportional: $\Delta P \sim \Delta T$. Calorimeters of this type ("power compensation DSC" or "differential power compensation scanning calorimeter, DPSC" or "dynamic power difference calorimeter") are widely used (cf. for example Watson et al., 1964; Hemminger, Höhne, 1984). They are discussed at full length in Sects. 2.2 and 3.2 of this book.

Heat-accumulating Calorimeters

In the case of this calorimetric method, the effect of the heat to be measured is not "suppressed" by compensation but leads to a temperature change in the sample substance and a "calorimeter substance" with which the heat to be determined is exchanged. This temperature change is measured. When the change is not too great, it is proportional to the amount of heat exchanged. The proportionality factor must be determined by calibration with a known amount of heat.

5th example: "Drop calorimeter"

---

1. Measurement of the temperature change of a substance due to the heat to be measured
2. Isoperibol
3. Single calorimeter

The temperature of the surroundings is kept constant with the aid of a thermostat ("isoperibol": uniform surroundings). The heat Q to be measured is exchanged with the "calorimeter substance" and the temperature change $\Delta T(t)$ is measured (Fig. A 2.4).

The following is valid: $Q = C_{cal} \cdot \Delta T^*$ (cf Fig. A 2.4c).

The proportionality factor C_{cal} is the heat capacity of the calorimeter substance (a liquid in Fig. A 2.4a) plus that of the other calorimeter components (stirrer, thermometer, etc.), which cannot be exactly defined. This factor is determined by calibration with electric energy (Joule's heat). As soon as there is a temperature difference between calorimeter substance and surroundings, heat is exchanged. This exchange must depend only on this temperature difference and must be reduced as far as possible by appropriate measures (Dewar vessel, radiation shields etc.). Otherwise, it cannot be determined by calibration and represents an error source. In order to guarantee strict repeatability of the heat exchange, ΔT must amount to only a few Kelvin. Since the temperature change of the calorimeter substance and the unavoidable heat exchange with the surroundings take place simultaneously, the temperature difference ΔT^* used to calculate Q must be determined according to defined rules (e.g. International Standard ISO 1928-1976 (E); Rossini, 1956; Gunn, 1971; Oetting, 1970; Sunner, Månsson, 1979) from the shape of the $\Delta T(t)$ curve measured before and after the sample has been placed into the calorimeter (cf. also 6th example). Simple drop calorimeters serve to measure mean heat capacities (temperature of the sample at the moment of its being placed into the calorimeter: up to about 500 °C; sample mass between 10 and 100 g).

In "aneroid" drop calorimeters (Fig. A 2.4b), the calorimeter substance is a solid body of good thermal conductivity. The advantage over calorimeters filled with liquid consists in that samples at high temperature (up to about 2000 °C) can be dropped without the risk of evaporation or splashing.

Other examples of calorimeters of this class are instruments in which the sample placed into it (solid body, liquid, gas) reacts with the calorimeter substance; this results in heat of reaction being released.

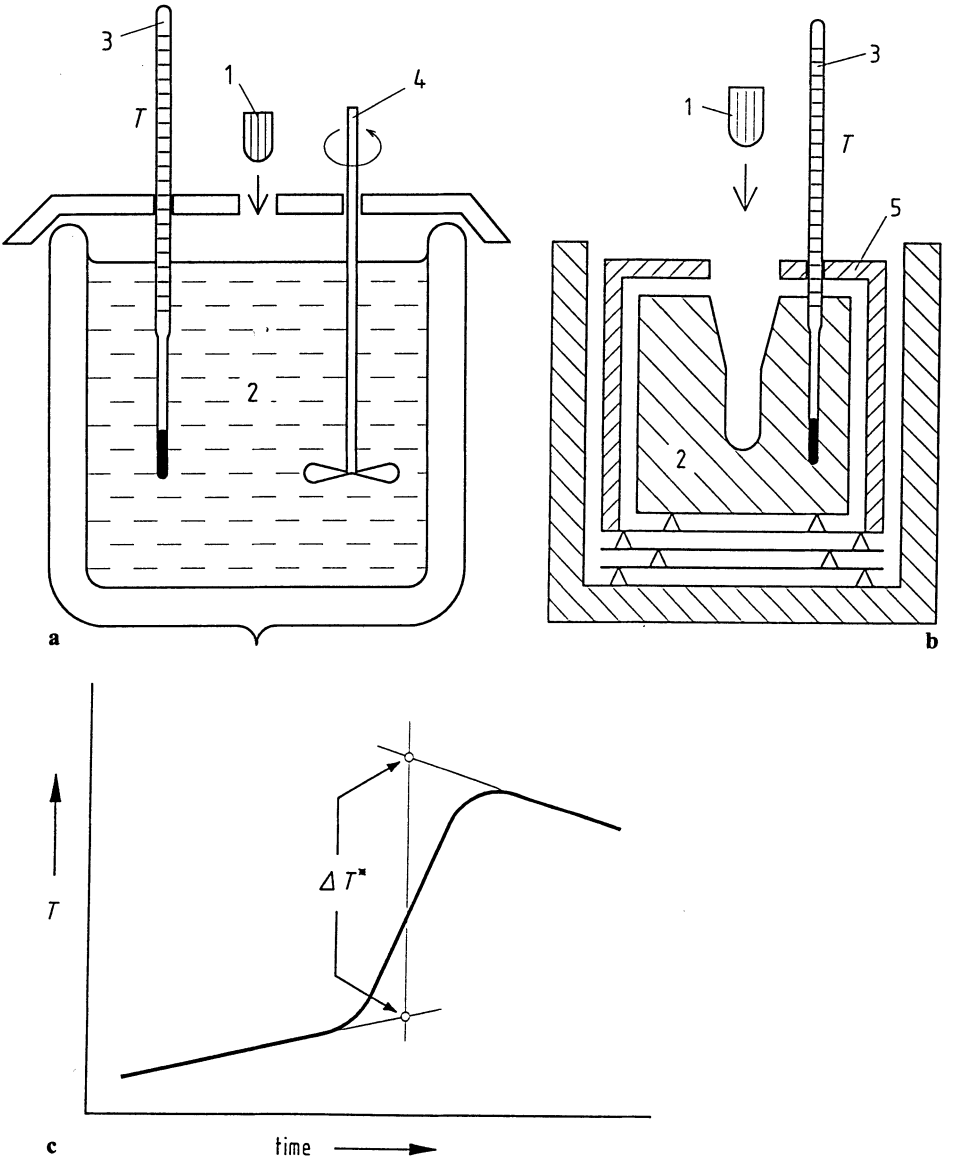

Fig. A 2.4. "Drop calorimeter" **a** with liquid, **b** with aneroid calorimeter substance (in isoperibol mode of operation) and **c** measured curve (acc. to Hemminger, 1994).
1 sample, 2 calorimeter substance: (**a**) liquid, (**b**) solid, 3 temperature sensor, 4 stirrer, 5 radiation shields.
The temperature change ΔT^* of the calorimeter substance has to be determined from the measured curve according to defined rules, taking the "preperiod" and the "postperiod" into account

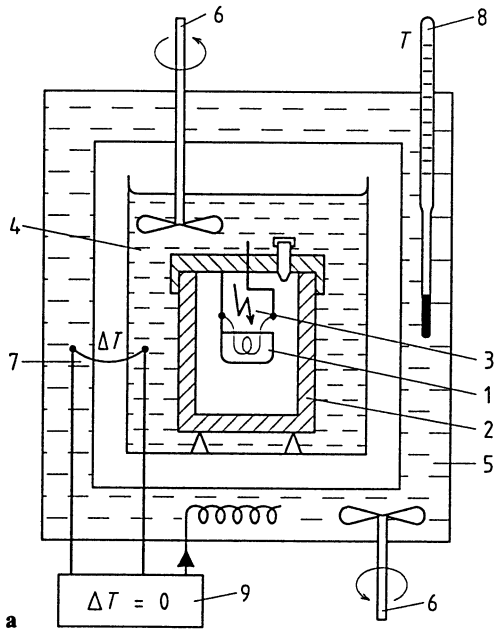

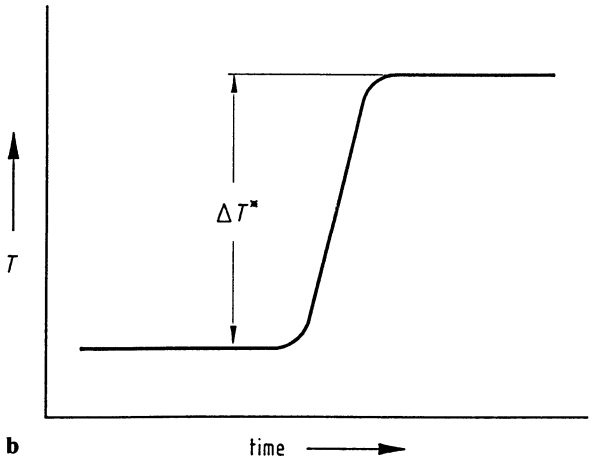

Fig. A 2.5. **a** Adiabatic "bomb calorimeter",
b Measured curve (acc. to Hemminger, 1994).
1 sample in combustion pan, 2 vessel, 3 ignition device (electrodes with heating filament), 4 calorimeter substance (water), 5 adiabatic jacket, 6 stirrer, 7 temperature difference sensor, 8 temperature sensor, 9 controller

6th example: "Adiabatic bomb calorimeter"

1. Measurement of the temperature change of a substance due to the heat to be measured
2. Adiabatic
3. Single calorimeter

In the case of the adiabatic bomb calorimeter (Fig. A 2.5), the "combustion bomb" which is (usually) filled with oxygen at high pressure immerses in water (calorimeter substance). The water temperature is continually measured before and after the electric ignition. With the aid of a controller, the temperature of the surroundings is always adapted to this temperature (adiabatic jacket). The temperature change with time in the surroundings serves as measurement signal; it is determined from the drift of the measured curve before the ignition (preperiod) and after the ignition (postperiod) (as with the "drop calorimeter", see 5th example).

Bomb calorimeters of this type (usually automated) are widely used to measure the calorific value of solids or liquids under standardized conditions. In general, they are calibrated with benzoic acid. Their uncertainty of measurement lies in the per mil range. (There are also "dry" bomb calorimeters, in which the temperature change of the combustion vessel itself (of the bomb) is measured; bomb calorimeters with isoperibol surroundings are also used.) For a detailed representation of bomb calorimetry, see Rossini, 1956; Skinner, 1962; Sunner, Månsson, 1979.

7th example: "Flow calorimeter"

1. Measurement of the temperature change of a substance due to the heat to be measured
2. Isoperibol
3. Single calorimeter (also designed as "twin")

In the case of the so-called "gas calorimeters", the heat to be measured is transferred, if possible completely, to a flowing medium (Fig. A 2.6). The temperature difference between the medium flowing in and the medium flowing out is proportional to the heat transferred. Calorimeters of this type are used to determine the calorific value of fuel gases; they are calibrated with gases of known calorific value (e.g. methane) so that the specific heat capacity of the heat-conveying medium must not be known. If an electric heater is used instead of the burner, the specific heat capacity of the heat-conveying medium can in principle be measured as well (cf. Hemminger, 1988).

In biology, biochemistry and chemistry, flow calorimeters with liquids serve to measure the heat development of microorganisms in certain nutrient solutions, or they are used to measure reaction heats. Two reacting solutions are, for example, mixed in a reaction tube (Fig. A 2.7). The uniform temperature of the reacting agents is measured before they are mixed and then at a point at which the reaction in the flowing liquid has come to an end. The temperature difference is a measure of the reaction heat. The calorimeter must be calibrated, either with the aid of known reaction heats of liquids or with an electric heater installed in the reaction tube.

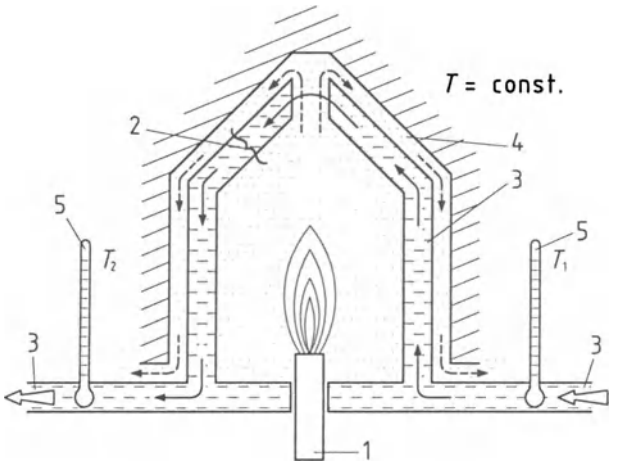

Fig. A 2.6. "Gas calorimeter".
1 burner in which the gas to be measured is burnt, 2 heat exchanger, 3 "heat conveying medium" (e.g. air or water), 4 combustion gases, 5 temperature sensor.
Inside the heat exchanger, the hot combustion gases convey their heat to the heat conveying medium whose temperature increase $T_2 - T_1$ is measured. The "calorific value" (the combustion heat) is proportional to $T_2 - T_1$

A sophisticated example of a flow calorimeter with stimulated cardiac muscle developing heat in the perfused tube has been described by Daut et al., 1991. (Flow calorimeters are also designed as twin calorimeters to cancel out the influence of the isoperibol surroundings (heat leaks)).

8th example: "Adiabatic calorimeter"

---

1. Measurement of the temperature change of a substance due to the supply of a known amount of heat
2. Adiabatic
3. Single calorimeter

This type of calorimeter (Fig. A 2.8) is not designed to measure an unknown heat; instead, a well-known, electrically generated heat $Q = W_{el}$ serves to change the sample temperature by ΔT. The temperature of the surroundings (adiabatic jacket) is adapted to the measurement temperature with high accuracy in order to avoid any heat exchange with the surroundings. Calorimeters of this type are used to determine the phenomenological coefficient of the heat supplied, Q, and the temperature change, ΔT, of a substance (at constant pressure): the heat capacity $C_p(T)$. The following is valid:

$$C_p = Q/\Delta T$$

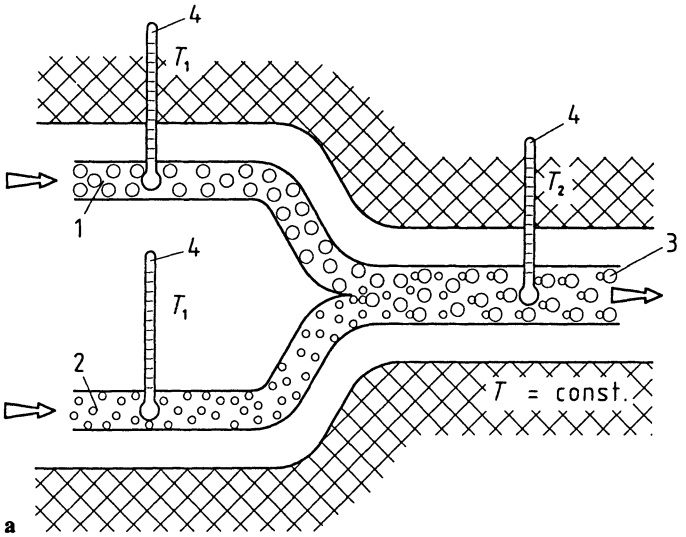

a

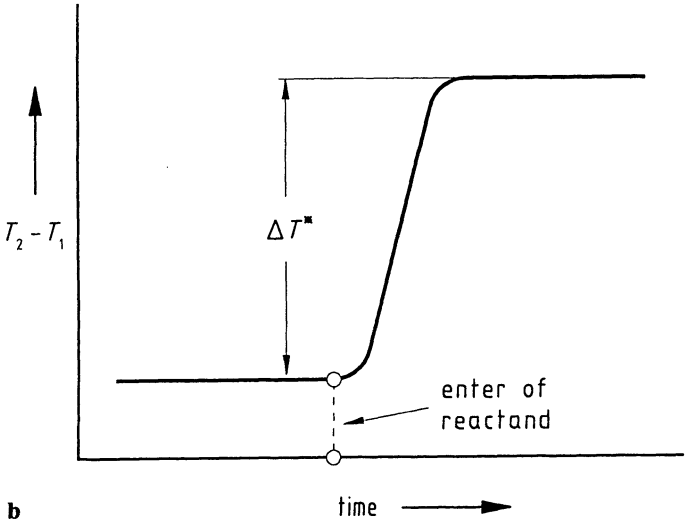

b

Fig. A 2.7. **a** "Flow-mix calorimeter",
b Measured curve.
1, 2 reactants, 3 reaction product, 4 temperature sensor.
As in the case of the "drop calorimeter", the temperature change ΔT^* required to determine the mixing or reaction heat is obtained from the pre- and postperiod (affected by a drift) of the measured curve $(T_2 - T_1)(t)$

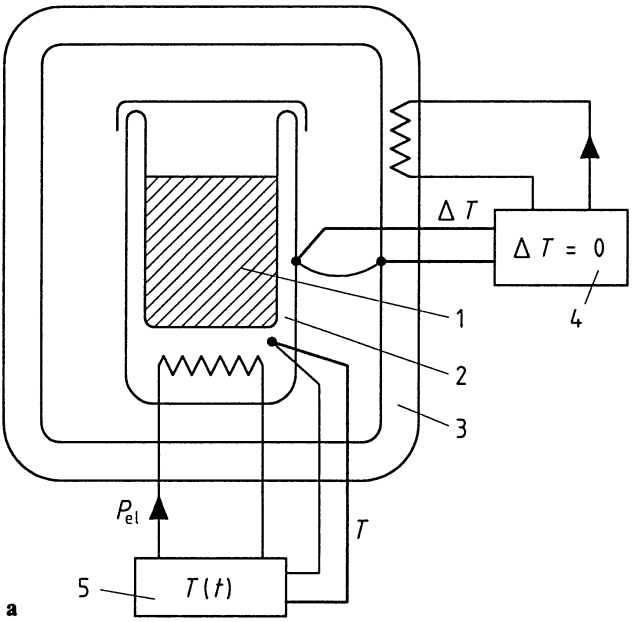

a

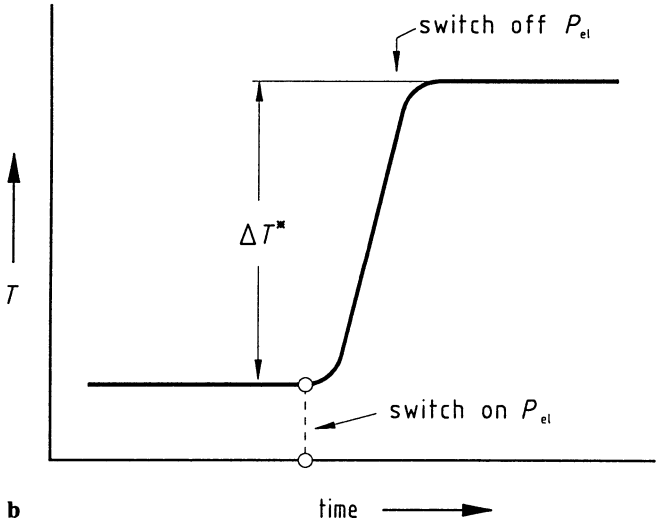

b

Fig. A 2.8. **a** "Adiabatic calorimeter",
b Measured curve (acc. to Hemminger, 1994).
1 sample, 2 heatable sample container, 3 adiabatic jacket, 4 controller, 5 programmer and controller, P_{el} electric heating power.
When the constant measurement temperature T is adjusted, the electric heating energy W_{el} is supplied to the sample, increasing the sample temperature by ΔT^*

Calorimeters of this type allow the specific heat capacity and latent heats to be measured with the greatest possible accuracy (Gmelin, Rödhammer, 1981; Jakobi et al., 1993).

Knowledge of the heat capacity and its temperature dependence is of utmost importance in solid state physics and thermodynamics. In practical application, ΔT is kept as small as possible in order to determine the temperature dependence of C_p as precisely as possible and to avoid errors due to inhomogeneous temperature fields. The limits are determined by the noise and the uncertainty of measurement of the temperature sensors (cf. Kagan, 1984; Zhiying, 1986).

Heat-exchanging Calorimeters

In calorimeters which measure the temperature change of the calorimeter substance, i. e. heat-accumulating calorimeters (e. g. drop calorimeters, bomb calorimeters), the heat exchange with the isoperibol surroundings is kept low to make the measured signal ΔT as great as possible. In the calorimeters referred to in this section, a defined exchange of the heat to be measured with the surroundings is deliberately aimed at, the reason for this being that the measured signal which describes the intensity of the exchange is then proportional to a heat flow rate Φ and not to a heat. This allows time dependences of a transition to be observed on the basis of the $\Phi(t)$ curve (the power compensation DSC also offers this possibility).

The twin design allows disturbances from the surroundings, which affect both systems in the same way, to be eliminated by taking only the difference between the individual measurement signals into account (Differential Scanning Calorimeter: DSC).

9th Example: "Heat flux differential scanning calorimeter"

---

1. Measurement of the exchange of the heat to be measured between sample and surroundings via a heat flow rate
2. Scanning of surroundings
3. Twin calorimeter

DSC with Disk-type Measuring System (cf. Sect. 2.1.1)

A metal, ceramic or quartz glass disk with the sample and the reference sample (or the pans) positioned on it symmetrical to the centre, is placed into a furnace (Fig. 2.1 a). Heat exchange between furnace ("surroundings") and samples takes place by heat conduction, radiation and convection. Strict repeatability of this heat exchange as a function of the temperature (with the atmosphere remaining unchanged) must be ensured. This is why a solid heat-conducting disk is used which guarantees that the properties of the measuring system dominate. As a result, the different characteristics of the individual samples contribute less strongly to the kind of heat exchange than in the case of the DTA (the measurement signal itself

must, of course, reflect the sample properties). The signal ΔT is measured on the solid heat conductor (disk) between the supports for sample and reference sample ($\Delta T = T_S - T_R$).

DSC with Cylinder-type Measuring System (cf. Sect. 2.1.2)

In another type of heat flux DSC, the two cylindrical containers for sample and reference sample are connected with the furnace ("surroundings") by one thermopile each (Fig. 2.2). The heat from the furnace to the samples preferably flows through the thermocouple wires which are at the same time the dominant heat conduction paths and the temperature difference sensors. When a differential connection is provided between the outputs of both thermopiles, the measured signal (ΔT) is proportional to the difference between the heat flow rates from the furnace to the sample ($\Delta T_{FS} \sim \Phi_{FS}$) and from the furnace to the reference sample ($\Delta T_{FR} \sim \Phi_{FR}$).

Survey of the classification of calorimeters

PRINCIPLE Of MEASUREMENT	MODE OF OPERATION	CONSTRUCTION
Measurement of the energy required to compensate the heat to be measured *(heat-compensating calorimeters)*	Static: isothermal isoperibol adiabatic	Single calorimeters
Measurement of the temperature change of the calorimeter substance measured *(heat-accumulating calorimeters)*	Dynamic: scanning of surroundings, isoperibol scanning adiabatic scanning	Twin (differential) calorimeters
Measurement of the heat flow rate between calorimeter substance and surroundings due to the heat to be measured *(heat-exchanging calorimeters)*		

References

Agrawal AJ (1989) Pol Sci: Part B, Pol Phys 27:1449
Aras L, Richardson MJ (1989) Polymer 30:2246
ASTM E 967-83 (1984) Standard Practice for Temperature Calibration of Differential Scanning Calorimeters and Differential Thermal Analyzers; Annual Book of ASTM Standards, vol 14.02:815
ASTM E 794-85 (1986) Standard Test Method for Melting and Crystallization Temperatures by Thermal Analysis; Annual Book of ASTM Standards, vol 14.02:703–707
Aston JG, Fink HL, Schumann SC (1943) J Amer Chem Soc 65:341–346
Bader RG, Schawe IEK, Höhne GWH (1993) Thermochim Acta 229:85
Barton JM (1980) Polymer 21:603–606
Barton JM (1985) In: Dusek K (ed) Advances in Polymer Sciences, Springer, Berlin, Heidelberg, New York: 111–154
Batzer H, Kreibich UT (1982) Angew Makromol Chem 105:113–130
Becker R (1976) Z phys Chem 257:667–677
Becker R (1977) Z phys Chem 258:953–966
Becker R (1978) Faserforschung und Textiltechnik 29:361–385
Beezer AE (1980) (ed) Biological microcalorimetry. Academic Press, London
Beford RE, Bonnier G, Maas H, Pavese F (1984) Metrologia 20:145–155
Blankenhorn K, Höhne GWH (1991) Thermochim Acta 187:219–224
Borchardt HJ, Daniels F (1957) J Am Chem Soc 79:41–46
Bouwstra JA, de Leevv VV, van Miltenberg JC (1985) J Chem Thermodyn 17:685–695
Bracewell RM (1965) The Fourier transform and its applications. McGraw-Hill, New York
Braun D, Kohl PR, Hellmann GP (1988) Makromol Chem 189:1671–1679
Brekner MJ, Schneider HA, Cantow HJ (1988) Polymer 29:78–85
Breuer K-H, Eysel W (1982) Thermochim Acta 57:317–329
Brezesinski G, Dörfler HD (1983) Colloid & Polymer 261:423–426
Brönsted JN (1906) Z Phys Chem 56:663–665
Bros JP (1989) J Less Common Metals 154:9–30
Brown WE, Dollimore D, Gallway AK (1980) In: Bamford CH, Tipper CF (eds) Comprehensive chemical kinetics, vol 2, Reactions in the solid state. Elsevier, Amsterdam
Bruzzone G (1985) Thermochim Acta 96:239–258
Bunsen RW (1870) Ann Phys 141:1–14
Calvet E (1948) CR hebd 226:1702–1704
Cammenga HK, Eysel W, Gmelin E, Hemminger W, Höhne GWH, Sarge SM (1993) Thermochim Acta 219:333–342
Chang SS (1988) Polym Commun 29:33–35
Chee KK (1985) Eur Polym J 21:29–31
Chekhovskoi VYa (1984) In: Maglic KD, Cezairliyan A, Peletsky VE (eds) Compendium of Thermophysical Property Measurement Methods 1. Plenum, New York
Christensen JJ, Johnston HD, Izatt RM (1968) Rev Sci Instrum 39:1356–1359

Chung TS (1984) J Appl Pol Sci 29:4403–4406
Couchman PR, Karasz FE (1978) Macromolecules 11:117–119
Cowie JMG, Ferguson R (1986) Polym Commun 27:258–260
CRC Handbook of Chemistry and Physics (1990–1991) 71st edn, CRC Press
Daut J, Groß T, Elzinga G (1991) Thermochim Acta 193:269–280
de Bolt MA, Easteal AJ, Macedo PB, Moynihan CT (1976) J Am Chem Soc 59:16–21
Doelman A, Gregges AR, Barrall EM (1977) In: Porter RS, Johnson JF (eds) Analytical Calorimetry, vol 4. Plenum, New York
Domen SR (1987) In: Kase KR, Bjärngard BE, Attix FH (eds) The dosimetry of ionizing radiation, vol II. Academic Press, Orlando, Florida
Doyle CD (1961) J Appl Pol Sci 5:285–292
Duncan JC, van de Welde JG, Wetton RE (1991) Kautschuk und Gummi 44:768–770
Eligehausen S, Sarge SM, Öhlschläger G, Cammenga HK (1989) J Therm Anal 35:515–526
Ellerstein SM (1968) In: Porter RS, Johnson JF (eds) Analytical Calorimetry, Vol 1. Plenum, New York
EN 45000 Series (European Standards)
EN 45001 (European Standards) General criteria for the operation of testing laboratories
Fan M, Müller F, Wilsmann W (1993) Thermochim Acta 224:19–32
Flammersheim HJ (1981) Wiss Beitr, Friedrich Schiller Universität Jena, 160–164
Flammersheim HJ (1988) J Therm Anal 33:55–65
Flammersheim HJ, Klemm E (1985) Acta Polymerica 36:443–446
Flammersheim HJ, Eckardt N, Kunze W (1991) Thermochim Acta 187:269–274
Flammersheim HJ, Eckardt N, Opfermann J (1993) Thermochim Acta 229:281–287
Flynn JH (1974) Thermochim Acta 8:69–81
Flynn JH (1990) Therm Anal 36:1579–1593
Flynn JH (1993) Thermochim Acta 217:129–149
Fox TG, Flory PJ (1950) J Appl Phys 21:581–590
Freeman ES, Carroll B (1958) J Phys Chem 62:394–397
Gilmour IW, Hay JN (1977) Polymer 18:281–285
Ginnings DC, Corruccini RJ (1947) Res Natl Bur Stand 38:538–591
Gmelin E (1987) Thermochim Acta 110:183–208
Gmelin E, Rödhammer P (1981) J Phys E: Sci Instrum 14:223–228
Godovsky YuK, Höhne GWH (eds) (1994) Special Issue: Deformation Calorimetry of Polymers; Thermochim Acta 247, 1:1–128
Gray AP (1968) In: Porter RS, Johnson JF (eds) Analytical Calorimetry, Vol 1 Plenum Press
Grewer T (1987) Thermochim Acta 119:1–15
Grewer T, Steinbach J (eds) (1993) Special Issue: Safety Techniques; Thermochim Acta 225, 2:143–301
Grønvold F (1967) Acta Chem Scand 21:1695–1715
Grønvold F (1993) J Chem Thermodynamics 25:1133–1144
Gunn SR (1971) J Chem Thermodynamics 3:19–34
Hale A, Macosko C, Bair HE (1991) Macromolecules 24:2610–2621
Hanitzsch E (1991) Thermochim Acta 187:275–281
Hay JN (1992) Progr Colloid Polym Sci 87:74–77
Hemminger W (ed) (1988) PTB Bericht PTB-W-37, Wirtschaftsverlag, Bremerhaven
Hemminger W (1994) Chapter 2 "Calorimetric Methods" in Calorimetry and Thermal Analysis of Polymers (Mathot VBF, ed), Hanser, Munich
Hemminger W, Schönborn K-H (1982) In: Miller B (ed) Thermal Analysis, Proc 7th ICTA, Vol 1, Wiley, New York 156–162
Hemminger W, Höhne GWH (1984) Calorimetry-Fundamentals and Practice; VCH Verlag, Weinheim

Hemminger WF, Cammenga HK (1989) Methoden der Thermischen Analyse. Springer, Berlin, Heidelberg, New York
Hemminger W, Raetz K (1989) PTB-Mitteilungen 99:83–88
Hemminger W, Sarge StM (1991) J Therm Anal 37:1455–1477
Hentze G (1984) Thermochim Acta 72:127–138
Hentze G, Krien G (1986) Thermochim Acta 107:61–74
Heublein G, Hallpap P, Hauptmann S, Mann G (1984) Einführung in die Reaktionstheorie. VEB Deutscher Verlag für Grundstoffindustrie, Leipzig
Hoff H (1991) Thermochim Acta 187:293–307
Höhne GWH (1983) Thermochim Acta 69:175–197
Höhne GWH, Glöggler E (1989) Thermochim Acta 151:295–304
Höhne GWH, Cammenga HK, Eysel W, Gmelin E, Hemminger W (1990) Thermochim Acta 160:1–12
Höhne GWH, Schawe JEK (1993) Thermochim Acta 229:27
Höhne GWH, Schawe JEK, Schick C (1993) Thermochim Acta 221:129–137
Horie K, Hiura H, Sawada M, Mita I, Kambe H (1970) J Pol Sci A1 8:1353–1372
Huguenin FGAE, Klein MT (1985) Ind Eng Chem, Prod Res Dev 24:166–171
Hutchinson JM (1990) J Pol Sci, Part B, Pol Phys 28:2127–2161
Hutchinson JM (1992) Progr Colloid Polym Sci 87:69–73
Hutchinson JM, Ruddy M (1988) J Polym Sci, Part B, Pol Phys 26, 2341–2366
Hutchinson JM, Ruddy M, Wilson MR (1988) Polymer 29:152–159
Hyde CG, Jones MW (1960) Gas Calorimetry, 2nd ed; Ernest Benn, London
International Vocabulary of Basic and General Terms in Metrology (1st ed 1984, 2nd ed 1994) Beuth, Berlin
IPTS-68 (1976) The International Practical Temperature Scale of 1968, Amended Edition of 1975; Metrologia 12:7–17
ITS-90: The International Temperature Scale of 1990 (1990) Metrologia 27:3–10
Jakobi R, Gmelin E, Ripka K (1993) J Therm Anal 40; Proc 10th ICTA (Morgan DJ, ed), 871–876, John Wiley, Chichester and Akadémiai Kiadó, Budapest
Jin Y, Wunderling B (1993) Thermochim Acta 226:155–161
Jorda R, Wilkes GL (1988) Polym Bull 20:479–485
Jung DH, Known TW, Bae DJ, Moon IK, Jeong YH (1992) Sci Technol 3:475
Kagan DN (1984) In: Maglic KD, Cezairliyan A, Peletsky VE (eds) Compendium of Thermophysical Property Measurement Methods 1. Plenum, New York
Kalachandra S, Turner DT (1987) J Pol Sci, Part B, Pol Phys 25:1971–1979
Keenan MR (1987) J Appl Pol Sci 33:1725–1734
Kemp RB (1993) Thermochim Acta 219:17–41
Kilian HG, Höhne GWH (1983) Thermochim Acta 69:199–219
Klee J, Hörhold HH, Flammersheim HJ (1990) Angew Makromol Chem 178:63–83
Klemm E, Flammersheim HJ, Märtin R, Hörhold HH (1985) Angew Makromol Chem 135:131–138
Kovacs AJ (1963) Fortschr Hochpol Forsch 3, 394–507
Kovacs AJ, Aklonis JJ, Hutchinson JM, Ramos AR (1979) J Polym Phys, Pol Phys Edn 17:1097–1162
Kovacs AJ, Hutchinson JM (1979) J Pol Sci, Pol Phys Edn 17:2031–2058
Lakshmikumar ST, Gopal ESR (1981) J Indian Inst Sci 63 (A):277–329
Lamprecht I, Schaarschmidt B (eds) (1977) Applications of Calorimetry in Life Sciences. de Gruyter, Berlin
Lamprecht I, Hemminger W, Höhne GWH (eds) (1991) Special Issue: Calorimetry in the Biological Sciences; Thermochim Acta 193:1–452
Lau SV, Suzuki H, Wunderlich B (1984) J Pol Sci Pol Phys Ed 22, 379–405

Lavoisier AL, de Laplace PS (1784) Histoire de L'Académie Royale des Sciences, Année 1780:355
Löblich K-R (1985a) Thermochim Acta 83:99–106
Löblich K-R (1986b) Thermochim Acta 85:263–266
Löblich K-R (1994) Thermochim Acta 231:7–20
Maglic KD, Cezairliyan A, Peletsky VE (eds) (1984) Compendium of Thermophysical Property Measurement Methods 1. Plenum, New York
Malavašič T, Osredkar U, Anzur I, Vizovisek I (1986) J Macromol Sci Chem A23:853–860
Marsh KN (ed) (1987) Recommended Reference Materials for the Realization of Physiochemical Properties. Blackwell Scientific Publications, Oxford
Mathot VBF (1984) Polymer 25:579–599
Mathot VBF, Pijpers MFJ (1983) J Thermal Anal 28:349–358
Mathot VBF, Pijpers MFJ (1989) Thermochim Acta 151:241–259
Mathot VBF (ed) (1994a) Calorimetry and Thermal Analysis of Polymers. Hanser, Munich
Mathot VBF (ed) (1994b) Special Issue: Thermal Analysis and Calorimetry in Polymer Physics; Thermochim Acta 238:321–415
Matuschek G, Ohrbach K-H, Kettrup A (1991) Thermochim Acta 190:111–123
Matuschek G, Ohrbach K-H, Kettrup A (1993) J Therm Anal 39:1141–1155
Mayorga OL, Navarro Rascon A, Freire E (1994) Thermochim Acta 238:309–319
Mijovic J, Lee CH (1989) J Appl Pol Sci 37:889–900
Min BG, Stachurski ZH, Hodgkin JH (1993) Polymer 34:4908–4912
Montserrat S (1992) J Appl Pol Sci 44:545–554
Montserrat-Ribas S (1992) Progr Colloid Polym Sci 87:78–82
Moratzky TH, Burkhardt G, Weyel W, Wegener G (1993) Thermochim Acta 229:193–204
Moynihan CT, Easteal AJ, de Bolt MA, Tucker J (1976) Am Ceram Soc 59:12–16 and 16–20
Narayanaswamy DS (1971) J Am Ceram Soc 54:491–498
Nölting J (1985) Thermochim Acta 94:1–15
O'Neill MJ (1964) Anal Chem 36:1238
Oetting FL (1970) Chem Thermodynamics 2:727–739
Ohrbach KH, Matuschek G, Kettrup A (1987) Thermochim Acta 121:87–96
Okui N (1990) Polymer 31:92–94
Opfermann J, Wilke G, Jung J, Ludwig W, Hagen S, Gebhardt M, Kaisersberger E (1991) Therm Analysenverf in Ind u Forschung. Wiss Z FSU Jena 51–68
Opfermann J (1992) Technical report concerning the peak separation. Netzsch-Gerätebau-GmbH, Selb, Germany
Oscarson JL, Izatt RM (1992) In: Rossiter BW, Baetzold RC (eds) Physical Methods of Chemistry, 2nd Eds. Wiley, New York
Parrish WmR (1986) Fluid Phase Equilibria 29:177–192
Pérez J, Cavaille JY, Calleja RD, Ribbeles JLG, Pradas MM, Greus AR (1991) Makromol Chem 192:2141–2161
Perrenot R, de Vallière P, Widmann G (1992) Therm Anal 38:381–390
Petit J-L, Sicard L, Eyraud L (1961) CR hebd 252:1740–1742
Petrie SEB (1972) J Pol Sci Part A-2 10:1255–1272
Peyser P (1983) J Macromol Sci-Phys, B22:185–196
Podešva J, Procházka O (1979) Makromol Chem 180:2525–2530
Poeßnecker W (1990) J Therm Anal 36:1123–1139
Poeßnecker W (1993) Thermochim Acta 229:97–109
Pomposo JA, Eguiazabal I, Calahorra E, Cortázar M (1993) Polymer 34:94–102
Preston-Thomas H (1976) Metrologia 12:7–17
Preston-Thomas H (1990) Metrologia 27:3–10
Privalov PL, Plotnikov VV (1989) Thermochim Acta 139:257–277

Raetz K (1989) Thermochim Acta 151:323–331
Rahm V, Gmelin E (1992) J Therm Anal 38:335–344
Rai US, Shekhar H (1993) J Therm Anal 39:415–428
Ramos AR, Hutchinson JM, Kovacs AJ (1984) J Pol Sci, Pol Phys, Edn 22:1655–1695
Reading M, Luget A, Wilson R (1994) Thermochim Acta 238:295–307
Regenass W (1985) Thermochim Acta 95:351–368
Reichelt J, Hemminger W (1983) Thermochim Acta 69:59–70
Richardson MJ (1976) Plastics and Rubber, Materials and Applications 1:162–167
Richardson MJ (1989) In: Booth C, Price C (eds) Comprehensive Polymer Science, Vol I, Pergamon, Oxford: 867–901
Richardson MJ (1992a) In: Maglic KD, Cezairliyan A and Peletsky VE (eds) Compendium of Thermophysical Property Measurement Methods 2. Plenum, New York 529
Richardson MJ (1992b) Pure Appl Chem 64:1790–1800
Richardson MJ (1993) Thermochim Acta 229:1–14
Richardson MJ, Savill NG (1975a) Polymer 16:753–757
Richardson MJ, Savill NG (1975b) Thermochim Acta 12:213–220
Roles KA, Wunderlich B (1993) J Pol Sci, Part B, Pol Phys 31:279–285
Rossini RD (ed) (1956) Experimental Themochemistry, Vol I. Interscience Publishers, New York
Rouquerol J, Zielenkiewicz W (1986) Thermochim Acta 109:121–137
Ryan ME, Dutta A (1979) Polymer 20:203–206
Sarge SM (1991) Thermochim Acta 198:323–334
Sarge SM, Cammenga HK (1985) Thermochim Acta 94:17–31
Sarge SM, Gmelin E, Höhne GWH, Cammenga HK, Hemminger W, Eysel W (1994) Thermochim Acta 247:129–168
Schawe JEK (1993) Thermochim Acta 229:69–84
Schawe JEK (1995) Thermochim Acta 261:183–194
Schawe JEK, Schick C (1991) Thermochim Acta 187:335–349
Schawe JEK, Schick C, Höhne GWH (1993) Thermochim Acta 229:37–52
Schawe JEK, Schick C, Höhne GWH (1994) Thermochim Acta 244:49–59
Schawe JEK, Winter W, Höhne GWK (1996) Thermochim Acta, submitted
Schick C, Krämer L, Mischok W (1985) Acta Polymerica 36:47–53
Schick C, Fabry F, Schnell U, Stoll G, Deutschbein L, Mischok W (1988) Acta Polymerica 39:705–710
Schmolz E, Lamprecht I, Schicker B (1993) Thermochim Acta 229:173–180
Schulze FW, Petrick HJ, Cammenga HK (1977) Z phys Chem NF 107:1–19
Schwanebeck W (1991) Thermochim Acta 187:201–210
Shultz AR (1984) J Pol Sci, Pol Phys Edn 22:1753–1771
Singh J (1993) Thermochim Acta 226:211–220
Skinner HA (ed) (1962) Experimental Thermochemistry, Vol II. Interscience Publishers, New York
Smith IT (1961) Polymer 2:95–108
Sourour S, Kamal MR (1976) Thermochim Acta 14:41–59
Spink H, Wadsö I (1976) In: Glick D (ed) Methods of Biochemical Analysis. Wiley, New York
Stevens GC, Richardson MJ (1985) Polym Commun 26:77–80
Struik LCE (1978) Physical Aging in Amorphous Polymers and Other Materials. Elsevier, Amsterdam
Sullivan PF, Seidel G (1968) Phys Rev 173:679
Sunner S, Månsson M (eds) (1979) Combustion Calorimetry. Pergamon Press, Oxford
Suzuki H, Grebowicz J, Wunderlich B (1984) Makromol Chem 186:1109–111
Suzuki H, Wunderlich B (1984) J Therm Anal 29:1369–1377

Takahashi Y, Asou M (1993) Thermochim Acta 223:7–22
Tanaka S (1992) Thermochim Acta 210:67–76
Ter Minassian L, Milliou F (1983) J Phys E: Sci Instrum 16:450–455
Tool AQ (1946) J Am Ceram Soc 29:240–253
Tryson GR, Shultz AR (1979) J Pol Sci: Pol Phys Ed 17:2059–2073
Tsitsilianis C, Staikos G (1992) Macromolecules 25:910–916
Ueberreiter K, Kanig G (1952) J Coll Sci 7:529
Ulbrich U, Cammenga HK (1993) Thermochim Acta 229:53–67
Vallebona G (1979) J Therm Anal 16:49–58
van der Plaats G (1984) Thermochim Acta 72:77–82
Von Stockar U, Marison IW (1991) Thermochim Acta 193:215–242
Wadsö I (1993) Thermochim Acta 219:1–15
Watson ES, O'Neill MJ, Justin J, Brenner N (1964) Anal Chem 36:1233–1238
White GK, Collocott SJ (1984) J Phys Chem Ref Data 13:1251–1257
Wiedemann HG (1991) Thermochim Acta 187:245–255
Wies S, Geyer W, Eysel W (1992) J Therm Anal 38:277–287
Wight FR, Hicks GW (1978) Polym Engn and Sci 18:378–381
Williams ML, Landel RF, Ferry JD (1955) J Am Chem Soc 77:3701–3707
Wisanrakkit G, Gillham JK (1990) Journal of Coatings Technology 62:35–50
Wolf G, Schmidt H-G, Bohmhammel K (1994) Thermochim Acta 235:23–29
Wunderlich B (1990) Thermal Analysis. Academic Press, Boston
Wunderlich B at al.: ATHAS databank update (1990) University of Tennessee, Knoxville, USA
Wunderlich B, Jin Y, Boller A (1994) Thermochim Acta 238:277–293
Wunderlich B, Jones LD (1969) J Macromol Sci 3:67–79
Zhiying Z (1986) Scienta Sinica B 24:1239–1247

Subject Index

Springer-Verlag and the Environment

We at Springer-Verlag firmly believe that an international science publisher has a special obligation to the environment, and our corporate policies consistently reflect this conviction.

We also expect our business partners – paper mills, printers, packaging manufacturers, etc. – to commit themselves to using environmentally friendly materials and production processes.

The paper in this book is made from low- or no-chlorine pulp and is acid free, in conformance with international standards for paper permanency.